BIOCONCENTRATION OF MUNITIONS COMPOUNDS IN PLANTS AND WORMS: EXPERIMENTS AND MODELING

by

Tifany L. Torralba–Sanchez

A dissertation submitted to the Faculty of the University of Delaware in partial fulfillment of the requirements for the degree of Doctor of Philosophy in Civil Engineering

Summer 2016

BIOCONCENTRATION OF MUNITIONS COMPOUNDS IN PLANTS AND WORMS: EXPERIMENTS AND MODELING

by

Tifany L. Torralba–Sanchez

Approved: _____
Harry W. Shenton III, Ph.D.
Chair of the Department of Civil and Environmental Engineering

Approved: _____
Babatunde A. Ogunnaike, Ph.D.
Dean of the College of Engineering

Approved: _____
Ann L. Ardis, Ph.D.
Senior Vice Provost for Graduate and Professional Education

I certify that I have read this dissertation and that in my opinion it meets the academic and professional standard required by the University as a dissertation for the degree of Doctor of Philosophy.

Signed: _____

Dominic M. Di Toro, Ph.D.
Professor in charge of dissertation

I certify that I have read this dissertation and that in my opinion it meets the academic and professional standard required by the University as a dissertation for the degree of Doctor of Philosophy.

Signed: _____

Herbert E. Allen, Ph.D.
Member of dissertation committee

I certify that I have read this dissertation and that in my opinion it meets the academic and professional standard required by the University as a dissertation for the degree of Doctor of Philosophy.

Signed: _____

Ronald T. Checkai, Ph.D.
Member of dissertation committee

I certify that I have read this dissertation and that in my opinion it meets the academic and professional standard required by the University as a dissertation for the degree of Doctor of Philosophy.

Signed: _____

Dave T.F. Kuo, Ph.D.
Member of dissertation committee

ACKNOWLEDGMENTS

This document has only one author, but the findings presented in this this doctoral dissertation are the result of the work of many more people than just myself.

God blessed me and made this achievement possible by prompting me in the right way to encounter very smart, proficient, and kindhearted people during my five years here at the University of Delaware. My adviser, Dr. Dominic Di Toro, is an outstanding example of this group of people. He kindly and enthusiastically welcomed me to his research team in the winter of 2011. Back then I arrived just as a young and inexperienced international student from a developing country, but Dr. Di Toro did not seem to regard me in that way. Based on what he had heard about me from my undergraduate thesis adviser, Dr. Di Toro trusted my judgement assigning me important research responsibilities right away, believed in my capabilities challenging me to take tough classes, and patiently gave me space to work at my own pace. This year Dr. Di Toro proudly graduates me along with three of my friends and colleagues as skilled researchers and competitive professionals. The transformation Dr. Di Toro's tutelage along with UD's high quality education made in my life is something my family and I will forever be grateful to this nation for!

In addition to Dr. Di Toro, I also had other valuable mentors to whom I am very thankful. In particular, Drs. H. Allen, D. Kuo, R. Checkai, P. Chiu, P. Imhoff, S. Patel selflessly offered me their treasured and vast knowledge, time, and advice always welcoming my questions with respectful cognizance and passionate curiosity. The meetings and discussions I had with them were opportunities for me to learn from

their exceptional talents and experience – they made me a more humble and ambitious engineer. Other examples of people who made this work possible are my coworkers who rapidly became my friends: now–Drs. Rosalina G., Andrew M., Yuzhen “Eva” L., Craig D., Solmaz M., and Olga D., and Drs.–to–be Kyle M. and Kathy B walked this bumpy but rewarding path with me. Every time we worked together they allowed me to learn from their distinct characters and skills and by doing so they made me a more understanding and efficient person. I also had great help from the undergraduate students who assisted me with my experiments in the laboratory: Caroline B., Kevin H., Samantha K., Lorraine S., and Mingze N.; guiding them, assigning their daily duties, and being responsible for their safety in the lab taught how to be a perceptive team leader. I am very thankful to the staff in our department for their kind, prompt, and effective assistance every time I asked them for help, in particular, Michael D, Rovshan M., Chris R., Karen G, and Marikka B. An interesting group of people that have been part of my life at UD are my colleagues including Drs.–to–be Shray S, Majid D., and Soohoon C; we spent moments of complains, laugh, and, of course, studying together – they always brought a spark of fun that boosted up my many days of monotonous routine.

Besides the people who helped me with the technical parts of this research, there are those who emotionally kept me going forward in the pursuance of this degree. My family has always been a main pillar for me given our very close relationship, we are like best friends; they were always aware of and present in my up and down moments during my life away from my home country, Colombia. Only with the precious values my parents, Ruth S. R. and Edgar T. V., instilled in me and the affecting support from my sisters, Dayan T. S. and Gilary T. S., was it possible for me

to cross this finish line – I know they are the most proud of me for this achievement. I am deeply thankful to my brilliant, loving, and calm boyfriend, Chongyang L.; during our four years together he has made great sacrifices for me and has always been there to willingly and generously help me with whatever I need. I have learned innumerable things from the very intense intellectual discussions he enjoys having so much and from the excellent education his parents, D. Zhang and D. Lin, gave him. Especially through his sharp mind and calm and wise reactions to problematic situations he has unintentionally taught me to be a more respectful, tolerant, and mature human being.

This degree is dedicated to my grandmother who passed away in the middle of my dissertation writing process. I will always remember what she told me about there not being challenges too big to overcome provided one enjoys good health: "*as long as you bear good health there are no reasons to be stressed out about, good health is a blessing that allows you to laugh about life's challenges*", she used to say. I will try to live my life with that in my heart and mind. Thank you!

TABLE OF CONTENTS

LIST OF TABLES

LIST OF FIGURES

ABSTRACT

Elevated concentrations of munitions compounds (MCs) – which include explosives and propellants – have been found in soils at military ranges and adjacent areas exposed to off–site migration of contaminants. Organisms such as plants and worms inhabiting these soils are exposed to and may take up the MCs, posing a risk to higher trophic levels. Experimental measurements and modeling tools are required to estimate the degree of bioconcentration to be expected.

Plant uptake assays, plant–water partitioning experiments, and two partition–based models for the estimation of MCs bioconcentration in plants and worms are presented. An experimental protocol for the plant uptake assays to obtain bioconcentration factors (BCFs), defined as the steady state ratio of the concentration in the organism to that available in the growth medium, was tested using barley (*Hordeum vulgare* L.). Unlike conventional methods, this protocol separated the effects of soil characteristics on the MCs bioavailability by using coarse quartz sand (99%, 0.85–1.27 mm effective diameter particles) rather than more complex field or synthetic soils. Applying the proposed protocol, steady state concentrations in both plant and exposure medium were achieved within a one–month period that produced BCFs. Standard partitioning experiments with plant biomass and water were also performed. The resulting plant–water partition coefficients effectually predicted the upper–bound of the experimental BCFs.

The models developed for the prediction of concentrations in plants and worms from soil exposures use polyparameter linear free energy relationships (pp–LFERs) to

estimate the partition coefficients of MCs between soil solids and soil interstitial water, and between organism biomass and water. The pp–LFERs were applied with a set of numerical descriptors computed from chemical structure only. These computations used quantum chemical methods that quantitatively characterize the molecular properties by which a MC interacts with soil solids, water, and organism biomass. Specifically soil organic carbon, plant cuticle, worm lipid, and worm protein were the phases considered in the soil–water–organism system. Concentrations of MCs in plants observed in independent validation uptake assays were predicted using pp–LFERs for the partitioning between soil organic carbon and interstitial water, and, subsequently, between water and plant cuticle. The resulting RMSE, root mean square error (log predicted - log observed concentration) of prediction, was 0.433. Similarly, concentrations in worms observed in independent validation uptake assays were predicted with the estimated concentrations in the soil interstitial water and pp–LFERs for the partitioning between water and worm lipid, and water and worm protein. The resulting RMSE was 0.396.

These results highlight the major role played by partitioning in the uptake of MCs by plants and worms from soil. Furthermore, these partition–based models yield estimates without the need for experimental measurements. They require only parameters computed from a compound's molecular structure using quantum chemical methods. These models are particularly useful when: (i) data for a specific organism are scarce, (ii) predictions need to be made for large libraries of compounds, and/or (iii) environmental risk needs to be assessed for compounds in the development stage.

Chapter 1

INTRODUCTION

1.1 Motivation

Elevated levels of munitions compounds (MCs) have been found in soils at military installations that involve munitions manufacturing, disposal, testing, and/or training [1] Off–site migration of MCs results in their contaminants appearance in underlying groundwater [2] and surrounding surface waters [3]. The presence of MCs in such systems poses a risk to ecological receptors such as plants and worms inhabiting the impacted locations and surrounding off-site areas, and simultaneously represents a potential for transference to higher trophic levels. Lethal, toxic (e.g., growth and reproduction inhibition), and/or avoidance response effects have been observed for MCs in different plant and worm species [4-7]. Limited evidence exists on the health effects of MCs in humans; however, animal studies have shown both liver and reproductive damages and presence of carcinomas in rats exposed to some MCs [8,9]. These results have led the US Environmental Protection Agency (US EPA) to assign a weight-of-evidence carcinogenic classification of C (possible human carcinogen) to those compounds along with their inclusion in the EPA's Integrated Risk Information System (IRIS) [8,9]. The information on the mobility, toxicity, and possible health effects has given rise to a pressing need for the US Department of Defense to minimize the residual environmental impacts of military testing and training operations. Both experimental and modeling approaches should be considered to assess the risk of MCs in the environment.

1.2 Experimental Approach

The degree to which a compound is transferred from the ambient environment (e.g., soil, water, air) into an organism has been typically expressed as a bioconcentration factor (BCF), calculated as the steady state ratio of the compound's concentration incorporated into an organism to the concertation available in the exposure medium [10-12]. Uptake assays with plants and worms have conventionally been performed using spiked or contaminated soils as the exposure medium to obtain BCFs for MCs [13-18]. While this experimental approach closely resembles the field conditions, it allows other biotic/abiotic processes, mediated by soil properties, to also influence the resulting MCs concentration in plants and worms. Some of those processes are the degradation/transformation of the parent compound and soil solid–soil interstitial water sorption–desorption, which determine the availability of the MCs for organism uptake [7,19-23]. As a result, BCFs spanning several orders of magnitude for the same MC in closely related species under similar nominal soil concentrations exist in the literature [14-18]. This greatly restricts the usefulness of extending soil–based BCFs to more generic exposure and soil conditions often found in regulatory and/or engineering cases [24]. Therefore, there is a need for a protocol that would reduce the variability in experimental BCFs by being less subjected to interferences from the aforementioned soil processes.

1.3 Modeling Approach

It has been shown that the concentration of contaminants that plants and worms are exposed to in the growth medium is that dissolved in the interstitial water [25-27]. However, due to the analytical difficulties to obtain reliable measurements of the concentration in the interstitial water, models able to predict the resulting

concentration in the organism without the need for interstitial water measurements have been proposed. For worms, these are dynamic models based on first–order kinetics that estimate the steady state concentration in the worm as

$$C_{i_{Worm}} = \frac{k_{i_u}}{k_{i_e}} C_{i_{Soil}} \quad (1\text{-}1)$$

where i is an organic compound of interest, $C_{i_{Soil}}$ = concentration of i in the soil (mg kg_{dwt}^{-1}, dwt: dry weight), k_{i_u} = uptake rate constant (d^{-1}), and k_{i_e} = elimination rate constant (d^{-1}). The rate constants k_{i_u} and k_{i_e} represent the summed contributions from various uptake and elimination processes. Similarly for plants, models often cited include elimination processes such as metabolism, photodegradation, volatilization from leaves, and growth dilution [28,29]. While these models provide a detailed representation of the mechanisms involved in the bioconcentration, they require parameter estimates that quantify each of these processes for a particular compound or species of interest (e.g., Jager [30], and Trapp and Eggen [29]). In the worm bioconcentration model by Jager [30], for example, up to six species-specific parameters and three chemical-specific parameters are determined through repeated numerical random sampling as experimental data or empirical correlations for their estimation are not available. Similarly, in the plant bioconcentration model by Trapp and Eggen [29], three species-specific parameters and four chemical-specific parameters are assumed from default datasets or taken as extrapolated values from considered-equivalent processes. Therefore, large datasets are needed to make these parameters available for each of the specific uptake and elimination processes. This limits the use of these models for most existing chemicals and for new proposed compounds for which only the molecular structure is known.

Models have also been formulated considering the uptake of nonionic organic compounds by plants and worms to be a passive diffusive process (i.e., no input of metabolic energy). In this way, the upper–bound of the concentration in the organism can be predicted using the partitioning between water and biomass components [25,31-35]. In most of these models, the organism lipid is regarded as the dominant phase for accumulation of compounds. Therefore, the estimation of the concentration in the organism is often based on the compound octanol–water partition coefficient, K_{OW}, or the partitioning to the organism–whole body is predicted with K_{OW}–based quantitative structure-activity relationships (QSARs) as shown, for example, in Eq. (1-2) and Eq. (1-3) from Li et al. [35] and Lord et al. [31], respectively.

$$C_{Plant} \approx C_{Water}\, f_{Lipid}\, K_{OW} \tag{1-2}$$

$$\log K_{Worm-Water} = 0.476\, (\log K_{OW}) + 1.04 \tag{1-3}$$

These models assume that octanol has similar solvation properties to those of the organism lipid, which has shown not to be the case for more polar compounds, compounds that interact by hydrogen-bonding when using octanol as a surrogate for other environmentally relevant organic phases [36-38]. Furthermore, the dependence on the K_{OW} as the sole parameter used to estimate the bioconcentration provides little insight into the chemical properties that make a compound more likely to accumulate in plants or worms. No model built with or for MCs was found in the literature; therefore, the bioconcentration of MCs would need to be predicted using these K_{OW}–based models. Hence, information on the chemical properties that determine the tendency of a MC to accumulate in plants and worms would not be available. This is

important knowledge to aid in selecting among proposed compounds, including MCs, early in the development stage, for example.

More recent models for estimating partitioning to organism components are polyparameter linear free energy relationships (pp-LFERs) [39,40]. Unlike single-parameter K_{OW}-based predictions, pp-LFERs predict partitioning by explicitly considering the contributions from different types of chemical interactions (e.g., hydrogen bonding, Van der Waals forces) between the solute and the condensed phase (e.g., soil organic carbon, plant cuticle, worm protein). Thus, pp-LFERs are able to more fully characterize the solvation properties of the condensed phase and the strength of its interactions with solutes relative to that of the aqueous phase. The chemical interactions pp-LFERs require can be obtained from chemical structure only, which eliminates the need for experimental measurements in the calibration of the model. This opens the possibility to estimate the MCs bioconcentration in plants and worms in challenging situations where experimental bioconcentration data are scarce or simply not available.

1.4 Research goals

In this dissertation the bioconcentration of MCs in plants and worms is regarded as being determined by both the bioavailability of the compound in the exposure medium and its tendency to sorb onto the organism biomass components. The bioavailability of the MCs is understood to be the result of soil solid–soil interstitial water sorption–desorption, which are processes largely controlled by soil properties such as organic carbon content.

The tendency of a MC to prefer an organic phase relative to the interstitial water is calculated as a partition coefficient, *K*. The *K* for the overall organism can be

obtained from the dominant contribution of a single phase or the sum of the contributions from multiple relevant phases. Fig. 1-1 illustrates the environmental phases considered to play a major role in the bioconcentration of MCs in plants and worms from soil: soil organic carbon, plant cuticle (lipid-like phase), worm lipid, worm protein, and worm internal water. The term for the internal water component in the partitioning between soil interstitial water and worm (Fig. 1-1) accounts for the contribution from the water phase inside the worm, which is assumed to be at the same concentration as that in the soil interstitial water. The mass fractions of the different phases, f, provide the characteristics of a particular plant or worm species or soil type.

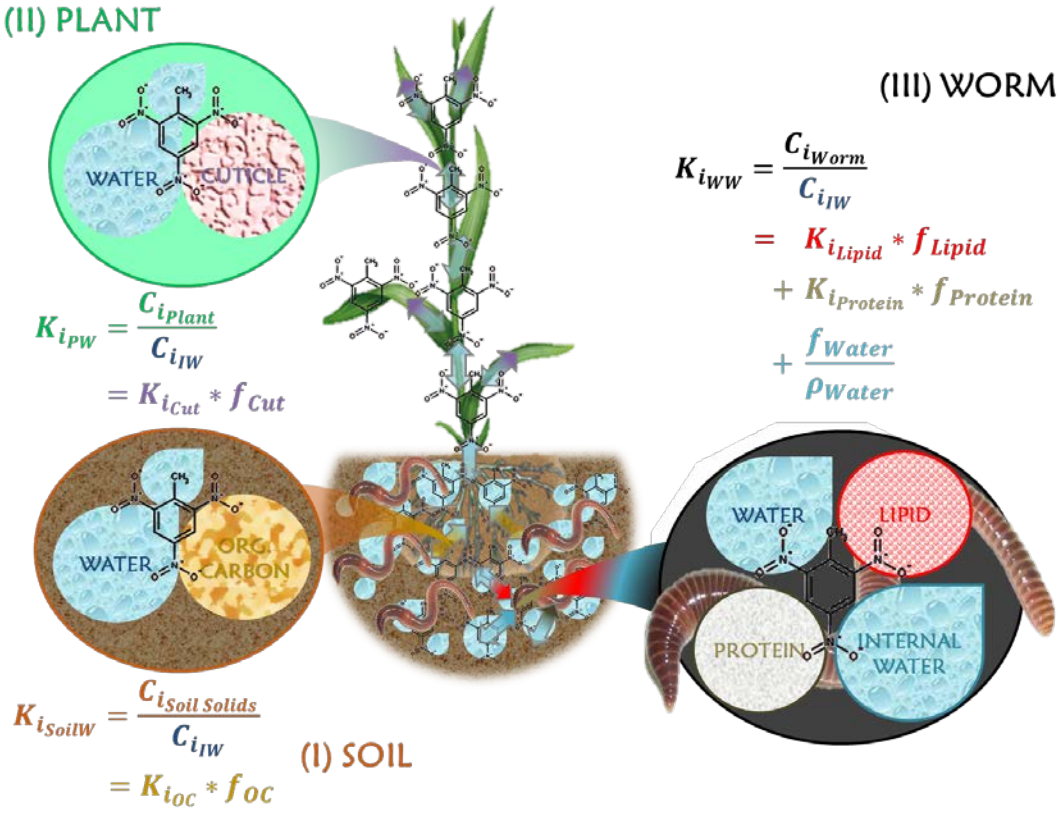

Figure 1-1 Schematics of the interactions between soil interstitial water (IW) and soil organic carbon (OC), plant cuticle (Cut), worm lipid, worm protein, and worm internal water for munitions compounds (displaying 2,4,6-trinitrotoluene). i: organic compound of interest, C: concentration, K: partition coefficient, SoilW: soil–water, PW: plant–water, WW: worm–water, f: mass fraction, and ρ: density. Colors identify the different components considered to play a major role in the soil–water–organism system.

Based on these considerations and the state of the art described above, these are the key objectives of this dissertation:

- Generating BCFs for plants with the use of an experimental protocol that allows separation of the effects of the growth medium on the MCs bioavailability for plant root uptake,

- Predicting BCFs for plants and worms with measurements or estimates of the MCs partitioning between water and organism biomass components, and
- Estimating concentrations in plants and worms exposed to MCs in soils with the prediction of the partitioning between soil solids and soil interstitial water, and between water and organism biomass components

This document comprises five chapters, including this Introductory Chapter. Chapter 2 presents an experimental protocol using coarse quartz sand (99% 0.85–1.27 mm effective diameter particles) as a substitute for conventional contaminated or spiked soil in uptake assays to obtain reproducible steady state plant BCFs for MCs. In addition, these BCFs are compared to measured plant–water partition coefficients to identify the extent to which partitioning can predict the upper–bound of the plant root uptake process. In Chapter 3, a bioconcentration model built with partition pp-LFERs between soil organic carbon and soil interstitial water, and between water and plant cuticle is validated for the prediction of MCs concentrations observed in independent plant uptake assays from soil. Similarly, Chapter 4 explores the dominant worm components for partitioning between water and organism biomass using pp-LFERs and together with a pp-LFER for partitioning between soil organic carbon and soil interstitial water form a bioconcentration model that is employed for the prediction of MCs concentrations observed in independent worm uptake assays in soil.

The core chapters (Chapter 2 to Chapter 4) are independent of each other for they were written to be published as individual articles in indexed scientific journals. Therefore, repetition of definitions for abbreviations and concepts are found across the chapters, and each contains an independent set of references, which also applies to

their individual appendices. Finally, Chapter 5 presents a summary of the findings, provides conclusions, and proposes future work.

REFERENCES

1. Jenkins TF, Hewitt AD, Grant CL, Thiboutot S, Ampleman G, Walsh ME, Ranney TA, Ramsey CA, Palazzo AJ, Pennington JC. Identity and distribution of residues of energetic compounds at army live-fire training ranges. *Chemosphere*. 2006;63(8):1280-1290.

2. Clausen JL, Korte N. Fate and transport of energetics from surface soils to groundwater. In: Chappell MA, Price CL, George RD, eds. Envir*onmental Chemistry of Explosives and Propellant Compounds in Soils and Marine Systems: Distributed Source Characterization and Remedial Technologies*. Washington, D.C: American Chemical Society. 2011;1069:273-316.

3. Ampleman G, Thiboutot S, Lewis J, Marois A, Gagnon A, Bouchard M, Jenkins T, Ranney TA, Pennington JC. Evaluation of the contamination by explosives and metals in soils, vegetation, surface water and sediment at Cold Lake Air Weapons Range (CLAWR), Alberta, Phase II Final report. Technical Report No. DRDC-Valcartier-TR-2004-204. Valcartier, Québec, Canada: Defence Research and Development Canada - Valcartier, Valcartier QUE (CAN); Cold Regions Research and Engineering Lab, Hanover NH (US). 2004;1-116.

4. Gorge E, Brandt S, Werner D. Uptake and metabolism of 2,4,6-trinitrotoluene in higher plants. *Environ Sci Pollut Res*. 1994;1(4):229-233.

5. Rocheleau S, Kuperman RG, Martel M, Paquet L, Bardai G, Wong S, Sarrazin M, Dodard S, Gong P, Hawari J, Checkai RT, Sunahara GI. Phytotoxicity of nitroaromatic energetic compounds freshly amended or weathered and aged in sandy loam soil. *Chemosphere*. 2006;62(4):545-558.

6. Dodard SG, Sarrazin M, Hawari J, Paquet L, Ampleman G, Thiboutot S, Sunahara GI. Ecotoxicological assessment of a high energetic and insensitive munitions compound: 2,4-dinitroanisole (DNAN). *J Hazard Mater*. 2013;262:143-150.

7. Kuperman RG, Checkai RT, Simini M, Phillips CT, Kolakowski JE, Lanno R. Soil properties affect the toxicities of 2,4,6-trinitrotoluene (TNT) and hexahydro-1,3,5-trinitro-1,3,5-triazine (RDX) to the enchytraeid worm *Enchytraeus crypticus*. *Environ Toxicol Chem*. 2013;32(11):2648-2659.

8. US Environmental Protection Agency. Integrated risk information system (IRIS): "2,4,6-trinitrotoluene (TNT)" Web site. https://cfpub.epa.gov/ncea/iris2/atoz.cfm. Accessed May, 2016.

9. US Environmental Protection Agency. Integrated risk information system (IRIS) multi-year agenda: "Hexahydro-1,3,5-trinitro-1,3,5-triazine (RDX)" Web site. https://www.epa.gov/iris/iris-agenda. Accessed May, 2016.

10. Jager T. Mechanistic approach for estimating bioconcentration of organic chemicals in earthworms (oligochaeta). *Environ Toxicol Chem*. 1998;17(10):2080-2090.

11. Arnot JA, Gobas FAPC. A review of bioconcentration factor (BCF) and bioaccumulation factor (BAF) assessments for organic chemicals in aquatic organisms. *Env Rev*. 2006;14(4):257-297.

12. McKone TE, Maddalena RL. Plant uptake of organic pollutants from soil: Bioconcentration estimates based on models and experiments. *Environ Toxicol Chem*. 2007;26(12):2494-2504.

13. Best EPH, Geter KN, Tatem HE, Lane BK. Effects, transfer, and fate of RDX from aged soil in plants and worms. *Chemosphere*. 2006;62(4):616-625.

14. Best EPH, Tatem HE, Geter KN, Wells ML, Lane BK. Effects, uptake, and fate of 2,4,6-trinitrotoluene aged in soil in plants and worms. *Environ Toxicol Chem*. 2008;27(12):2539-2547.

15. Rocheleau S, Lachance B, Kuperman RG, Hawari J, Thiboutot S, Ampleman G, Sunahara GI. Toxicity and uptake of cyclic nitramine explosives in ryegrass *Lolium perenne*. *Environ Pollut*. 2008;156(1):199-206.

16. Sarrazin M, Dodard SG, Savard K, Lachance B, Bobidoux PY, Kuperman RG, Hawari J, Ampleman G, Thiboutot S, Sunahara GI. Accumulation of hexahydro-1,3,5-trinitro-1,3,5-triazine by the earthworm eisenia andrei in a sandy loam soil. *Environ Toxicol Chem*. 2009;28(10):2125-2133.

17. Zhang B, Pan X, Cobb GP, Anderson TA. Uptake, bioaccumulation, and biodegradation of hexahydro-1,3,5-trinitro-1,3,5-triazine (RDX) and its reduced metabolites (MNX and TNX) by the earthworm (*Eisenia fetida*). *Chemosphere*. 2009;76(1):76-82.

18. Sunahara GI. Development of toxicity benchmarks and bioaccumulation data for N-based organic explosives for terrestrial plants and soil invertebrates. Final Report No. SERDP ER-1416. Québec, Canada: National Research Council of Canada Montreal (Québec) Biotechnology Research Institute. 2012;1-289.

19. Renoux AY, Sarrazin M, Hawari J, Sunahara GI. Transformation of 2,4,6-trinitrotoluene in soil in the presence of the earthworm eisenia andrei. *Environ Toxicol Chem*. 2000;19(6):1473-1480.

20. Berthelot Y, Valton É, Auroy A, Trottier B, Robidoux PY. Integration of toxicological and chemical tools to assess the bioavailability of metals and energetic compounds in contaminated soils. *Chemosphere*. 2008;74(1):166-177.

21. Savard K, Sarrazin M, Dodard SG, Monteil-Rivera F, Kuperman RG, Hawari J, Sunahara GI. Role of soil interstitial water in the accumulation of hexahydro-1,3,5-trinitro-1,3,5-triazine in the earthworm *Eisenia andrei*. *Environ Toxicol Chem*. 2010;29(4):998-1005.

22. Huang Q, Liu B, Hosiana M, Guo X, Wang T, Gui M. Bioavailability of 2, 4, 6-trinitrotoluene (TNT) to earthworms in three different types of soils in china. *Soil Sed Contam*. 2016;25(1):38-49.

23. Kuperman RG, Simini M, Checkai RT, Dodard SG, Sarrazin M, Hawari J, Paquet L, Sunahara GI, Di Toro DM, Allen HE, Kuo DTF, Torralba-Sanchez TL. Developing earthworm bioconcentration factors of nitrogen-based compounds for predicting environmentally significant parameters for new munition compounds in soil. *Appl Soil Ecol*. 2016;104:25-30.

24. Yong RN, Nakano M, Pusch R. Environmental soil properties and behaviour. Boca Raton, FL: CRC Press, Inc. 2012;455.

25. Connell DW, Markwell RD. Bioaccumulation in the soil to earthworm system. *Chemosphere*. 1990;20(1):91-100.

26. Cunningham SD, Anderson TA, Schwab AP, Hsu FC. Phytoremediation of soils contaminated with organic pollutants. In: Sparks DL, ed. *Advances in agronomy*. San Diego, CA: Academic Press. 1996;56:55-114.

27. Collins C, Fryer M, Grosso A. Plant uptake of non-ionic organic chemicals. *Environ Sci Technol*. 2006;40(1):45-52.

28. Trapp S, Matthies M. Generic one-compartment model for uptake of organic chemicals by foliar vegetation. *Environ Sci Technol*. 1995;29(9):2333-2338.

29. Trapp S, Eggen T. Simulation of the plant uptake of organophosphates and other emerging pollutants for greenhouse experiments and field conditions. *Environ Sci Pollut R*. 2013;20(6):4018-4029.

30. Jager T. Modeling ingestion as an exposure route for organic chemicals in earthworms (oligochaeta). *Ecotoxicol Environ Saf*. 2004;57(1):30-38.

31. Lord KA, Briggs GG, Neale MC, Manlove R. Uptake of pesticides from water and soil by earthworms. *Pestic Sci*. 1980;11(4):401-408.

32. Briggs GG, Bromilow RH, Evans AA. Relationships between lipophilicity and root uptake and translocation of non-ionised chemicals by barley. *Pestic Sci*. 1982;13(5):495-504.

33. Briggs GG, Bromilow RH, Evans AA, Williams M. Relationships between lipophilicity and the distribution of non-ionised chemicals in barley shoots following uptake by the roots. *Pestic Sci*. 1983;14(5):492-500.

34. Chiou CT, Sheng G, Manes M. A partition-limited model for the plant uptake of organic contaminants from soil and water. *Environ Sci Technol*. 2001;35(7):1437-1444.

35. Li H, Sheng G, Chiou CT, Xu O. Relation of organic contaminant equilibrium sorption and kinetic uptake in plants. *Environ Sci Technol*. 2005;39(13):4864-4870.

36. von Oepen B, Kördel W, Klein W, Schüürmann G. QSAR in environmental toxicology predictive QSPR models for estimating soil sorption coefficients: Potential and limitations based on dominating processes. *Sci Total Environ*. 1991;109/110:343-354.

37. Wei DB, Wu CD, Wang LS, Hu HY. QSPR-based prediction of adsorption of halogenated aromatics on yellow-brown soil. *SAR QSAR Environ Res*. 2003;14(3):191-198.

38. Kozerski GE, Xu S, Miller J, Durham J. Determination of soil-water sorption coefficients of volatile methylsiloxanes. *Environ Toxicol Chem*. 2014;33(9):1937-1945.

39. Abraham MH. Scales of solute hydrogen-bonding: Their construction and application to physicochemical and biochemical processes. *Chem Soc Rev*. 1993;22(2):73-83.

40. Goss KU. Predicting the equilibrium partitioning of organic compounds using just one linear solvation energy relationship (LSER). *Fluid Phase Equilibr*. 2005;233(1):19-22.

Chapter 2

BIOCONCENTRATION FACTORS AND PLANT–WATER PARTITION COEFFICIENTS OF MUNITIONS COMPOUNDS IN BARLEY

2.1 Introduction

Elevated concentrations of munitions compounds (MCs) – which include explosives and propellants – have been found in soils at various military installations [1-5] as well as in underlying groundwater [6-12] and surrounding surface water bodies [13,14]. MCs dissolve into the soil solution and can be taken up by plants. Such mobility makes MCs an environmental concern for organisms growing in the soils at military ranges and surrounding locations. Therefore, risk assessments of these MCs should include an evaluation of their uptake by plants.

The uptake of a chemical substance by plant tissues (e.g., roots, stem, leaves) from the ambient environment (e.g., soil, water, air) has been typically measured by bioconcentration factors (BCFs). BCFs for plants are calculated as the ratio of the steady state concentration measured in the plant relative to that in the exposure medium [15]. These BCFs are generally determined through laboratory scale experiments where plants are grown in spiked or contaminated field soils [16-20] or hydroponically in nutrient solutions containing dissolved contaminants [21,22]. In the case of solid growth media, various types of BCFs have been used depending on whether expressed relative to the concentration in the medium solids (dry mass) or relative to that in the medium water solution (interstitial/pore water) [15]. The latter BCF is chemically more meaningful since the concentration available for plant root

uptake is only that dissolved in the interstitial water [23,24]. Therefore, BCFs should be calculated as

$$BCF_i = \left(\frac{C_{i_{Organism}}}{C_{i_{Available\ in\ growth\ medium.}}}\right)_{SS} = \left(\frac{C_{i_{Plant}}}{C_{i_{IW}}}\right)_{SS} \quad (2\text{-}1)$$

where i refers to a compound of interest (e.g., a MC), BCF_i = bioconcentration factor of i expressed in $L_{water}\ kg_{plant\ dwt}^{-1}$ (dwt: dry weight), SS denotes steady state, $C_{i_{Plant}}$ = concentration of i in the plant expressed in mg kg_{dwt}^{-1}, and $C_{i_{IW}}$ = dissolved concentration of i in the interstitial water (IW) expressed in mg L^{-1}.

Studies have measured uptake by plants from soils at the laboratory scale for some of the most extensively studied MCs: 2,4,6-trinitrotoluene (TNT); 2,4-dinitrotoluene (2,4-DNT); 2,4-dinitroanisole (2,4-DNAN); hexahydro-1,3,5-trinitro-1,3,5-triazine (RDX); and octahydro-1,3,5,7-tetranitro-1,3,5,7-tetrazocine (HMX) [16,17,19,20,25-30]. The set of plant concentrations observed in these studies is graphically summarized in Fig. 2-1A. The BCFs are presented in Fig. 2-1B when available. They are BCFs as ratio of the MC concentration in the plant to that in the soil solids (this ratio is hereafter referred to as "BCF_{Solids}"). Fig. 2-1 reveals large variations among both plant concentrations and BCF_{Solids} for a single MC. The variations in plant concentrations are expected since the corresponding exposure concentration is not considered. The variations found in BCF_{Solids} (up to three orders of magnitude for the same MC) are primarily due to three main factors: plant type, exposure time, and available concentration for plant root uptake. These are key elements to consider in the experimental design of uptake assays for the determination of MCs bioconcentration in plants.

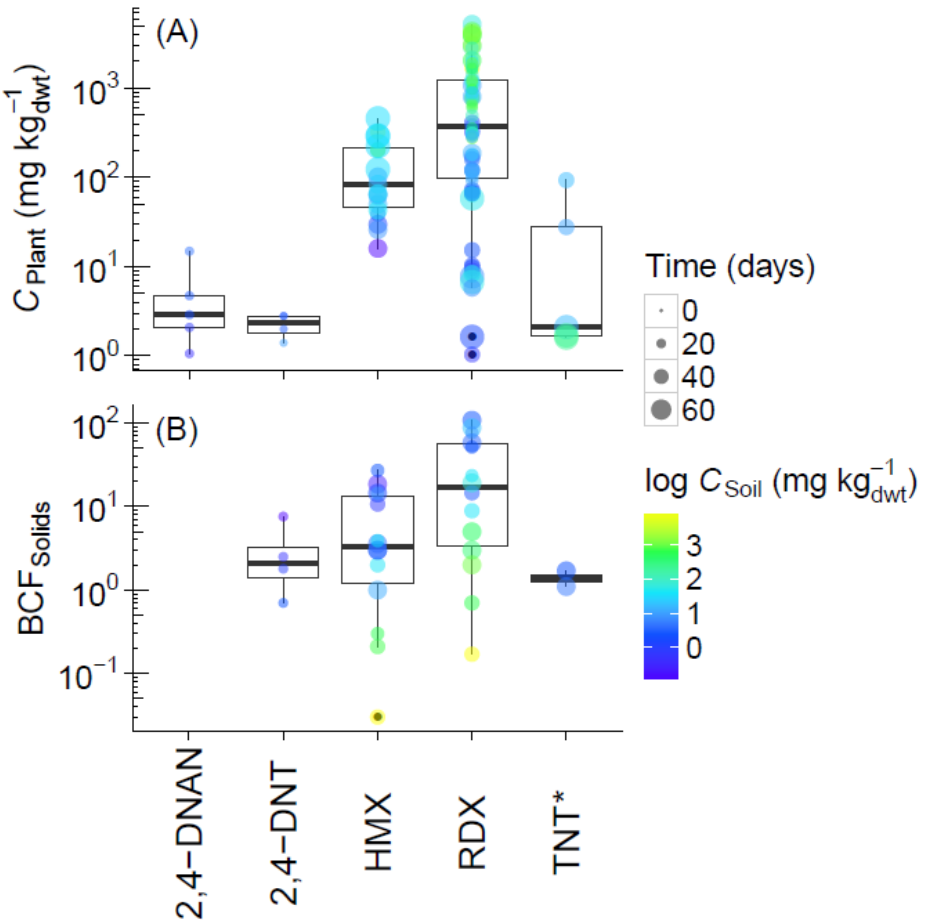

Figure 2-1 Results from published uptake studies: (A) MCs concentrations in plants on the last day of exposure (C_{Plant}), and (B) bioconcentration factors expressed relative to concentrations in soil solids (BCF_{Solids}) as kg_{dwt} soil $(kg_{dwt}\ plant)^{-1}$. C_{Soil}: Concentration in soil at the beginning of exposure. Circles' size proportional to the exposure duration. Data presented for the whole plant or only for the aboveground plant parts when available. TNT* = TNT or TNT degradation products; TNT is reported as not detected in plant tissues in some references.

Plant type: General differences in the potential to take up MCs have been shown between aquatic and terrestrial plant types [31,32], while those between more similar plant types, terrestrial monocotyledons and dicotyledons, have not been

observed [33]. Most of the species investigated in the studies included in Fig. 2-1 are terrestrial herbaceous plants that belong to closely related families: graminoids (grasses), legumes, and amaryllis. This likely reduces the significance of plant type as a factor for the large variations shown in Fig. 2-1.

Exposure time: In contrast to the similarity in plant types, the uptake assays included in Fig. 2-1 have exposure times varying from 19 to 77 days. Plant concentrations obtained with longer exposure time (i.e., > 40 days) were generally higher than those measured in short–exposure experiments (Fig. 2-1A). However, these comparisons should only be made once growth dilution effects [24] (increasing biomass during the growing period dilutes chemical concentrations in the plant tissues) have been taken into account, the concentration in the plant has reached a temporal steady state (i.e., no significant variations with longer exposure time), and the BCF is relative to the MC concentration in the medium water solution (i.e., reporting BCF defined in Eq. (2-1) instead of BCF_{Solids}).

Available concentration for plant root uptake: Soils with diverse physicochemical properties are used in the studies included in Fig. 2-1. Soil properties such as organic carbon content have been shown to determine MCs bioavailability as a result of sorption processes [34-38]. The available concentration for plant root uptake is further limited by the transformation/degradation of the parent compound in the growth medium during the plant exposure. Aqueous solubility also plays an important role in the bioavailability of MCs, as it controls the maximum concentration that will dissolve in the soil interstitial water. Therefore, contrary to what might be expected, increments in soil concentration treatments do not necessarily lead to higher BCF_{Solids} in plants. Fig. 2-1B, for example, shows decreasing BCF_{Solids} with increasing soil

concentrations [16,17,19] for exposures up to 1×10^4 mg kg_{dwt}^{-1} for RDX and HMX [19], which have considerably lower solubilities than other MCs (Table 2-1). This decrease in BCF_{Solids} wrongly points to conclude that large MCs concentrations in the soil do not result in higher plant bioconcentration. However, what is actually happening is that the concentration available for plant root uptake is overestimated when: (i) further increments in soil concentration treatments do not lead to higher concentrations in the soil interstitial water as the MC aqueous solubility has been reached, and/or (ii) the rate of MC degradation in the soil plus plant uptake exceeds the rate of MC dissolution decreasing the exposure concentration.

The most common alternative to field or synthetic soil growth media has been the use of hydroponic systems with water only exposure. While it is clear what the MC concentration available for plant root uptake is, these type of experiments have shown plants with delayed and less frequent root branching than those growing in a solid medium [39,40]. Root morphology and architecture determine the accessibility of plants to both nutrients and contaminants, thus a solid growth medium represents field conditions more closely than a hydroponic system with water only. Normal plant root development and minimal influence of the growth medium in the concentration available for plant root uptake dictate the choice of using essentially inert solids such as coarse quartz sand (99%, 0.85–1.27 mm effective diameter particles) as growth media (hereafter referred to as “sand”).

The uptake assays in the work presented here were designed in order to provide data for the development of a model to predict the steady state BCFs of MCs and compounds with similar chemical structure functionalities referred to as munition-like compounds (MLCs). This requires the concentrations in the plant and available

for plant root uptake to be at steady state. Therefore, using sand as the solid growth medium in this work is particularly convenient because, in addition to the advantages mentioned previously, sand allows to: (i) easily conduct fluids thereby providing a more uniform exposure concentration, and (ii) make interstitial water sampling, measured in the displaced solution, more representative compared to that obtained in studies using more complex soil(s) (hereafter referred to as "soil").

Separating the contributions of the growth medium characteristics and the MCs, or MLCs, properties to the BCFs can also aid in understanding the uptake process from a mechanistic perspective. The uptake of nonionic organic contaminants through plant roots has already been shown to be a passive diffusive process [24] (i.e., no input of metabolic energy). The uptake of nonionic organic contaminants through plant roots has already been shown to be a passive (i.e., no input of metabolic energy) diffusive process [24]. This suggests the uptake of nonionic organic MCs and MLCs is largely governed by their aqueous concentrations and sorption onto plant tissues. Partition–dominated steady state sorption of nonionic organic contaminants by plant materials has been tested and shown to serve as an estimate for the upper–bound of the bioconcentration resulting from the overall uptake process [41-43].

In this work, five nonionic organic compounds were studied for both plant uptake and plant–water partitioning by barley (*Hordeum vulgare* L.). Two objectives were: (i) provide BCFs that are predominantly a function of the compound chemical properties, using steady state measurements and sand as the solid growth medium; and (ii) estimate the upper–bound of the plant uptake process via plant–water partitioning measurements. The compounds included three MCs: TNT; 2,4-DNT; and 2,4-DNAN; and two MLCs: 4-nitroanisole (4-NAN) and 2-methoxy-5-nitropyridine (2-M-5-

NPYNE). Additionally, in order to increase chemical variety, three more compounds were studied for plant–water partitioning. These compounds comprised two MCs: RDX and HMX, and a MLC: 2,5-dimethoxy-4-nitroaniline (2,5-DM-4-NANE). While the MLCs here might not be used in current explosives and propellants formulations, their structural resemblance to MCs including the presence of nitro functional groups ($-NO_2$) and N-substituted rings (Table 2-1) makes them likely to be related to future MCs for which MLCs can serve as validation proxies. Differences among all eight compounds include the position and number of the nitro groups, as well as the presence of other functional groups, methoxy ($O-CH_3$) and amino ($-NH_2$), in the structures. This diversity in functionalities and physicochemical properties determines the bioavailability of both MCs and MLCs and is likely to influence the extent of their uptake and partitioning from water into plants.

Table 2-1 Selected characteristics and physicochemical properties of the MCs and MLCs studied.

Class	Compound[a]	CAS #	Molecular Weight	Structure	Aqueous Solubility[b] mg L^{-1}	log K_{OW}[b]
MCs: Nitroaromatics	TNT	118-96-7	227.13	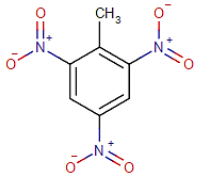	115	1.60
	2,4-DNT	121-14-2	182.14	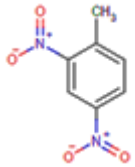	200	1.98
	2,4-DNAN	119-27-7	198.14	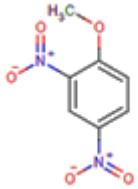	155	1.58[c]
MCs: Nitramines	RDX	121-82-4	222.12	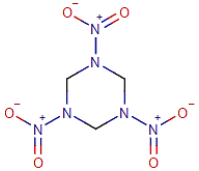	60	0.87

	HMX	2691-41-0	296.16	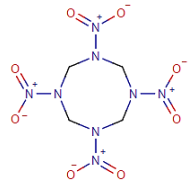	5	0.16
	4-NAN	100-17-4	153.14	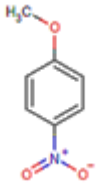	590	2.03
MLCs	2-M-5-NPYNE	5446-92-4	154.13	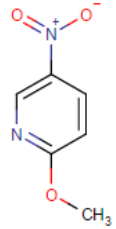	1406[d]	1.55
	2,5-DM-4-NANE	6313-37-7	198.18	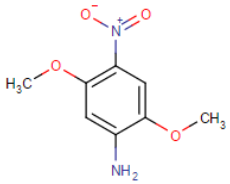	1801[d]	1.63[d]

[a] Chemicals: 2,4,6-trinitrotoluene (TNT); 2,4-dinitrotoluene (2,4-DNT); 2,4-dinitroanisole (2,4-DNAN); hexahydro-1,3,5-trinitro-1,3,5-triazine (RDX); octahydro-1,3,5,7-tetranitro-1,3,5,7-tetrazocine (HMX); 4-nitroanisole (4-NAN); 2-methoxy-5-nitropyridine (2-M-5-NPYNE); 2,5-dimethoxy-4-nitroaniline (2,5-DM-4-NANE)
[b] Experimental data from EPI Suite database [44]
[c] Experimental value from Hawari et al. [45]
[d] Estimate from EPI Suite [44] in absence of an experimental value

2.2 Materials and Methods

2.2.1 Chemicals and Reagents

Aqueous solutions of TNT; 2,4-DNT; RDX; and HMX at nominal concentrations of 100, 100, 50, and 5 mg L^{-1}, respectively, were obtained from U.S Army Edgewood Chemical Biological Center (Aberdeen Proving Ground, MD, USA). The other compounds: 2,4-DNAN; 4-NAN; 2,5-DM-4-NANE; and 2-M-5-NPYNE were obtained from Sigma-Aldrich, Inc. (Milwaukee, WI, USA), all with purity ≥ 97%. Reference standards for TNT; 2,4-DNT; RDX; HMX; and 4-NAN were from AccuStandard, Inc. (New Haven, CT, USA) or Crescent Chemical Co., Inc. (Islandia, New York, USA). Reference solutions for 2,4-DNAN; 2,5-DM-4-NANE; and 2-M-5-NPYNE were prepared in either methanol or ethanol. High performance liquid chromatography (HPLC)–grade methanol was from Fisher Scientific Co., Inc. (Suwanee, GA, USA). All other chemicals were either analytical or certified grade. Deionized water (18.1 MΩ) was obtained using a Neu–Ion, Inc. (Baltimore, MD, USA) water purification system and was used throughout the studies.

Sand (Ottawa ACS grade, CAS: 14808-60-7, quartz, particle size: 20–30 mesh, specific gravity: 2.65) was obtained from VWR International, LLC (Radnor, PA, USA). Sand was triple rinsed with water and used as the solid growth medium.

2.2.2 Plant Growth Conditions

The plant species selected was based on its wide geographical distribution, rapid growth, and ease of cultivation in the laboratory. Barley is an important cereal crop; in 2013 it ranked fourth (both in area harvested and production) among cereal crops in the world [46]. The monocotyledon *Hordeum vulgare* L. (barley) belongs to the

Poaceae family (true grasses) which has several species established in standard test procedures that are accepted for plant uptake and translocation tests [47,48]. *H. vulgare* has been listed as one of the species used routinely to study phytotoxicity [48]. Additionally, barley has been used at military locations as vegetation cover to control wind (mainly dust) and water erosion [49].

The studies presented here were performed using seeds of hulless barley (*H. vulgare*) obtained from Keystone Group AG Seeds (New Columbia, PA, USA). Plant tests were carried out in a dark fabric–surrounded growth chamber with natural light lamp (AGROSUN®, Full Spectrum Grow Light) to maintain an average luminosity of 1281±10 lux (mean ± standard deviation) for a duration of 16 h per day. Temperature and relative humidity in the growth chamber were 25.7±0.4 °C and 38 to 51%, respectively.

Seeds of barley were sterilized following the procedure proposed in Abdul–Baki [50], and germinated in darkness for 24 h on wet (water) paper towels in plastic dishes at room temperature (23.3±0.5 °C). Sets of 10 to 20 germinated seeds were sown in individual glass pots (diameter: 6 cm, and height: 14 cm) containing 500 g_{dwt} of sand. Glass pots had a drainage nozzle at the bottom for sampling of displaced solution. A square of stainless steel mesh (40 mesh, 4 cm side) was placed at the bottom to prevent the loss of quartz grains. In order to supply needed nutrients for plant growth in sand, a fixed aliquot (4 mL per day) of modified Hoagland aqueous solution [51,52] was added per pot throughout both the toxicity experiments and uptake assays described below in Sections 2.2.4 and 2.2.5, respectively. Nutrient solution composition is shown in Table A-1 in Appendix A.

2.2.3 Plant Growth in Sand

In order to address possible concerns about limited growth for plants sown in media like sand or mixtures of sand and soil relative to those planted in only soil, a test comparing plant height of barley (unexposed to MCs or MLCs) among three different growth media was performed. The media were: (i) sand (plant growth supported using nutrient solution as described above in Section 2.2.2), (ii) 50% (w/w) sand-Matapeake soil (silt loam texture, 21% sand, 57% silt, 22% clay, 1.5% total organic carbon, 9.9 cmol kg^{-1} cation-exchange capacity, and pH 5.7), and (iii) only Matapeake soil.

2.2.4 Toxicity Screening

In order to determine MCs and MLCs exposure concentrations that were low enough to avoid lethal or inhibitory effects in plant growth during the uptake assays but were high enough to be quantified reliably, toxicity screening tests were performed. Procedures for determining toxicity were adapted from the ASTM Standard Guide E1963-09 [48] and the OECD Guidelines Test 227 [53]. Tests were initiated after one day of emergence (2 days after being sown in sand) by adding 4 pore volumes (pore volume = 100 mL, determined by fluid displacement method) of the corresponding compound solution per pot at one of four nominal aqueous concentrations (1, 10, 50, and 100 mg L^{-1}; hereafter referred to as solutions added). Nutrients for plant growth were supplied separately from the solutions added using a fixed aliquot per pot, as described previously in Sec. 2.2.2. To ensure that the desired exposure level had been reached, a set of displaced solution samples were collected from the pot's bottom drainage nozzle and analyzed by HPLC at the end of each of the 4 pore volumes added. All treatments were carried out with a minimum of two

replicates. A set of replicate pots per compound not treated with MCs or MLCs were used as negative controls.

The exposure solution was regarded to be that available for barley root uptake in the interstitial water. The concentration of this exposure solution, i.e., exposure concentration, was considered to be that measured in the displaced solution samples collected from the pot's bottom drainage nozzle. In order to maintain an approximately constant exposure concentration throughout the experiment, daily replenishment of 2 pore volumes was applied using the corresponding solution added. Displaced solution samples were collected at the end of each pore volume and subsequently analyzed by HPLC for MCs and MLCs concentrations. The displaced solution samples collected from each pore volume are hereafter referred to as first– and last–fraction of displaced solution. These samples also served to quantify the extent of the overnight degradation of the compound in the interstitial water.

Shoot height was measured periodically to monitor growth over time. Plants were harvested 6 or 8 days after the beginning of the exposure to MCs or MLCs and the shoot and root lengths of every plant were recorded. Shoots were measured to the tallest point and the longest root was measured to the end of the root tip [48].

2.2.5 Uptake Assays

Seeds preparation and planting, nutrient solution supply, MCs and MLCs solutions loading protocol, and displaced solution sampling for the uptake assays followed the same procedures described previously for the toxicity screening in Section 2.2.4. However, exposure time and MCs and MLCs concentrations in solutions added were modified for the uptake assays as follows: plants were initially grown for 2-3 weeks using only nutrient solution and were then exposed to a MC or

MLC solution at a single non-toxic concentration for various exposure times. The initial MC-free period enabled the plants to reach steady state shoots height to avoid growth dilution effects [24]. Immediately after the MC-free growth period, the exposure to a MC or MLC nominal concentration of 10 mg L^{-1} was initiated following the loading procedures described previously in Section 2.2.4.

Plants were harvested at each of four exposure times: 1, 2, 3, and 4 weeks, and the roots were rinsed with water to remove residual sand. A minimum of two pots were sampled per exposure time. The biomass (shoots and roots together) of each pot was cut into small pieces (approx. 0.5 cm) to facilitate extraction, and then placed into a 10 mL centrifuge glass tube for subsequent acetonitrile extraction. The extraction was performed adding 3 mL of a 0.01 mol L^{-1} $CaCl_2$ and NaN_3 solution to repress microbial activity and 5 mL of acetonitrile per tube. The biomass-acetonitrile suspensions were tumbled end-to-end in darkness at 20 rpm for 1 h, supernatants were transferred with disposable glass pipettes into disposable glass culture tubes (10 mL), filtered through Durapore® polyvinylidene difluoride (PVDF) membranes (0.45 µm pore size, EMD Millipore Corp., Billerica, MA), and analyzed for MCs and MLCs concentrations by HPLC. Four consecutive extractions were performed for each biomass tube.

In order to verify the reproducibility of the BCFs obtained, uptake assays for one of each MCs and MLCs (2,4-DNAN and 4-NAN, respectively) were performed more than once.

2.2.6 Plant-Water Partitioning

Fresh plant mass (0.2 - 0.5 g_{dwt}, shoots and roots together) grown for a 2-3 weeks MC-free period was harvested, cut into small pieces (approx. 0.5 cm), and

mixed with 5 mL of the corresponding MC or MLC aqueous solution and 3 mL of a 0.01 mol L^{-1} $CaCl_2$ and NaN_3 solution to repress microbial activity, in a 10 mL glass tube. In order to establish the effect of the compound initial concentration in the resulting partition coefficient, most partitioning tests were performed at both a low and high concentration (listed in Table A-8 in Appendix A) determined based on the compound aqueous solubility using either experimental values or estimates from EPI Suite [44] (Table 2-1). The ratios of initial concentration to aqueous solubility for the low and high concentration treatments ranged from 0.01 to 0.09 and 0.06 to 0.87, respectively. All treatments were carried out with a minimum of two replicates.

The biomass–MC or –MLC suspensions were tumbled end–to–end in darkness at 20 rpm for 24 h. This contact time had been shown to be sufficient for the equilibration of organic compounds during plant sorption experiments in previous work [41,54]. However, a kinetic sorption experiment using 4-NAN was completed separately to confirm that 24 h was sufficient to achieve steady state concentrations. Following the equilibration period, the aqueous phase from each tube was transferred with disposable glass pipettes into disposable glass culture tubes (10 mL), filtered through PVDF membranes (0.45 µm pore size), and analyzed by HPLC. The plant phase from each tube was subjected to four consecutive acetonitrile extractions using the same procedure described previously for the uptake assays in Section 2.2.5. Plant extracts were transferred, filtered, and analyzed for MCs and MLCs concentrations by HPLC in the same fashion as the aqueous phases.

2.2.7 Analytical Methods

MCs and MLCs concentrations in the filtered aqueous phase samples and plant extracts were analyzed and quantified in an Agilent Technologies (Wilmington, DE,

USA) 1200 series HPLC system using modifications of the US EPA Method 8330B [55]. Separation was made on a ZORBAX SB-C18 column (4.6 × 50 mm; 3.5 µm particle size) maintained at 16.5 °C (36.5 °C for RDX and 2,5-DM-4-NANE to avoid overlap with background signals). The sample injection volume was 100 µL. A water and methanol gradient was used at a flow rate of 2 mL min^{-1}. The initial solvent system consisted of 70% water and 30% methanol, which was held for 2.80 min. A linear gradient was built from 30% methanol to 65% methanol between 2.80 min and 3.15 min. Subsequently, the solvent ratio was changed to the initial conditions and maintained until the end of the total run time (4.50 min). Chromatograms were generated at a wavelength of 214 nm.

2.2.8 Data Analyses

Two–way analysis of variance (ANOVA) with repeated measures was used to establish the effect of three different growth media in plant height over time. Two–way ANOVA tests were performed to identify statistically significant differences in the means of plant responses among carrier controls and MCs–, or MLCs–, exposed subjects for the toxicity screening. Subsequently, Tukey honest significant difference (Tukey HSD) tests were carried out for multiple comparisons to determine statistically significant differences between mean pairs, and to establish values for the No–Observed–Adverse–Effect–Concentration (NOAEC) and the Lowest–Observed–Adverse–Effect–Concentration (LOAEC) for each compound. Effective concentrations producing a 50% decrease (EC_{50}) in the plant responses relative to carrier controls were determined fitting the endpoint shoot height, or root elongation, measurements to either of these models

Logistic Gompertz Model:

$$y = a \times e^{\left\{[\log(1-p)]\times\left(\frac{C}{EC_p}\right)^b\right\}} \quad (2\text{-}2)$$

Logistic Hormetic Model:

$$y = \frac{a \times [1 + (h \times C)]}{1 + \left[\frac{p + (h \times C)}{(1-p)} \times \left(\frac{C}{EC_p}\right)^b\right]} \quad (2\text{-}3)$$

where y = measured endpoint shoot height or root elongation (cm), a = control response, i.e., y-axis intercept (cm), p = value for the p effect (0.5 for 50%), C = measured exposure concentration (mg L^{-1}), EC_p = estimate of effect concentration for the specified percent effect (mg L^{-1}), b = scale parameter, and h = hormetic effect parameter [56,57]. Toxicity screening results that exhibited hormesis (stimulation effects at doses below the toxicity threshold, while causing toxicity at doses above the threshold [58]) were fitted to the hormetic model.

ANOVA with repeated measures tests were conducted to examine the fluctuation of exposure concentrations throughout the toxicity screening and the uptake assays. One–way ANOVA was used to assess the dependence of the ratios of concentrations in the plant to concentrations in the interstitial water on the exposure duration in the uptake tests. In all these statistical tests, a p-value ≤ 0.05 was accepted as significant and these analyses were performed using the R software for statistical computing [59].

2.3 Results and Discussion

2.3.1 Plant Growth in Sand

Fig. 2-2 compares the shoot height for plants grown in sand and sand–Matapeake soil relative to that of those growing in only Matapeake soil over a period of 21 days. Ratios were ≥ 1.0 after the average shoot height started to reach a plateau

(approx. 10 days) and until the end of the tested period. There was no statistically significant difference (p-value = 0.68) in shoots height among plants growing in sand, sand–Matapeake soil, and only Matapeake soil throughout the 21 days. This result supports the use of sand as the solid growth medium. Additionally, the use of sand made it possible to maintain nearly constant MCs and MLCs exposure concentrations in both toxicity screening and uptake assays, as described below in Sections 2.3.2 and 2.3.3.

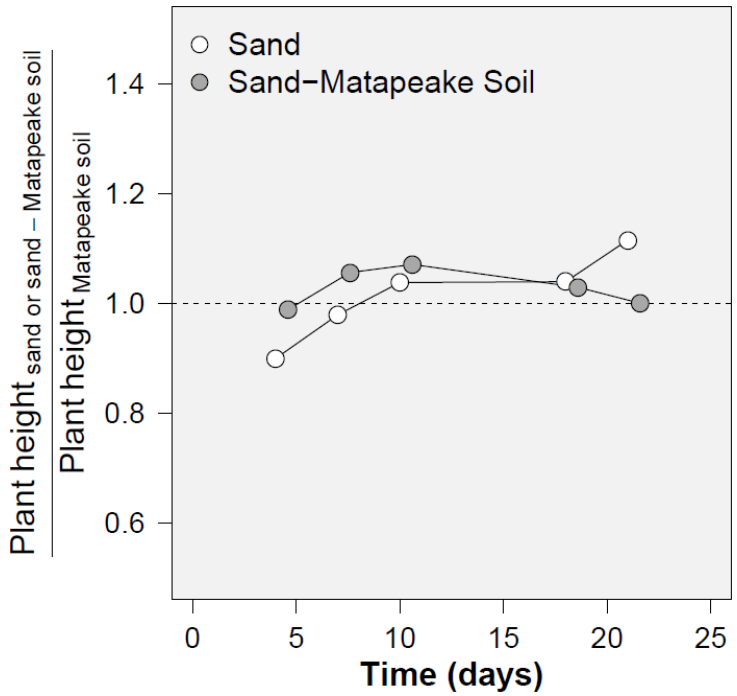

Figure 2-2 Growth of barley (unexposed to MCs or MLCs) in three different solid media over a period of 21 days. Data presented as the ratios of the average shoot height of plants grown in either sand or sand–Matapeake soil relative to that of those growing in only Matapeake soil. Horizontal dotted line is a visual reference at ratio = 1.

2.3.2 Toxicity Screening

Results of the toxicity screening tests for barley exposed to single MCs or MLCs for 6 or 8 days are shown in Fig.2-3 (Table A-2 in Appendix A), a comparison of endpoint shoot height and root elongation versus measured exposure concentrations. The nominal exposure concentration chosen for the uptake assays is shown as a vertical line at 10 mg L^{-1} in Fig.2-3.

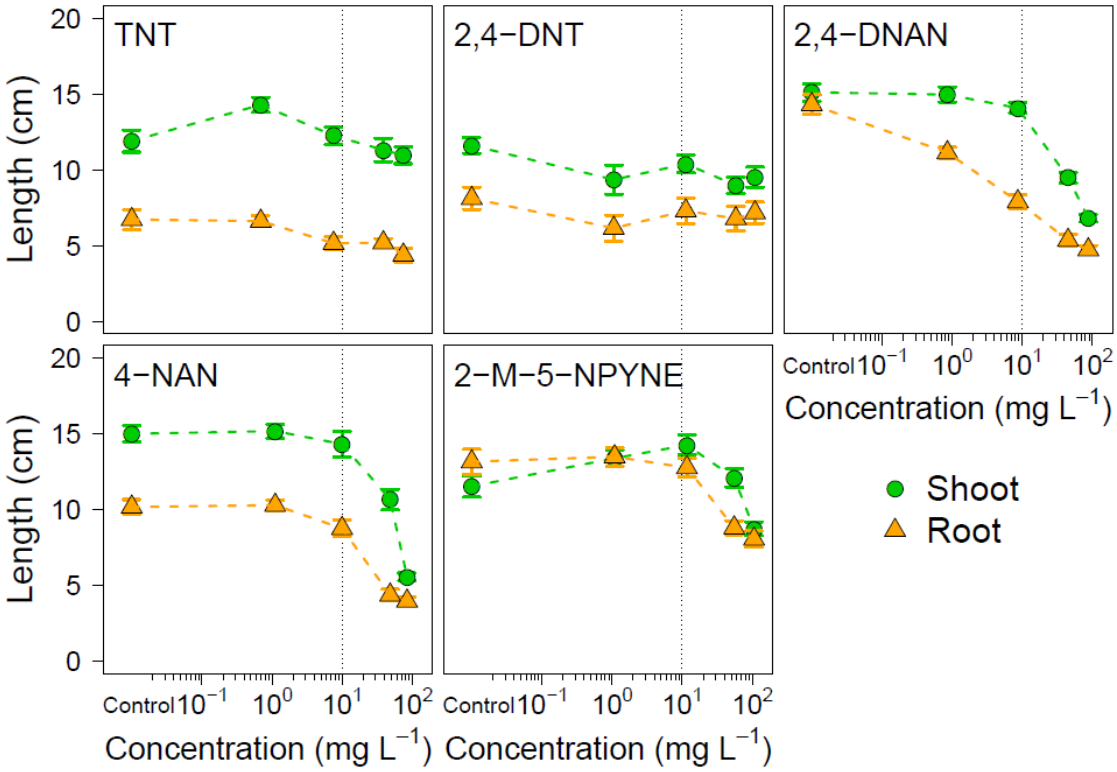

Figure 2-3 Barley shoot and root lengths versus measured exposure concentrations of MCs and MLCs. Vertical dotted line shows nominal concentration chosen to perform uptake assays (10 mg L^{-1}). Data presented as means ± standard error of the mean (SEM). Dashed colored lines are visual guides for data trends. If not visible, error bars are smaller than the symbol.

The NOAEC, LOAEC, and EC_{50} values for shoot and root length are listed in Table 2-2. Both the shoot length LOAEC and EC_{50} were > 10 mg L^{-1} for all the compounds. This was also the case for root length LOAEC for all compounds except 2,4-DNAN. Since the shoot lengths were not affected and only the root elongation for 2,4-DNAN showed an effect, 10 mg L^{-1} (nominal) was chosen to perform the uptake assays. This also ensured that the concentration of MCs or MLCs in the plant biomass after extraction would be high enough to be quantified reliably.

Plant biomass exhibited a typical exponential growth at all concentrations during toxicity screening (Fig. A-1 in Appendix A). Measured exposure concentrations are reported in Fig. A-2 in Appendix A. For sand as the solid growth medium with daily replenishment of the exposure solution, the fluctuations in the measured exposure concentrations were not different from the mean concentration at the 5% level of statistical significance for any of the compounds in the toxicity screening (Table A-3 in Appendix A). Overnight degradation in the growth medium during the toxicity screening was never > 26% for any of the compounds except TNT, which had a one-time maximum of 34%. This was expected since TNT has been shown to be readily transformed in comparison to other MCs [38,60]. Addition of four consecutive pore volumes was sufficient to reach the desired concentrations on the day the exposure to MCs, or MLCs, began (Fig. A-3 in Appendix A).

Table 2-2 NOAEC, LOAEC, and EC_{50} for MCs and MLCs in toxicity screening test with barley.

Plant Part	Summary Statistics	MCs and MLCs				
		TNT	2,4-DNT	2,4-DNAN	4-NAN	2-M-5-NYPNE
Shoot	NOAEC[a]	74.675±1.443	109.411±1.036	8.668±0.300	9.972±0.074	55.274±0.872
	p-value[b]	0.87	0.22	0.73	0.93	0.98
	LOAEC[c]	> 74.675±1.443	> 109.411±1.036	45.211±1.774	48.358±0.976	105.984±2.196
	p-value	ND[d]	ND	< 0.001	< 0.001	0.01
	EC_{50}[e]	> 74.675±1.443	> 109.411±1.036	26.156±4.200	47.098±3.813	>105.984±2.196
	95% CI[f]	ND	ND	17.874–34.430	39.577–54.619	ND
	Model[g]	Hormetic	Gompertz	Gompertz	Gompertz	Hormetic
Root	NOAEC	74.675±1.443	109.411±1.036	< 0.859±0.055	9.972±0.074	11.703±0.366
	p-value	0.95	0.96	ND	0.19	1.00
	LOAEC	> 74.675±1.443	> 109.411±1.036	0.859±0.055	48.358±0.976	55.274±0.872
	p-value	ND	ND	< 0.001	< 0.001	< 0.001
	EC_{50}	> 74.675±1.443	> 109.411±1.036	0.916±0.492	15.135±4.768	46.736±13.266
	95% CI	ND	ND	-0.054–1.887	5.730–24.540	20.556–72.916
	Model	Hormetic	Gompertz	Gompertz	Gompertz	Gompertz

[a] No–Observed–Adverse–Effect–Concentration in mg L^{-1} (measured): mean ± standard error of the mean (SEM)
[b] A p-value ≤ 0.05 was accepted as significant
[c] Lowest–Observed–Adverse–Effect–Concentration in mg L^{-1} (measured): mean ± SEM
[d] Not determinable
[e] Effect Concentration (mg L^{-1}) producing a 50% effect relative to carrier control ± SEM
[f] 95 % Confidence Interval (mg L^{-1})
[g] Defined in Eq. (2-2) and Eq. (2-3). Fitted to toxicity screening results for the determination of EC_{50}

2.3.3 Uptake Assays

Measured exposure concentrations in the uptake assays are shown in Fig. 2-4. The fluctuations in these concentrations over time were not different from the mean concentration at the 5% level of statistical significance for any of the compounds except TNT (Table A-4 in Appendix A), which reached a steady concentration at the third week of exposure. These significant TNT fluctuations were not the result of a failure of the daily replenishment protocol. They were already observed in the solution added to the pots as seen in Fig. 2-4, where the concentrations in the solution added follow the same trend as those of the displaced solutions. Nevertheless, the TNT exposure concentrations eventually stabilized in week 3 when the BCF was determined.

With the use of sand as the solid growth medium and daily replenishment of the exposure solution, overnight degradation of the MCs and MLCs in the growth medium never exceeded 11% during the uptake assays. Also, there was no significant sorption of these compounds by sand (Table A-5 in Appendix A). Therefore, it was possible to maintain approximately constant exposure concentrations throughout the time tested. The assurance of a nearly constant exposure is one of the advantages and improvements of this experimental protocol as it reduces the uncertainty in BCFs caused by the transformation/degradation of the parent compound in the growth medium. These processes lead to non–constant exposures in uptake experiments with soils where endpoint concentrations of TNT and 2,4-DNT have been shown to be below detection limits or only 20 to 50% of the initial soil concentrations [20,25,28], and even in carrier controls (i.e., without plants added) or during preliminary soil

incubation periods TNT and 2,4-DNT concentrations have been observed to decrease by 20 to 80% in less than a month [20,25,28].

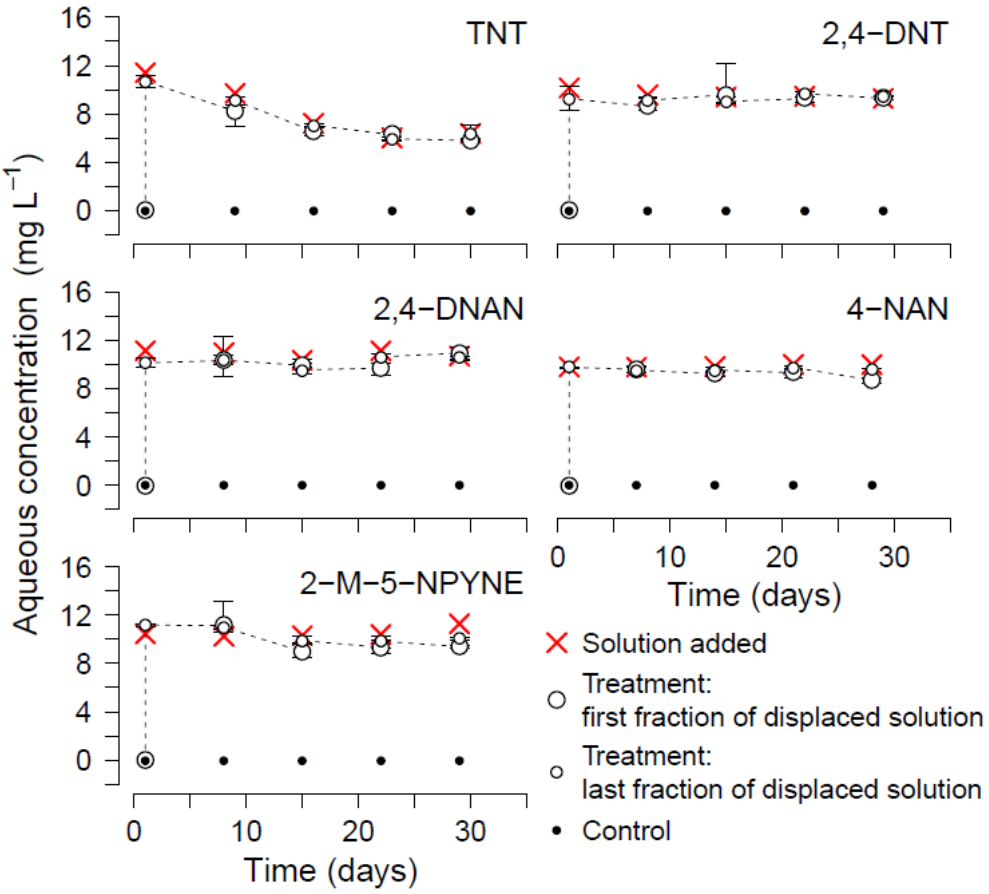

Figure 2-4 Exposure concentrations over time for MCs and MLCs in uptake assays with barley. Legend: Solution added is the aqueous solution sampled just before being loaded into plant pots; Treatment are samples from displaced solutions of pots exposed to MCs or MLCs; first and last fraction of displaced solution refer to the first and last pore volume replenished daily; Control are samples from displaced solutions of untreated plant pots (not exposed to MCs or MLCs). Displaying 2nd trial for 2,4-DNAN and 1st trial for 4-NAN. Data presented as means and error bars represent the range. If not visible, error bars are smaller than the symbol.

The ratios of concentration in the plant to concentration in the interstitial water, $\frac{C_{i_{Plant}}}{C_{i_{IW}}}$, for MCs and MLCs versus time of exposure are shown in Fig. 2-5. These values did not vary significantly with time of exposure for any of the compounds except 4-NAN (Table A-6 in Appendix A). However, steady state values were reached after three weeks of constant exposure for all compounds including 4-NAN (1st trial, Table A-6 in Appendix A). Therefore, steady state log BCFs were calculated with the values from week 3 and 4 (Fig. 2-5 and Table A-7 in Appendix A), using Eq. (2-1): log (BCF) ± standard error of the mean (SEM) = 0.618±0.017, 0.698±0.032, 1.300±0.057, 0.515±0.027, and 0.403±0.052 L kg_{dwt}^{-1} for TNT; 2,4-DNT; 2,4-DNAN; 4-NAN; and 2-M-5-NPYNE, respectively. The log BCFs results for TNT and 2,4-DNT are larger or on the higher end relative to the log BCF_{Solids} reported by Best et al. [17] and Sunahara [20] for perennial ryegrass (*Lolium perenne*), a plant species closely related to barley, which range from 0.04 to 0.23 and from -0.15 to 0.88 for TNT metabolites (TNT reported as not detected in plant material) and 2,4-DNT, respectively. This is perhaps due to both the uncertainty of whether the BCF_{Solids} were steady state values and the reduced availability of the compounds for plant uptake in the soil exposures relative to that in the sand medium. No plant BCF or BCF_{Solids} values were found in the literature for 2,4-DNAN; 4-NAN; or 2-M-5-NPYNE.

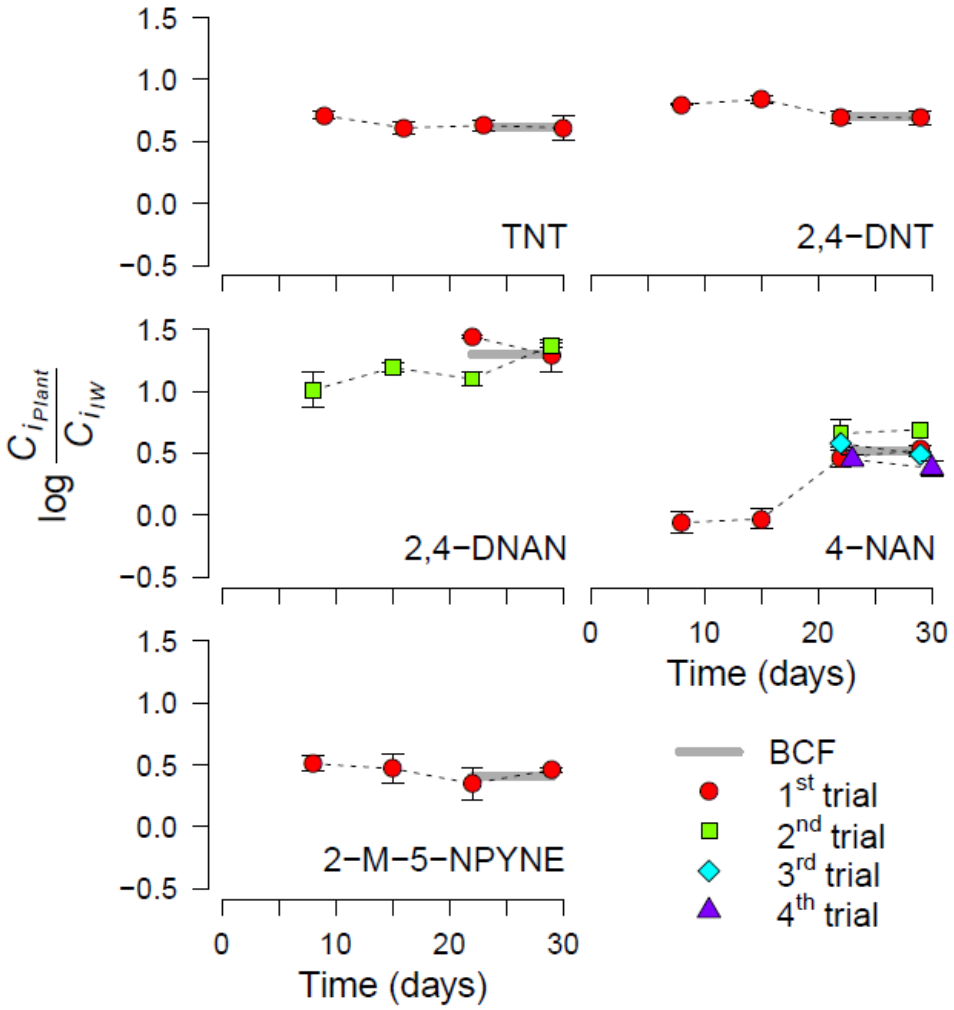

Figure 2-5 Logarithmic ratios of concentration in the plant to concentration in the interstitial water $\left(\log\frac{C_{i_{Plant}}}{C_{i_{IW}}}\right)$ versus time of exposure for MCs and MLCs in uptake assays with barley. $C_{i_{Plant}}$: concentration of compound i in barley (mg kg_{dwt}^{-1}), $C_{i_{IW}}$: concentration of compound i in the interstitial water - displaced solution (mg L^{-1}). BCF: steady state bioconcentration factor (L kg_{dwt}^{-1}). Trials refer to repetitions of a particular uptake assay. Data presented as means ± standard error of the mean (SEM). If not visible, error bars smaller than the symbol.

Reproducible BCFs were obtained for both of the compounds tested for more than one trial: 2,4-DNAN and 4-NAN (Fig. 2-5 and Table A-7 in Appendix A). Differences in log BCF values among trials for 2,4-DNAN and 4-NAN were not statistically significant (p-value = 0.13 and 0.08, respectively). No trend was observed in log BCF as a function of the compound being a MC or a MLC. Biomass profiles showed a stable behavior throughout the uptake assays for all compounds (Fig. A-4 in Appendix A).

2.3.4 Plant–Water Partitioning vs. Uptake

Plant–water partitioning experiments were performed to obtain the plant-water partition coefficients for MCs and MLCs. In order to establish the exposure time necessary to reach steady state, a kinetic sorption experiment was conducted using 4-NAN to confirm that 24 h was sufficient time to achieve steady state concentrations, as shown in previous work [41,54]. The result showed no statistically significant difference in the log plant-water partition coefficient (log K_{PW}) between 24, 48, and 144 h contact times (p-value = 0.18; Table A-8 in Appendix A). Therefore, 24 h contact time was used in the plant–water partitioning experiments. Differences in log K_{PW} between experiments performed at a low and high initial MC or MLC concentration were not statistically significant at the 5% level for any of the compounds (Table A-9 in Appendix A).

The K_{PW} values for MCs and MLCs with barley are shown in Fig. 2-6. K_{PW} values were calculated as the concentration in the plant (mg $kg_{plant\ dwt}^{-1}$) divided by the concentration in the water phase (mg L^{-1}), both measured at the end of the 24 h equilibration period (Table A-10 in Appendix A). Experimental octanol–water partition coefficients (K_{OW}) are also displayed in Fig. 2-6 as a reference. All MCs,

except HMX, and 4-NAN had a median log K_{PW} value between 1.180 and 1.520 L kg_{dwt}^{-1} showing similar partition affinity for barley biomass to that of undissociated polar aromatic/cyclic compounds including o-chlorophenol and 2,4-dichlorophenol for rice shoots biomass ($1.08 < \log K_{PW} < 1.68$ L kg_{dwt}^{-1}) [22], while being low relative to those of nonpolar aromatic/cyclic compounds such as 1,2-dichlorobenzene and lindane for plant biomass of grasses belonging to the same family as barley ($2.32 < \log K_{PW} < 4.58$ L kg_{dwt}^{-1}) [41,42]. Median log K_{PW} values for 2,5-DM-4-NANE, HMX, and 2-M-5-NPYNE were even lower: 0.795, 0.830, 0.960 L kg_{dwt}^{-1}, respectively. No bias in log K_{PW} was observed due to the compound being either a MC or MLC.

Overall, the range of K_{PW} values for the eight compounds evaluated spans only approximately one order of magnitude (Fig. 2-6) despite the differences expected at least for the nitramine MCs (HMX and RDX) given their low affinities for organic phases relative to the aqueous phase (log K_{OW} = 0.16 and 0.87 values for HMX and RDX, respectively – Table 2-1). In fact, there is no apparent relationship between log K_{PW} and log K_{OW}. This suggests barley biomass components have solvation properties that are quite different than those commonly accounted for using lipid surrogates like octanol, something that has also been proposed in published sorption experiments of aromatic contaminants by grasses [41,43].

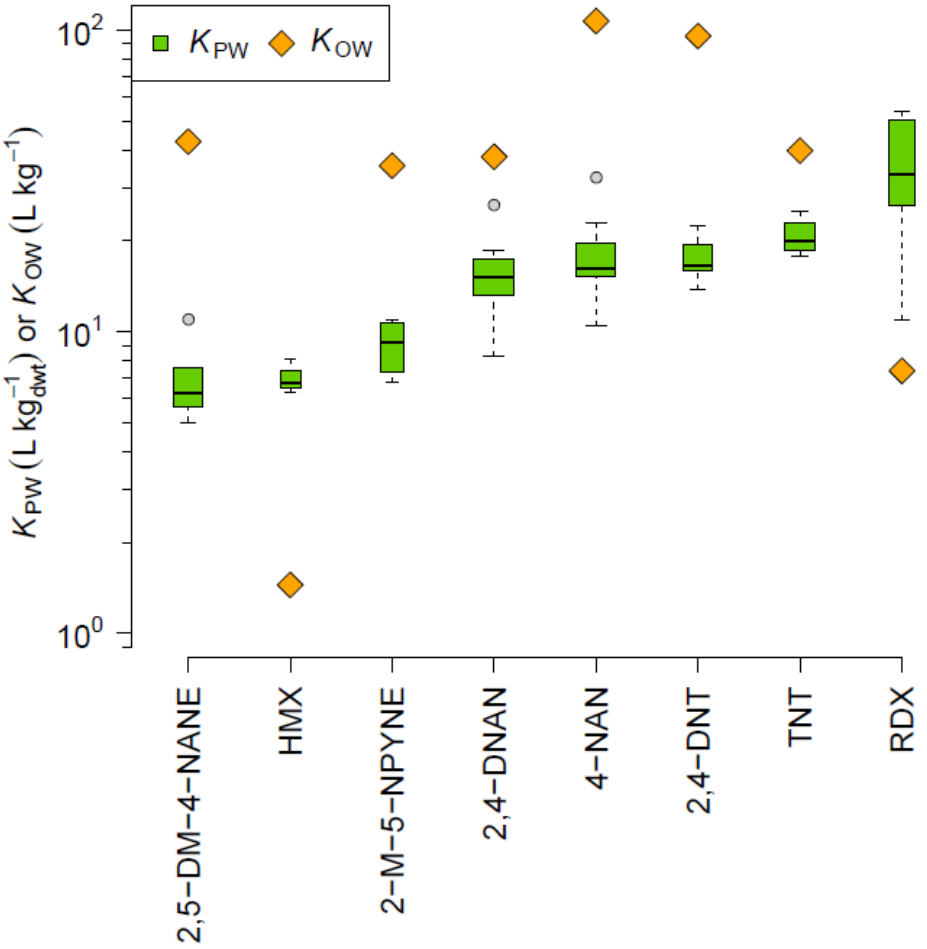

Figure 2-6 Plant-water partition coefficients (K_{PW}) for MCs and MLCs with barley and their respective octanol-water partition coefficients (K_{OW}). Data ordered by K_{PW}. K_{OW} values are experimental data obtained from EPI Suite database [44] for all compounds except 2,4-DNAN that was reported by Hawari et al. [45] and 2,5-DM-4-NANE that was an estimate from EPI Suite [44] in absence of an experimental value. Box width proportional to the square-root of the number of observations in the group.

The extent to which the bioconcentration of nitroaromatic MCs and MLCs, as measured by log BCFs, is related to their plant–water partitioning is illustrated in Fig. 2-7. Absolute differences between the median values of the log K_{PW} and log BCF were

between 0.190 and 0.690, with the BCF in most cases smaller than K_{PW}. These relatively small differences indicate that simple partition between the barley biomass and aqueous phase largely reflects the extent to which these compounds bioconcentrate in the plant. Studies have reported similar observations for uptake of compounds including toluene, hexachlorobenzene, and perfluorooctane sulfonate (PFOS) by several plant species, showing the "kinetic uptake limit" or maximum concentration in the plant to be predicted satisfactorily using the equilibrium sorption of the solute by the plant [42,54,61].

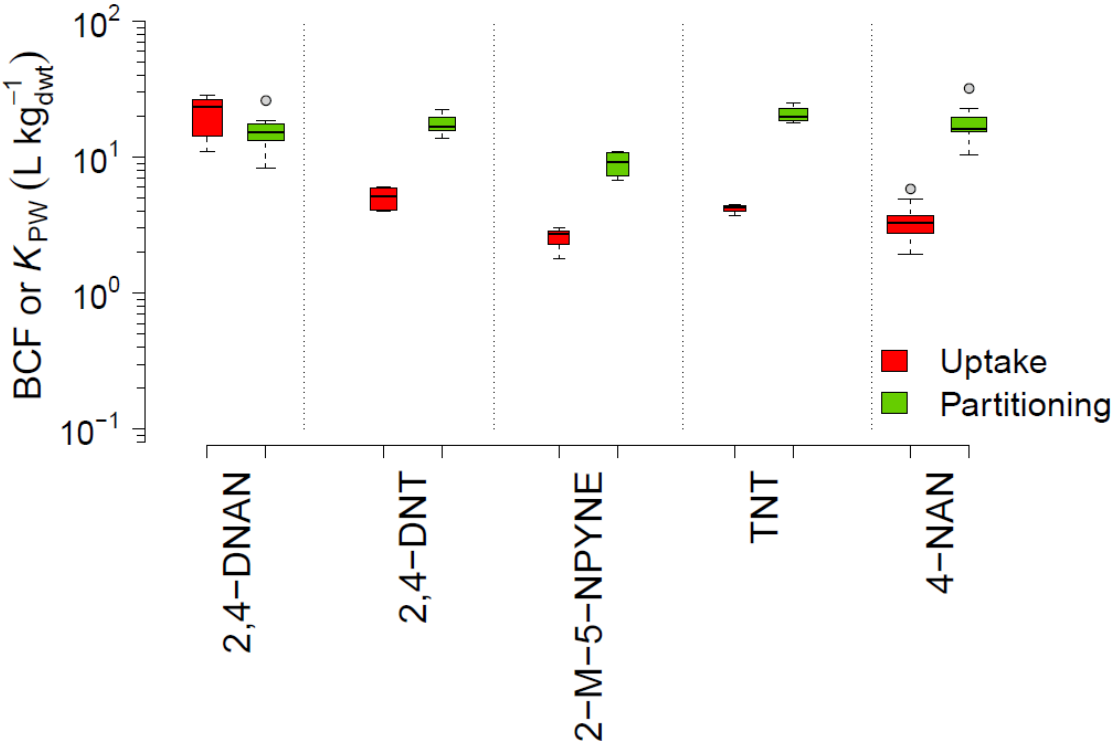

Figure 2-7 Comparison between uptake (as measured by BCF) and plant-water partition coefficient (K_{PW}) for MCs and MLCs. Compounds ordered from small to larger discrepancy between log K_{PW} and log BCF. Box width proportional to the square-root of the number of observations in the group.

The differences between K_{PW} and BCF could be due to the compounds being transformed and/or metabolized within the plant. Evidence of the transformation of TNT; 2,4-DNT; and 2,4-DNAN in the interior of grasses and related plants species, for example, has been reported [20,30,62-65]. Of the three compounds, TNT has been shown to be so readily biotransformed in plants that often only its transformation products have been observed in plant shoots [17,20,32]. In contrast, 2,4-DNT and 2,4-DNAN and their metabolites have been observed in various plant tissues [20,30,65]. It is worth noting, however, that 2,4-DNAN has not been studied as extensively as TNT or 2,4-DNT since it has not been as widely utilized due to its novelty as a MC [66].

In order to provide a quantitative analysis for the extent to which the transformation/degradation of the compounds within the plant can explain the differences found between K_{PW} and BCF, degradation rates ($k_{degradation}$) were estimated for TNT; 2,4-DNT; and 2,4-DNAN by fitting an exponential decay model to a time course dataset of concentrations in perennial ryegrass (*L. perenne*) observed during soil uptake assays by Sunahara [20] and Dodard et al. [30] (Table A-11 and Fig. A-5 in Appendix A). No time course data were found for 2-M-5-NPYNE or 4-NAN. While the estimated $k_{degradation}$ values are not the result of degradation processes occurring exclusively within the plant tissues, but also account for those taking place in the soil, they do indicate how susceptible to degradation/transformation each compound is relative to the other MCs. The estimated $k_{degradation}$ values were: 0.066, 0.083, 0.189 d^{-1} for 2,4-DNAN; 2,4-DNT; and TNT, respectively. This increasing sequence is in agreement with that of the discrepancies found between K_{PW} and BCF for these compounds as shown in Fig. 2-8, a comparison of the $k_{degradation}$ to $\frac{K_{PW}}{BCF}$, the ratio of

plant-water partitioning to uptake. The increase in $\frac{K_{PW}}{BCF}$ is matched by the increase in $k_{degradation}$ suggesting that degradation is causing the difference between BCF and K_{PW}.

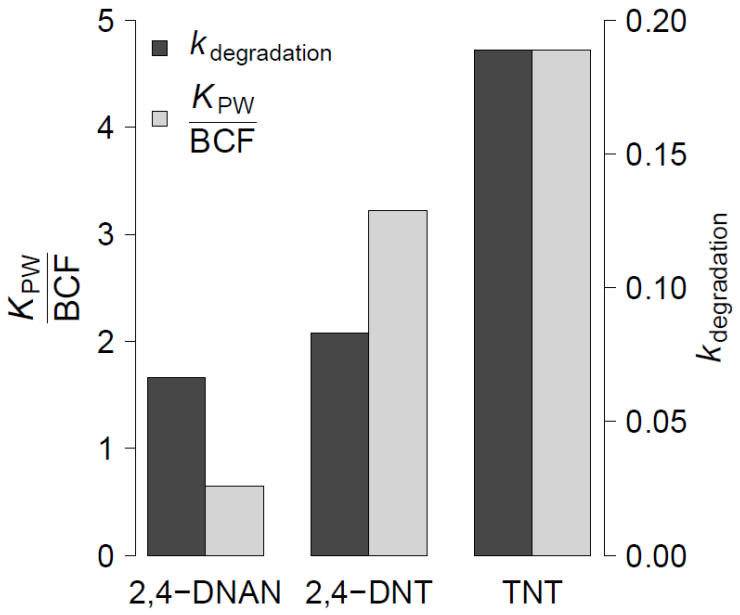

Figure 2-8 Comparison between the ratios of plant-water partitioning to uptake $\left(\frac{K_{PW}}{BCF}\right)$ and estimated degradation/transformation rates ($k_{degradation}$) for MCs.

2.4 Conclusions

Reproducible steady state bioconcentration factors for MCs and MLCs in barley can be generated using coarse quartz sand as the solid growth medium with daily replenishment of the exposure solution. The use of a solid growth medium like sand also provides for normal development of plant roots.

Even though plants are complex organisms, simple plant-water partition coefficients are able to estimate the BCFs of the tested compounds with a difference between log K_{PW} and log BCF of 0.2 to 0.7 log units. The plant-water partition

coefficients, therefore, can be used as the upper-bounds for the bioconcentration of these compounds in barley.

The fact that no particular difference between MCs and MLCs was observed in neither BCFs nor K_{PW} values, indicates that the estimation of upper-bounds for the uptake process using plant-water partition coefficients is also applicable to compounds with particular functionalities like those in the MLCs, including methoxy ($O\text{-}CH_3$) and amino ($\text{-}NH_2$) groups (Table 2-1). Although according to the findings in this work, the evaluated MCs and MLCs have rather low plant uptake upper-bounds, as measured by K_{PW}, relative to other nonpolar aromatic/cyclic contaminants, they can bioconcentrate in barley and thus constitute a risk for ecological receptors and point to the potential for transference to higher trophic levels from plants. A quantitative model for the prediction of partitioning and BCFs for MCs and other compounds is presented in the following chapter.

REFERENCES

This list includes references cited in Appendix A.

1. Simini M, Wentsel RS, Checkai RT, Phillips CT, Chester NA, Major MA, Amos JC. Evaluation of soil toxicity at joliet army ammunition plant. *Environ Toxicol Chem*. 1995;14(4):623-630.

2. Jenkins TF, Hewitt AD, Grant CL, Thiboutot S, Ampleman G, Walsh ME, Ranney TA, Ramsey CA, Palazzo AJ, Pennington JC. Identity and distribution of residues of energetic compounds at army live-fire training ranges. *Chemosphere*. 2006;63(8):1280-1290.

3. Walsh ME, Ramsey CA, Taylor S, Hewitt AD, Bjella K, Collins CM. Subsampling variance for 2,4-DNT in firing point soils. *Soil Sed Contam*. 2007;16(5):459-472.

4. Walsh MR, Walsh ME, Hewitt AD. Energetic residues from field disposal of gun propellants. *J Hazard Mater*. 2010;173(1–3):115-122.

5. Taylor S, Bigl S, Packer B. Condition of *in situ* unexploded ordnance. *Sci Total Environ*. 2015;505:762-769.

6. Spalding RF, Fulton JW. Groundwater munition residues and nitrate near Grand Island, Nebraska, U.S.A. *J Contam Hydrol*. 1988;2(2):139-153.

7. Best EPH, Sprecher SL, Larson SL, Fredrickson HL, Bader DF. Environmental behavior of explosives in groundwater from the Milan Army Ammunition Plant in aquatic and wetland plant treatments. Uptake and fate of TNT and RDX in plants. *Chemosphere*. 1999;39(12):2057-2072.

8. Best EPH, Sprecher SL, Larson SL, Fredrickson HL, Bader DF. Environmental behavior of explosives in groundwater in groundwater from the Milan Army Ammunition Plant in aquatic and wetland plant treatments. Removal, mass balances and fate in groundwater of TNT and RDX. *Chemosphere*. 1999;38(14):3383-3396.

9. Spiegel K, Headley JV, Peru KM, Haidar N, Gurprasard NP. Residues of explosives in groundwater leached from soils at a military site in Eastern Germany. *Commun Soil Sci Plant Anal*. 2005;36(1-3):133-153.

10. Weeks KR, Veenstra SC, Hill DL. Bioremediation of perchlorate and explosives in groundwater. In: Calabrese EJ, Kostecki PT, Dragun J, eds. *Contaminated Soils, Sediment and Water: Science in the Real World.* New York, NY: Springer US. 2005;9:123-134.

11. Amaral HIF, Fernandes J, Berg M, Schwarzenbach RP, Kipfer R. Assessing TNT and DNT groundwater contamination by compound-specific isotope analysis and ^{3}H–^{3}He groundwater dating: A case study in Portugal. *Chemosphere*. 2009;77(6):805-812.

12. Clausen JL, Korte N. Fate and transport of energetics from surface soils to groundwater. In: Chappell MA, Price CL, George RD, eds. Envir*onmental Chemistry of Explosives and Propellant Compounds in Soils and Marine Systems: Distributed Source Characterization and Remedial Technologies*. Washington, D.C: American Chemical Society. 2011;1069:273-316.

13. Talmage SS, Opresko DM, Maxwell CJ, Welsh CJE, Cretella FM, Reno PH, Daniel FB. Nitroaromatic munition compounds: Environmental effects and screening values. In: Ware GW, ed. *Reviews of Environmental Contamination and Toxicology*. New York, NY: Springer US. 1999;161:1-156.

14. Ampleman G, Thiboutot S, Lewis J, Marois A, Gagnon A, Bouchard M, Jenkins T, Ranney TA, Pennington JC. Evaluation of the contamination by explosives and metals in soils, vegetation, surface water and sediment at Cold Lake Air Weapons Range (CLAWR), Alberta, Phase II Final report. Technical Report No. DRDC-Valcartier-TR-2004-204. Valcartier, Québec, Canada: Defence Research and Development Canada - Valcartier, Valcartier QUE (CAN); Cold Regions Research and Engineering Lab, Hanover NH (US). 2004;1-116.

15. McKone TE, Maddalena RL. Plant uptake of organic pollutants from soil: Bioconcentration estimates based on models and experiments. *Environ Toxicol Chem*. 2007;26(12):2494-2504.

16. Best EPH, Geter KN, Tatem HE, Lane BK. Effects, transfer, and fate of RDX from aged soil in plants and worms. *Chemosphere*. 2006;62(4):616-625.

17. Best EPH, Tatem HE, Geter KN, Wells ML, Lane BK. Effects, uptake, and fate of 2,4,6-trinitrotoluene aged in soil in plants and worms. *Environ Toxicol Chem*. 2008;27(12):2539-2547.

18. Kobayashi T, Navarro RR, Tatsumi K, Iimura Y. Influence of compost amendment on pyrene availability from artificially spiked soil to two subspecies of *Cucurbita pepo*. *Sci Total Environ*. 2008;404(1):1-9.

19. Rocheleau S, Lachance B, Kuperman RG, Hawari J, Thiboutot S, Ampleman G, Sunahara GI. Toxicity and uptake of cyclic nitramine explosives in ryegrass *Lolium perenne*. *Environ Pollut*. 2008;156(1):199-206.

20. Sunahara GI. Development of toxicity benchmarks and bioaccumulation data for N-based organic explosives for terrestrial plants and soil invertebrates. Final Report No. SERDP ER-1416. Québec, Canada: National Research Council of Canada Montreal (Québec) Biotechnology Research Institute. 2012;1-289.

21. Li H, Sheng G, Sheng W, Xu O. Uptake of trifluralin and lindane from water by ryegrass. *Chemosphere*. 2002;48(3):335-341.

22. Su Y, Zhu Y, Liang Y. Interactions of mixed organic contaminants in uptake by rice seedlings. *Chemosphere*. 2009;74(7):890-895.

23. Cunningham SD, Anderson TA, Schwab AP, Hsu FC. Phytoremediation of soils contaminated with organic pollutants. In: Sparks DL, ed. *Advances in agronomy*. San Diego, CA: Academic Press. 1996;56:55-114.

24. Collins C, Fryer M, Grosso A. Plant uptake of non-ionic organic chemicals. *Environ Sci Technol*. 2006;40(1):45-52.

25. Pennington JC. Plant uptake of 2,4,6-trinitrotoluene, 4-amino-2,6-dinitrotoluene, and 2-amino- 4,6-dinitrotoluene using ^{14}C-labeled and unlabeled compounds. Technical Report No. EL-88-20. Vicksburg, MS: U,S. Army Waterways Experiment Station, Corps of Engineers. 1988;1-68.

26. Groom CA, Halasz A, Paquet L, Morris N, Olivier L, Dubois C, Hawari J. Accumulation of HMX (octahydro-1,3,5,7-tetranitro-1,3,5,7-tetrazocine) in indigenous and agricultural plants grown in HMX-contaminated anti-tank firing-range soil. *Environ Sci Technol*. 2002;36(1):112-118.

27. Price RA, Pennington JC, Larson SL, Neumann D, Hayes CA. Uptake of RDX and TNT by agronomic plants. *Soil Sediment Contam*. 2002;11(3):307-326.

28. Duringer JM, Craig AM, Smith DJ, Chaney RL. Uptake and transformation of soil [^{14}C]-trinitrotoluene by cool-season grasses. *Environ Sci Technol*. 2010;44(16):6325-6330.

29. Chen D, Liu ZL, Banwart W. Concentration-dependent RDX uptake and remediation by crop plants. *Environ Sci Pollut Res*. 2011;18(6):908-917.

30. Dodard SG, Sarrazin M, Hawari J, Paquet L, Ampleman G, Thiboutot S, Sunahara GI. Ecotoxicological assessment of a high energetic and insensitive munitions compound: 2,4-dinitroanisole (DNAN). *J Hazard Mater*. 2013;262:143-150.

31. Hannink NK, Rosser SJ, Bruce NC. Phytoremediation of explosives. *Crit Rev Plant Sci*. 2002;21(5):511-538.

32. Panz K, Miksch K. Phytoremediation of explosives (TNT, RDX, HMX) by wild-type and transgenic plants. *J Environ Manage*. 2012;113:85-92.

33. Scheidemann P, Klunk A, Sens C, Werner D. Species dependent uptake and tolerance of nitroaromatic compounds by higher plants. *J Plant Physiol*. 1998;152(2-3):242-247.

34. Pennington JC, Myers TE, Davis WM, Olin TJ, McDonald TA, Hayes CA, Townsend DM. Impacts of sorption on *in situ* bioremediation of explosives-contaminated soils. Technical Report No. IRRP-95-1. Vicksburg, MS: U,S. Army Waterways Experiment Station, Corps of Engineers. 1995;1-54.

35. Larson SL, Martin WA, Escalon BL, Thompson M. Dissolution, sorption, and kinetics involved in systems containing explosives, water, and soil. *Environ Sci Technol*. 2007;42(3):786-792.

36. Berthelot Y, Valton É, Auroy A, Trottier B, Robidoux PY. Integration of toxicological and chemical tools to assess the bioavailability of metals and energetic compounds in contaminated soils. *Chemosphere*. 2008;74(1):166-177.

37. Savard K, Sarrazin M, Dodard SG, Monteil-Rivera F, Kuperman RG, Hawari J, Sunahara GI. Role of soil interstitial water in the accumulation of hexahydro-1,3,5-trinitro-1,3,5-triazine in the earthworm *Eisenia andrei*. *Environ Toxicol Chem*. 2010;29(4):998-1005.

38. Kalderis D, Juhasz AL, Boopathy R, Comfort S. Soils contaminated with explosives: Environmental fate and evaluation of state-of-the-art remediation processes (IUPAC technical report). *Pure Appl Chem*. 2011;83(7):1407-1484.

39. Crush JR, Care DA, Gourdin A, Woodfield DR. Root growth media effects on root morphology and architecture in white clover. *New Zea J Agric Res*. 2005;48(2):255-263.

40. Lin Y, Allen HE, Di Toro DM. Barley root hair growth and morphology in soil, sand, and water solution media and relationship with nickel toxicity. *Environ Toxicol Chem*. 2016; 35(8): 2125-2133.

41. Barbour JP, Smith JA, Chiou CT. Sorption of aromatic organic pollutants to grasses from water. *Environ Sci Technol*. 2005;39(21):8369-8373.

42. Li H, Sheng G, Chiou CT, Xu O. Relation of organic contaminant equilibrium sorption and kinetic uptake in plants. *Environ Sci Technol*. 2005;39(13):4864-4870.

43. Chiou CT, Sheng G, Manes M. A partition-limited model for the plant uptake of organic contaminants from soil and water. *Environ Sci Technol*. 2001;35(7):1437-1444.

44. US Environmental Protection Agency. Estimation Programs Interface (EPI) Suite™ for Microsoft® Windows, v. 4.11. Washington, D.C: US EPA. 2012.

45. Hawari J, Monteil-Rivera F, Perreault NN, Halasz A, Paquet L, Radovic-Hrapovic Z, Deschamps S, Thiboutot S, Ampleman G. Environmental fate of 2,4-dinitroanisole (DNAN) and its reduced products. *Chemosphere*. 2015;119:16-23.

46. Food and Agriculture Organization of the United Nations. FAO Statistical Database (FAOSTAT) Web site. http://faostat3.fao.org/compare/E. Accessed October, 2015.

47. US Environmental Protection Agency. OCSPP 850.4800: Plant uptake and translocation test. In: *Ecological effects test guidelines EPA 712-C-002.* Office of chemical safety and pollution prevention. Washington, D.C: US EPA. 2012.

48. American Society for Testing and Materials. E1963 − 09: Standard guide for conducting terrestrial plant toxicity tests. West Conshohocken, PA: ASTM International. 2014.

49. Nielson AB, Reid EH. Use of vegetation in military construction. *J Soil Water Conserv*. 1948;3(3):113-118.

50. Abdul-Baki AA. Hypochlorite and tissue sterilization. *Planta*. 1974;115(4):373-376.

51. Cheng T, Allen HE. Prediction of uptake of copper from solution by lettuce (*Lactuca sativa* Romance). *Environ Toxicol Chem*. 2001;20(11):2544-2551.

52. Organisation for Economic Co-operation and Development. Test No. 208: Terrestrial plant test: Seedling emergence and seedling growth test. In: *OECD guidelines for the testing of chemicals, Section 2.* Paris, France: OECD Publishing. 2006.

53. Chang M, Wang M, Kuo DTF, Shih Y. Sorption of selected aromatic compounds by vegetables. *Ecol Eng*. 2013;61, Part A:74-81.

54. US Environmental Protection Agency. Method 8330B: Nitroaromatics, nitramines, and nitrate esters by high performance liquid chromatography (HPLC). In: *Test methods for evaluating solid waste, physical/chemical methods (SW-846).*Washington, D.C: Office of solid waste and emergency response. 2006.

55. Rocheleau S, Kuperman RG, Simini M, Hawari J, Checkai RT, Thiboutot S, Ampleman G, Sunahara GI. Toxicity of 2,4-dinitrotoluene to terrestrial plants in natural soils. *Sci Total Environ*. 2010;408(16):3193-3199.

56. Kuperman RG, Checkai RT, Simini M, Phillips CT, Kolakowski JE, Lanno R. Soil properties affect the toxicities of 2,4,6-trinitrotoluene (TNT) and hexahydro-1,3,5-trinitro-1,3,5-triazine (RDX) to the enchytraeid worm *Enchytraeus crypticus*. *Environ Toxicol Chem*. 2013;32(11):2648-2659.

57. Calabrese EJ, Baldwin LA, Holland CD. Hormesis: A highly generalizable and reproducible phenomenon with important implications for risk assessment. *Risk Anal*. 1999;19(2):261-281.

58. R Development Core Team. R: A language and environment for statistical computing, v.3.2.0. Vienna, Austria: R Foundation for Statistical Computing. 2015.

59. Esteve-Nunez A, Caballero A, Ramos JL. Biological degradation of 2,4,6-trinitrotoluene. *Microbiol Mol Biol Rev*. 2001;65(3):335-352.

60. Zhao HX, Guan Y, Zhang GL, Zhang Z, Tan F, Quan X, Chen JW. Uptake of perfluorooctane sulfonate (PFOS) by wheat (*Triticum aestivum* L.) plant. *Chemosphere*. 2013;91(2):139-144.

61. Palazzo AJ, Leggett DC. Effect and disposition of TNT in a terrestrial plant. *J Environ Qual*. 1986;15(1):49-52.

62. Gorge E, Brandt S, Werner D. Uptake and metabolism of 2,4,6-trinitrotoluene in higher plants. *Environ Sci Pollut Res*. 1994;1(4):229-233.

63. Nepovim A, Hebner A, Soudek P, Gerth A, Thomas H, Smrcek S, Vanek T. Degradation of 2,4,6-trinitrotoluene by selected helophytes. *Chemosphere*. 2005;60(10):1454-1461.

64. Yoon JM, Oliver DJ, Shanks JV. Phytotransformation of 2,4-dinitrotoluene in *Arabidopsis thaliana*: Toxicity, fate, and gene expression studies in vitro. *Biotechnol Prog*. 2006;22(6):1524-1531.

65. Richard T, Weidhaas J. Dissolution, sorption, and phytoremediation of IMX-101 explosive formulation constituents: 2,4-dinitroanisole (DNAN), 3-nitro-1,2,4-triazol-5-one (NTO), and nitroguanidine. *J Hazard Mater*. 2014;280:561-569.

Chapter 3

PREDICTING PLANT–SOIL BIOCONCENTRATION OF MUNITIONS COMPOUNDS FROM MOLECULAR STRUCTURE

3.1 Introduction

Munitions compounds (MCs) are widely used in commercial and military activities, and are often released into the environment [1-3]. As a result, organisms such as plants growing in the soils at military ranges and surrounding locations are exposed and are likely to bioconcentrate MCs. This causes concerns regarding the potential for environmental risk due to both the direct ecological toxicity and the transference of these compounds to higher trophic levels. Hence the need for modeling tools to estimate the extent of bioconcentration to be expected.

Studies proposing models to predict bioconcentration of organic compounds in plants from various growth media have been published [4-11]. Some of these models account for transformation and degradation of the parent compound within the plant (e.g., metabolism, photodegradation), volatilization from leaves, and plant physiological processes such as growth and water transpiration [7,11]. However, in order to be applied to a specific compound, these models require parameter estimates that quantify each of these mechanisms for that compound. This limits their general applicability.

Models have also been formulated assuming that the plant–root uptake of nonionic organic compounds is a passive diffusive process (i.e., no input of metabolic energy) for which the upper–bound of the plant concentration can be predicted [10,12]. This type of uptake is driven by concentration gradients between the plant and the

external phase(s) where the organic compound is present (e.g., soil), and it operates through the plant transpiration stream [4,5,13]. In this way, the process can be described as partition–dominated steady state between the soil solids, soil solution (interstitial water), and plant. It is governed by the bioavailable concentration of the compound in the growth medium and its tendency to sorb to plant tissues.

The concentration of an organic compound available for plant-root uptake in soils is that freely dissolved in the interstitial water [14,15]. This concentration is the result of soil solid-soil interstitial water adsorption-desorption and is largely controlled by soil properties such as content of organic carbon and clay size particles [16-20]. For MCs, organic carbon plays a dominant role relative to clay size particles in soils with organic carbon content > ≈ 2%, as concluded by Miglino [21]. The ratio of the concentration of an organic compound between soil organic carbon and the aqueous phase is expressed quantitatively as a partition coefficient, K_{OC}. These coefficients are most commonly estimated with single-parameter quantitative structure-activity relationships (QSARs) that are developed using a log-log correlation of K_{OC} with the octanol–water partition coefficient (K_{OW}). This assumes that n-octanol is a good surrogate for soil organic carbon [22,23]. While these QSARs have been shown to work reasonably well in predicting K_{OC} for mostly nonpolar hydrophobic organic chemicals [24], they have failed for more polar compounds, compounds that interact by hydrogen-bonding, and for highly hydrophobic compounds [25-27]. Consequently, a need for comprehensive models of K_{OC} that perform well for a wide range of compound classes has been identified [28].

Steady state sorption of organic contaminants by plant tissue components, such as carbohydrates and lipids, has also been measured and modeled [29-31]. The majority of

these partition coefficients refer to sorption by lipids rather than other plant components. Since many organic contaminants of concern are lipophilic, their capacity to dissolve in more polar phases like carbohydrates is far less than that in lipids [30,31]. Similarly to the estimation methods for K_{OC}, n-octanol is commonly used as a surrogate to model sorption to plant lipids. While practical, this approach has not been able to fully characterize the interactions between organic compounds and plant tissues [12,29].

An alternative approach is to use a polyparameter linear free energy relationship (pp–LFER) model [32,33]. Unlike single-parameter K_{OW}-based predictions, pp–LFERs predict partitioning by explicitly considering the contributions from different types of chemical interactions (e.g., hydrogen bonding, van der Waals forces) between the solute and the condensed phase (e.g., soil organic carbon, plant lipids). Thus, pp–LFERs are able to more fully characterize the solvation properties of the condensed phase and the strength of its interactions with solutes relative to that of the aqueous phase.

In order to achieve these results, however, the estimation of pp–LFERs parameters require a significantly larger and more chemically diverse training dataset of partition coefficients than is needed for the single-parameter K_{OW}-based models. In the case of plants, the pp–LFERs require sufficient data to quantify both the solvation properties of a specific biomass component (e.g., lipids, carbohydrates, proteins) and the molecular properties of the organic contaminant of interest [9,31,34].

The purpose of this work is to predict the bioconcentration of MCs and compounds with similar chemical structural functionalities (Table B-1 in Appendix B), which are hereafter referred to as munition-like compounds (MLCs), in plants

based on the partitioning between soil solids, interstitial water, and plant. This is achieved using pp–LFERs for the prediction of K_{OC} to estimate the dissolved concentration in the growth medium, and, subsequently, the partitioning between water and plant cuticle, a lipid-like plant component, to estimate the sorption to plant tissue. This procedure is validated by predicting concentrations in plant biomass compiled from published uptake assays in an independent dataset (90 observations). The pp–LFER developed in this work uses only molecular structure to compute the required model parameters. Therefore, it can also be used to evaluate the bioconcentration potential for proposed compounds early in the development stage of new MCs.

3.2 Methodology

3.2.1 Polyparameter Linear Free Energy Relationship (pp–LFER) Models

The pp–LFER models for partitioning between soil organic carbon and water, and between plant cuticle and water used in this work are based on the Abraham polyparameter model [32]

$$\log K_{SW} = c + eE + sS + aA + bB + vV \qquad (3\text{-}1)$$

where K_{SW}, the dependent variable, is the partition coefficient between a solvation phase (e.g., organic carbon, plant cuticle) and water, and the independent variables, the right hand side of Eq. (3-1), are the parameters that account for the free energy contributions from different types of molecular interactions. The uppercase letters in Eq. (3-1) are solute (e.g., MC, MLC) descriptors and the lowercase letters quantify the complementary effect of the solvation phase on the corresponding interaction. The eE term represents the dispersion interactions that are predominant between nonpolar (no

permanent multipole moments) molecules. The sS term is the dipolarity/polarizability that arises from dipole-dipole and dipole-induced dipole interactions. The aA and bB terms account for the donation and acceptance of hydrogen bonds (where aA is solvent acceptor–solute donor and bB is solvent donor–solute acceptor). Hydrogen bonds are bonds between certain types of hydrogen atoms and highly electronegative atoms in polar molecules. Finally, vV accounts for the energy required for cavity formation, and c is a regression constant [32].

3.2.1.1 Plant Cuticle–Water pp–LFER

Using a multiple linear regression analysis (MLRA) and experimentally obtained solute descriptors (uppercase letters in Eq. (3-1)), Platts and Abraham [9] fitted a pp–LFER model to a dataset of plant cuticle–water partition coefficients, K_{Cut}, for tomato (*Lycopersicum esculentum* Mill) cuticle, for various volatile organic compounds (-0.77 < log K_{OW} < 6.25) yielding

$$\log K_{Cut} = -0.415 + 0.596E - 0.413S - 0.508A - 4.096B + 3.908V \quad (3\text{-}2)$$
$$62 \text{ compounds; } N = 62;\ R^2 = 0.981;\ SD = 0.236;\ F = 566$$

where K_{Cut} = plant cuticle–water partition coefficient ($L_{water}\ kg_{cuticle}^{-1}$), N = number of data points used to estimate the regression equation coefficients, R^2 = coefficient of determination, SD = regression standard deviation, and F = Fischer's F statistic.

The cuticle is an extracellular hydrophobic membrane composed of interconnected long-chain fatty acids and alkyls [35,36] that coats plant organs such as fruits, leaves, and stems [37], and protects and waterproofs the plant surface. According to Eq. (3-2), this hydrophobic membrane is more competitive for solutes than water through π- and n- electron pairs dispersion interactions ($e = 0.596 > 0$), and via cavity formation in the cuticle that requires much less free energy than in water ($v =$

$3.908 > 0$). This model also indicates that the cuticle is less polar/polarizable ($s = -0.413 < 0$) and accepts hydrogen bonds ($a = -0.508 < 0$) and donates hydrogen bonds ($b = -4.096 < 0$) much less readily than water [9].

In order to broaden the chemical and plant species diversity and to incorporate MCs and MLCs functionalities, such as aromatic compounds with multiple C-NO_2 groups and non-aromatic cyclic structures with N-NO_2 bonds (Table B-1 in Appendix B), into the training set used by Platts and Abraham [9], additional K_{Cut} data (Table B-2 in Appendix B) were collected and included in deriving the plant cuticle–water pp–LFER. Sources for these data are described below (Sec. 3.2.2.1).

The pp–LFER model of cuticle partitioning is the basis for the plant bioconcentration model developed below. Since new chemicals and new plant cuticle data were added to the dataset, it was necessary that the solute parameters (uppercase letters in Eq. (3-1)) be obtained from consistent sources. Therefore, solute descriptors were obtained from three sources: Absolv estimated Abraham Parameters (Absolv–AP) from the Absolv software module (part of ACD Labs proprietary ACD/PhysChem Suite [38]), Experimentally derived Abraham Parameters (Exp–AP), and Quantum Chemically estimated Abraham Parameters (QCAP) both from Liang [39] (Tables B-4 to B-6 in Appendix B). These three sources were selected because Absolv–AP have been widely used and are recommended by Platts and Abraham [9] for the estimation of descriptors for any organic structure, and Exp–AP and QCAP have been shown to successfully predict K_{SW} values for a wide variety of organic compounds including MCs and MLCs [39]. Three updated plant cuticle-water pp–LFERs were obtained using MLRA with each Absolv–AP, Exp–AP, and QCAP as the solute parameters and the

full K_{Cut} dataset as the independent variable. The MLRAs were performed using the `lm` function of the R software for statistical computing [40].

3.2.1.2 Soil Organic Carbon-Water pp–LFER

The K_{OC} that are used below (Sec. 3.2.3) were calculated using the pp–LFER model developed by Kipka and Di Toro [41]

$$\begin{aligned}\log K_{OC} = {} & 0.670\ (\pm 0.088) + 1.075\ (\pm 0.061)E - 0.277\ (\pm 0.083)S \\ & - 0.363\ (\pm 0.100)A - 1.697\ (\pm 0.085)B \\ & + 1.468\ (\pm 0.077)V \\ & 440 \text{ compounds};\ \mathrm{N} = 440;\ \mathrm{RMSE} = 0.48\end{aligned} \tag{3-3}$$

where K_{OC} = soil organic carbon–water partition coefficient ($L_{water}\ kg_{OC}^{-1}$), values in parenthesis = $\pm$ the standard error, and RMSE = root mean square error of prediction. This model was built with a large and chemically diverse dataset of nonionic organic compounds using Absolv–AP for the solute parameters. The solvent parameters reveal that the soil organic carbon phase has similar solvation capabilities to those shown by plant cuticle in Eq. (3-2). The solute descriptors used to apply this model were the appropriate QCAP reported by Liang [39] (Table B-8 in Appendix B).

3.2.2 Experimental Data

Two types of experimental data were collected from the literature: (i) reported K_{Cut} values, and (ii) measurements of concentrations in plant biomass made during uptake assays where plants were exposed to MCs, or MLCs, in the growth medium. The former dataset was added to the training set used by Platts and Abraham [9], while the latter served to validate the pp–LFER models.

3.2.2.1 Plant Cuticle–Water Partition Coefficients (K_{Cut}) Data

Partition coefficients between plant cuticle and water are commonly determined by individually equilibrating either isolated cuticular membranes (CM) or cuticle matrices (MX, the dewaxed CM) [37,42,43] with an aqueous solution of an organic compound (i) and calculating the cuticle partition coefficient

$$K_{i_{Cut}} = \frac{C_{i_{CM\ or\ MX}}}{C_{i_{Water}}} \tag{3-4}$$

where $C_{i_{CM\ or\ MX}}$ = concentration of compound i in CM or MX (mg kg_{dwt}^{-1}; dwt: dry weight), and $C_{i_{Water}}$ = concentration of compound i in the water phase (mg L^{-1}). The K_{Cut} dataset (Table B-2 in Appendix B) includes values obtained with CM or MX since the presence of wax in the cuticle component proved to have no significant effect on the resulting K_{Cut} (Table B-3 in Appendix B).

In addition to K_{Cut} from isolated plant cuticle components, values obtained from experiments performed with whole plant biomass were also included in the dataset after normalization of the plant–water partition coefficient by the mass fraction of plant cuticle

$$K_{i_{Cut}} = \frac{K_{i_{PW}}}{f_{Cut}} \tag{3-5}$$

where $K_{i_{PW}}$ = plant–water partition coefficient of compound i (L_{water} $kg_{dwt\ plant}^{-1}$) and f_{Cut} = dry weight fraction of cuticle in the plant ($kg_{cuticle}$ $kg_{dwt\ plant}^{-1}$). A total of 143 experimental K_{Cut} for undissociated organic compounds were compiled for the plant cuticle pp–LFER training set (Table B-2 in Appendix B). The plant species in the K_{Cut} dataset are, as reported in the sources: *Lycopersicum esculentum* Mill (*L. esculentum*); *Ficus elastica* Roxb. var. decora (*F. elastica*); *Capiscum annuum* L. (*C. annuum*); *Citrus aurantium* L. (*C. aurantium*); *Prunus laurocerasus* L. (*P. laurocerasus*);

Ginkgo biloba L. (*G. biloba*); *Juglans regia* L. (*J. regia*:); *Solanum lycopersicum* (*S. lycopersicum*); *Malus domestica* (*M. domestica*:); *Solanum tuberosum* (*S. tuberosum*); *Vitis heyneana* Roem. et Schult (*V. heyneana*:); *Lolium multiflorum* Lam. (*L. multiflorum*); *Lolium arundinaceium* (*L. arundinaceium*); *Festuca rubra* L. (*F. rubra*); *Spinacia oleracea* (*S. oleracea*); *Hordeum vulgare* L. (*H. vulgare*).

3.2.2.2 Data from Plant Uptake Assays

A dataset was compiled from measurements reported in published uptake assays with grasses and other plants belonging to closely related families exposed to MCs, or MLCs, in the growth medium (Table B-9 in Appendix B). The plant species in this dataset are, as reported in the sources: *Cyperus esculentus* (*C. esculentus*); *H. vulgare*; *Lolium perenne* (*L. perenne*); *Medicago sativa* (*M. sativa*); *Zea mays* (*Z. mays*); *Glycine max* (*G. max*); *Sorghum Sudanese* (*S. Sudanese*); *Triticum aestivum* (*T. aestivum*); *Phaseolus vulgaris* (*P. vulgaris*); *Brassica rapa*.(*B. rapa*).

In addition to experiments performed in spiked or contaminated field soil (hereafter referred to as "soil"), assays using either coarse quartz sand (99%, 0.85–1.27 mm effective diameter particles, hereafter referred to as "sand") or aqueous solutions as the growth medium were also included in the dataset. The inclusion of these datasets had two purposes: (i) compare the predictions relative to those in soil exposures, and (ii) test only the plant cuticle–water pp–LFER without the need for a soil organic carbon–water pp–LFER. The full dataset includes the concentration in the plant, concentration in the growth medium, exposure time, and dry weight fraction of organic carbon in the soil (f_{OC}) when applicable. Details of the experiments are described in Table B-9 in Appendix B. Concentrations in the plant were for the whole plant or only for the aboveground plant parts when available; measurements in fruits

(e.g., corn kernels) were not included. Concentrations below reported analytical quantification limits or without clarification on whether they were expressed on a dry or fresh weight basis were excluded. Data from studies not reporting either the soil organic carbon or organic matter content were also excluded.

3.2.3 Prediction of Concentrations in Plants from Independent Uptake Assays

Concentrations in grasses and closely related plants reported in published uptake assays were predicted using models of the appropriate partition coefficients. The concentration of MCs and MLCs available for plant–root uptake in soil growth medium was estimated using

$$C_{i_{IW}} = \frac{C_{i_{Soil\ Solids}}}{K_{i_{SoilW}}} = \frac{C_{i_{Soil\ Solids}}}{K_{i_{OC}} f_{OC}} \quad (3\text{-}6)$$

where $C_{i_{IW}}$ = concentration of compound i in the growth medium interstitial water (IW) (mg L^{-1}), $C_{i_{Soil\ Solids}}$ = concentration of compound i in the soil solids (mg kg_{dwt}^{-1}), $K_{i_{SoilW}}$ = soil–water partition coefficient of compound i (L_{water} $kg_{dwt\ soil}^{-1}$), and f_{OC} = dry weight fraction of organic carbon in the soil (kg_{OC} $kg_{dwt\ soil}^{-1}$).

Values for $C_{i_{Soil\ Solids}}$ were those reported by the sources as the concentration at the beginning of the exposure or a steady state concentration when available. Values for f_{OC} were also obtained from the sources. However, soil organic matter content (as f_{OM} or $\%_{OM}$, w/w) is reported in most of the sources. A factor of 0.50 was used to convert f_{OM} to f_{OC} ($f_{OC} = 0.5\ f_{OM}$) when needed [44]. $K_{i_{OC}}$ were estimated using the pp–LFER in Eq. (3-3) described previously in Sec. 3.2.1.

Using the predicted $C_{i_{IW}}$, the concentration of MCs and MLCs in plant biomass was estimated as

$$C_{i_{Plant}} = K_{i_{PW}} C_{i_{IW}} = K_{i_{Cut}}\ f_{Cut}\ C_{i_{IW}} \quad (3\text{-}7)$$

where $C_{i_{Plant}}$ = concentration of compound i in the plant biomass (mg kg_{dwt}^{-1}). A single f_{Cut} appropriate for barley (*H. vulgare*) was used for all plant species in the independent dataset since they belong to the same family as barley, Poaceae (true grasses), or to closely related families (Table B-9 in Appendix B). The barley f_{Cut} was calculated using the cuticle content per leaf area (616.3 µg cm^{-2}) and the average specific leaf area (0.3 cm^2 mg_{dwt}^{-1}) measured and reported by Chun et al. [45] and Gunn et al. [46], respectively, resulting in f_{Cut} = 0.18 kg kg_{dwt}^{-1}. $K_{i_{Cut}}$ were estimated using the pp–LFER in Eq. (3-8) described below in Sec. 3.3.1. The $C_{i_{Plant}}$ for the experiments performed in either sand or aqueous solutions was predicted using the measured concentration available for plant root uptake in the exposure medium as reported in the corresponding study. This value was used for the $C_{i_{IW}}$ in Eq.(3-7).

3.3 Results and Discussion

3.3.1 Plant Cuticle-Water pp–LFER

Predicted K_{Cut} using Eq. (3-2) versus observed K_{Cut} are shown in Fig. 3-1 (Tables B-4 to B-6 in Appendix B). The accuracy of the predictions varied with the source of the Abraham solute descriptors (Absolv–AP, Exp–AP, and QCAP). The predicted K_{Cut} for the nitramine MCs, RDX and HMX (abbreviations for all MCs and MLCs are explained in Table B-1 in Appendix B), using Absolv–AP were seven orders of magnitude smaller than the observed K_{Cut} (Fig. 3-1A). A reason for these large underpredictions is the absence of the nitramine (N-NO_2) functional group in the Absolv fragment descriptors set [47]. Missing fragments has been identified as a major drawback for the group contribution approach in the estimation of solute descriptors

[39,48]. N-NO_2 is a highly electronegative group and it increases the potential reactive sites of these MCs [49], therefore the fragment descriptor needs to be included.

Exp–AP were used for RDX, HMX, TNT, and 4-NAN (Fig. 3-1B) in lieu of Absolv–AP. The predictions for RDX and HMX improved by more than six orders of magnitude and the RMSE decreased from RMSE = 1.173 (Fig. 3-1A) to RMSE = 0.611 (Fig. 3-1B). While the experimental derivation of molecular properties generally results in high-quality solute descriptors, its application to large collections of compounds or proposed MCs early in the development stage is limited by time and feasibility constrains. Consequently, an alternative method for the determination of solute descriptors that depends only on molecular structure was also tested. QCAP are derived from quantum chemically computed solvent–water partition coefficients and molecular polarizability [39]. Using this method, solute descriptors S, A, and B are simultaneously estimated with a MLRA to quantum chemically computed solvent–water partition coefficients, while E and V are independently obtained from molecular polarizability calculations and a continuum solvation model based on molecular electrostatic interactions, respectively [39,50]. These QCAP were used for all the compounds to predict the observed K_{Cut} (Fig. 3-1C). A further improvement relative to using Exp–AP resulted with RMSE = 0.513 (Fig. 3-1C).

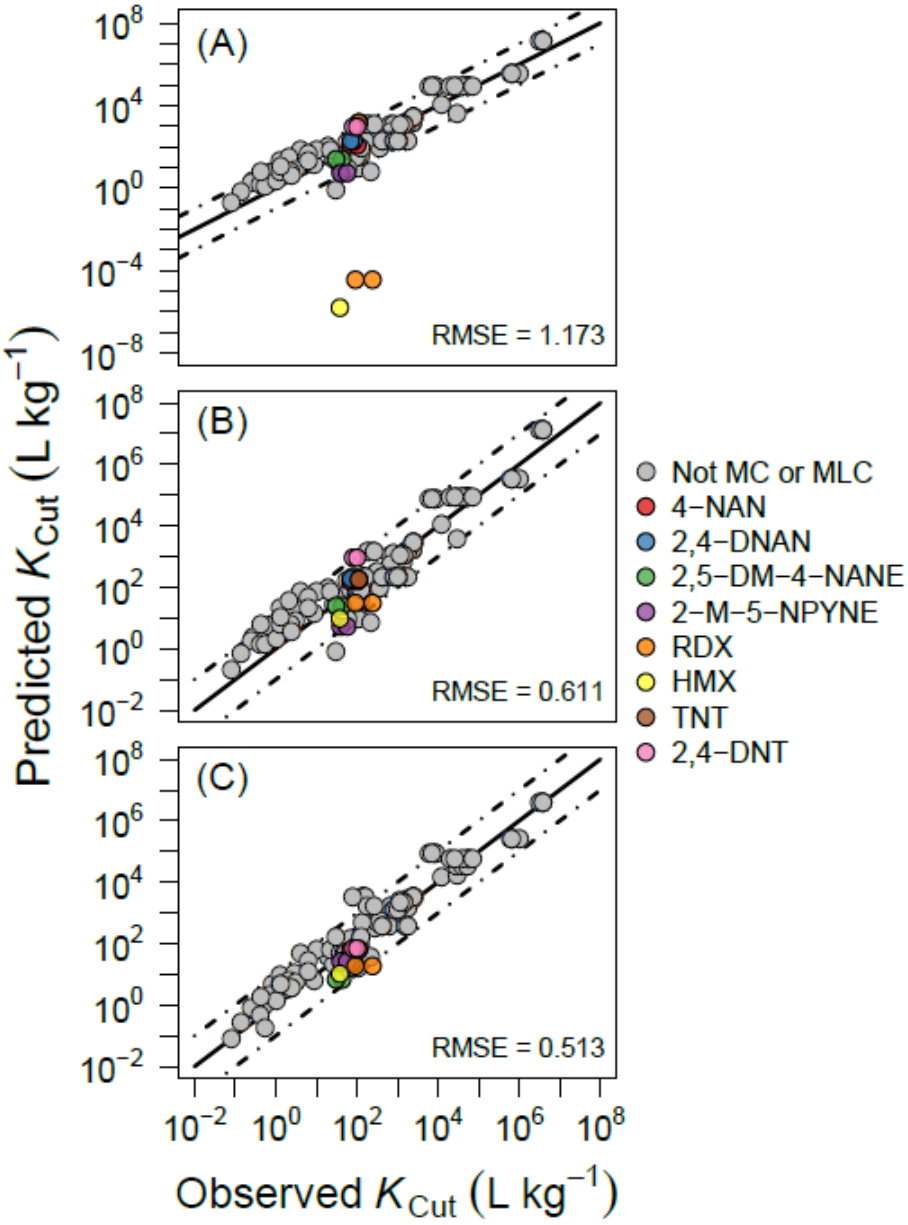

Figure 3-1 pp–LFER–predicted K_{Cut} versus observed K_{Cut} for organic compounds (Tables B-2 and B-4 to B-6 in Appendix B). Predictions made using pp–LFER model from Platts and Abraham [9], Eq. (3-2), for K_{Cut} data collected from the literature. Solute descriptors, uppercase letters for Eq. (3-2), are: (A) Absolv–AP [38], (B) Absolv–AP for all compounds except RDX, HMX, TNT, and 4-NAN for which S, A, and B are Exp–AP [39]; and (C) QCAP [39]. RMSE: root mean square error of prediction (log predicted - log observed). The solid line indicates the best agreement (unity), dashed lines are spaced at 1 log unit from unity.

The dataset employed by Platts and Abraham [9] to develop the K_{Cut} pp–LFER in Eq. (3-2), used to make the predictions in Fig. 3-1, did not contain MCs or MLCs. Therefore, pp–LFERs were developed with a MLRA fitting the general Abraham model (Eq. (3-1)) to the expanded K_{Cut} dataset compiled from the literature (described previously in Sec. 3.2.2.1), which also includes a more heterogeneous group of plant species. The results are shown in Fig. 3-2 and the pp–LFERs are listed in Table B-7 in Appendix B. The solute descriptors used parallel the sequence in Fig. 3-1 (Absolv–AP, Exp–AP, QCAP).

The goodness of fit, evaluated by the RMSE, varied with the solute descriptors. The pp–LFER obtained using Absolv–AP improved the RMSE relative to that yielded by the predictions with Platts and Abraham's pp–LFER [9] (1.173 to 0.786; Fig.3-1A and Fig. 3-2A, respectively), but in order to fit the MCs and MLCs it produced misfits for many of the other compounds (Fig. 3-2A). Predicted K_{Cut} were biased high in order to compensate for the poor Absolv–AP for the nitramine MCs. Using Exp–AP for some of the MCs and MLCs improved the overall fit but still produced misfits for compounds other than MCs or MLCs (Fig. 3-2B).

The best fit was obtained when QCAP were used for all the compounds. The resulting pp–LFER satisfactorily captured the overall variations in the dataset (Fig. 3-2C) yielding a RMSE = 0.395, which indicates that approximately 68% of predicted K_{Cut} fall within ± 0.395 log units (a factor of ± 2.48) of the corresponding observed K_{Cut}. The resulting plant cuticle-water pp–LFER using QCAP is

$$\begin{aligned}\log K_{Cut} = {} & -0.617\ (\pm 0.101) + 0.417\ (\pm 0.088)E + 0.919\ (\pm 0.168)S \\ & - 0.546\ (\pm 0.102)A - 5.449\ (\pm 0.259)B \\ & + 3.479\ (\pm 0.208)V \end{aligned} \qquad (3\text{-}8)$$

$$77\ \text{compounds; N} = 143;\ \text{RMSE} = 0.395;\ R^2_{Adj.} = 0.936;\ \text{SE} = 0.403;\ F = 418$$

where $R^2_{Adj.}$ = adjusted R^2 and SE = regression residual standard error. The system parameters in Eq. (3-8), which are the lowercase variables in Eq. (3-1), quantify the extent to which compounds partition to plant cuticle relative to water. The signs of the system parameters in Eq. (3-8) are consistent with those obtained by Platts and Abraham [9] (Eq. (3-2)) for all molecular interactions except the dipolarity/polarizability term, s, which is negative $s = -0.413$ in Eq. (3-2) and positive $s = 0.919$ in Eq. (3-8). The $s > 0$ in Eq. (3-8) suggests that plant cuticle is a stronger solvation phase than water when interacting with polar/polarizable solutes, which is an unexpected result. This is because water is usually stronger than many environmental and biological phases through polarizability interactions [51], i.e., $s < 0$. However, the resulting s is highly dependent on the quality of the estimated S values used in the pp–LFER calibration. A difficulty in the common simultaneous estimation of E, S, A, and B with MLRA fitting directly to experimental partitioning data, is the inability of multiple linear regression to reliably distinguish between E and S effects as they are cross correlated. One of the advantages of the QCAP E and S is that they are obtained from independently computed molecular properties and are therefore more reliably estimated [39].

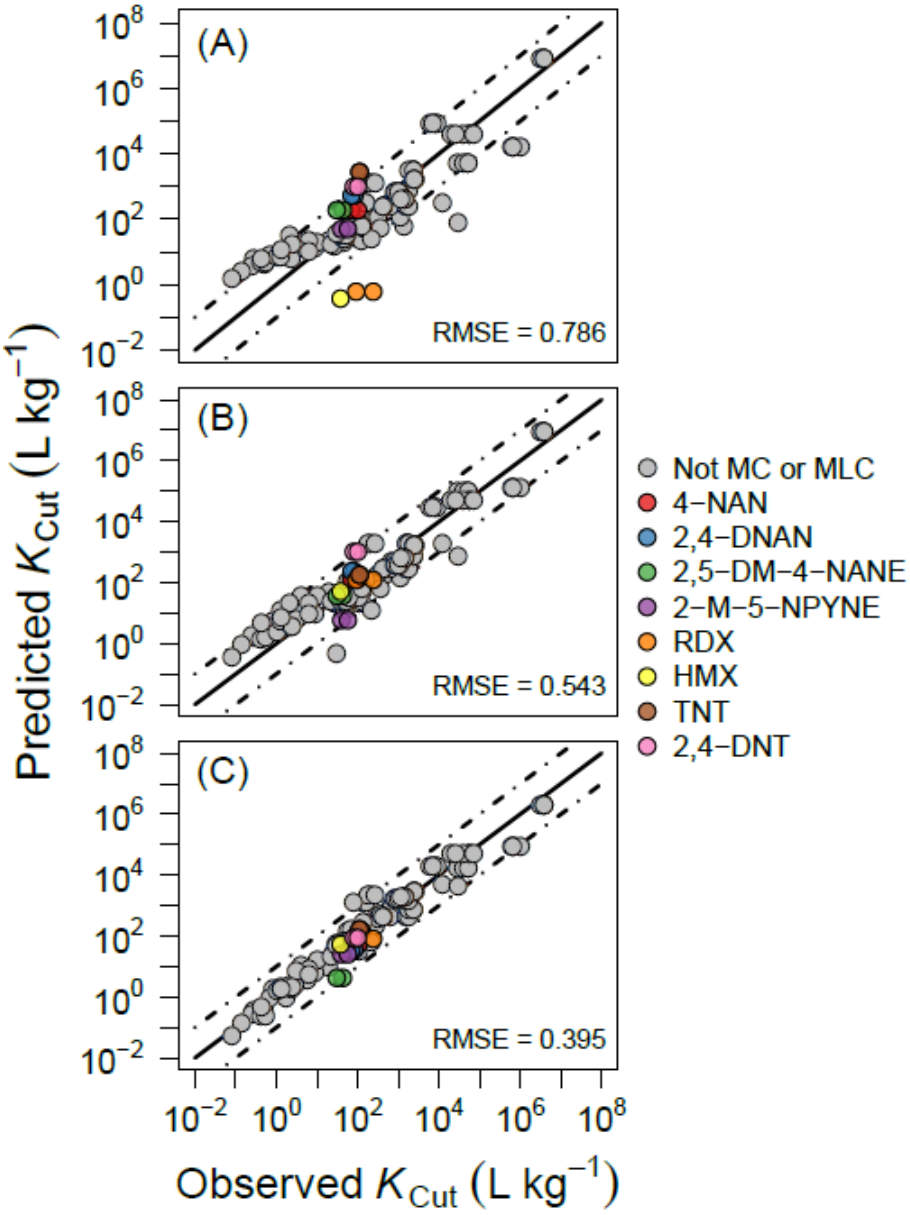

Figure 3-2 pp–LFER-predicted K_{Cut} versus observed K_{Cut} for organic compounds (Tables B-2 and B-4 to B-6 in Appendix B). Predictions made using pp–LFERs, Eq. (3-1), fitted to K_{Cut} data collected from the literature. Solute descriptors, uppercase letters for Eq. (3-1), are: (A) Absolv–AP [38]; (B) Absolv–AP for all compounds except 4-NAN, RDX, HMX, and TNT for which *S*, *A*, and *B* are Exp–AP [39]; and (C) QCAP [39]. RMSE: root mean square error of prediction (log predicted - log observed). The solid line indicates the best agreement (unity), dashed lines are spaced at 1 log unit from unity.

The ability of a pp–LFER to characterize correctly the properties of a solvation phase like the plant cuticle, thus largely relies on the quality and diversity of the solute descriptors used in the calibration dataset. The quality of the QCAP used in Eq. (3-8) surpasses or matches that of both the Absolv–AP and Exp–AP for estimating the observed K_{Cut}, as discussed previously. The solute descriptors used to generate Eq. (3-2), reported as experimentally obtained, produced an excellent agreement to the observed values in Platts and Abraham [9]. However, in terms of solute descriptors diversity, the training set used for Eq. (3-8) covers a considerably wider descriptor space in E and S values than that for Eq. (3-2), as shown in Table 3-1. The high end of the S range for Eq. (3-8) comes mostly from the MCs and MLCs. These compounds provided the response of the plant cuticle to more polar solutes, which can behave through both specific and nonspecific molecular interactions [52]. Eq. (3-8) suggests that the plant cuticle relative to water has the ability to polarize in response to a polar solute and cause the partition coefficient to increase. This might be due to the polar characteristics of the ester and ether bonds interconnecting the fatty acids and long-chain alkyls in the cutin and cutan components of the plant cuticle [35,36], and/or to the recent evidence of the presence of aqueous polar pores embedded in plant cuticular membranes [53]. These reasons supported the choice of Eq. (3-8) over Eq. (3-2) for the prediction of concentrations in plants from published uptake assays.

Table 3-1 Range of solute descriptor space for the plant cuticle–water pp–LFERs by Platts and Abraham [9] and this work.

		Platts and Abraham[a]	This work[b]
E	Min.	0.00	0.47
	Max.	3.26	4.76
S	Min.	0.00	0.12
	Max.	1.76	2.45
A	Min.	0.00	0.00
	Max.	0.96	1.09
B	Min.	0.00	-0.05
	Max.	1.67	1.31
V	Min.	0.308	0.295
	Max.	2.674	2.498

[a] Eq. (3-2). Range reported in Platts and Abraham [9]
[b] Eq. (3-8). QCAP range from Table B-6 in Appendix B

3.3.2 Prediction of Concentrations in Plants from Independent Uptake Assays

Estimated versus observed concentrations in plants for five MCs and two MLCs are shown in Fig. 3-3 (Tables B-9 and B-10 in Appendix B). Predictions were made based on the partitioning between soil organic carbon, interstitial water, and plant cuticle, as described previously in Sec. 3.2.3. The K_{OC} model, Eq. (3-3), was used to estimate the concentration of the MC, or MLC, in the soil interstitial water (i.e., exposure concentration), and the K_{Cut} model, Eq. (3-8), was used to predict the corresponding concentration in the plant biomass. The final equation used to predict the plant concentrations is Eq. (3-9) in Table 3-2, which contains the equations used ordered in the sequence to generate a prediction.

Table 3-2 Sequence of equations for the prediction of concentrations in plants exposed to MCs, or MLCs, in the growth medium.

A partition–based plant bioconcentration model[a]:

$$C_{i_{Plant}} = \frac{K_{i_{Cut}}\, f_{Cut}\, C_{i_{Soil\ Solids}}}{K_{i_{OC}}\, f_{OC}} \quad (3\text{-}9)$$

Var.	Equation	#
$K_{i_{OC}}$:	$\log K_{OC} = 0.670 + 1.075E - 0.277S - 0.363A - 1.697B + 1.468V$	(3-3)
$C_{i_{IW}}$:	$C_{i_{IW}} = \frac{C_{i_{Soil\ Solids}}}{K_{i_{OC}}\, f_{OC}}$	(3-6)
$K_{i_{Cut}}$:	$\log K_{Cut} = -0.617 + 0.417E + 0.919S - 0.546A - 5.449B + 3.479V$	(3-8)
$C_{i_{Plant}}$:	$C_{i_{Plant}} = K_{i_{Cut}}\, f_{Cut}\, C_{i_{IW}}$	(3-7)

[a] Var.: Variables; i: MC, or MLC, of interest; $C_{i_{Plant}}$: concentration of compound i in the plant biomass (mg kg_{dwt}^{-1}); $K_{i_{Cut}}$: plant cuticle–water partition coefficient of i (L_{water} $kg_{cuticle}^{-1}$); f_{Cut}: dry weight fraction of cuticle in the plant ($kg_{cuticle}$ $kg_{dwt\ plant}^{-1}$); $C_{i_{Soil\ Solids}}$: concentration of i in the soil solids (mg kg_{dwt}^{-1}); $K_{i_{OC}}$: soil organic carbon–water partition coefficient of i (L_{water} kg_{OC}^{-1}); f_{OC}: dry weight fraction of organic carbon in the soil (kg_{OC} $kg_{dwt\ soil}^{-1}$); E, S, A, B, and V: QCAP for i (Tables B-6 and B-8 in Appendix B); $C_{i_{IW}}$: concentration of i in the growth medium interstitial water (IW) (mg L^{-1})

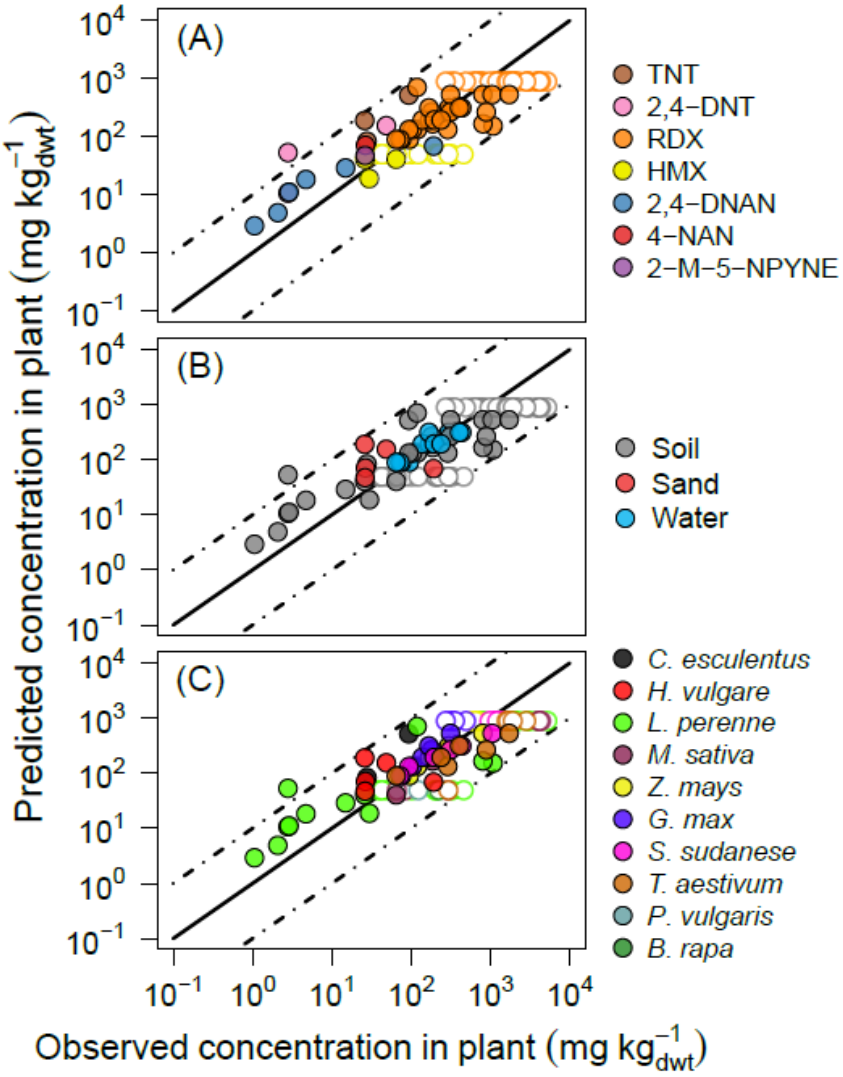

Figure 3-3 pp–LFER–predicted concentrations in the plant versus observed values from published uptake studies (Tables B-9 and B-10 in Appendix B). Color coding assigned based on: (A) MCs and MLCs (Table B-1 in Appendix B), (B) growth medium, and (C) plant species (abbreviations in Table B-9 in Appendix B). Unfilled symbols represent predictions made with concentrations in the interstitial water at aqueous solubility for those observations for which the predicted concentration in the interstitial water exceeded the aqueous solubility of the compound. See text for details. Their border color corresponds to the color identification in each panel legend. Root mean square error of prediction (log predicted - log observed), excluding predictions at aqueous solubility, RMSE = 0.425. The solid line indicates the best agreement (unity), dashed lines are spaced at 1 log unit from unity.

The panels in Fig. 3-3 contain the same predicted and observed concentrations in the plant but with different coding by (A) compound, (B) growth medium, and (C) plant species. These are the main factors that affect the performance of the partitioning model. Measured concentrations in plants range across three orders of magnitude for five different compounds including nitroaromatic, nitramines, and nitropyridines. They were predicted within an order of magnitude (Fig. 3-3A). No bias in the predictions was observed for either MCs or MLCs.

The data included plant uptake assays carried out in three different growth media: soil, sand, and water (Fig. 3-3B). The accuracy of the predictions increased in the order of soil < sand < water as shown by the logarithmic residuals ranging (minimum to maximum) from -0.850 to 1.280, -0.444 to 0.866, and -0.142 to 0.272, respectively (Table B-10 in Appendix B). This can be due to both the complexity of the experimental procedure increasing in the order of water < sand < soil and the inclusion of a K_{OC} model to make the estimations from soil, which contributes to a larger prediction uncertainty relative to that for uptake assays in water or in a simple sand that does not have an appreciable content of organic matter. Predictions made using only the plant cuticle pp–LFER (Eq. (3-8)) produced RMSE values of 0.538 and 0.121 for experiments performed with sand and water as the growth medium, respectively. This indicates that the plant cuticle pp–LFER model is capable of estimating within a reasonable uncertainty the bioconcentration of compounds that are available for plant root uptake using only the measured concentration in the water (interstitial water in the case of sand), f_{Cut}, and QCAP.

It is difficult to maintain a nearly constant exposure concentration in soils, unlike in water or sand as the respective growth medium, due to both the promoted

degradation of the parent compound and the inhomogeneous distribution of the compound in the soil. Unfortunately, for the majority of the data in Fig. 3-3 the concentrations in the growth medium were not monitored or prevented from significantly fluctuating. Only the initial concentrations in the growth medium were available (Table B-9 in Appendix B). The loss of the parent compound led to the overestimation of some of the resulting plant concentrations (Fig. 3-3A and 3-3B), especially for compounds like TNT which have been shown to be readily transformed [20,54].

In order to circumvent the problem of significant compound degradation in the growth medium and/or to ensure that the resulting concentration in the plant is above analytical quantification limits, large amounts of chemicals are usually applied to soil as the initial exposure treatment during uptake assays (Table B-9 in Appendix B). However, under these large soil treatments (unfilled symbols in Fig. 3-3), the predicted concentration in the interstitial water exceeded the aqueous solubility of the compound. Given that the concentration available for plant–root uptake is only that dissolved in the interstitial water, for these cases the prediction of the concentration in the plant was made using the aqueous solubility of the compound as the exposure concentration. This yielded single predictions for concentration in the plant (shown as horizontal trends in Fig. 3-3), especially for MCs with low aqueous solubilities, such as RDX and HMX (Table B-1 in Appendix B).

Fig. 3-3C shows the ten plant species in the dataset (abbreviations explained in Table B-9 in Appendix B). No bias in the quality of predictions was observed as a function of plant species. This indicates that using a single f_{Cut} value for ten different organisms is not an unreasonable simplification.

Despite the lack of uniformity in the plant concentration data and some uncertainty in the soil concentration over the duration of the exposure, the prediction of concentrations from independent uptake assays for all three growth media using Eq. (3-9) yielded a RMSE = 0.425 (excluding predictions at aqueous solubility). This RMSE is considerably smaller than that produced by a dynamic model based on physiological plant uptake by Trapp and Eggen [11], RMSE = 0.578 (calculated using data in their Fig. 2). Their model predicts concentrations in plants, such as barley and carrot (leaves, steams, and/or roots; excluding fruits for comparison to this work), from greenhouse experiments for nonionic polar organic compounds. Unfortunately, comparison to the other models for bioconcentration of organic compounds in plants cited previously in Sec. 3.1 was not possible as a validation to an independent dataset is often not presented or it is performed as a cross–validation [8].

3.4 Conclusions

Bioconcentration of MCs and MLCs in plants can be estimated based on the partitioning between the growth medium solids, interstitial water, and plant. Partitioning between soil organic carbon and interstitial water, and between interstitial water and plant cuticle for MCs, MLCs, and other organic compounds can be predicted with pp–LFERs. The smallest estimation error (RMSE = 0.395) for the plant cuticle–water pp–LFER was obtained using QCAP as the solute descriptors in lieu of Absolv–AP or Exp–AP. The superior quality of the QCAP and the diversity of the K_{Cut} solute training dataset, which covers a wide range of descriptor space, enabled the better characterization of the solvation properties of the plant cuticle phase.

A demonstration of the prediction capabilities of the partitioning–based model to estimate concentrations from independent plant uptake assays was presented.

Concentrations of five MCs and two MLCs measured in ten plant species during uptake experiments with three different types of growth media were estimated with a RMSE = 0.425. Residual errors were smaller for the prediction of plant concentrations from assays performed in sand or water than those in complex soils. This is likely due to both the straightforward exposure procedures for sand and water as growth media and the fact that the estimations for soil assays involve not only a plant cuticle–water pp–LFER but also a soil organic carbon–water pp–LFER to account for the sorption processes affecting the concentration available for plant root uptake.

The RMSE = 0.425 indicates that approximately 68% of predicted concentrations in the plant fall within ± 0.425 log units (a factor of ± 2.66) of the corresponding observed concentration in the plant. This result suggests that the partition–based plant bioconcentration model presented (Eq. (3-9)), which utilizes quantum chemically computed Abraham parameters and two pp–LFERs, can be used to predict the plant concentrations of MCs from molecular structure only.

REFERENCES

This list includes references cited in Appendix B.

1. Ampleman G, Thiboutot S, Lewis J, Marois A, Gagnon A, Bouchard M, Jenkins T, Ranney TA, Pennington JC. Evaluation of the contamination by explosives and metals in soils, vegetation, surface water and sediment at Cold Lake Air Weapons Range (CLAWR), Alberta, Phase II Final report. Technical Report No. DRDC-Valcartier-TR-2004-204. Valcartier, Québec, Canada: Defence Research and Development Canada - Valcartier, Valcartier QUE (CAN); Cold Regions Research and Engineering Lab, Hanover NH (US). 2004;1-116.

2. Jenkins TF, Hewitt AD, Grant CL, Thiboutot S, Ampleman G, Walsh ME, Ranney TA, Ramsey CA, Palazzo AJ, Pennington JC. Identity and distribution of residues of energetic compounds at army live-fire training ranges. *Chemosphere*. 2006;63(8):1280-1290.

3. Clausen JL, Korte N. Fate and transport of energetics from surface soils to groundwater. In: Chappell MA, Price CL, George RD, eds. Envir*onmental Chemistry of Explosives and Propellant Compounds in Soils and Marine Systems: Distributed Source Characterization and Remedial Technologies*. Washington, D.C: American Chemical Society. 2011;1069:273-316.

4. Briggs GG, Bromilow RH, Evans AA. Relationships between lipophilicity and root uptake and translocation of non-ionised chemicals by barley. *Pestic Sci*. 1982;13(5):495-504.

5. Briggs GG, Bromilow RH, Evans AA, Williams M. Relationships between lipophilicity and the distribution of non-ionised chemicals in barley shoots following uptake by the roots. *Pestic Sci*. 1983;14(5):492-500.

6. Travis CC, Arms AD. Bioconcentration of organics in beef, milk, and vegetation. *Environ Sci Technol*. 1988;22(3):271-274.

7. Trapp S, Matthies M. Generic one-compartment model for uptake of organic chemicals by foliar vegetation. *Environ Sci Technol*. 1995;29(9):2333-2338.

8. Dowdy DL, McKone TE. Predicting plant uptake of organic chemicals from soil or air using octanol/water and octanol/air partition ratios and a molecular connectivity index. *Environ Toxicol Chem*. 1997;16(12):2448-2456.

9. Platts JA, Abraham MH. Partition of volatile organic compounds from air and from water into plant cuticular matrix: An LFER analysis. *Environ Sci Technol*. 2000;34(2):318-323.

10. Chiou CT, Sheng G, Manes M. A partition-limited model for the plant uptake of organic contaminants from soil and water. *Environ Sci Technol*. 2001;35(7):1437-1444.

11. Trapp S, Eggen T. Simulation of the plant uptake of organophosphates and other emerging pollutants for greenhouse experiments and field conditions. *Environ Sci Pollut R.* 2013;20(6):4018-4029.

12. Li H, Sheng G, Chiou CT, Xu O. Relation of organic contaminant equilibrium sorption and kinetic uptake in plants. *Environ Sci Technol*. 2005;39(13):4864-4870.

13. Bromilow RH, Chamberlain K. Principles governing uptake and transport of chemicals. In: Trapp S, McFarlane JC, eds. *Plant contamination: Modeling and simulation of organic chemical processes.* Boca Raton, FL: CRC Press, Inc. 1995;37-68.

14. Cunningham SD, Anderson TA, Schwab AP, Hsu FC. Phytoremediation of soils contaminated with organic pollutants. In: Sparks DL, ed. *Advances in agronomy.* San Diego, CA: Academic Press. 1996;56:55-114.

15. Collins C, Fryer M, Grosso A. Plant uptake of non-ionic organic chemicals. *Environ Sci Technol*. 2006;40(1):45-52.

16. Pennington JC, Myers TE, Davis WM, Olin TJ, McDonald TA, Hayes CA, Townsend DM. Impacts of sorption on *in situ* bioremediation of explosives-contaminated soils. Technical Report No. IRRP-95-1. Vicksburg, MS: U,S. Army Waterways Experiment Station, Corps of Engineers. 1995;1-54.

17. Larson SL, Martin WA, Escalon BL, Thompson M. Dissolution, sorption, and kinetics involved in systems containing explosives, water, and soil. *Environ Sci Technol*. 2007;42(3):786-792.

18. Berthelot Y, Valton É, Auroy A, Trottier B, Robidoux PY. Integration of toxicological and chemical tools to assess the bioavailability of metals and energetic compounds in contaminated soils. *Chemosphere*. 2008;74(1):166-177.

19. Savard K, Sarrazin M, Dodard SG, Monteil-Rivera F, Kuperman RG, Hawari J, Sunahara GI. Role of soil interstitial water in the accumulation of hexahydro-1,3,5-trinitro-1,3,5-triazine in the earthworm *Eisenia andrei*. *Environ Toxicol Chem*. 2010;29(4):998-1005.

20. Kalderis D, Juhasz AL, Boopathy R, Comfort S. Soils contaminated with explosives: Environmental fate and evaluation of state-of-the-art remediation processes (IUPAC technical report). *Pure Appl Chem*. 2011;83(7):1407-1484.

21. Miglino AN. Modeling the adsorption and desorption of munition constituents on soils using reversible and resistant components. Newark, DE: University of Delaware. 2015;[Doctoral Dissertation].

22. Sabljić A, Güsten H, Verhaar H, Hermens J. QSAR modelling of soil sorption. improvements and systematics of log KOC vs. log KOW correlations. *Chemosphere*. 1995;31(11–12):4489-4514.

23. Gawlik BM, Sotiriou N, Feicht EA, Schulte-Hostede S, Kettrup A. Alternatives for the determination of the soil adsorption coefficient, KOC, of non-ionicorganic compounds — a review. *Chemosphere*. 1997;34(12):2525-2551.

24. Doucette WJ. Quantitative structure-activity relationships for predicting soil-sediment sorption coefficients for organic chemicals. *Environ Toxicol Chem*. 2003;22(8):1771-1788.

25. von Oepen B, Kördel W, Klein W, Schüürmann G. QSAR in environmental toxicology predictive QSPR models for estimating soil sorption coefficients: Potential and limitations based on dominating processes. *Sci Total Environ*. 1991;109/110:343-354.

26. Wei DB, Wu CD, Wang LS, Hu HY. QSPR-based prediction of adsorption of halogenated aromatics on yellow-brown soil. *SAR QSAR Environ Res*. 2003;14(3):191-198.

27. Kozerski GE, Xu S, Miller J, Durham J. Determination of soil-water sorption coefficients of volatile methylsiloxanes. *Environ Toxicol Chem*. 2014;33(9):1937-1945.

28. Goss KU, Schwarzenbach RP. Linear free energy relationships used to evaluate equilibrium partitioning of organic compounds. *Environ Sci Technol*. 2001;35(1):1-9.

29. Barbour JP, Smith JA, Chiou CT. Sorption of aromatic organic pollutants to grasses from water. *Environ Sci Technol*. 2005;39(21):8369-8373.

30. Zhang M, Zhu L. Sorption of polycyclic aromatic hydrocarbons to carbohydrates and lipids of ryegrass root and implications for a sorption prediction model. *Environ Sci Technol*. 2009;43(8):2740-2745.

31. Hung H, Lin T, Chiou CT. Partition coefficients of organic contaminants with carbohydrates. *Environ Sci Technol*. 2010;44(14):5430-5436.

32. Abraham MH. Scales of solute hydrogen-bonding: Their construction and application to physicochemical and biochemical processes. *Chem Soc Rev*. 1993;22(2):73-83.

33. Goss KU. Predicting the equilibrium partitioning of organic compounds using just one linear solvation energy relationship (LSER). *Fluid Phase Equilibr*. 2005;233(1):19-22.

34. Hale SE, Cornelissen G, Arp HPH. Comment on 'partition coefficients of organic contaminants with carbohydrates'. *Environ Sci Technol*. 2011;45(3):1158-1158.

35. Bargel H, Koch K, Cerman Z, Neinhuis C. Structure-function relationships of the plant cuticle and cuticular waxes - a smart material? *Funct Plant Biol*. 2006;33(10):893-910.

36. Dominguez E, Cuartero J, Heredia A. An overview on plant cuticle biomechanics. *Plant Sci*. 2011;181(2):77-84.

37. Schreiber L, Schonherr J. Water and solute permeability of plant cuticles: Measurement and data analysis. Berlin, Germany: Springer Berlin Heidelberg. 2009;1-299

38. Advanced Chemistry Development, Inc. ACD/PhysChem suite: Absolv module, v.5.0. Toronto, ON, Canada: ACD/Labs. 2013.

39. Liang Y. Determining Abraham solute and system parameters for neutral organic compounds using quantum chemical methods. Newark, DE: University of Delaware. 2016;[Doctoral Dissertation].

40. R Development Core Team. R: A language and environment for statistical computing, v.3.2.0. Vienna, Austria: R Foundation for Statistical Computing. 2015.

41. Kipka U, Di Toro DM. A linear solvation energy relationship model of organic chemical partitioning to particulate organic carbon in soils and sediments. *Environ Toxicol Chem*. 2011;30(9):2013-2022.

42. Holloway PJ, Baker EA. Isolation of plant cuticles with zinc chloride-hydrochloric acid solution. *Plant Physiol*. 1968;43(11):1878-1879.

43. Riederer M, Schonherr J. Accumulation and transport of (2,4-dichlorophenoxy)acetic acid in plant cuticles: I. sorption in the cuticular membrane and its components. *Ecotoxicol Environ Saf*. 1984;8(3):236-247.

44. Pribyl DW. A critical review of the conventional SOC to SOM conversion factor. *Geoderma*. 2010;156(3–4):75-83.

45. Chun JC, Lee HJ, Lim SJ, Kim SE, Guh JO. Comparative absorption, translocation, and metabolism of foliar-applied oxyfluorfen in wheat and barley. *Pestic Biochem Physiol*. 2001;70(2):118-125.

46. Gunn S, Farrar JF, Collis BE, Nason M. Specific leaf area in barley: Individual leaves versus whole plants. *New Phytol*. 1999;143(1):45-51.

47. Platts JA, Butina D, Abraham MH, Hersey A. Estimation of molecular linear free energy relation descriptors using a group contribution approach. *J Chem Inf Comput Sci*. 1999;39(5):835-845.

48. Hou TJ, Xia K, Zhang W, Xu XJ. ADME evaluation in drug discovery. 4. prediction of aqueous solubility based on atom contribution approach. *J Chem Inf Comput Sci*. 2004;44(1):266-275.

49. Kandhakumar G, Jothi M, Kumaradhas P. Probing the effect of nitro groups in nitramine based energetic molecules: A DFT and charge density study. *Mol Simul*. 2016;42(3):173-185.

50. Lin ST, Sandler SI. A priori phase equilibrium prediction from a segment contribution solvation model. *Ind Eng Chem Res*. 2002;41(5):899-913.

51. Endo S, Goss KU. Applications of polyparameter linear free energy relationships in environmental chemistry. *Environ Sci Technol*. 2014;48(21):12477-12491.

52. Schwarzenbach RP, Gschwend PM, Imboden DM. Environmental organic chemistry. Hoboken, NJ: John Wiley & Sons, Inc. 2005;60-62.

53. Schreiber L. Polar paths of diffusion across plant cuticles: New evidence for an old hypothesis. *Ann Bot*. 2005;95(7):1069-1073.

54. Esteve-Nunez A, Caballero A, Ramos JL. Biological degradation of 2,4,6-trinitrotoluene. *Microbiol Mol Biol Rev*. 2001;65(3):335-352.

55. US Environmental Protection Agency. Estimation Programs Interface (EPI) Suite™ for Microsoft® Windows, v. 4.11. Washington, D.C: US EPA. 2012.

56. Hawari J, Monteil-Rivera F, Perreault NN, Halasz A, Paquet L, Radovic-Hrapovic Z, Deschamps S, Thiboutot S, Ampleman G. Environmental fate of 2,4-dinitroanisole (DNAN) and its reduced products. *Chemosphere*. 2015;119:16-23.

57. Sabljic A, Gusten H, Schonherr J, Riederer M. Modeling plant uptake of airborne organic-chemicals .1. plant cuticle water partitioning and molecular connectivity. *Environ Sci Technol*. 1990;24(9):1321-1326.

58. Chen B, Johnson EJ, Chefetz B, Zhu L, Xing B. Sorption of polar and nonpolar aromatic organic contaminants by plant cuticular materials: Role of polarity and accessibility. *Environ Sci Technol*. 2005;39(16):6138-6146.

59. Kirsch T, Kaffarnik F, Riederer M, Schreiber L. Cuticular permeability of the three tree species *Prunus Iaurocerasus* L., *Ginkgo biloba* L. and *Juglans regia* L.: comparative investigation of the transport properties of intact leaves, isolated cuticles and reconstituted cuticular waxes. *J Exp Bot*. 1997;48(5):1035-1045.

60. Chen B, Li Y, Guo Y, Zhu L, Schnoor JL. Role of the extractable lipids and polymeric lipids in sorption of organic contaminants onto plant cuticles. *Environ Sci Technol*. 2008;42(5):1517-1523.

61. Li Y, Chen B. Phenanthrene sorption by fruit cuticles and potato periderm with different compositional characteristics. *J Agric Food Chem*. 2009;57(2):637-644.

62. Pennington JC. Plant uptake of 2,4,6-trinitrotoluene, 4-amino-2,6-dinitrotoluene, and 2-amino- 4,6-dinitrotoluene using ^{14}C-labeled and unlabeled compounds. Technical Report No. EL-88-20. Vicksburg, MS: U,S. Army Waterways Experiment Station, Corps of Engineers. 1988;1-68.

63. Sunahara GI. Development of toxicity benchmarks and bioaccumulation data for N-based organic explosives for terrestrial plants and soil invertebrates. Final

Report No. SERDP ER-1416. Québec, Canada: National Research Council of Canada Montreal (Québec) Biotechnology Research Institute. 2012;1-289.

64. Rocheleau S, Lachance B, Kuperman RG, Hawari J, Thiboutot S, Ampleman G, Sunahara GI. Toxicity and uptake of cyclic nitramine explosives in ryegrass *Lolium perenne*. *Environ Pollut*. 2008;156(1):199-206.

65. Best EPH, Tatem HE, Geter KN, Wells ML, Lane BK. Effects, uptake, and fate of 2,4,6-trinitrotoluene aged in soil in plants and worms. *Environ Toxicol Chem*. 2008;27(12):2539-2547.

66. Best EPH, Geter KN, Tatem HE, Lane BK. Effects, transfer, and fate of RDX from aged soil in plants and worms. *Chemosphere*. 2006;62(4):616-625.

67. Chen D, Liu ZL, Banwart W. Concentration-dependent RDX uptake and remediation by crop plants. *Environ Sci Pollut Res*. 2011;18(6):908-917.

68. Groom, Carl A., Halasz, Annamaria, Paquet, Louise, Morris, Neil, Olivier, Lucie, Dubois, Charles, Hawari, Jalal. Accumulation of HMX (octahydro-1,3,5,7-tetranitro-1,3,5,7-tetrazocine) in indigenous and agricultural plants grown in HMX-contaminated anti-tank firing-range soil. *Environ Sci Technol*. 2002;36(1):112-118.

69. Dodard SG, Sarrazin M, Hawari J, Paquet L, Ampleman G, Thiboutot S, Sunahara GI. Ecotoxicological assessment of a high energetic and insensitive munitions compound: 2,4-dinitroanisole (DNAN). *J Hazard Mater*. 2013;262:143-150.

Chapter 4

PREDICTING WORM–SOIL BIOCONCENTRATION OF MUNITIONS COMPOUNDS FROM MOLECULAR STRUCTURE

4.1 Introduction

Residues of munitions compounds (MCs) deposited on soils at military ranges and areas exposed to off-site migration of contaminants come in direct contact with biota inhabiting the soils in those locations. As a result, soil dwelling organisms such as earthworms are exposed, and are likely to accumulate MCs posing risks not only of direct toxicity but also of transference to higher trophic levels. Modeling tools are required to estimate the degree of bioconcentration to be expected.

Worms are crucial for the structure, recycling of nutrients, and fertility of soils [1]. Terrestrial and aquatic worms are routinely used as test organisms to assess the environmental risk of contaminants [2,3]. Their abundance, behavior, and substance body burden are bioindicators of soil and sediment quality [4]. The bioconcentration of organic compounds in worms is defined as the steady state ratio of the compound concentration in the worm to that in the soil or sediment interstitial/pore water [5], and it is expressed as

$$BCF_i = \left(\frac{C_{i_{Organism}}}{C_{i_{Available\ in\ growth\ medium.}}}\right)_{SS} = \left(\frac{C_{i_{Worm}}}{C_{i_{IW}}}\right)_{SS} \quad (4\text{-}1)$$

where i refers to a compound of interest (e.g., a MC), BCF_i = bioconcentration factor of i ($L_{water}\ kg_{worm\ dwt}^{-1}$; dwt: dry weight), SS denotes steady state, $C_{i_{Worm}}$ =

concentration of i in the worm (mg kg_{dwt}^{-1}), and $C_{i_{IW}}$ = dissolved concentration of i in the interstitial water (IW) (mg L^{-1}).

Because of the analytical challenges associated with separating the interstitial water from soil or sediment solids, preferred models are those able to estimate the concentration of organic compounds in worms using the soil concentration rather than the measured interstitial water concentration. Dynamic models based on first–order kinetics have been proposed [6-12] to predict the steady state concentration in the worm using

$$C_{i_{Worm}} = \frac{k_{i_u}}{k_{i_e}} C_{i_{Solid\ growth\ medium}} \quad (4\text{-}2)$$

where $C_{i_{Solid\ growth\ medium}}$ = concentration of i in the solid growth medium (mg kg_{dwt}^{-1}), k_{i_u}= uptake rate constant (d^{-1}), and k_{i_e} = elimination rate constant (d^{-1}). The rate constants $k_{i_u}$and k_{i_e} represent the summed contributions from various uptake and elimination processes. Although Eq. (4-2) does not have the need for measurements of concentrations in the interstitial water, it requires both uptake and elimination kinetic data to determine the rate constants. Since worms can take up contaminants through two main routes: (i) dermal, diffusion of the contaminant dissolved in the interstitial water through the skin, and (ii) intestinal, ingestion of contaminated particles [9,13], dynamic models may include both of these uptake routes [10]. However, with the exception of very hydrophobic chemicals (octanol–water partition coefficient, log K_{OW} > 6) for which the second route is of major importance, the first route has been shown to be dominant for a variety of organic compounds [9,14]. These dynamic models incorporate a detailed representation of the mechanisms involved in the uptake process, but they often require a large number of fitting parameters for each chemical

(e.g., Jager [10]). Therefore, a large dataset is needed to estimate the parameters for each of the specific uptake and elimination processes. This limits the use of these models for most existing chemicals and for new proposed compounds for which only the molecular structure is known.

Models that include only the passive partitioning between soil (or sediment) solids and soil interstitial water, and between soil interstitial water and worm components have been published [15-18]. These models consider only the organic phases present in soil and worms to estimate the distribution of contaminants. Soil organic carbon, worm lipid, and worm protein have been suggested as the phases playing a major role [5,19-21]. To estimate the partition coefficients between organic carbon and water (K_{OC}), lipid and water (K_{Lipid}), and protein and water ($K_{Protein}$), these models often use single-parameter quantitative structure-activity relationships (QSARs) that are developed using a log-log correlation of each $K_{OC,}$ K_{Lipid}, and $K_{Protein}$ with the K_{OW}. This assumes that octanol has similar solvation properties to those of soil OC and worm components. However, this is not the case for more polar compounds, compounds that interact by hydrogen-bonding [22-24], and certain worm species [17]. The reliance on the K_{OW} as the sole chemical property used to estimate the BCF provides little insight into the chemical properties that make a compound more likely to bioconcentrate in worms. This is important information that can be used to aid in selecting among proposed MCs early in the development stage.

More recent models for estimating K_{OC}, K_{Lipid}, and $K_{Protein}$ employ polyparameter linear free energy relationships (pp–LFERs) [25,26]. Contrary to single-parameter K_{OW}-based predictions, pp–LFERs estimate partitioning by considering the contributions from different types of interactions between the solute and the

condensed phase (e.g., soil organic carbon, worm lipid). Thus, pp–LFERs are able to more fully characterize the solvation properties of the condensed phase and the strength of its interactions with solutes relative to that of water. In order to achieve these results, however, pp–LFERs demand a significantly larger and more chemically diverse training dataset of partition coefficients than that for single-parameter K_{OW}-based models.

Unfortunately, the database available for partitioning of organic compounds between worm and water is rather limited. However, if the uptake of these compounds from soil is mainly driven by passive partitioning between interstitial water and worm components like lipid and protein, and thus less dependent on active physiological processes inherent to a particular organism, then the sources of data for the calibration of K_{Lipid} and $K_{Protein}$ pp–LFERs can be expanded to other organisms such as fish for which numerous measurements exist in the literature. Moreover, experimental fish BCFs have been found to be in the same order of magnitude as worm BCFs for organic compounds including MCs [27-29]. This suggests that the numerous fish data could be used to build models that produce a baseline estimate of the MCs bioconcentration in worms.

The objective of this work is to predict the bioconcentration of MCs (Table C-1 in Appendix C) in earthworms based on the partitioning between soil solids, interstitial water, and worm components. This is achieved using pp–LFERs for the prediction of K_{OC} to estimate the concentration in soil available for dermal uptake, and, subsequently, K_{Lipid} and $K_{Protein}$ to estimate the sorption to worm tissue. Two K_{Lipid} pp–LFERs are compared for the prediction of the bioconcentration in worms. The first is fitted exclusively to worm data, while the second is an existing model that was

calibrated to lipid partitioning data from various organisms. The same $K_{Protein}$ pp–LFER is used for both models.

The procedure for the prediction of concentrations in worms from soil concentration is validated by estimating concentrations in worms compiled from published uptake assays in an independent dataset (23 observations). The pp–LFERs involved in this work use only molecular structure to compute the required model parameters. Therefore, they can also be used to assess the bioconcentration potential for proposed MCs early in the development stage.

4.2 Methodology

Two types of predictions are made: (i) estimation of observed worm BCFs, as defined in Eq. (4-1), for those experiments that employed measured concentrations in the interstitial water, and (ii) estimation of concentrations in worms observed during uptake experiments for which the concentration in the interstitial water was unknown or not reported and, therefore, needs to be predicted. The first set of predictions test the partition–based BCFs models using measured exposure concentrations, while the second set of predictions examine whether the K_{OC}, K_{Lipid}, and $K_{Protein}$ pp–LFERs can be used to estimate MCs concentrations in worms within a reasonable uncertainty for situations where only soil concentration measurements are available.

4.2.1 Prediction of Worm Bioconcentration Factors (BCFs)

The bioconcentration model employed for worms is similar to that employed for fish [30]. Three phases are assumed to represent the components in the worm for which partitioning determines the BCF: lipid, protein, and internal water. A three phase partitioning model, based on the BCF definition in Eq. (4-1), is

$$BCF_i = \left(f_{Lipid}\, K_{i_{Lipid}} + f_{Protein}\, K_{i_{Protein}} + \frac{f_{Water}}{\rho_{Water}}\right) \frac{1}{f_{dwt}} \qquad (4\text{-}3)$$

where i is an organic compound of interest (e.g., a MC); $K_{i_{Lipid}}$ and $K_{i_{Protein}}$ are the lipid–water and protein–water partition coefficients of compound i, respectively (L_{water} kg_{lipid}^{-1} and L_{water} $kg_{protein}^{-1}$); f_{Lipid} and $f_{Protein}$ are the wet weight worm fraction of lipid and protein, respectively (kg_{lipid} $kg_{wwt\ worm}^{-1}$ and $kg_{protein}$ $kg_{wwt\ worm}^{-1}$, wwt: wet weight); f_{Water} and f_{dwt} are the worm mass fraction of water and dry weight, respectively (kg_{water} $kg_{wwt\ worm}^{-1}$ and kg_{dwt} $kg_{wwt\ worm}^{-1}$); and ρ_{Water} is the density of water (kg_{water} L_{water}^{-1}). The $\frac{1}{f_{dwt}}$ term is included since most of the literature BCFs data are reported on a dry weight basis and the worm fractions of lipid and protein are most commonly found on a wet weight basis. Eq. (4-3) represents a worm as a three component system: lipid, protein, and internal water, and the BCF is the sum of the individual contributions of compound i in each of the three components. The sources for the BCFs data (Table C-2 in Appendix C) are described below in Sec. 4.2.3.1 together with the sources for the fractions of lipid, protein, water, and dry weight (Table C-3 in Appendix C). $K_{i_{Lipid}}$ and $K_{i_{Protein}}$ were predicted using the pp–LFERs described below in Sec. 4.2.2.

4.2.2 Polyparameter Linear Free Energy Relationship (pp–LFER) Models

The pp–LFER models for partitioning between water and soil organic carbon, lipid, and protein used in this work are based on the Abraham polyparameter model [25]

$$\log K_{SW} = c + eE + sS + aA + bB + vV \qquad (4\text{-}4)$$

where K_{SW}, the dependent variable, is the partition coefficient between a solvation phase (e.g., organic carbon, worm lipid) and water, and the independent variables, the right hand side of Eq. (4-4), account for the free energy contributions from different

types of molecular interactions. The uppercase letters in Eq. (4-4) are solute descriptors for the compound being modeled (e.g., a MC) and the lowercase letters refer to the complementary effect of the solvation phase on the corresponding interaction. The eE term represents the dispersion interactions that occur between non-polar (no permanent multipole moments) molecules. The sS term is the dipolarity/polarizability that arises from dipole-dipole and dipole-induced dipole interactions. The aA and bB terms account for the donation and acceptance of hydrogen bonds, which are bonds between certain types of hydrogen atoms and highly electronegative atoms in polar molecules. The aA term refers to solvent acceptor (a)–solute donor (A) and bB to solvent donor (b)–solute acceptor (B). Finally, vV accounts for the energy required for cavity formation, and c is a regression constant [25].

4.2.2.1 Lipid–Water and Protein–Water pp–LFERs

Two K_{Lipid} pp–LFERs were tested for the prediction of worm BCFs and the validation for the estimation of concentrations in worms from independent uptake experiments. The same K_{Protein} pp–LFER was used for both tests. The first K_{Lipid} pp–LFER was obtained using Eq. (4-4) substituted into Eq. (4-3) and fit exclusively to BCF worm data collected from the literature, sources described below in Sec. 4.2.3.1. The solute descriptors, uppercase letters in Eq. (4-4), were Quantum Chemically estimated Abraham Parameters (QCAP) from Liang [31] (Table C-5 in Appendix C). Briefly, the QCAP E and V are obtained from the compound's computed molecular polarizability and molecular volume, respectively. The QCAP S, A, and B are simultaneously estimated with a multiple linear regression analysis (MLRA) applied to Eq. (4-4) using quantum chemically computed solvent–water partition coefficients for 60 solvents with known lowercase parameters [31,32]. The primary reason for using

QCAP for the development of the worm lipid–water pp–LFER is the failure of other available Abraham parameter estimation methods for certain MCs, whereas QCAP have been shown to successfully predict K_{SW} values for a wide variety of organic compounds including MCs and compounds with similar chemical structural functionalities, which are referred to as munition-like compounds (MLCs; Table C-1 in Appendix C) [31].

The second K_{Lipid} and the $K_{Protein}$ pp–LFERs were obtained from recent publications by Kuo and Di Toro [30,33]

$$\begin{aligned}\log K_{Lipid} = {} & 0.84\ (\pm 0.14) + 0.77\ (\pm 0.10)E - 1.10\ (\pm 0.19)S \\ & - 0.47\ (\pm 0.22)A - 3.52(\pm 0.20)B + 3.37(\pm 0.13)V \\ & 248 \text{ compounds; } N = 248;\ R^2 = 0.88;\ RMSE = 0.57\end{aligned} \quad (4\text{-}5)$$

$$\begin{aligned}\log K_{Protein} = {} & -0.88\ (\pm 0.17) + 0.74\ (\pm 0.13)E - 0.37\ (\pm 0.15)S \\ & - 0.13\ (\pm 0.15)A - 1.37\ (\pm 0.16)B + 1.06\ (\pm 0.14)V \\ & 69 \text{ compounds; } N = 69;\ R^2 = 0.76;\ RMSE = 0.38\end{aligned} \quad (4\text{-}6)$$

where K_{Lipid} and $K_{Protein}$ are expressed as $L_{water}\ kg_{lipid}^{-1}$ and $L_{water}\ kg_{protein}^{-1}$, respectively, values in parenthesis are $\pm$ the standard error, N = number of data points used to estimate the regression equation coefficients, R^2 = coefficient of determination, and RMSE is the root mean square error of prediction. Kuo and Di Toro [30,33] calibrated Eq. (4-5) using data from multiple sources including partitioning experiments with fish fat/oil for a diverse set of organic compounds ($1.0 < \log K_{OW} < 8.5$). Eq. (4-6) was trained with data from partitioning to human serum albumin as a protein surrogate for compounds with low log K_{OW} ($0.0 < \log K_{OW} < 4.5$) for which partitioning to protein is more dominant than partitioning to lipids.

The solvent parameters for lipid–water partitioning in Eq. (4-5) can be used to determine which phase, lipid or water, is more competitive for solutes. A positive

solvent coefficient causes an increase in the partition coefficient indicating that lipid is preferred relative to water. For example, dispersion interactions (e = 0.77 > 0) favor lipid, and cavity formation in the lipid requires less free energy than in water (v = 3.37 > 0), so again lipid is favored. Eq. (4-5), however, shows that the lipid is less polar/polarizable (s = - 1.10 < 0) and accepts hydrogen bonds (a = - 0.47 < 0) and donates hydrogen bonds (b = - 3.52 < 0) less readily than water, indicating that for these type of interactions water is favored over lipid.

The protein solvent parameters in Eq. (4-6) depict protein as a phase with solvation tendencies similar to those of the lipid phase relative to water as the signs for all the solvent parameters are the same in Eq. (4-6) and Eq. (4-5). The competitiveness for solutes between protein and lipid, however, varies with the type of molecular interaction as listed in Table 4-1, which contains the differences in solvent parameters between the two phases. Negative differences in Table 4-1 indicate the molecular interaction type represented by that solvent parameter favors protein over lipid. In this way, protein is stronger than lipid for polarizability (s), acceptance of hydrogen bonds (a), and donation of hydrogen bonds (b). Lipid is favored for dispersion (e) and cavity formation (v).

The solute descriptors, uppercase letters in Eq. (4-4), for the partition coefficient pp–LFERs used here, Eq. (4-5) and Eq. (4-6), were the appropriate QCAP reported by Liang [31] (Table C-5 in Appendix C).

Table 4-1 Comparison of the competitiveness for solutes between lipid and protein, calculated as the difference between the solvent parameters in the K_{Lipid} and $K_{Protein}$ pp–LFERs obtained by Kuo and Di Toro [30,33], Eq. (4-5) and Eq. (4-6), respectively.

Solvent parameter	Phase		Difference
	Lipid	Protein	
e	0.77	0.74	0.03
s	-1.1	-0.37	-0.73
a	-0.47	-0.13	-0.34
b	-3.52	-1.37	-2.15
v	3.37	1.06	2.31

4.2.2.2 Soil Organic Carbon-Water pp–LFER

The K_{OC} values were estimated using the pp–LFER model developed by Kipka and Di Toro [34]

$$\begin{aligned}\log K_{OC} = {} & 0.670\ (\pm 0.088) + 1.075\ (\pm 0.061)E - 0.277\ (\pm 0.083)S \\ & - 0.363\ (\pm 0.100)A - 1.697\ (\pm 0.085)B \\ & + 1.468\ (\pm 0.077)V \\ & 440 \text{ compounds; } \mathrm{N} = 440; \mathrm{RMSE} = 0.48\end{aligned} \tag{4-7}$$

where K_{OC} is expressed as $L_{water}\ kg_{OC}^{-1}$. This model was built with a wide and chemically varied dataset for nonionic organic compounds. The solvent parameters in Eq. (4-7) indicate that the soil organic carbon phase has similar solvation tendencies than those of the lipid and protein phases shown in Eq. (4-5) and Eq. (4-6), respectively, as the signs for all the molecular interactions are the same among these three pp–LFERs. A comparison of the difference in solvent parameters between lipid and organic carbon is presented in Table 4-2. Negative differences in Table 4-2 indicate the molecular interaction type represented by that solvent parameter favors organic carbon over lipid. In this way, the organic carbon phase is stronger than lipid

for all molecular interactions with the exception of cavity formation (v). The solute descriptors used to apply this model here were the appropriate QCAP reported by Liang [31] (Table C-5 in Appendix C).

Table 4-2 Comparison of the competitiveness for solutes between lipid and organic carbon, calculated as the difference between the solvent parameters in the K_{Lipid} pp–LFER by Kuo and Di Toro [30,33], Eq. (4-5), and K_{OC} pp–LFER by Kipka and Di Toro [34], Eq. (4-7).

Solvent parameter	Phase		Difference
	Lipid	OC	
e	0.77	1.08	-0.31
s	-1.1	-0.28	-0.82
a	-0.47	-0.36	-0.11
b	-3.52	-1.70	-1.82
v	3.37	1.47	1.90

4.2.3 Experimental Data

Two datasets were compiled from published uptake assays: worm BCFs from studies with measured concentrations in the interstitial water, and concentrations in worms from studies performed in soil for which measured concentrations in the interstitial water were unavailable. Data exclusion criteria were: (1) compounds with experimental log K_{OW} > 6.0 (values from the EPI Suite database [35]) given that the worm intestinal uptake route becomes predominant for these highly hydrophobic chemicals, (2) compounds for which QCAP were not available (Liang [31]), (3) measurements obtained at exposures concentrations causing lethal or inhibitory effects to worms, (4) concentrations below reported analytical quantification limits or without

clarification on whether they were expressed on a dry or fresh weight basis, and (5) studies not reporting either the soil organic carbon or organic matter content. The data are listed in Tables C-2 and C-8 in Appendix C.

4.2.3.1 Worm Bioconcentration Factors

A BCF dataset was assembled that is both chemically diverse and has worm species variety as well. The compounds include MCs, MLCs, polycyclic aromatic hydrocarbons (PAHs), and organochlorines for studies with seven different terrestrial and aquatic worm species (Table C-2 in Appendix C). The exposure media include coarse quartz sand (0.5–1.0 mm effective diameter particles, hereafter referred to as "sand"), spiked or contaminated soil more complex than simple sand (hereafter referred to as "soil"), spiked or contaminated sediment, and water. A total of 60 observed worm BCFs values for undissociated organic compounds were compiled (Table C-2 in Appendix C). The worm species in the BCFs dataset are: *Eisenia andrei* (*E. andrei*); *Lumbriculus variegatus* (*L. variegatus*); *Lumbricus terrestris* (*L. terrestris*); *Eisenia fetida* (*E. fetida*); *Lumbricus rubellus* (*L. rubellus*); *Tubifex tubifex* (*T. tubifex*); *Monopylephorus rubroniveu* (*M. rubroniveus*).

Values for f_{Lipid}, $f_{Protein}$, f_{Water}, and f_{dwt} were found in the literature for five of the seven worm species in the dataset (Table C-3 in Appendix C). Values for the missing species were calculated as the average among worms of the same type, i.e., terrestrial or aquatic (Table C-4 in Appendix C).

4.2.3.2 Concentrations in Worms

A dataset was compiled from measurements reported in published uptake assays with worms exposed to MCs in soil (Table C-8 in Appendix C). The dataset

includes the concentration in the worm, concentration in the soil, exposure time, and mass fraction of organic carbon in the soil (f_{OC}). A total of 23 observations were compiled. Further details of the experiments are described in Table C-8 in Appendix C. The worm species included in this dataset are *E. andrei* and *E. fetida*.

4.2.4 Prediction of Concentrations in Worms from Independent Uptake Assays

Concentrations of MCs in worms reported in published soil uptake assays (Table C-8 in Appendix C) were predicted using the K_{OC}, K_{Lipid}, and $K_{Protein}$ pp–LFERs. The concentration of MCs available for worm passive uptake in soil exposure medium was estimated using

$$C_{i_{IW}} = \frac{C_{i_{Soil\ Solids}}}{K_{i_{SoilW}}} = \frac{C_{i_{Soil\ Solids}}}{K_{i_{OC}} f_{OC}} \quad (4\text{-}8)$$

where $C_{i_{IW}}$ = concentration of compound i in the growth medium interstitial water (IW) (mg L^{-1}), $C_{i_{Soil\ Solids}}$ = concentration of compound i in the soil solids (mg kg_{dwt}^{-1}), $K_{i_{SoilW}}$ = soil-water partition coefficient of compound i (L_{water} $kg_{dwt\ soil}^{-1}$), and f_{OC} = dry weight fraction of organic carbon in the soil (kg_{OC} $kg_{dwt\ soil}^{-1}$).Values for $C_{i_{Soil\ Solids}}$ were those reported by the sources as the concentration at the beginning of the exposure or a steady state exposure concentration when available. Values for f_{OC} were also obtained from the sources when available. However, soil organic matter content (as f_{OM} or %, w/w) is reported in most of the sources. A factor of 0.50 was used to convert f_{OM} to f_{OC} when needed [36]. $K_{i_{OC}}$ were estimated using Eq. (4-7), described previously in Sec. 4.2.2.2.

Using the predicted $C_{i_{IW}}$, the concentration of MCs in worm biomass was estimated as

$$C_{i_{Worm}} = K_{i_{WW}} C_{i_{IW}} = \left(f_{Lipid}\, K_{i_{Lipid}} + f_{Protein}\, K_{i_{Protein}} + \frac{f_{Water}}{\rho_{Water}} \right) \frac{C_{i_{IW}}}{f_{dwt}} \quad (4\text{-}9)$$

where $K_{i_{WW}}$ = worm–water partition coefficient of compound i (L_{water} $kg_{dwt\ worm}^{-1}$). $K_{i_{Lipid}}$ were estimated using both of the pp–LFERs described previously in Sec. 4.2.2.1. $K_{i_{Protein}}$ were estimated using Eq. (4-6). Values for f_{Lipid}, $f_{Protein}$, f_{Water}, and f_{dwt} were obtained from the literature (Table C-3 in Appendix C).

4.3 Results and Discussion

4.3.1 Lipid–Water and Protein–Water pp–LFERs and Prediction of Worm BCFs

The prediction of worm BCFs was performed substituting Eq. (4-4) into Eq. (4-3) for the K_{Lipid}, which yields

$$BCF_i = \left[f_{Lipid}\, 10^{(c+eE+sS+aA+bB+vV)} + f_{Protein}\, K_{i_{Protein}} + \frac{f_{Water}}{\rho_{Water}} \right] \frac{1}{f_{dwt}} \quad (4\text{-}10)$$

where values for f_{Lipid}, $f_{Protein}$, f_{Water}, and f_{dwt} were obtained from the literature (Table C-4 in Appendix C), $K_{i_{Protein}}$ were estimated using Eq. (4-6), and the solute descriptors, uppercase letters in Eq. (4-4), were QCAP reported by Liang [31] (Table C-5 in Appendix C), and the solvent parameters, lowercase letters in Eq. (4-4), were the result of the MLRA to the worm BCFs.

The predicted BCFs using Eq. (4-10) are shown in Fig. 4-1. The regression yielded a RMSE = 0.499, indicating that approximately 68% of the predicted BCFs fall within ± 0.499 log units (a factor of ± 3.16) of the corresponding observed BCF. The color coding in Fig. 4-1 allows to identify each data point by compound (Fig. 4-1A), exposure medium (Fig. 4-1B), and worm species (Fig. 4-1C). The BCFs

covered a range of approximately five orders of magnitude ($0.664 < \log BCF < 5.389$) for which MCs and MLCs constitute the lower end of the range (Fig. 4-1A). No bias was observed for the prediction of any compound.

On the other hand, the RMSE of the predictions depended on the exposure media (Fig. 4-1B) with RMSEs for each group increasing in the order of sand < water < soil < sediment (0.177, 0.365, 0.467, and 0.768, respectively). This was expected as the concentrations measured in worms and exposure phase in experiments with sediments or soils are less reliable than those in assays with sand or water. This is due to the analytical challenges to collect worms or interstitial water (i.e., exposure phase) from sediment or soil without also disturbing the sample and changing it in some way, for example by oxidation.

No trend was observed in the prediction as a function of the worm being terrestrial or aquatic (Fig. 4-1C), suggesting that the model could be applied to a variety of worm species.

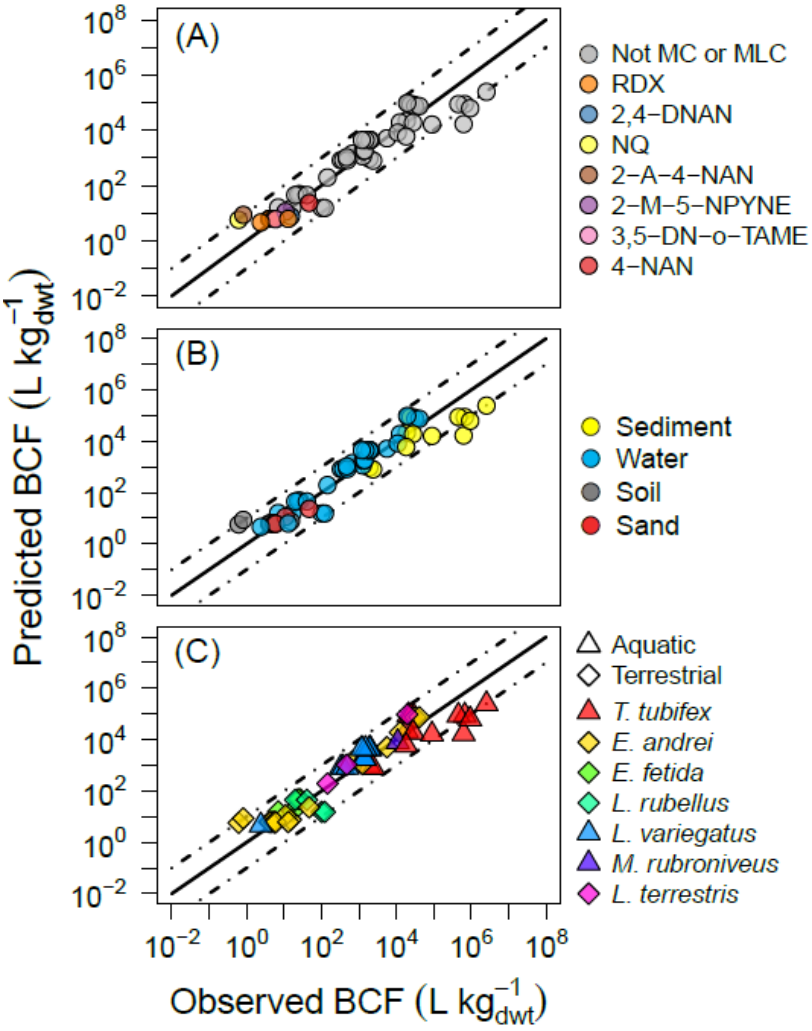

Figure 4-1 Predicted versus observed BCFs for organic compounds (Table C-6 in Appendix C). Predictions made using a BCF model (Eq. (4-10)) with partitioning to three worm components, lipid (Eq. (4-11)), protein (Eq. (4-6)), and internal water. Color coding assigned based on: (A) organic compound, (B) exposure medium, and (C) worm species. Root mean square error of prediction (log predicted - log observed BCF), RMSE = 0.499. Abbreviations defined in Tables C-1 and C-2 in Appendix C. The solid line indicates the best agreement (unity), dashed lines are spaced at 1 log unit from unity.

The K_{Lipid} pp–LFER obtained in this work with the MLRA described for Eq. (4-10) using exclusively BCF worm data was

$$\begin{aligned}\log K_{Lipid} = {} & 0.751\ (\pm 0.780) + 0.431\ (\pm 0.189)E - 2.409\ (\pm 0.387)S \\ & - 0.787\ (\pm 0.393)A - 2.106\ (\pm 0.793)B \\ & + 4.553\ (\pm 0.673)V \\ & 27 \text{ compounds; } \mathrm{N} = 60\end{aligned} \tag{4-11}$$

where the solvent parameters, lowercase variables in Eq. (4-4), resulted to be very similar to those in the K_{Lipid} pp–LFER obtained by Kuo and Di Toro [30,33] with lipid–water partitioning data from multiple sources including fish fat/oil (Eq. (4-5)). Both Eq. (4-5) and Eq. (4-11) exhibit the same competitiveness of the lipid phase relative to water as the signs of the solvent parameters are the same for all types of molecular interactions and, with the exception of s, the values are not different at the 5% level of statistical significance (Table C-7 in Appendix C).

Given the similarities between these two K_{Lipid} pp–LFERs, a comparison of predictions for the BCF worm data was performed using either the K_{Lipid} pp–LFER by Kuo and Di Toro [30,33] (Eq. (4-5)) or that obtained in this work (Eq. (4-11)) and shown in Fig. 4-2. The BCF model (Eq. (4-3)) was able to capture the linear variation in the observed worm BCFs in spite of using a K_{Lipid} pp–LFER not trained specifically with worm data (Fig. 4-2B). The underprediction of three organochlorines in the higher end of the dataset (Fig. 4-2) appears to be an artifact of the experimental measurements as all three observations are from the same study and are approximately two orders of magnitude higher than values corresponding to the same compounds (1,2,3,4-tetrachlorobenzene; pentachlorobenzene; and hexachlorobenzene) and worm species (*Tubifex tubifex*) reported by other studies also included in the set (Tables C-2 in

Appendix C). No bias was observed in the prediction of any of the eight chemical classes in particular.

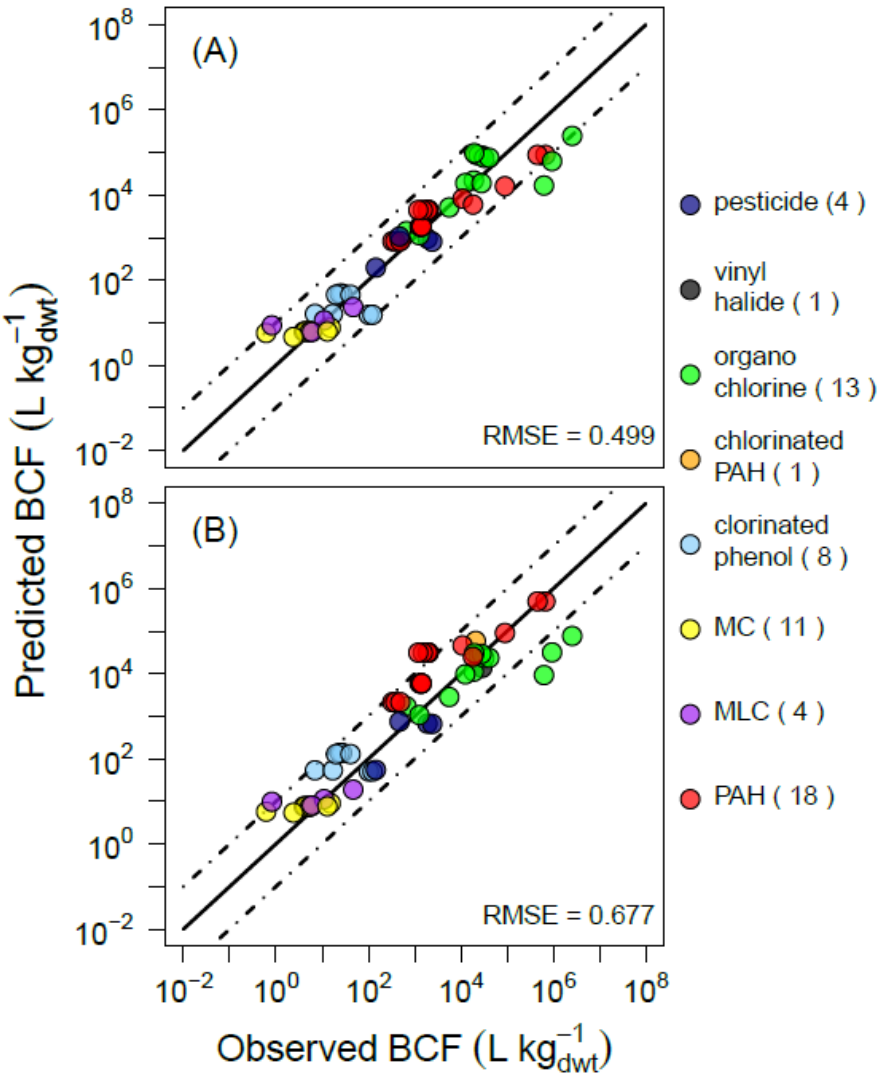

Figure 4-2 Predicted versus observed BCFs for organic compounds (Table C-6 in Appendix C). Predictions made using a partition–based BCF model (Eq. (4-3)) with the K_{Lipid} pp–LFER from (A) this work (Eq. (4-11)) or (B) Kuo and Di Toro [30,33] (Eq. (4-5)). Legend: Chemical class with corresponding count; PAH: polycyclic aromatic hydrocarbon. RMSE: Root mean square error of prediction (log predicted - log observed BCF). The solid line indicates the best agreement (unity), dashed lines are spaced at 1 log unit from unity.

Obtaining a RMSE for the prediction with Eq. (4-5) (RMSE = 0.677) that is larger than that using Eq. (4-11) (RMSE = 0.499) is expected since unlike the K_{Lipid} pp–LFER built in this work, the K_{Lipid} pp–LFER by Kuo and Di Toro [30,33] is not fitted to the data. Fig. 4-2B is an independent prediction of the observed worm BCFs. The fact that a reasonable uncertainty in the estimation of worm BCFs is obtained using a K_{Lipid} pp–LFER not specific to worms suggests that the solvation properties of worm lipid and lipid from other organisms such as fish are indeed similar. Therefore, it appears that the resulting concentration in the worm is mostly chemical–specific, rather than species–specific.

The contribution of the three worm components (lipid, protein, and water) to the predicted BCFs varied among chemical classes, as shown in Fig. 4-3, a comparison of the fraction contributed to the BCFs by each worm component. Considerable differences were also found within the MCs (NQ; RDX; 2,4-DNAN) and MLCs (3,5-DN-o-TAME; 2-A-4-NAN; 2-M-5-NPYNE; 4-NAN) and thus they are not grouped together in Fig. 4-3. The contributions were more uniform within the other chemical classes; therefore, the values in Fig. 4-3 are the average for each of these classes.

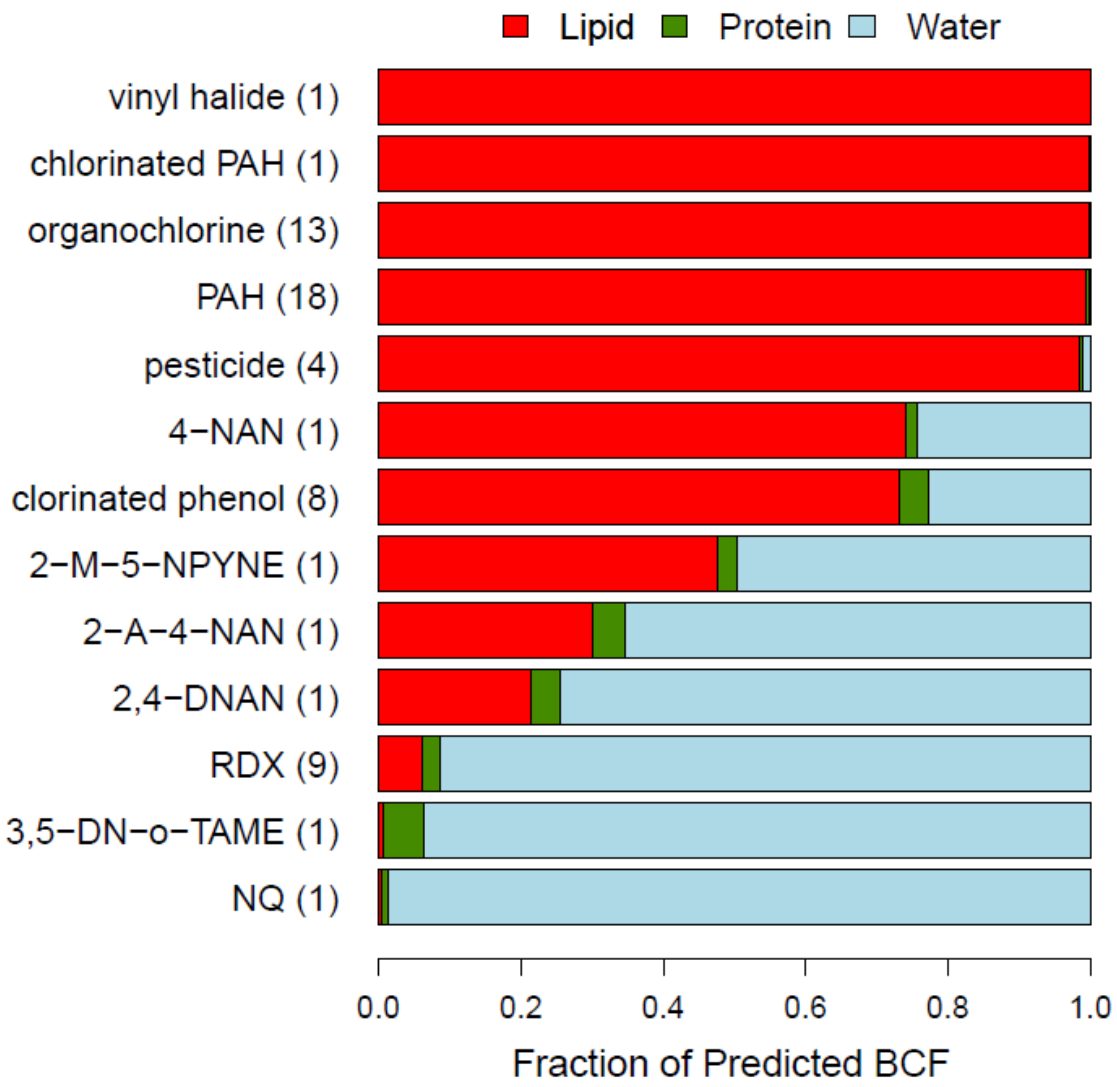

Figure 4-3 Contribution of worm components (lipid, protein and internal water) to the predcited BCF (Eq.(4-3)) for MCs, MLCs, and other chemical classes in the worm dataset presented in Fig. 4-1. Prediction of partitioning to lipid component made using K_{Lipid} pp–LFER from this work (Eq. (4-11)), and to protein component using $K_{Protein}$ pp–LFER from Kuo and Di Toro [30,33] (Eq. (4-6)). Numbers in parenthesis are the corresponding count. Abbreviations are defined in Tables C-1 and C-2 in Appendix C.

Lipid rose to be the dominant phase for chlorinated phenols, pesticides, PAHs, organochlorines, chlorinated PAHs, and vinyl halides (Fig. 4-3), while water

contributed the most to the worm BCFs for all MCs and MLCs with the exception of 4-NAN. Protein resulted to be the phase with no dominant contributions to the BCFs for all chemicals classes including MCs and MLCs (Fig. 4-3). A reason is that despite the high content of this phase in worms (approximately $10\%_{wwt}$, Table C-3 in Appendix C), the energy required for cavity formation in protein is considerably larger in comparison to that needed in lipid. This is indicated by the wide positive difference for v in Table 4-3 (3.49), a comparison of the solvent parameters between lipid (K_{Lipid} pp–LFER from this work) and protein. In addition to v, a large difference was also found for the dipolarity/polarizability solvent descriptor, s, (Table 4-3), but in this case the discrepancy favors the protein phase (-2.04).

Table 4-3 Comparison of the competitiveness for solutes between lipid and protein, calculated as the difference between the solvent parameters in the K_{Lipid} obtained in this work and $K_{Protein}$ pp–LFER obtained by Kuo and Di Toro [30,33], Eq. (4-11) and Eq. (4-6), respectively.

Solvent parameter	Phase		Difference
	Lipid	Protein	
e	0.43	0.74	-0.31
s	-2.41	-0.37	-2.04
a	-0.79	-0.13	-0.66
b	-2.11	-1.37	-0.74
v	4.55	1.06	3.49

The effect of these contrasting solvation capabilities on the resulting K_{Lipid} and $K_{Protein}$, and ultimately on the predicted worm BCF, for this set of organic compounds is examined more in depth in Fig. 4-4. Fig. 4-4 pairs the effect of the solvation capabilities with the complementary response from the compounds studied, i.e., a

solvent–solute product (xX). Most of the xX values for the protein phase are near 0 and none are above 3 (Fig. 4-4). This illustrates the very low effectiveness of protein to solvate these organic compounds, especially relative to lipid for which some xX values go up to approximately 8. Furthermore, the dipolarity/polarizability term that based only on the solvent parameters favors partition to protein over lipid (Table 4-3), shows sS values that while not being as negative as the lipid sS are all < 0, making protein noncompetitive for solutes relative to water neither.

The major role in the partitioning between lipid and water is played by the cavity formation (vV) and dipolarity/polarizability (sS) interactions which are -6.3 < sS < -1.2 and 3.0 < vV < 8.3, respectively (Fig. 4-4). Chemical classes of a less polar nature and demanding more energy for cavity formation due to their larger molecular volumes, such as PAHs and organochlorines, have larger values for sS and vV (Fig. 4-4), and thus show the most substantial contributions from the lipid phase to the predicted worm BCF (Fig.4-4). In contrast, compounds that have smaller molecular volumes and are of a more polar nature, such as most of the MCs and MLCs, have smaller values for sS and vV (Fig. 4-4), and thus show the most substantial contributions from the water phase to the predicted worm BCF (Fig.4-3). The effect from the dispersion interactions (eE) and the donation and acceptance of hydrogen bonds (aA and bB) to either the K_{Lipid} or the K_{Protein} were very small with values between -1.80 and 2.61 (Fig. 4-4), which is a very narrow range relative to that covered by the sS and vV terms (-6.3 to 8.3).

These results add to the importance of chemical–specificity and molecular interactions on the bioconcentration of nonionic organic compounds in worms.

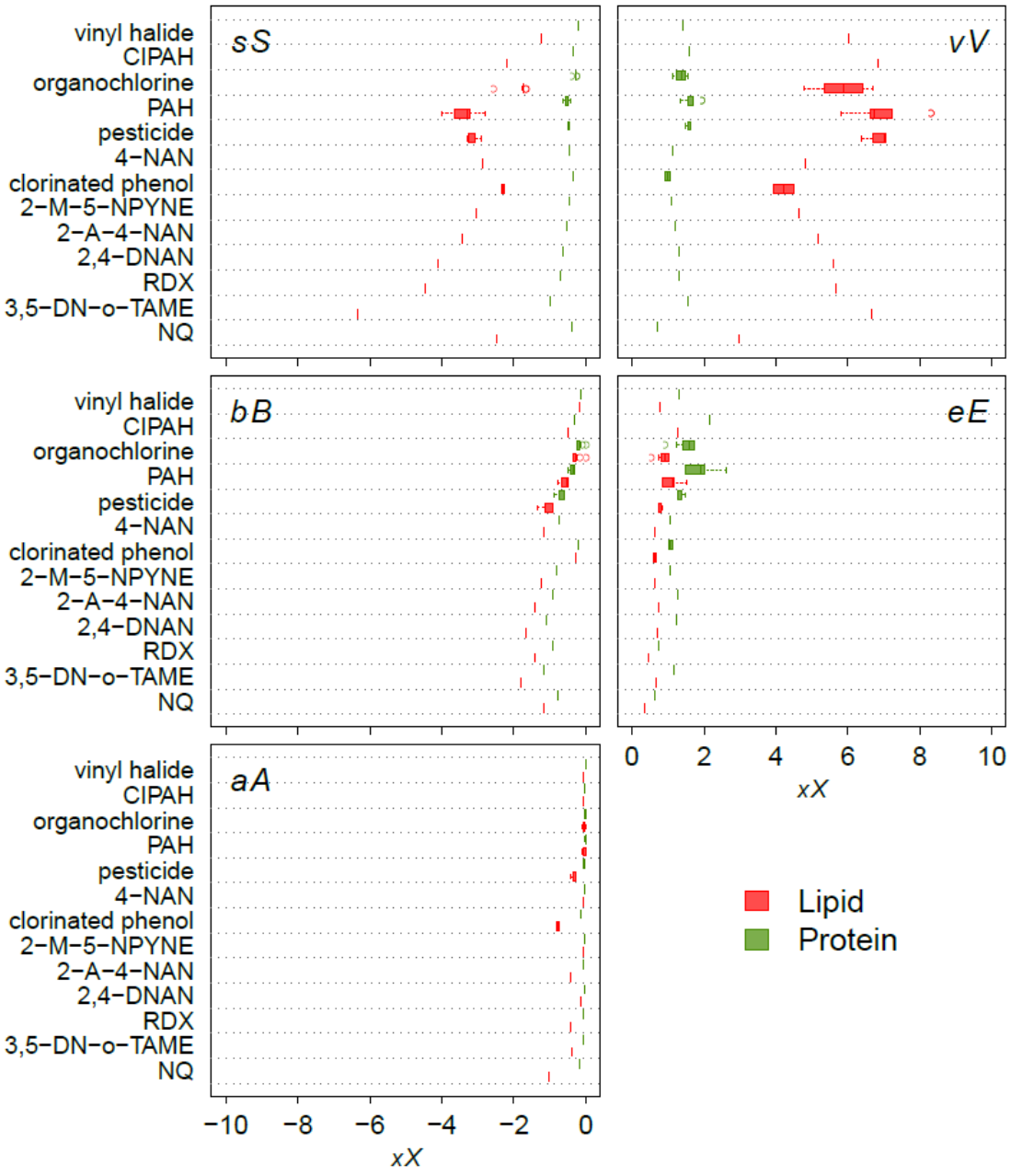

Figure 4-4 Contribution from solute–solvent products (xX, Eq. (4-4)) to the predicted log K_{Lipid} (Eq. (4-11)) and log $K_{Protein}$ (Eq. (4-6)) for MCs, MLCs, and other chemical classes in the worm BCF dataset presented in Fig. 4-1.

4.3.2 Prediction of Concentrations in Worms from Independent Uptake Assays

Predictions of concentrations in worms for MCs using the BCF model are shown in Fig. 4-5 (Tables C-8 to C-11 in Appendix C). The final equation used to predict the worm concentration is Eq. (4-12) in Table 4-4, which contains the equations used ordered in the sequence to generate a prediction. In Eq. (4-12), the $C_{i_{Soil}}$ and f_{OC} were obtained directly from the source of the uptake assay (Table C-8 in Appendix C), worm values for f_{Lipid}, $f_{Protein}$, f_{Water}, and f_{dwt} were from the literature (Table C-9 in Appendix C), and $K_{i_{Lipid}}$, $K_{i_{Protein}}$, and K_{OC} were estimated using the pp–LFERs in Eq. (4-5) (or Eq. (4-11)), Eq. (4-6), and Eq. (4-7), respectively.

Table 4-4 Sequence of equations for the prediction of concentrations in worms exposed to MCs, or MLCs, in soil.

A partition–based worm bioconcentration model[a]:

$$C_{i_{Worm}} = \left(f_{Lipid}\, K_{i_{Lipid}} + f_{Protein}\, K_{i_{Protein}} + \frac{f_{Water}}{\rho_{Water}}\right)\frac{C_{i_{Soil\,Solids}}}{f_{dwt}\, f_{OC}\, K_{i_{OC}}} \qquad (4\text{-}12)$$

Var.	Equation	#
$K_{i_{OC}}$	$\log K_{OC} = 0.670 + 1.075E - 0.277S - 0.363A - 1.697B + 1.468V$	(4-7)
$C_{i_{IW}}$	$C_{i_{IW}} = \frac{C_{i_{Soil\,Solids}}}{K_{i_{OC}} f_{OC}}$	(4-8)
$K_{i_{Lipid}}$	$\log K_{Lipid} = 0.84 + 0.77E - 1.10S - 0.47A - 3.52B + 3.37V$	(4-5)
$K_{i_{Lipid}}$	$\log K_{Lipid} = 0.751 + 0.431E - 2.409S - 0.787A - 2.106B + 4.553V$	(4-11)
$K_{i_{Protein}}$	$\log K_{Protein} = -0.88 + 0.74E - 0.37S - 0.13A - 1.37B + 1.06V$	(4-6)
$C_{i_{Worm}}$	$C_{i_{Worm}} = \left(f_{Lipid}\, K_{i_{Lipid}} + f_{Protein}\, K_{i_{Protein}} + \frac{f_{Water}}{\rho_{Water}}\right)\frac{C_{i_{IW}}}{f_{dwt}}$	(4-9)

[a] Var.: Variables; i: MC, or MLC, of interest; $C_{i_{Worm}}$: concentration of i in the worm (mg kg_{dwt}^{-1}); f_{Lipid} and $f_{Protein}$: wet weight worm fraction of lipid and protein, respectively (kg_{lipid} $kg_{wwt\ worm}^{-1}$ and $kg_{protein}$ $kg_{wwt\ worm}^{-1}$, wwt: wet weight); $K_{i_{Lipid}}$ and $K_{i_{Protein}}$: lipid–water and protein–water partition coefficients of i, respectively (L_{water} kg_{lipid}^{-1} and L_{water} $kg_{protein}^{-1}$); f_{Water} and f_{dwt}: worm mass fraction of water and dry weight, respectively (kg_{water} $kg_{wwt\ worm}^{-1}$ and kg_{dwt} $kg_{wwt\ worm}^{-1}$); ρ_{Water}: density of water (kg_{water} L_{water}^{-1}); $C_{i_{Soil\ Solids}}$: concentration of compound i in the soil solids (mg kg_{dwt}^{-1}); f_{OC}: dry weight fraction of organic carbon in the soil (kg_{OC} $kg_{dwt\ soil}^{-1}$); $K_{i_{OC}}$: organic carbon–water partition coefficient of i (L_{water} kg_{OC}^{-1}); E, S, A, B, and V: QCAP for i (Table C-9 in Appendix C); $C_{i_{IW}}$: dissolved concentration of i in the interstitial water (IW) (mg L^{-1})

Concentrations exceeding the aqueous solubility in the soil interstitial water were obtained when predicting the dissolved concentration from the reported soil concentrations for RDX and HMX (Table C-1 in Appendix C), as shown in Fig. 4-5. Often very large concentrations, up to 10000 mg kg_{dwt}^{-1}, of a compound of interest are applied to the soil at the beginning of uptake assays in order to compensate for the losses of the parent compound due to transformation/degradation processes and/or to overcome analytical limitations in the detection of compounds with low aqueous solubilities [37-39]. However, these large concentrations result in both sorbed and pure compound in the soil. In order to predict the concentration in the worm for these cases, it was assumed that the dissolved concentration was at the solubility of the compound and not at the predicted concentration based on a measured soil concentration. This is the reason that the predicted worm concentration is constant for RDX and HMX in Fig. 4-5. Also, because the prediction was based on an assumed concentration (solubility of the compound) these data were not included in the calculation of the RMSE for the models.

The RMSEs for the model using either K_{Lipid} pp–LFER (Eq. (4-11) or Eq. (4-5)) were RMSE = 0.396 (Fig. 4-5A) and RMSE = 0.523 (Fig. 4-5B), which

parallels the result obtained for the predictions of BCFs from experiments with measured concentrations in the interstitial water (RMSE = 0.499) (Fig. 4-2A) and (RMSE = 0.677) (Fig. 4-2B). The reason for the difference is that the model in panel (A) uses the K_{Lipid} pp–LFER fitted to the BCF worm data, whereas the model in panel (B) uses the K_{Lipid} pp–LFER by Kuo and Di Toro [30,33], which was calibrated to a set of partitioning data from various lipid sources.

The BCF model (Eq. (4-12)) was able to predict worm concentrations for a small but chemically heterogeneous MCs dataset including nitramines (e.g., RDX, abbreviations for MCs are defined in Table C-1 in Appendix C) and nitroaromatics (e.g., TNT) as well as new insensitive MCs (e.g., 2,4-DNAN) [40]. These MCs have diverse molecular structures and functional groups that interact to a different degree with the lipid and protein phases making the prediction of the concentration in the worm components challenging. While the differences among MCs are considerably smaller than those relative to other chemical classes, the BCF model employs pp–LFERs that are sensitive to these variations via the solute Abraham parameters. For example, RDX, TNT, and 2,4-DNAN are described by different values for their ability to undergo hydrogen bonding donation (A: 0.528, 0.302, 0.187, respectively; Table C-9 in Appendix C), and RDX and TNT have distinctive values for the extent of their interactions through dispersion forces (E: 1.020 and 1.660, respectively; Table C-9 in Appendix C).

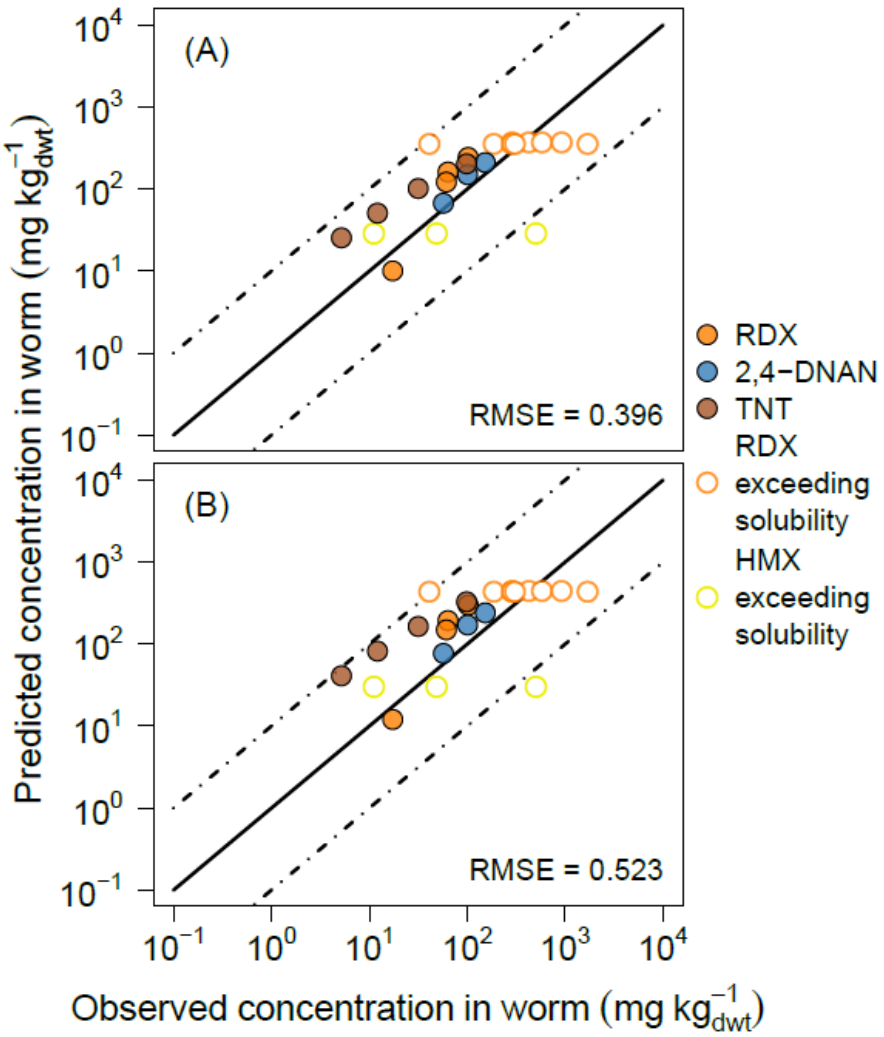

Figure 4-5 Predicted versus observed concentrations of MCs in worms from independent studies. Predictions made using a partition–based model (Eq. (4-12)) with the K_{Lipid} pp–LFER from (A) this work (Eq. (4-11)) or (B) Kuo and Di Toro [30,33] (Eq. (4-5)). Unfilled symbols represent predictions made with concentrations in the interstitial water at aqueous solubility. RMSE: Root mean square error (log predicted - log observed concentration in worm), excluding predictions at aqueous solubility. The solid line indicates the best agreement (unity), dashed lines are spaced at 1 log unit from unity.

The results shown in Fig. 4-5 are for the prediction of data that were not part of the calibration of either BCF model. In this way, Fig. 4-5 serves as a validation for the underlying assumptions of the BCF model (Eq. (4-12)), those are, (1) the uptake from soil is mainly from passive diffusion, and (2) the worm components playing a major role in the bioconcentration of MCs are lipid, protein, and water.

4.4 Conclusions

Worm bioconcentration factors can be predicted based on the partitioning to three main worm components: lipid, protein, and internal water. The individual contribution of the components to the bioconcentration was dependent on the chemical compound. Compounds that interact mostly through dispersive forces embedded in the cavity formation (vV) and dispersion (eE) terms, such as PAHs and organochlorines, showed a large preference for worm lipid. Compounds that are of a more polar nature interacting predominantly through polarizability (sS) and hydrogen bonding (aA and bB), such as RDX and NQ, concentrated mostly in the worm internal water. The prediction uncertainties for the estimation of the worm BCFs were low using either a lipid–water pp–LFER trained exclusively with worm data (RMSE = 0.499; Eq. (4-11)) or one trained with data from various sources of lipids including fish fat/oil (RMSE = 0.677; Eq. (4-5)). No bias was observed in the model predictions as a function of the worm being a terrestrial or aquatic species, suggesting partitioning to the lipid phase has little dependence on the organism species, something which would be expected for a chemical–dominated process. In this way, the abundant amount of lipid–water partitioning data available for organisms like fish can be used to make a baseline prediction of the BCFs for worms for which limited data exists.

Concentrations in worms exposed to MCs in soil during independent uptake assays were estimated based only on the partitioning between soil organic carbon and interstitial water, and between water and worm components. Using this modeling frame, observed values were predicted within ± 0.396 log units (or ± 0.523, depending on the K_{Lipid} pp–LFER used for the lipid contribution). This indicates that the concentration available for worm uptake can be predicted from partitioning between soil interstitial water organic carbon, and that partitioning to worm components can estimate the extent of the bioconcentration to be expected.

These results demonstrate the ability of the BCF model to make reasonable estimates without relying on experimental measurements and using only molecular structure to compute the required model parameters. This is particularly useful when data for a specific organism are scarce, predictions need to be made for large libraries of compounds, and/or environmental risk needs to be assessed for compounds in the development stage.

REFERENCES

This list includes references cited in Appendix C.

1. Grdisa M, Grsic K, Grdisa MD. Earthworms - role in soil fertility to the use in medicine and as a food. *Isj-Invert Surviv J*. 2013;10(1):38-45.

2. Organisation for Economic Co-operation and Development. Test No. 315: Bioaccumulation in sediment-dwelling benthic oligochaetes. In: *OECD guidelines for the testing of chemicals, Section 3.* Paris, France: OECD Publishing. 2008.

3. Organisation for Economic Co-operation and Development. Test No. 317: Bioaccumulation in terrestrial oligochaetes. In: *OECD guidelines for the testing of chemicals, Section 3.* Paris, France: OECD Publishing. 2010.

4. Frund HC, Graefe U, Tischer S. Earthworms as bioindicators of soil quality. In: Karaca A, ed. *Biology of earthworms. Soil biology*. Berlin, Heidelberg, Germany: Springer Berlin Heidelberg; 2011:261-278.

5. Jager T. Mechanistic approach for estimating bioconcentration of organic chemicals in earthworms (oligochaeta). *Environ Toxicol Chem*. 1998;17(10):2080-2090.

6. Frank AP, Landrum PF, Eadie BJ. Polycyclic aromatic hydrocarbon rates of uptake, depuration, and biotransformation by lake michigan stylodrilus heringianus. *Chemosphere*. 1986;15(3):317-330.

7. Gabric AJ, Connell DW, Bell PRF. A kinetic model for bioconcentration of lipophilic compounds by oligochaetes. *Water Res*. 1990;24(10):1225-1231.

8. Belfroid AC, Seinen W, van Gestel KCAM, Hermens JLM, van Leeuwen KJ. Modelling the accumulation of hydrophobic organic chemicals in earthworms - application of the equilibrium partitioning theory. *Environ Sci Pollut Res*. 1995;2(1):5-15.

9. Belfroid AC, Sijm DTHM, Van Gestel CAM. Bioavailability and toxicokinetics of hydrophobic aromatic compounds in benthic and terrestrial invertebrates. *Env Rev*. 1996;4(4):276-299.

10. Jager T. Modeling ingestion as an exposure route for organic chemicals in earthworms (oligochaeta). *Ecotoxicol Environ Saf*. 2004;57(1):30-38.

11. Hu XY, Wen B, Shan XQ, Zhang SZ. Bioavailability of pentachlorophenol to earthworms (eisenia fetida) in artificially contaminated soils. *J Environ Sci Health A Tox hazard Subst Environ Eng*. 2005;40(10):1905-1916.

12. Henson-Ramsey H, Levine J, Kennedy-Stoskopf S, Taylor SK, Shea D, Stoskopf MK. Development of a dynamic pharmacokinetic model to estimate

bioconcentration of xenobiotics in earthworms. *Environ Model Assess*. 2009;14(3):411-418.

13. Peijnenburg W, Capri E, Kula C, Liess M, Luttik R, Montforts M, Nienstedt K, Rombke J, Sousa JP, Jensen J. Evaluation of exposure metrics for effect assessment of soil invertebrates. *Crit Rev Environ Sci Technol*. 2012;42(17):1862-1893.

14. Jager T, Fleuren RHLJ, Hogendoorn EA, De Korte G. Elucidating the routes of exposure for organic chemicals in the earthworm, eisenia andrei (oligochaeta). *Environ Sci Technol*. 2003;37(15):3399-3404.

15. Lord KA, Briggs GG, Neale MC, Manlove R. Uptake of pesticides from water and soil by earthworms. *Pestic Sci*. 1980;11(4):401-408.

16. van Gestel CAM, Ma WC. Toxicity and bioaccumulation of chlorophenols in earthworms, in relation to bioavailability in soil. *Ecotoxicol Environ Saf*. 1988;15(3):289-297.

17. Connell DW, Markwell RD. Bioaccumulation in the soil to earthworm system. *Chemosphere*. 1990;20(1):91-100.

18. Belfroid A, van Wezel A, Sikkenk M, van Gestel K, Seinen W, Hermens J. The toxicokinetic behavior of chlorobenzenes in earthworms (eisenia andrei): Experiments in water. *Ecotoxicol Environ Saf*. 1993;25(2):154-165.

19. Bruns E, Egeler P, Roembke J, Scheffczyk A, Spoerlein P. Bioaccumulation of lindane and hexachlorobenzene by the oligochaetes enchytraeus luxuriosus and enchytraeus albidus (enchytraeidae, oligochaeta, annelida). *Hydrobiologia*. 2001;463(1-3):185-196.

20. Larson SL, Martin WA, Escalon BL, Thompson M. Dissolution, sorption, and kinetics involved in systems containing explosives, water, and soil. *Environ Sci Technol*. 2007;42(3):786-792.

21. Sharma P, Mayes MA, Tang G. Role of soil organic carbon and colloids in sorption and transport of TNT, RDX and HMX in training range soils. *Chemosphere*. 2013;92(8):993-1000.

22. von Oepen B, Kördel W, Klein W, Schüürmann G. QSAR in environmental toxicology predictive QSPR models for estimating soil sorption coefficients: Potential and limitations based on dominating processes. *Sci Total Environ*. 1991;109/110:343-354.

23. Wei DB, Wu CD, Wang LS, Hu HY. QSPR-based prediction of adsorption of halogenated aromatics on yellow-brown soil. *SAR QSAR Environ Res*. 2003;14(3):191-198.

24. Kozerski GE, Xu S, Miller J, Durham J. Determination of soil-water sorption coefficients of volatile methylsiloxanes. *Environ Toxicol Chem*. 2014;33(9):1937-1945.

25. Abraham MH. Scales of solute hydrogen-bonding: Their construction and application to physicochemical and biochemical processes. *Chem Soc Rev*. 1993;22(2):73-83.

26. Goss KU. Predicting the equilibrium partitioning of organic compounds using just one linear solvation energy relationship (LSER). *Fluid Phase Equilibr*. 2005;233(1):19-22.

27. Oliver BG. Biouptake of chlorinated hydrocarbons from laboratory-spiked and field sediments by oligochaete worms. *Environ Sci Technol*. 1987;21(8):785-790.

28. Belden JB, Lotufo GR, Lydy MJ. Accumulation of hexahydro-1,3,5-trinitro-1,3,5-triazine in channel catfish (*ictalurus punctatus*) and aquatic oligochaetes (*lumbriculus variegatus*). *Environ Toxicol Chem*. 2005;24(8):1962-1967.

29. Savard K, Sarrazin M, Dodard SG, Monteil-Rivera F, Kuperman RG, Hawari J, Sunahara GI. Role of soil interstitial water in the accumulation of hexahydro-1,3,5-trinitro-1,3,5-triazine in the earthworm *Eisenia andrei*. *Environ Toxicol Chem*. 2010;29(4):998-1005.

30. Kuo DTF, Di Toro DM. A reductionist mechanistic model for bioconcentration of neutral and weakly polar organic compounds in fish. *Environ Toxicol Chem*. 2013;32(9):2089-2099.

31. Liang Y. Determining Abraham solute and system parameters for neutral organic compounds using quantum chemical methods. Newark, DE: University of Delaware. 2016;[Doctoral Dissertation].

32. Lin ST, Sandler SI. A priori phase equilibrium prediction from a segment contribution solvation model. *Ind Eng Chem Res*. 2002;41(5):899-913.

33. Kuo DTF, Di Toro DM. Biotransformation model of neutral and weakly polar organic compounds in fish incorporating internal partitioning. *Environ Toxicol Chem*. 2013;32(8):1873-1881.

34. Kipka U, Di Toro DM. A linear solvation energy relationship model of organic chemical partitioning to particulate organic carbon in soils and sediments. *Environ Toxicol Chem*. 2011;30(9):2013-2022.

35. US Environmental Protection Agency. Estimation Programs Interface (EPI) Suite™ for Microsoft® Windows, v. 4.11. Washington, D.C: US EPA. 2012.

36. Pribyl DW. A critical review of the conventional SOC to SOM conversion factor. *Geoderma*. 2010;156(3–4):75-83.

37. Best EPH, Geter KN, Tatem HE, Lane BK. Effects, transfer, and fate of RDX from aged soil in plants and worms. *Chemosphere*. 2006;62(4):616-625.

38. Sarrazin M, Dodard SG, Savard K, Lachance B, Bobidoux PY, Kuperman RG, Hawari J, Ampleman G, Thiboutot S, Sunahara GI. Accumulation of hexahydro-1,3,5-trinitro-1,3,5-triazine by the earthworm eisenia andrei in a sandy loam soil. *Environ Toxicol Chem*. 2009;28(10):2125-2133.

39. Sunahara GI. Development of toxicity benchmarks and bioaccumulation data for N-based organic explosives for terrestrial plants and soil invertebrates. Final Report No. SERDP ER-1416. Québec, Canada: National Research Council of Canada Montreal (Québec) Biotechnology Research Institute. 2012;1-289.

40. Hawari J, Monteil-Rivera F, Perreault NN, Halasz A, Paquet L, Radovic-Hrapovic Z, Deschamps S, Thiboutot S, Ampleman G. Environmental fate of 2,4-dinitroanisole (DNAN) and its reduced products. *Chemosphere*. 2015;119:16-23.

41. Kuperman RG, Simini M, Checkai RT, Dodard SG, Sarrazin M, Hawari J, Paquet L, Sunahara GI, Di Toro DM, Allen HE, Kuo DTF, Torralba-Sanchez TL. Developing earthworm bioconcentration factors of nitrogen-based compounds for predicting environmentally significant parameters for new munition compounds in soil. *Appl Soil Ecol*. 2016;104:25-30.

42. Branquart E, Deleu R, Copin A, Gaspar C. Bioaccumulation and metabolisation of isoproturon, linuron and lindane by *Lumbricus terrestris* L. *Meded Fac Landbouwkd Toegep Biol Wet Univ Gent*. 1995;609(2b):511-519.

43. Ankley GT, Erickson RJ, Sheedy BR, Kosian PA, Mattson VR, Cox JS. Evaluation of models for predicting the phototoxic potency of polycyclic aromatic hydrocarbons. *Aquat Toxicol*. 1997;37(1):37-50.

44. Kraaij RH, Tolls J, Sijm D, Cornelissen G, Heikens A, Belfroid A. Effects of contact time on the sequestration and bioavailability of different classes of hydrophobic organic chemicals to benthic oligochaetes (tubificidae). *Environ Toxicol Chem*. 2002;21(4):752-759.

45. Kraaij R, Mayer P, Busser FJM, van het Bolscher M, Seinen W, Tolls J. Measured pore-water concentrations make equilibrium partitioning work - A data analysis. *Environ Sci Technol*. 2003;37(2):268-274.

46. van der Wal L, Jager T, Fleuren RHLJ, Barendregt A, Sinnige TL, van Gestel CAM, Hermens JLM. Solid-phase microextraction to predict bioavailability and accumulation of organic micropollutants in terrestrial organisms after exposure to a field-contaminated soil. *Environ Sci Technol*. 2004;38(18):4842-4848.

47. Sun Z, Liu X, Sun L, Song C. Earthworm as a potential protein resource. *Ecol Food Nutr*. 1997;36(2-4):221-236.

48. Albro PW, Schroeder JL, Corbett JT. Lipids of the earthworm *Lumbricus-terrestris*. *Lipids*. 1992;27(2):136-143.

49. Finke MD. Complete nutrient composition of commercially raised invertebrates used as food for insectivores. *Zoo Biol*. 2002;21(3):269-285.

50. Liebig M, Egeler P, Oehlmann J, Knacker T. Bioaccumulation of ^{14}C-17α-ethinylestradiol by the aquatic oligochaete *Lumbriculus variegatus* in spiked artificial sediment. *Chemosphere*. 2005;59(2):271-280.

51. Croce V, De Angelis S, Patrolecco L, Polesello S, Valsecchi S. Uptake and accumulation of sediment-associated 4-nonylphenol in a benthic invertebrate (lumbriculus variegatus, freshwater oligochaete). *Environ Toxicol Chem*. 2005;24(5):1165-1171.

52. Ankley GT, Cook PM, Carlson AR, Call DJ, Swenson JA, Corcoran HF, Hoke RA. Bioaccumulation of pcbs from sediments by oligochaetes and fishes - comparison of laboratory and field studies. *Can J Fish Aquat Sci*. 1992;49(10):2080-2085.

53. Egeler P, Meller M, Roembke J, Spoerlein P, Streit B, Nagel R. Tubifex tubifex as a link in food chain transfer of hexachlorobenzene from contaminated sediment to fish. *Hydrobiologia*. 2001;463:171-184.

54. Gong P, Loh PR, Barker ND, Tucker G, Wang N, Zhang C, Escalon BL, Berger B, Perkins EJ. Building quantitative prediction models for tissue residue of two explosives compounds in earthworms from microarray gene expression data. *Environ Sci Technol*. 2012;46(1):19-26.

55. Dodard SG, Sarrazin M, Hawari J, Paquet L, Ampleman G, Thiboutot S, Sunahara GI. Ecotoxicological assessment of a high energetic and insensitive munitions compound: 2,4-dinitroanisole (DNAN). *J Hazard Mater*. 2013;262:143-150.

Chapter 5

SUMMARY, CONCLUSIONS, AND RECOMMENDATIONS

In this dissertation, experiments were designed and performed in a manner that the data produced could be used to build and evaluate a model for the estimation of MCs bioconcentration in plants. This and another model for worms were used to predict MCs concentrations in the organisms based on the partitioning between soil organic carbon, plant cuticle, worm lipid, worm protein, and water. Partition coefficients were estimated applying pp–LFERs with solute descriptors computed from molecular structure only using quantum chemical methods. The partition–based models were tested with independent data to evaluate their validity.

The experimental protocol presented in Chapter 2 had the objectives to generate reproducible steady state BCFs and evaluate the role that partitioning plays in the uptake of MCs by plants from contaminated growth media. These objectives determined the experimental design. The effects of other processes, such as degradation/transformation of the MCs in the exposure medium, on the resulting plant bioconcentration needed to be minimized. The use of coarse quartz sand, regarded as an essentially chemically and biologically inert material, in lieu of conventional spiked or contaminated field or synthetic soil together with the daily replenishment of the exposure solution, maintained an approximately constant concentration of the compound in the growth medium throughout the uptake assays. This showed that the proposed experimental protocol enabled to diminish the effects of the degradation/transformation processes on the resulting MCs bioconcentration. The use

of coarse quartz sand as the solid growth medium provided three additional advantages: (i) kept the MC concentration locally constant for plant root uptake as sorption onto the medium solids was not significant; (ii) allowed monitoring the exposure concentration with a simpler procedure than in a more complex soil as fluids drain through sand more readily; (iii) provided a solid exposure medium for normal plant root development. Using this experimental protocol, within a month reproducible steady state BCFs for barley were obtained for three nitroaromatic MCs and two MLCs. Exposure in sand with daily replenishment of the exposure solution was found to be a better alternative than exposure in a more complex soil with a one–time amendment of the compound for the determination of BCFs and the elucidation of mechanisms for barley uptake of MCs. Future investigation is suggested to measure BCFs with other plant species besides barley, including some outside the grasses family. These BCFs should be determined for both the MCs studied for plant uptake in this work and additional MCs, especially nitramines that have different chemical properties such as significantly lower aqueous solubilities. This would determine the extent to which the BCFs for MCs are plant species specific, and serve as further evaluation of the prediction capabilities for the plant cuticle–water partitioning model developed in this dissertation.

In Chapter 2, results from plant–water partitioning experiments were used to predict the barley BCFs. The log K_{PW} (plant–water partition coefficient) estimated the log BCF with less than an order of magnitude (0.2 to 0.7 log units) difference. BCFs for MCs that are known to be less susceptible to transformation/degradation processes, e.g., 2,4–DNAN, were predicted with smaller discrepancies relative to those for MCs known to be easily transformed, e.g., TNT. These discrepancies were attributed to the

transformation/degradation of the compounds within the plant during the uptake assays. The other possibilities were excluded by the experimental design. The effect of transformation/degradation processes taking place in the growth medium were minimized by maintaining an approximately constant exposure concentration of the parent compound and the partitioning experiments were performed in the presence of a biocide that suppressed microbial activity. This indicates that partitioning can be used as a baseline prediction of the uptake process. Future work would strengthen the K_{PW} prediction of BCFs by coupling it with estimates or measurements of the degradation rates of these compounds within plants.

Chapter 3 presented a model for the prediction of concentrations in plants exposed to MCs–contaminated growth media. The model was based on the partitioning of the compound between the growth medium solids and interstitial water, and between water and plant cuticle. A pp–LFER for the estimation of K_{Cut} (plant cuticle–water partition coefficient) was obtained by fitting partitioning data, including those obtained in Chapter 2, from a variety of plant species and nonionic organic compounds to a general Abraham polyparameter model using quantum chemically derived Abraham parameters (QCAP). This pp–LFER yielded a RMSE = 0.395 for the prediction of log K_{Cut}, the smallest RMSE among those obtained using other methods to estimate the Abraham parameters. Using the K_{Cut} pp–LFER and an existing K_{OC} pp–LFER for the prediction of the concertation in the soil interstitial water, the partition–based model estimated plant concentrations from independent validation uptake assays with a RMSE = 0.433. This suggests that the uptake from soil proceeds from the concentration in the interstitial water and that the subsequent tendency to sorb to plant biomass can be modeled using partitioning to cuticle. The cuticle content for many of

the plant species in the independent dataset were estimated from a similar species. A further refinement of the predictions could be made if specific values became available.

Finally, in Chapter 4, a similar partition–based model was built to predict the bioconcentration of MCs in worms. In addition to a lipid phase, however, partitioning to worm protein and worm internal water were also considered. Despite the larger content of protein than lipid in the worms on a wet weight basis (approximately an order of magnitude), the contribution from protein to the BCFs was not dominant for any compound in a training set that included MCs, PAHs, and organochlorines. Lipid was the favored phase for compounds undergoing molecular interactions almost exclusively through dispersion and polarizability, such as PAHs, while compounds with more tendency to interact through hydrogen bonds, such as NQ, preferred the worm internal water phase. Two pp–LFERs for the lipid–water partition coefficient K_{Lipid} were tested. One was built exclusively using worm data. The second one was an existing model calibrated to lipid–water partitioning data for lipids from various sources. Similar estimation uncertainties for the prediction of BCFs were obtained using either pp–LFER. This suggests that differences due to processes specific to the worm species examined in the training set are of secondary importance, and it highlights the relevance of chemical specificity. Using the partition–based model with the contributions from the three worm components (lipid, protein, and internal water) and the K_{OC} pp–LFER for the prediction of the concertation in the soil interstitial water, concentrations of MCs in worms observed in independent uptake experiments were predicted with a RMSE = 0.396. This adds support to the results obtained for plants in Chapter 3 that highlight the importance soil solid–soil interstitial water

sorption-desorption processes have in the bioavailability of MCs for uptake by plants and worms. Also, these results elucidate that a partition–based model with partition coefficients calculated from only molecular structure can serve as an estimation tool for the prediction of the bioconcentration of MCs in worms. Parallel to the recommendation for the plant model, a further refinement of the predictions for worms would likely be achieved if specific values for the content of lipid, water, and protein became available for the species in the BCF training set.

Overall, this dissertation shows that the uptake of MCs by plants and worms from soil is to a large extent determined by the partitioning between soil solids and soil interstitial water, and between water and organism biomass components. In this regard, the models developed in this work, which rely on predicted partition coefficients, can be used to estimate the upper–bound of the MCs bioconcentration in plants and worms from contaminated growth media.

Two extensions to this work would be (i) applying the plant and worm partition–based models to other nonionic organic contaminants of concern, this would test the underlying principles considered to build the models using compounds with a different suite of chemical functionalities; (ii) including an *in Vivo* biotransformation model analogous to that proposed for fish BCF in the work where the K_{Lipid} and K_{Protein} pp-LFERs for Chapter 4 were taken from. This biotransformation model uses pp-LFERs to estimate the whole–body biotransformation half–life for chemicals freely dissolved in the organism internal water that may bind with enzymes and subsequently undergo biotransformation reactions. The incorporation of *in Vivo* biotransformation into the partition–based models developed in this dissertation would refine their

predictions and support a new framework for the estimation of chemical reactivity in biological systems.

Appendix A

EXPERIMENTS WITH BARLEY EXPOSED TO MUNITIONS COMPOUNDS AND MUNITIONS –LIKE COMPOUNDS: SUPPORTING INFORMATION

Sections in this appendix are corresponding to those in Chapter 2. References cited are listed in the "REFERENCES" section of Chapter 2.

A.1 Plant Growth Conditions

Table A-1 Composition of aqueous solution used to supply nutrients for plant growth in sand.

Chemical	Concentration
	mol L^{-1}
$MgSO_4$	9.98×10^{-4}
KH_2PO_4	1.25×10^{-4}
KNO_3	2.50×10^{-3}
H_3BO_3	2.31×10^{-5}
$MnCl_2$	4.60×10^{-6}
$ZnSO_4$	3.83×10^{-7}
Na_2MoO_4	1.86×10^{-7}
$CaCl_2$	2.00×10^{-3}
MES	2.93×10^{-3}

A.2 Toxicity Screening

Table A-2 Barley shoot height and root elongation for each measured exposure concentration in toxicity screening with MCs and MLCs.

Compound	Exposure Concentration[a]	Replicate	Plant	Leaf Height	Root Elongation
	mg L^{-1}			cm	cm
TNT	0.00E+00	A	1	1.26E+01	6.60E+00
TNT	0.00E+00	A	2	1.86E+01	1.52E+01
TNT	0.00E+00	A	3	7.90E+00	4.40E+00
TNT	0.00E+00	A	4	1.10E+01	4.90E+00
TNT	0.00E+00	A	5	9.90E+00	6.30E+00
TNT	0.00E+00	A	6	1.06E+01	5.50E+00
TNT	0.00E+00	A	7	8.00E+00	5.50E+00
TNT	0.00E+00	A	8	5.60E+00	4.20E+00
TNT	0.00E+00	A	9	1.39E+01	8.50E+00
TNT	0.00E+00	A	10	1.31E+01	3.80E+00
TNT	0.00E+00	B	1	1.16E+01	6.80E+00
TNT	0.00E+00	B	2	1.18E+01	3.20E+00
TNT	0.00E+00	B	3	1.70E+01	1.45E+01
TNT	0.00E+00	B	4	1.31E+01	6.90E+00
TNT	0.00E+00	B	5	1.72E+01	1.08E+01
TNT	0.00E+00	B	6	1.36E+01	5.90E+00
TNT	0.00E+00	B	7	1.07E+01	4.00E+00
TNT	0.00E+00	B	8	8.80E+00	3.60E+00
TNT	0.00E+00	B	9	1.29E+01	5.20E+00
TNT	0.00E+00	B	10	1.02E+01	4.40E+00
TNT	0.00E+00	C	1	1.54E+01	1.20E+01
TNT	0.00E+00	C	2	7.20E+00	4.90E+00

TNT	0.00E+00	C	3	9.80E+00	6.10E+00
TNT	0.00E+00	C	4	1.57E+01	1.26E+01
TNT	0.00E+00	C	5	4.20E+00	1.90E+00
TNT	0.00E+00	C	6	6.10E+00	7.90E+00
TNT	0.00E+00	C	7	4.20E+00	4.00E+00
TNT	0.00E+00	C	8	5.50E+00	3.00E+00
TNT	0.00E+00	C	9	8.30E+00	6.00E+00
TNT	0.00E+00	C	10	1.25E+01	1.35E+01
TNT	6.90E-01	A	1	1.74E+01	1.05E+01
TNT	6.90E-01	A	2	1.01E+01	5.50E+00
TNT	6.90E-01	A	3	1.32E+01	6.30E+00
TNT	6.90E-01	A	4	1.45E+01	7.60E+00
TNT	6.90E-01	A	5	1.46E+01	4.90E+00
TNT	6.90E-01	A	6	1.51E+01	7.40E+00
TNT	6.90E-01	A	7	1.51E+01	7.60E+00
TNT	6.90E-01	A	8	1.61E+01	6.40E+00
TNT	6.90E-01	A	9	1.41E+01	6.30E+00
TNT	6.90E-01	A	10	1.52E+01	5.30E+00
TNT	6.90E-01	B	1	1.22E+01	5.10E+00
TNT	6.90E-01	B	2	1.46E+01	8.70E+00
TNT	6.90E-01	B	3	1.48E+01	1.20E+01
TNT	6.90E-01	B	4	1.61E+01	7.90E+00
TNT	6.90E-01	B	5	7.70E+00	4.30E+00
TNT	6.90E-01	B	6	1.53E+01	9.50E+00
TNT	6.90E-01	B	7	1.40E+01	7.60E+00
TNT	6.90E-01	B	8	1.54E+01	8.00E+00
TNT	6.90E-01	B	9	1.50E+01	7.40E+00
TNT	6.90E-01	B	10	1.54E+01	7.40E+00
TNT	6.90E-01	C	1	7.50E+00	7.00E+00
TNT	6.90E-01	C	2	6.30E+00	4.00E+00

TNT	6.90E-01	C	3	6.20E+00	7.50E+00
TNT	6.90E-01	C	4	6.50E+00	5.30E+00
TNT	6.90E-01	C	5	7.80E+00	6.20E+00
TNT	6.90E-01	C	6	7.90E+00	6.10E+00
TNT	6.90E-01	C	7	8.10E+00	5.20E+00
TNT	6.90E-01	C	8	7.00E+00	2.70E+00
TNT	6.90E-01	C	9	9.90E+00	3.90E+00
TNT	6.90E-01	C	10	1.16E+01	5.30E+00
TNT	7.54E+00	A	1	1.32E+01	1.04E+01
TNT	7.54E+00	A	2	1.72E+01	9.90E+00
TNT	7.54E+00	A	3	1.03E+01	6.60E+00
TNT	7.54E+00	A	4	1.21E+01	7.90E+00
TNT	7.54E+00	A	5	1.36E+01	7.00E+00
TNT	7.54E+00	A	6	1.01E+01	5.50E+00
TNT	7.54E+00	A	7	1.41E+01	8.00E+00
TNT	7.54E+00	A	8	9.60E+00	4.60E+00
TNT	7.54E+00	A	9	1.47E+01	7.70E+00
TNT	7.54E+00	A	10	1.44E+01	7.30E+00
TNT	7.54E+00	B	1	1.36E+01	5.40E+00
TNT	7.54E+00	B	2	1.04E+01	6.50E+00
TNT	7.54E+00	B	3	1.60E+01	4.50E+00
TNT	7.54E+00	B	4	1.02E+01	2.70E+00
TNT	7.54E+00	B	5	1.01E+01	4.40E+00
TNT	7.54E+00	B	6	1.34E+01	7.60E+00
TNT	7.54E+00	B	7	1.02E+01	5.90E+00
TNT	7.54E+00	B	8	1.44E+01	6.00E+00
TNT	7.54E+00	B	9	8.00E+00	4.10E+00
TNT	7.54E+00	B	10	9.60E+00	5.60E+00
TNT	7.54E+00	C	1	8.30E+00	3.50E+00
TNT	7.54E+00	C	2	6.00E+00	1.40E+00

TNT	7.54E+00	C	3	5.50E+00	1.30E+00
TNT	7.54E+00	C	4	4.60E+00	3.00E+00
TNT	7.54E+00	C	5	5.50E+00	4.10E+00
TNT	7.54E+00	C	6	8.50E+00	2.30E+00
TNT	7.54E+00	C	7	5.20E+00	2.80E+00
TNT	7.54E+00	C	8	7.80E+00	2.20E+00
TNT	7.54E+00	C	9	6.80E+00	3.50E+00
TNT	7.54E+00	C	10	9.20E+00	3.40E+00
TNT	3.87E+01	A	1	8.20E+00	7.00E+00
TNT	3.87E+01	A	2	1.54E+01	7.00E+00
TNT	3.87E+01	A	3	9.50E+00	6.10E+00
TNT	3.87E+01	A	4	1.04E+01	4.60E+00
TNT	3.87E+01	A	5	1.09E+01	6.50E+00
TNT	3.87E+01	A	6	9.10E+00	7.60E+00
TNT	3.87E+01	A	7	1.11E+01	6.80E+00
TNT	3.87E+01	A	8	1.12E+01	6.50E+00
TNT	3.87E+01	A	9	1.19E+01	5.80E+00
TNT	3.87E+01	A	10	1.55E+01	6.00E+00
TNT	3.87E+01	B	1	5.50E+00	4.90E+00
TNT	3.87E+01	B	2	5.80E+00	6.10E+00
TNT	3.87E+01	B	3	6.10E+00	3.50E+00
TNT	3.87E+01	B	4	6.50E+00	2.50E+00
TNT	3.87E+01	B	5	1.00E+01	4.40E+00
TNT	3.87E+01	B	6	8.70E+00	5.20E+00
TNT	3.87E+01	B	7	8.70E+00	3.10E+00
TNT	3.87E+01	B	8	1.28E+01	3.30E+00
TNT	3.87E+01	B	9	7.50E+00	4.40E+00
TNT	3.87E+01	B	10	1.16E+01	4.50E+00
TNT	3.87E+01	C	1	7.50E+00	4.50E+00
TNT	3.87E+01	C	2	5.40E+00	5.20E+00

TNT	3.87E+01	C	3	4.40E+00	3.90E+00
TNT	3.87E+01	C	4	5.10E+00	3.00E+00
TNT	3.87E+01	C	5	7.20E+00	4.10E+00
TNT	3.87E+01	C	6	6.30E+00	3.70E+00
TNT	3.87E+01	C	7	8.00E+00	7.00E+00
TNT	3.87E+01	C	8	6.10E+00	5.00E+00
TNT	3.87E+01	C	9	1.23E+01	7.10E+00
TNT	3.87E+01	C	10	6.10E+00	6.90E+00
TNT	7.47E+01	A	1	8.70E+00	5.10E+00
TNT	7.47E+01	A	2	9.50E+00	6.20E+00
TNT	7.47E+01	A	3	1.23E+01	8.00E+00
TNT	7.47E+01	A	4	1.17E+01	7.90E+00
TNT	7.47E+01	A	5	8.80E+00	6.10E+00
TNT	7.47E+01	A	6	1.17E+01	1.00E+01
TNT	7.47E+01	A	7	9.50E+00	4.90E+00
TNT	7.47E+01	A	8	1.18E+01	7.90E+00
TNT	7.47E+01	A	9	1.40E+01	1.01E+01
TNT	7.47E+01	A	10	1.16E+01	5.30E+00
TNT	7.47E+01	B	1	7.10E+00	4.00E+00
TNT	7.47E+01	B	2	4.80E+00	1.50E+00
TNT	7.47E+01	B	3	6.60E+00	3.20E+00
TNT	7.47E+01	B	4	4.30E+00	1.50E+00
TNT	7.47E+01	B	5	4.40E+00	2.10E+00
TNT	7.47E+01	B	6	6.40E+00	2.20E+00
TNT	7.47E+01	B	7	7.90E+00	2.00E+00
TNT	7.47E+01	B	8	6.10E+00	1.40E+00
TNT	7.47E+01	B	9	6.20E+00	2.30E+00
TNT	7.47E+01	B	10	6.70E+00	5.60E+00
TNT	7.47E+01	C	1	4.90E+00	3.40E+00
TNT	7.47E+01	C	2	9.20E+00	5.40E+00

TNT	7.47E+01	C	3	5.70E+00	4.30E+00
TNT	7.47E+01	C	4	8.60E+00	3.50E+00
TNT	7.47E+01	C	5	7.50E+00	5.50E+00
TNT	7.47E+01	C	6	4.70E+00	1.90E+00
TNT	7.47E+01	C	7	6.50E+00	5.00E+00
TNT	7.47E+01	C	8	5.40E+00	2.10E+00
TNT	7.47E+01	C	9	5.20E+00	1.50E+00
TNT	7.47E+01	C	10	6.00E+00	2.00E+00
2,4-DNT	0.00E+00	A	1	1.40E+01	9.10E+00
2,4-DNT	0.00E+00	A	2	9.80E+00	1.12E+01
2,4-DNT	0.00E+00	A	3	1.12E+01	3.70E+00
2,4-DNT	0.00E+00	A	4	1.47E+01	1.16E+01
2,4-DNT	0.00E+00	A	5	9.90E+00	5.50E+00
2,4-DNT	0.00E+00	A	6	1.35E+01	5.70E+00
2,4-DNT	0.00E+00	A	7	7.40E+00	3.70E+00
2,4-DNT	0.00E+00	A	8	1.40E+01	1.17E+01
2,4-DNT	0.00E+00	A	9	1.40E+01	1.40E+01
2,4-DNT	0.00E+00	A	10	1.18E+01	6.50E+00
2,4-DNT	0.00E+00	B	1	1.22E+01	1.22E+01
2,4-DNT	0.00E+00	B	2	1.31E+01	5.50E+00
2,4-DNT	0.00E+00	B	3	1.15E+01	9.00E+00
2,4-DNT	0.00E+00	B	4	1.09E+01	1.19E+01
2,4-DNT	0.00E+00	B	5	9.00E+00	1.05E+01
2,4-DNT	0.00E+00	B	6	8.60E+00	2.90E+00
2,4-DNT	0.00E+00	B	7	8.00E+00	6.00E+00
2,4-DNT	0.00E+00	B	8	1.27E+01	7.20E+00
2,4-DNT	0.00E+00	B	9	1.05E+01	5.60E+00
2,4-DNT	0.00E+00	B	10	1.55E+01	9.00E+00
2,4-DNT	1.06E+00	A	1	1.00E+01	2.50E+00
2,4-DNT	1.06E+00	A	2	6.20E+00	2.50E+00

2,4-DNT	1.06E+00	A	3	1.02E+01	9.00E+00
2,4-DNT	1.06E+00	A	4	9.20E+00	1.50E+00
2,4-DNT	1.06E+00	A	5	3.90E+00	6.10E+00
2,4-DNT	1.06E+00	A	6	1.46E+01	3.40E+00
2,4-DNT	1.06E+00	A	7	1.75E+01	1.40E+01
2,4-DNT	1.06E+00	A	8	1.21E+01	1.13E+01
2,4-DNT	1.06E+00	A	9	1.71E+01	1.40E+01
2,4-DNT	1.06E+00	A	10	5.30E+00	4.40E+00
2,4-DNT	1.06E+00	B	1	1.30E+01	8.50E+00
2,4-DNT	1.06E+00	B	2	6.50E+00	3.20E+00
2,4-DNT	1.06E+00	B	3	4.70E+00	6.60E+00
2,4-DNT	1.06E+00	B	4	3.10E+00	4.00E+00
2,4-DNT	1.06E+00	B	5	1.00E+01	7.20E+00
2,4-DNT	1.06E+00	B	6	1.11E+01	5.00E+00
2,4-DNT	1.06E+00	B	7	7.10E+00	3.10E+00
2,4-DNT	1.06E+00	B	8	1.34E+01	1.00E+01
2,4-DNT	1.06E+00	B	9	5.10E+00	2.50E+00
2,4-DNT	1.06E+00	B	10	7.10E+00	4.50E+00
2,4-DNT	1.13E+01	A	1	1.51E+01	1.21E+01
2,4-DNT	1.13E+01	A	2	1.30E+01	1.00E+01
2,4-DNT	1.13E+01	A	3	9.80E+00	7.60E+00
2,4-DNT	1.13E+01	A	4	9.40E+00	1.03E+01
2,4-DNT	1.13E+01	A	5	1.43E+01	1.30E+01
2,4-DNT	1.13E+01	A	6	1.23E+01	2.20E+00
2,4-DNT	1.13E+01	A	7	1.54E+01	1.23E+01
2,4-DNT	1.13E+01	A	8	8.80E+00	2.10E+00
2,4-DNT	1.13E+01	A	9	8.80E+00	4.70E+00
2,4-DNT	1.13E+01	A	10	7.90E+00	7.00E+00
2,4-DNT	1.13E+01	B	1	1.00E+01	1.02E+01
2,4-DNT	1.13E+01	B	2	6.80E+00	2.10E+00

2,4-DNT	1.13E+01	B	3	1.10E+01	6.40E+00
2,4-DNT	1.13E+01	B	4	6.00E+00	3.10E+00
2,4-DNT	1.13E+01	B	5	8.10E+00	3.80E+00
2,4-DNT	1.13E+01	B	6	8.70E+00	7.50E+00
2,4-DNT	1.13E+01	B	7	1.00E+01	7.60E+00
2,4-DNT	1.13E+01	B	8	1.21E+01	9.50E+00
2,4-DNT	1.13E+01	B	9	1.18E+01	3.40E+00
2,4-DNT	1.13E+01	B	10	8.60E+00	1.13E+01
2,4-DNT	5.83E+01	A	1	8.70E+00	8.00E+00
2,4-DNT	5.83E+01	A	2	1.50E+01	1.45E+01
2,4-DNT	5.83E+01	A	3	8.90E+00	4.50E+00
2,4-DNT	5.83E+01	A	4	1.02E+01	1.02E+01
2,4-DNT	5.83E+01	A	5	8.60E+00	4.90E+00
2,4-DNT	5.83E+01	A	6	6.00E+00	2.00E+00
2,4-DNT	5.83E+01	A	7	1.07E+01	4.10E+00
2,4-DNT	5.83E+01	A	8	1.30E+01	1.20E+01
2,4-DNT	5.83E+01	A	9	6.60E+00	3.80E+00
2,4-DNT	5.83E+01	A	10	1.06E+01	5.60E+00
2,4-DNT	5.83E+01	B	1	5.80E+00	1.90E+00
2,4-DNT	5.83E+01	B	2	7.30E+00	5.20E+00
2,4-DNT	5.83E+01	B	3	7.90E+00	7.20E+00
2,4-DNT	5.83E+01	B	4	1.04E+01	1.03E+01
2,4-DNT	5.83E+01	B	5	8.90E+00	1.00E+01
2,4-DNT	5.83E+01	B	6	6.00E+00	2.00E+00
2,4-DNT	5.83E+01	B	7	6.70E+00	8.50E+00
2,4-DNT	5.83E+01	B	8	1.24E+01	1.07E+01
2,4-DNT	5.83E+01	B	9	7.70E+00	6.00E+00
2,4-DNT	5.83E+01	B	10	8.40E+00	4.50E+00
2,4-DNT	1.09E+02	A	1	6.90E+00	4.00E+00
2,4-DNT	1.09E+02	A	2	1.12E+01	1.20E+01

2,4-DNT	1.09E+02	A	3	7.00E+00	1.02E+01
2,4-DNT	1.09E+02	A	4	1.33E+01	8.30E+00
2,4-DNT	1.09E+02	A	5	1.13E+01	9.60E+00
2,4-DNT	1.09E+02	A	6	1.19E+01	9.30E+00
2,4-DNT	1.09E+02	A	7	8.10E+00	6.00E+00
2,4-DNT	1.09E+02	A	8	1.26E+01	9.40E+00
2,4-DNT	1.09E+02	A	9	7.70E+00	1.01E+01
2,4-DNT	1.09E+02	A	10	1.00E+01	6.20E+00
2,4-DNT	1.09E+02	B	1	7.80E+00	6.20E+00
2,4-DNT	1.09E+02	B	2	1.72E+01	1.32E+01
2,4-DNT	1.09E+02	B	3	1.21E+01	3.10E+00
2,4-DNT	1.09E+02	B	4	1.05E+01	9.00E+00
2,4-DNT	1.09E+02	B	5	9.40E+00	7.00E+00
2,4-DNT	1.09E+02	B	6	5.40E+00	1.90E+00
2,4-DNT	1.09E+02	B	7	5.40E+00	4.10E+00
2,4-DNT	1.09E+02	B	8	7.50E+00	5.30E+00
2,4-DNT	1.09E+02	B	9	6.30E+00	6.10E+00
2,4-DNT	1.09E+02	B	10	8.90E+00	2.70E+00
2,4-DNAN	0.00E+00	A	1	1.70E+01	1.50E+01
2,4-DNAN	0.00E+00	A	2	1.47E+01	1.30E+01
2,4-DNAN	0.00E+00	A	3	1.32E+01	1.25E+01
2,4-DNAN	0.00E+00	A	4	1.90E+01	1.54E+01
2,4-DNAN	0.00E+00	A	5	1.77E+01	1.60E+01
2,4-DNAN	0.00E+00	A	6	1.15E+01	1.79E+01
2,4-DNAN	0.00E+00	A	7	1.43E+01	1.20E+01
2,4-DNAN	0.00E+00	A	8	1.11E+01	1.14E+01
2,4-DNAN	0.00E+00	A	9	1.62E+01	1.45E+01
2,4-DNAN	0.00E+00	A	10	1.43E+01	1.80E+01
2,4-DNAN	0.00E+00	A	11	1.31E+01	1.16E+01
2,4-DNAN	0.00E+00	A	12	1.65E+01	1.58E+01

2,4-DNAN	0.00E+00	A	13	1.65E+01	1.44E+01
2,4-DNAN	0.00E+00	A	14	1.60E+01	1.71E+01
2,4-DNAN	0.00E+00	A[c]	15	1.57E+01	1.00E+01
2,4-DNAN	8.60E-01	A	1	9.50E+00	5.70E+00
2,4-DNAN	8.60E-01	A	2	1.03E+01	1.10E+01
2,4-DNAN	8.60E-01	A	3	1.27E+01	9.70E+00
2,4-DNAN	8.60E-01	A	4	1.54E+01	1.31E+01
2,4-DNAN	8.60E-01	A	5	1.70E+01	8.00E+00
2,4-DNAN	8.60E-01	A	6	2.08E+01	5.30E+00
2,4-DNAN	8.60E-01	A	7	1.70E+01	1.20E+01
2,4-DNAN	8.60E-01	A	8	1.77E+01	1.24E+01
2,4-DNAN	8.60E-01	A	9	1.70E+01	1.31E+01
2,4-DNAN	8.60E-01	A	10	1.30E+01	1.03E+01
2,4-DNAN	8.60E-01	A	11	1.53E+01	1.22E+01
2,4-DNAN	8.60E-01	A	12	1.55E+01	1.45E+01
2,4-DNAN	8.60E-01	A	13	1.40E+01	1.20E+01
2,4-DNAN	8.60E-01	A	14	1.55E+01	1.32E+01
2,4-DNAN	8.60E-01	A	15	1.10E+01	9.65E+00
2,4-DNAN	8.60E-01	B	1	1.01E+01	1.18E+01
2,4-DNAN	8.60E-01	B	2	1.46E+01	1.37E+01
2,4-DNAN	8.60E-01	B	3	1.56E+01	1.43E+01
2,4-DNAN	8.60E-01	B	4	1.86E+01	1.18E+01
2,4-DNAN	8.60E-01	B	5	6.90E+00	1.10E+01
2,4-DNAN	8.60E-01	B	6	1.43E+01	1.45E+01
2,4-DNAN	8.60E-01	B	7	1.06E+01	1.10E+01
2,4-DNAN	8.60E-01	B	8	1.96E+01	1.30E+01
2,4-DNAN	8.60E-01	B	9	1.44E+01	1.60E+01
2,4-DNAN	8.60E-01	B	10	1.10E+01	1.05E+01
2,4-DNAN	8.60E-01	B	11	1.57E+01	1.04E+01
2,4-DNAN	8.60E-01	B	12	1.90E+01	1.15E+01

2,4-DNAN	8.60E-01	B	13	1.46E+01	1.00E+01
2,4-DNAN	8.60E-01	B	14	1.50E+01	1.35E+01
2,4-DNAN	8.60E-01	B	15	1.54E+01	9.00E+00
2,4-DNAN	8.60E-01	C	1	8.00E+00	8.20E+00
2,4-DNAN	8.60E-01	C	2	1.83E+01	8.00E+00
2,4-DNAN	8.60E-01	C	3	1.77E+01	1.02E+01
2,4-DNAN	8.60E-01	C	4	1.73E+01	1.30E+01
2,4-DNAN	8.60E-01	C	5	1.43E+01	1.30E+01
2,4-DNAN	8.60E-01	C	6	1.60E+01	1.10E+01
2,4-DNAN	8.60E-01	C	7	2.08E+01	1.70E+01
2,4-DNAN	8.60E-01	C	8	1.75E+01	7.00E+00
2,4-DNAN	8.60E-01	C	9	1.45E+01	1.05E+01
2,4-DNAN	8.60E-01	C	10	1.66E+01	9.60E+00
2,4-DNAN	8.60E-01	C	11	1.50E+01	6.70E+00
2,4-DNAN	8.60E-01	C	12	1.63E+01	1.00E+01
2,4-DNAN	8.60E-01	C	13	1.96E+01	1.05E+01
2,4-DNAN	8.60E-01	C	14	1.02E+01	1.15E+01
2,4-DNAN	8.60E-01	C	15	1.40E+01	1.11E+01
2,4-DNAN	8.67E+00	A	1	1.22E+01	7.50E+00
2,4-DNAN	8.67E+00	A	2	1.70E+01	5.20E+00
2,4-DNAN	8.67E+00	A	3	1.39E+01	5.10E+00
2,4-DNAN	8.67E+00	A	4	8.50E+00	3.40E+00
2,4-DNAN	8.67E+00	A	5	1.27E+01	4.80E+00
2,4-DNAN	8.67E+00	A	6	1.30E+01	4.00E+00
2,4-DNAN	8.67E+00	A	7	1.42E+01	8.50E+00
2,4-DNAN	8.67E+00	A	8	1.20E+01	3.40E+00
2,4-DNAN	8.67E+00	A	9	1.37E+01	1.00E+01
2,4-DNAN	8.67E+00	A	10	1.80E+01	8.20E+00
2,4-DNAN	8.67E+00	A	11	1.30E+01	2.80E+00
2,4-DNAN	8.67E+00	A	12	1.20E+01	2.80E+00

2,4-DNAN	8.67E+00	A	13	1.63E+01	7.40E+00
2,4-DNAN	8.67E+00	A	14	1.40E+01	2.50E+00
2,4-DNAN	8.67E+00	A	15	1.30E+01	4.40E+00
2,4-DNAN	8.67E+00	B	1	1.40E+01	8.20E+00
2,4-DNAN	8.67E+00	B	2	1.27E+01	1.17E+01
2,4-DNAN	8.67E+00	B	3	1.64E+01	7.30E+00
2,4-DNAN	8.67E+00	B	4	1.50E+01	9.50E+00
2,4-DNAN	8.67E+00	B	5	1.72E+01	1.10E+01
2,4-DNAN	8.67E+00	B	6	1.76E+01	8.60E+00
2,4-DNAN	8.67E+00	B	7	1.42E+01	1.01E+01
2,4-DNAN	8.67E+00	B	8	1.16E+01	7.90E+00
2,4-DNAN	8.67E+00	B	9	1.41E+01	9.30E+00
2,4-DNAN	8.67E+00	B	10	1.24E+01	1.13E+01
2,4-DNAN	8.67E+00	B	11	1.17E+01	7.00E+00
2,4-DNAN	8.67E+00	B	12	1.17E+01	1.17E+01
2,4-DNAN	8.67E+00	B	13	1.70E+01	1.35E+01
2,4-DNAN	8.67E+00	B	14	1.35E+01	3.00E+00
2,4-DNAN	8.67E+00	C	1	1.10E+01	7.50E+00
2,4-DNAN	8.67E+00	C	2	1.73E+01	5.10E+00
2,4-DNAN	8.67E+00	C	3	9.00E+00	8.10E+00
2,4-DNAN	8.67E+00	C	4	1.70E+01	9.00E+00
2,4-DNAN	8.67E+00	C	5	1.23E+01	1.05E+01
2,4-DNAN	8.67E+00	C	6	1.76E+01	1.35E+01
2,4-DNAN	8.67E+00	C	7	1.25E+01	1.06E+01
2,4-DNAN	8.67E+00	C	8	1.34E+01	5.40E+00
2,4-DNAN	8.67E+00	C	9	1.32E+01	9.00E+00
2,4-DNAN	8.67E+00	C	10	1.85E+01	8.40E+00
2,4-DNAN	8.67E+00	C	11	1.40E+01	1.04E+01
2,4-DNAN	8.67E+00	C	12	1.31E+01	3.60E+00
2,4-DNAN	8.67E+00	C	13	1.60E+01	1.15E+01

2,4-DNAN	8.67E+00	C	14	1.55E+01	1.06E+01
2,4-DNAN	8.67E+00	C	15	1.74E+01	8.00E+00
2,4-DNAN	8.67E+00	C	16	1.32E+01	1.50E+01
2,4-DNAN	4.52E+01	A	1	1.01E+01	6.00E+00
2,4-DNAN	4.52E+01	A	2	6.50E+00	7.20E+00
2,4-DNAN	4.52E+01	A	3	1.10E+01	5.00E+00
2,4-DNAN	4.52E+01	A	4	1.16E+01	8.20E+00
2,4-DNAN	4.52E+01	A	5	1.20E+01	7.50E+00
2,4-DNAN	4.52E+01	A	6	9.50E+00	4.30E+00
2,4-DNAN	4.52E+01	A	7	8.50E+00	6.30E+00
2,4-DNAN	4.52E+01	A	8	9.50E+00	2.10E+00
2,4-DNAN	4.52E+01	A	9	1.10E+01	6.50E+00
2,4-DNAN	4.52E+01	A	10	1.14E+01	6.40E+00
2,4-DNAN	4.52E+01	A	11	1.20E+01	4.80E+00
2,4-DNAN	4.52E+01	A	12	8.40E+00	6.80E+00
2,4-DNAN	4.52E+01	A	13	1.07E+01	5.70E+00
2,4-DNAN	4.52E+01	A	14	7.00E+00	2.00E+00
2,4-DNAN	4.52E+01	A	15	1.02E+01	5.00E+00
2,4-DNAN	4.52E+01	B	1	5.70E+00	8.00E-01
2,4-DNAN	4.52E+01	B	2	9.10E+00	5.70E+00
2,4-DNAN	4.52E+01	B	3	6.00E+00	5.60E+00
2,4-DNAN	4.52E+01	B	4	8.50E+00	3.50E+00
2,4-DNAN	4.52E+01	B	5	1.14E+01	6.40E+00
2,4-DNAN	4.52E+01	B	6	1.03E+01	6.60E+00
2,4-DNAN	4.52E+01	B	7	1.05E+01	5.60E+00
2,4-DNAN	4.52E+01	B	8	6.50E+00	9.10E+00
2,4-DNAN	4.52E+01	B	9	9.20E+00	2.00E+00
2,4-DNAN	4.52E+01	B	10	9.60E+00	1.60E+00
2,4-DNAN	4.52E+01	B	11	8.90E+00	3.80E+00
2,4-DNAN	4.52E+01	B	12	1.15E+01	7.00E+00

2,4-DNAN	4.52E+01	B	13	1.05E+01	7.80E+00
2,4-DNAN	4.52E+01	B	14	7.90E+00	2.80E+00
2,4-DNAN	4.52E+01	B	15	9.80E+00	9.00E+00
2,4-DNAN	8.78E+01	A	1	3.20E+00	5.10E+00
2,4-DNAN	8.78E+01	A	2	6.60E+00	5.20E+00
2,4-DNAN	8.78E+01	A	3	7.20E+00	7.60E+00
2,4-DNAN	8.78E+01	A	4	7.00E+00	4.60E+00
2,4-DNAN	8.78E+01	A	5	8.50E+00	1.50E+00
2,4-DNAN	8.78E+01	A	6	4.90E+00	2.40E+00
2,4-DNAN	8.78E+01	A	7	7.50E+00	6.00E+00
2,4-DNAN	8.78E+01	A	8	9.40E+00	3.50E+00
2,4-DNAN	8.78E+01	A	9	7.50E+00	4.50E+00
2,4-DNAN	8.78E+01	A	10	6.60E+00	4.50E+00
2,4-DNAN	8.78E+01	A	11	9.50E+00	5.20E+00
2,4-DNAN	8.78E+01	A	12	8.30E+00	6.00E+00
2,4-DNAN	8.78E+01	A	13	9.60E+00	5.00E+00
2,4-DNAN	8.78E+01	A	14	4.90E+00	3.60E+00
2,4-DNAN	8.78E+01	B	1	4.00E+00	5.20E+00
2,4-DNAN	8.78E+01	B	2	7.50E+00	5.60E+00
2,4-DNAN	8.78E+01	B	3	7.90E+00	3.20E+00
2,4-DNAN	8.78E+01	B	4	7.60E+00	6.00E+00
2,4-DNAN	8.78E+01	B	5	7.50E+00	2.10E+00
2,4-DNAN	8.78E+01	B	6	7.90E+00	6.00E+00
2,4-DNAN	8.78E+01	B	7	5.00E+00	3.50E+00
2,4-DNAN	8.78E+01	B	8	8.20E+00	2.10E+00
2,4-DNAN	8.78E+01	B	9	5.50E+00	5.50E+00
2,4-DNAN	8.78E+01	B	10	5.10E+00	4.20E+00
2,4-DNAN	8.78E+01	B	11	7.20E+00	5.40E+00
2,4-DNAN	8.78E+01	B	12	5.20E+00	8.60E+00
2,4-DNAN	8.78E+01	B	13	7.10E+00	3.00E+00

2,4-DNAN	8.78E+01	B	14	5.30E+00	6.20E+00
2,4-DNAN	8.78E+01	B	15	NR[b]	4.20E+00
2,4-DNAN	8.78E+01	C	1	4.20E+00	2.60E+00
2,4-DNAN	8.78E+01	C	2	6.50E+00	6.00E+00
2,4-DNAN	8.78E+01	C	3	6.50E+00	7.00E+00
2,4-DNAN	8.78E+01	C	4	6.40E+00	2.70E+00
2,4-DNAN	8.78E+01	C	5	4.10E+00	1.30E+00
2,4-DNAN	8.78E+01	C	6	6.20E+00	2.50E+00
2,4-DNAN	8.78E+01	C	7	7.90E+00	3.60E+00
2,4-DNAN	8.78E+01	C	8	7.00E+00	2.90E+00
2,4-DNAN	8.78E+01	C	9	6.20E+00	7.50E+00
2,4-DNAN	8.78E+01	C	10	7.80E+00	6.80E+00
2,4-DNAN	8.78E+01	C	11	7.00E+00	5.30E+00
2,4-DNAN	8.78E+01	C	12	7.30E+00	4.70E+00
2,4-DNAN	8.78E+01	C	13	6.20E+00	5.20E+00
2,4-DNAN	8.78E+01	C	14	9.30E+00	7.10E+00
2,4-DNAN	8.78E+01	C	15	9.40E+00	8.10E+00
4-NAN	0.00E+00	A	1	1.60E+01	9.40E+00
4-NAN	0.00E+00	A	2	1.65E+01	5.20E+00
4-NAN	0.00E+00	A	3	1.47E+01	1.02E+01
4-NAN	0.00E+00	A	4	1.55E+01	1.30E+01
4-NAN	0.00E+00	A	5	1.40E+01	9.50E+00
4-NAN	0.00E+00	A	6	1.47E+01	8.50E+00
4-NAN	0.00E+00	A	7	1.60E+01	1.65E+01
4-NAN	0.00E+00	A	8	1.30E+01	8.00E+00
4-NAN	0.00E+00	A	9	1.30E+01	1.23E+01
4-NAN	0.00E+00	A	10	1.95E+01	1.33E+01
4-NAN	0.00E+00	A	11	1.60E+01	1.05E+01
4-NAN	0.00E+00	A	12	1.70E+01	1.75E+01
4-NAN	0.00E+00	A	13	1.77E+01	1.05E+01

4-NAN	0.00E+00	A	14	1.60E+01	1.10E+01
4-NAN	0.00E+00	A	15	1.44E+01	1.05E+01
4-NAN	0.00E+00	A	16	1.75E+01	1.20E+01
4-NAN	0.00E+00	A	17	1.75E+01	1.00E+01
4-NAN	0.00E+00	A	18	1.37E+01	8.50E+00
4-NAN	0.00E+00	A	19	1.13E+01	9.30E+00
4-NAN	0.00E+00	A	20	6.70E+00	1.45E+01
4-NAN	0.00E+00	B	1	1.76E+01	8.00E+00
4-NAN	0.00E+00	B	2	1.41E+01	9.50E+00
4-NAN	0.00E+00	B	3	1.90E+01	9.20E+00
4-NAN	0.00E+00	B	4	1.70E+01	1.00E+01
4-NAN	0.00E+00	B	5	1.55E+01	7.00E+00
4-NAN	0.00E+00	B	6	1.95E+01	1.35E+01
4-NAN	0.00E+00	B	7	1.40E+01	8.00E+00
4-NAN	0.00E+00	B	8	1.85E+01	1.00E+01
4-NAN	0.00E+00	B	9	1.20E+01	9.00E+00
4-NAN	0.00E+00	B	10	1.42E+01	9.00E+00
4-NAN	0.00E+00	B	11	1.55E+01	1.00E+01
4-NAN	0.00E+00	B	12	1.60E+01	1.45E+01
4-NAN	0.00E+00	B	13	1.20E+01	1.00E+01
4-NAN	0.00E+00	B	14	1.48E+01	7.50E+00
4-NAN	0.00E+00	B	15	1.60E+01	8.00E+00
4-NAN	0.00E+00	B	16	1.50E+01	1.10E+01
4-NAN	0.00E+00	B	17	3.00E+00	1.50E+00
4-NAN	1.11E+00	A	1	1.70E+01	1.00E+01
4-NAN	1.11E+00	A	2	1.80E+01	1.06E+01
4-NAN	1.11E+00	A	3	1.25E+01	9.00E+00
4-NAN	1.11E+00	A	4	1.55E+01	1.20E+01
4-NAN	1.11E+00	A	5	1.50E+01	1.06E+01
4-NAN	1.11E+00	A	6	1.91E+01	9.00E+00

4-NAN	1.11E+00	A	7	1.57E+01	1.05E+01
4-NAN	1.11E+00	A	8	1.50E+01	1.05E+01
4-NAN	1.11E+00	A	9	1.80E+01	1.04E+01
4-NAN	1.11E+00	A	10	1.55E+01	1.15E+01
4-NAN	1.11E+00	A	11	1.63E+01	1.20E+01
4-NAN	1.11E+00	A	12	1.45E+01	1.06E+01
4-NAN	1.11E+00	A	13	1.61E+01	9.50E+00
4-NAN	1.11E+00	A	14	1.80E+01	1.05E+01
4-NAN	1.11E+00	A	15	1.90E+01	1.00E+01
4-NAN	1.11E+00	A	16	1.95E+01	1.15E+01
4-NAN	1.11E+00	A	17	1.90E+01	1.10E+01
4-NAN	1.11E+00	A	18	1.72E+01	9.50E+00
4-NAN	1.11E+00	A	19	1.67E+01	1.03E+01
4-NAN	1.11E+00	A	20	1.76E+01	1.00E+01
4-NAN	1.11E+00	B	1	1.30E+01	1.08E+01
4-NAN	1.11E+00	B	2	1.73E+01	1.53E+01
4-NAN	1.11E+00	B	3	1.20E+01	1.00E+01
4-NAN	1.11E+00	B	4	8.80E+00	1.00E+00
4-NAN	1.11E+00	B	5	1.85E+01	1.13E+01
4-NAN	1.11E+00	B	6	1.78E+01	8.50E+00
4-NAN	1.11E+00	B	7	1.20E+01	1.10E+01
4-NAN	1.11E+00	B	8	1.52E+01	1.37E+01
4-NAN	1.11E+00	B	9	1.65E+01	1.15E+01
4-NAN	1.11E+00	B	10	1.42E+01	9.00E+00
4-NAN	1.11E+00	B	11	1.45E+01	7.20E+00
4-NAN	1.11E+00	B	12	1.80E+01	1.00E+01
4-NAN	1.11E+00	B	13	1.84E+01	1.00E+01
4-NAN	1.11E+00	B	14	1.55E+01	1.04E+01
4-NAN	1.11E+00	B	15	1.51E+01	1.15E+01
4-NAN	1.11E+00	B	16	1.26E+01	1.14E+01

4-NAN	1.11E+00	B	17	4.50E+00	NR
4-NAN	1.11E+00	B	18	1.41E+01	1.10E+01
4-NAN	1.11E+00	C	1	1.60E+01	8.30E+00
4-NAN	1.11E+00	C	2	2.00E+01	1.35E+01
4-NAN	1.11E+00	C	3	1.35E+01	1.20E+01
4-NAN	1.11E+00	C	4	1.55E+01	1.00E+01
4-NAN	1.11E+00	C	5	1.55E+01	1.30E+01
4-NAN	1.11E+00	C	6	1.72E+01	1.03E+01
4-NAN	1.11E+00	C	7	1.23E+01	9.80E+00
4-NAN	1.11E+00	C	8	1.15E+01	1.01E+01
4-NAN	1.11E+00	C	9	1.53E+01	9.00E+00
4-NAN	1.11E+00	C	10	1.75E+01	1.00E+01
4-NAN	1.11E+00	C	11	1.23E+01	1.20E+01
4-NAN	1.11E+00	C	12	1.45E+01	1.38E+01
4-NAN	1.11E+00	C	13	1.62E+01	1.05E+01
4-NAN	1.11E+00	C	14	1.48E+01	9.30E+00
4-NAN	1.11E+00	C	15	1.30E+01	7.70E+00
4-NAN	1.11E+00	C	16	1.02E+01	1.25E+01
4-NAN	1.11E+00	C	17	1.25E+01	4.00E+00
4-NAN	1.11E+00	C	18	1.13E+01	9.00E+00
4-NAN	1.11E+00	C	19	1.50E+01	9.70E+00
4-NAN	1.11E+00	C	20	1.20E+01	9.00E+00
4-NAN	9.97E+00	A	1	1.90E+01	1.00E+01
4-NAN	9.97E+00	A	2	1.55E+01	1.00E+01
4-NAN	9.97E+00	A	3	1.35E+01	1.00E+01
4-NAN	9.97E+00	A	4	1.37E+01	7.00E+00
4-NAN	9.97E+00	A	5	1.30E+01	5.50E+00
4-NAN	9.97E+00	A	6	1.45E+01	1.00E+01
4-NAN	9.97E+00	A	7	1.58E+01	8.80E+00
4-NAN	9.97E+00	A	8	9.80E+00	1.14E+01

4-NAN	9.97E+00	A	9	1.80E+01	1.15E+01
4-NAN	9.97E+00	A	10	6.60E+00	7.60E+00
4-NAN	9.97E+00	A	11	1.35E+01	8.00E+00
4-NAN	9.97E+00	A	12	7.50E+00	2.50E+00
4-NAN	9.97E+00	A	13	1.67E+01	1.25E+01
4-NAN	9.97E+00	A	14	9.50E+00	8.00E+00
4-NAN	9.97E+00	A	15	1.80E+01	9.00E+00
4-NAN	9.97E+00	A	16	1.80E+01	8.80E+00
4-NAN	9.97E+00	A	17	1.85E+01	8.20E+00
4-NAN	9.97E+00	A	18	1.47E+01	1.05E+01
4-NAN	9.97E+00	A[c]	19	1.60E+01	7.00E+00
4-NAN	4.84E+01	A	1	5.30E+00	2.50E+00
4-NAN	4.84E+01	A	2	8.50E+00	1.70E+00
4-NAN	4.84E+01	A	3	1.60E+01	6.00E+00
4-NAN	4.84E+01	A	4	1.63E+01	7.00E+00
4-NAN	4.84E+01	A	5	6.80E+00	2.00E+00
4-NAN	4.84E+01	A	6	1.57E+01	3.80E+00
4-NAN	4.84E+01	A	7	1.60E+01	9.70E+00
4-NAN	4.84E+01	A	8	1.48E+01	3.00E+00
4-NAN	4.84E+01	A	9	1.20E+01	3.50E+00
4-NAN	4.84E+01	A	10	1.50E+01	7.70E+00
4-NAN	4.84E+01	A	11	9.70E+00	1.80E+00
4-NAN	4.84E+01	A	12	8.50E+00	2.00E+00
4-NAN	4.84E+01	A	13	1.45E+01	7.00E+00
4-NAN	4.84E+01	A	14	9.20E+00	5.50E+00
4-NAN	4.84E+01	A	15	4.00E+00	7.30E+00
4-NAN	4.84E+01	A	16	1.57E+01	4.00E+00
4-NAN	4.84E+01	A	17	2.30E+00	NR
4-NAN	4.84E+01	B	1	1.26E+01	3.00E+00
4-NAN	4.84E+01	B	2	7.00E+00	2.50E+00

4-NAN	4.84E+01	B	3	1.32E+01	5.00E+00
4-NAN	4.84E+01	B	4	9.00E+00	5.00E+00
4-NAN	4.84E+01	B	5	9.00E+00	3.50E+00
4-NAN	4.84E+01	B	6	1.10E+01	5.50E+00
4-NAN	4.84E+01	B	7	1.19E+01	6.00E+00
4-NAN	4.84E+01	B	8	1.20E+01	4.30E+00
4-NAN	4.84E+01	B	9	1.35E+01	7.00E+00
4-NAN	4.84E+01	B	10	8.80E+00	2.00E+00
4-NAN	4.84E+01	B	11	1.45E+01	4.00E+00
4-NAN	4.84E+01	B	12	5.80E+00	NR
4-NAN	4.84E+01	B	13	1.22E+01	6.50E+00
4-NAN	4.84E+01	B	14	1.20E+01	5.00E+00
4-NAN	4.84E+01	B	15	8.40E+00	2.00E+00
4-NAN	4.84E+01	B	16	7.00E+00	3.00E+00
4-NAN	4.84E+01	B	17	4.00E+00	8.00E-01
4-NAN	8.43E+01	A	1	2.70E+00	8.00E-01
4-NAN	8.43E+01	A	2	8.00E+00	2.00E+00
4-NAN	8.43E+01	A	3	6.50E+00	5.00E+00
4-NAN	8.43E+01	A	4	8.00E+00	5.50E+00
4-NAN	8.43E+01	A	5	5.80E+00	2.00E+00
4-NAN	8.43E+01	A	6	4.00E+00	1.00E+00
4-NAN	8.43E+01	A	7	NR	3.20E+00
4-NAN	8.43E+01	A	8	7.00E+00	3.30E+00
4-NAN	8.43E+01	A	9	2.30E+00	7.00E-01
4-NAN	8.43E+01	A	10	7.50E+00	4.50E+00
4-NAN	8.43E+01	A	11	6.00E+00	2.00E+00
4-NAN	8.43E+01	A	12	2.00E+00	NR
4-NAN	8.43E+01	A	13	4.40E+00	NR
4-NAN	8.43E+01	B	1	5.50E+00	4.70E+00
4-NAN	8.43E+01	B	2	5.70E+00	5.20E+00

4-NAN	8.43E+01	B	3	6.80E+00	6.70E+00
4-NAN	8.43E+01	B	4	5.50E+00	2.10E+00
4-NAN	8.43E+01	B	5	7.00E+00	6.70E+00
4-NAN	8.43E+01	B	6	7.50E+00	1.00E+00
4-NAN	8.43E+01	B	7	5.00E+00	3.60E+00
4-NAN	8.43E+01	B	8	7.00E+00	4.30E+00
4-NAN	8.43E+01	B	9	7.00E+00	4.60E+00
4-NAN	8.43E+01	B	10	7.00E+00	4.80E+00
4-NAN	8.43E+01	B	11	5.70E+00	4.10E+00
4-NAN	8.43E+01	B	12	4.80E+00	1.40E+00
4-NAN	8.43E+01	B	13	8.00E+00	6.70E+00
4-NAN	8.43E+01	B	14	3.00E+00	4.00E-01
4-NAN	8.43E+01	B	15	5.80E+00	7.10E+00
4-NAN	8.43E+01	B	16	5.50E+00	5.80E+00
4-NAN	8.43E+01	B	17	3.00E+00	4.90E+00
4-NAN	8.43E+01	B	18	7.00E+00	9.60E+00
4-NAN	8.43E+01	C	1	5.50E+00	2.50E+00
4-NAN	8.43E+01	C	2	8.00E+00	3.50E+00
4-NAN	8.43E+01	C	3	7.00E+00	5.00E+00
4-NAN	8.43E+01	C	4	6.00E+00	6.50E+00
4-NAN	8.43E+01	C	5	5.50E+00	6.00E+00
4-NAN	8.43E+01	C	6	5.50E+00	5.00E+00
4-NAN	8.43E+01	C	7	7.00E+00	6.50E+00
4-NAN	8.43E+01	C	8	4.50E+00	5.50E+00
4-NAN	8.43E+01	C	9	2.50E+00	2.50E+00
4-NAN	8.43E+01	C	10	5.00E+00	5.00E+00
4-NAN	8.43E+01	C	11	6.00E+00	3.20E+00
4-NAN	8.43E+01	C	12	5.50E+00	5.00E+00
4-NAN	8.43E+01	C	13	6.10E+00	4.10E+00
4-NAN	8.43E+01	C	14	6.00E+00	3.80E+00

4-NAN	8.43E+01	C	15	4.00E+00	2.00E+00
4-NAN	8.43E+01	C	16	6.00E+00	2.00E+00
4-NAN	8.43E+01	C	17	4.20E+00	4.00E+00
4-NAN	8.43E+01	C	18	1.00E+00	5.00E-01
4-NAN	8.43E+01	C	19	6.50E+00	4.00E+00
2-M-5-NPYNE	0.00E+00	A	1	1.35E+01	2.14E+01
2-M-5-NPYNE	0.00E+00	A	2	1.66E+01	1.30E+01
2-M-5-NPYNE	0.00E+00	A	3	1.82E+01	2.10E+01
2-M-5-NPYNE	0.00E+00	A	4	1.32E+01	1.80E+01
2-M-5-NPYNE	0.00E+00	A	5	1.01E+01	1.20E+01
2-M-5-NPYNE	0.00E+00	A	6	1.10E+01	1.60E+01
2-M-5-NPYNE	0.00E+00	A	7	1.33E+01	1.80E+01
2-M-5-NPYNE	0.00E+00	A	8	1.22E+01	1.37E+01
2-M-5-NPYNE	0.00E+00	A	9	1.10E+01	1.55E+01
2-M-5-NPYNE	0.00E+00	A	10	9.40E+00	1.00E+01
2-M-5-NPYNE	0.00E+00	B	1	1.44E+01	1.40E+01
2-M-5-NPYNE	0.00E+00	B	2	1.09E+01	3.00E+00
2-M-5-NPYNE	0.00E+00	B	3	6.70E+00	1.10E+01
2-M-5-NPYNE	0.00E+00	B	4	1.01E+01	5.90E+00
2-M-5-NPYNE	0.00E+00	B	5	1.42E+01	1.80E+01
2-M-5-NPYNE	0.00E+00	B	6	1.15E+01	1.45E+01
2-M-5-NPYNE	0.00E+00	B	7	1.87E+01	1.37E+01
2-M-5-NPYNE	0.00E+00	B	8	1.05E+01	1.50E+01
2-M-5-NPYNE	0.00E+00	B	9	2.00E+01	1.80E+01
2-M-5-NPYNE	0.00E+00	B	10	1.42E+01	1.72E+01
2-M-5-NPYNE	0.00E+00	C	1	7.00E+00	8.00E+00
2-M-5-NPYNE	0.00E+00	C	2	1.26E+01	1.30E+01
2-M-5-NPYNE	0.00E+00	C	3	9.50E+00	1.14E+01
2-M-5-NPYNE	0.00E+00	C	4	8.00E+00	1.12E+01
2-M-5-NPYNE	0.00E+00	C	5	8.00E+00	8.40E+00

2-M-5-NPYNE	0.00E+00	C	6	1.07E+01	1.65E+01
2-M-5-NPYNE	0.00E+00	C	7	7.10E+00	1.10E+01
2-M-5-NPYNE	0.00E+00	C	8	1.32E+01	1.25E+01
2-M-5-NPYNE	0.00E+00	C	9	5.60E+00	1.00E+01
2-M-5-NPYNE	0.00E+00	C	10	4.30E+00	3.50E+00
2-M-5-NPYNE	1.09E+00	A	1	1.42E+01	1.36E+01
2-M-5-NPYNE	1.09E+00	A	2	1.24E+01	1.12E+01
2-M-5-NPYNE	1.09E+00	A	3	1.11E+01	1.20E+01
2-M-5-NPYNE	1.09E+00	A	4	1.50E+01	1.56E+01
2-M-5-NPYNE	1.09E+00	A	5	1.21E+01	7.50E+00
2-M-5-NPYNE	1.09E+00	A	6	1.46E+01	1.45E+01
2-M-5-NPYNE	1.09E+00	A	7	1.75E+01	1.60E+01
2-M-5-NPYNE	1.09E+00	A	8	1.41E+01	1.35E+01
2-M-5-NPYNE	1.09E+00	A	9	1.52E+01	1.09E+01
2-M-5-NPYNE	1.09E+00	A	10	7.00E+00	4.40E+00
2-M-5-NPYNE	1.09E+00	B	1	1.55E+01	1.60E+01
2-M-5-NPYNE	1.09E+00	B	2	1.50E+01	1.45E+01
2-M-5-NPYNE	1.09E+00	B	3	1.76E+01	1.35E+01
2-M-5-NPYNE	1.09E+00	B	4	1.17E+01	1.16E+01
2-M-5-NPYNE	1.09E+00	B	5	1.09E+01	1.25E+01
2-M-5-NPYNE	1.09E+00	B	6	1.80E+01	1.50E+01
2-M-5-NPYNE	1.09E+00	B	7	1.55E+01	1.60E+01
2-M-5-NPYNE	1.09E+00	B	8	1.09E+01	1.10E+01
2-M-5-NPYNE	1.09E+00	B	9	1.83E+01	2.05E+01
2-M-5-NPYNE	1.09E+00	B	10	6.40E+00	1.00E+01
2-M-5-NPYNE	1.09E+00	C	1	1.32E+01	1.55E+01
2-M-5-NPYNE	1.09E+00	C	2	1.35E+01	2.10E+01
2-M-5-NPYNE	1.09E+00	C	3	1.45E+01	1.35E+01
2-M-5-NPYNE	1.09E+00	C	4	1.42E+01	1.45E+01
2-M-5-NPYNE	1.09E+00	C	5	8.50E+00	1.15E+01

2-M-5-NPYNE	1.09E+00	C	6	1.05E+01	1.00E+01
2-M-5-NPYNE	1.09E+00	C	7	1.25E+01	1.27E+01
2-M-5-NPYNE	1.09E+00	C	8	1.06E+01	1.50E+01
2-M-5-NPYNE	1.09E+00	C	9	1.65E+01	1.50E+01
2-M-5-NPYNE	1.09E+00	C	10	1.41E+01	1.56E+01
2-M-5-NPYNE	1.17E+01	A	1	9.10E+00	4.60E+00
2-M-5-NPYNE	1.17E+01	A	2	1.85E+01	1.65E+01
2-M-5-NPYNE	1.17E+01	A	3	1.30E+01	1.40E+01
2-M-5-NPYNE	1.17E+01	A	4	1.71E+01	1.86E+01
2-M-5-NPYNE	1.17E+01	A	5	9.80E+00	1.00E+01
2-M-5-NPYNE	1.17E+01	A	6	7.60E+00	8.50E+00
2-M-5-NPYNE	1.17E+01	A	7	1.66E+01	1.50E+01
2-M-5-NPYNE	1.17E+01	A	8	1.60E+01	1.55E+01
2-M-5-NPYNE	1.17E+01	A	9	1.80E+01	1.70E+01
2-M-5-NPYNE	1.17E+01	A	10	1.20E+01	1.17E+01
2-M-5-NPYNE	1.17E+01	B	1	1.28E+01	1.08E+01
2-M-5-NPYNE	1.17E+01	B	2	1.50E+01	1.34E+01
2-M-5-NPYNE	1.17E+01	B	3	1.50E+01	1.31E+01
2-M-5-NPYNE	1.17E+01	B	4	8.50E+00	7.50E+00
2-M-5-NPYNE	1.17E+01	B	5	2.02E+01	1.65E+01
2-M-5-NPYNE	1.17E+01	B	6	9.80E+00	1.05E+01
2-M-5-NPYNE	1.17E+01	B	7	1.36E+01	1.45E+01
2-M-5-NPYNE	1.17E+01	B	8	1.71E+01	1.45E+01
2-M-5-NPYNE	1.17E+01	B	9	1.72E+01	1.53E+01
2-M-5-NPYNE	1.17E+01	B	10	1.40E+01	1.37E+01
2-M-5-NPYNE	1.17E+01	C	1	1.64E+01	1.28E+01
2-M-5-NPYNE	1.17E+01	C	2	1.50E+01	1.30E+01
2-M-5-NPYNE	1.17E+01	C	3	1.50E+01	1.22E+01
2-M-5-NPYNE	1.17E+01	C	4	1.11E+01	6.40E+00
2-M-5-NPYNE	1.17E+01	C	5	1.33E+01	1.02E+01

2-M-5-NPYNE	1.17E+01	C	6	1.90E+01	1.70E+01
2-M-5-NPYNE	1.17E+01	C	7	6.40E+00	8.20E+00
2-M-5-NPYNE	1.17E+01	C	8	1.97E+01	1.40E+01
2-M-5-NPYNE	1.17E+01	C	9	1.60E+01	1.10E+01
2-M-5-NPYNE	1.17E+01	C	10	1.45E+01	1.65E+01
2-M-5-NPYNE	5.53E+01	A	1	1.33E+01	7.50E+00
2-M-5-NPYNE	5.53E+01	A	2	1.55E+01	1.05E+01
2-M-5-NPYNE	5.53E+01	A	3	1.72E+01	1.05E+01
2-M-5-NPYNE	5.53E+01	A	4	1.37E+01	1.05E+01
2-M-5-NPYNE	5.53E+01	A	5	9.00E+00	7.70E+00
2-M-5-NPYNE	5.53E+01	A	6	8.40E+00	6.20E+00
2-M-5-NPYNE	5.53E+01	A	7	1.32E+01	7.00E+00
2-M-5-NPYNE	5.53E+01	A	8	5.20E+00	6.00E+00
2-M-5-NPYNE	5.53E+01	A	9	1.05E+01	1.00E+01
2-M-5-NPYNE	5.53E+01	A	10	8.50E+00	5.20E+00
2-M-5-NPYNE	5.53E+01	B	1	1.60E+01	8.00E+00
2-M-5-NPYNE	5.53E+01	B	2	1.05E+01	7.50E+00
2-M-5-NPYNE	5.53E+01	B	3	1.00E+01	9.50E+00
2-M-5-NPYNE	5.53E+01	B	4	1.33E+01	9.70E+00
2-M-5-NPYNE	5.53E+01	B	5	1.56E+01	8.20E+00
2-M-5-NPYNE	5.53E+01	B	6	1.58E+01	1.14E+01
2-M-5-NPYNE	5.53E+01	B	7	1.14E+01	1.00E+01
2-M-5-NPYNE	5.53E+01	B	8	1.55E+01	1.17E+01
2-M-5-NPYNE	5.53E+01	B	9	1.31E+01	1.30E+01
2-M-5-NPYNE	5.53E+01	B	10	1.50E+01	1.37E+01
2-M-5-NPYNE	5.53E+01	C	1	1.14E+01	3.50E+00
2-M-5-NPYNE	5.53E+01	C	2	5.60E+00	5.50E+00
2-M-5-NPYNE	5.53E+01	C	3	1.30E+01	1.10E+01
2-M-5-NPYNE	5.53E+01	C	4	1.15E+01	4.70E+00
2-M-5-NPYNE	5.53E+01	C	5	7.70E+00	6.00E+00

2-M-5-NPYNE	5.53E+01	C	6	1.20E+01	1.05E+01
2-M-5-NPYNE	5.53E+01	C	7	6.00E+00	8.70E+00
2-M-5-NPYNE	5.53E+01	C	8	1.57E+01	1.00E+01
2-M-5-NPYNE	5.53E+01	C	9	1.45E+01	1.00E+01
2-M-5-NPYNE	5.53E+01	C	10	1.41E+01	1.00E+01
2-M-5-NPYNE	1.06E+02	A	1	9.70E+00	8.50E+00
2-M-5-NPYNE	1.06E+02	A	2	1.17E+01	1.27E+01
2-M-5-NPYNE	1.06E+02	A	3	8.40E+00	9.50E+00
2-M-5-NPYNE	1.06E+02	A	4	1.20E+01	1.00E+01
2-M-5-NPYNE	1.06E+02	A	5	8.00E+00	8.50E+00
2-M-5-NPYNE	1.06E+02	A	6	1.00E+01	8.50E+00
2-M-5-NPYNE	1.06E+02	A	7	6.50E+00	5.00E+00
2-M-5-NPYNE	1.06E+02	A	8	7.50E+00	7.00E+00
2-M-5-NPYNE	1.06E+02	A	9	1.05E+01	9.00E+00
2-M-5-NPYNE	1.06E+02	A	10	1.00E+01	7.00E+00
2-M-5-NPYNE	1.06E+02	B	1	6.00E+00	3.00E+00
2-M-5-NPYNE	1.06E+02	B	2	7.50E+00	3.00E+00
2-M-5-NPYNE	1.06E+02	B	3	6.00E+00	8.00E+00
2-M-5-NPYNE	1.06E+02	B	4	6.50E+00	7.60E+00
2-M-5-NPYNE	1.06E+02	B	5	1.10E+01	8.60E+00
2-M-5-NPYNE	1.06E+02	B	6	1.20E+01	8.50E+00
2-M-5-NPYNE	1.06E+02	B	7	1.20E+01	9.70E+00
2-M-5-NPYNE	1.06E+02	B	8	1.15E+01	1.10E+01
2-M-5-NPYNE	1.06E+02	B	9	9.20E+00	9.50E+00
2-M-5-NPYNE	1.06E+02	B	10	6.00E+00	3.00E+00
2-M-5-NPYNE	1.06E+02	C	1	6.50E+00	7.50E+00
2-M-5-NPYNE	1.06E+02	C	2	6.20E+00	4.00E+00
2-M-5-NPYNE	1.06E+02	C	3	5.00E+00	9.40E+00
2-M-5-NPYNE	1.06E+02	C	4	6.60E+00	1.28E+01
2-M-5-NPYNE	1.06E+02	C	5	1.32E+01	1.08E+01

2-M-5-NPYNE	1.06E+02	C	6	5.70E+00	2.50E+00
2-M-5-NPYNE	1.06E+02	C	7	1.05E+01	1.35E+01
2-M-5-NPYNE	1.06E+02	C	8	5.70E+00	8.20E+00
2-M-5-NPYNE	1.06E+02	C	9	1.05E+01	1.08E+01
2-M-5-NPYNE	1.06E+02	C	10	9.60E+00	4.40E+00

[a] Average of measured exposure concentrations across replicates for the corresponding solution added. The 0 mg L^{-1} concentration represents controls (pots not exposed to MCs, or MLCs)

[b] Not recorded

[c] Replicate B was accidentally exposed to the wrong solution added few days after the beginning of the experiment, so it was excluded for further measurements

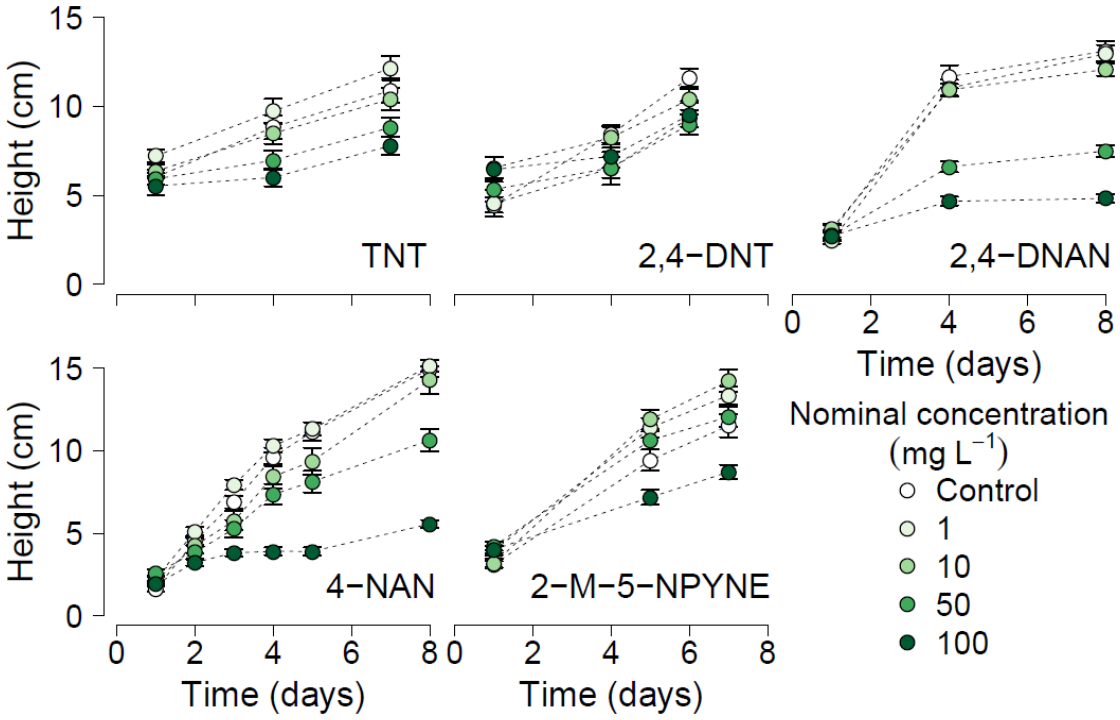

Figure A-1 Biomass profiles (shoot height) for barley exposed to individual munitions compounds (MCs) or munitions-like compounds (MLCs) at increasing concentration of solution added (nominal: Control, 1, 10, 50, and 100 mg L^{-1}) during toxicity screening. Data presented as means ± standard error of the mean (SEM). If not visible, error bars are smaller than the symbol.

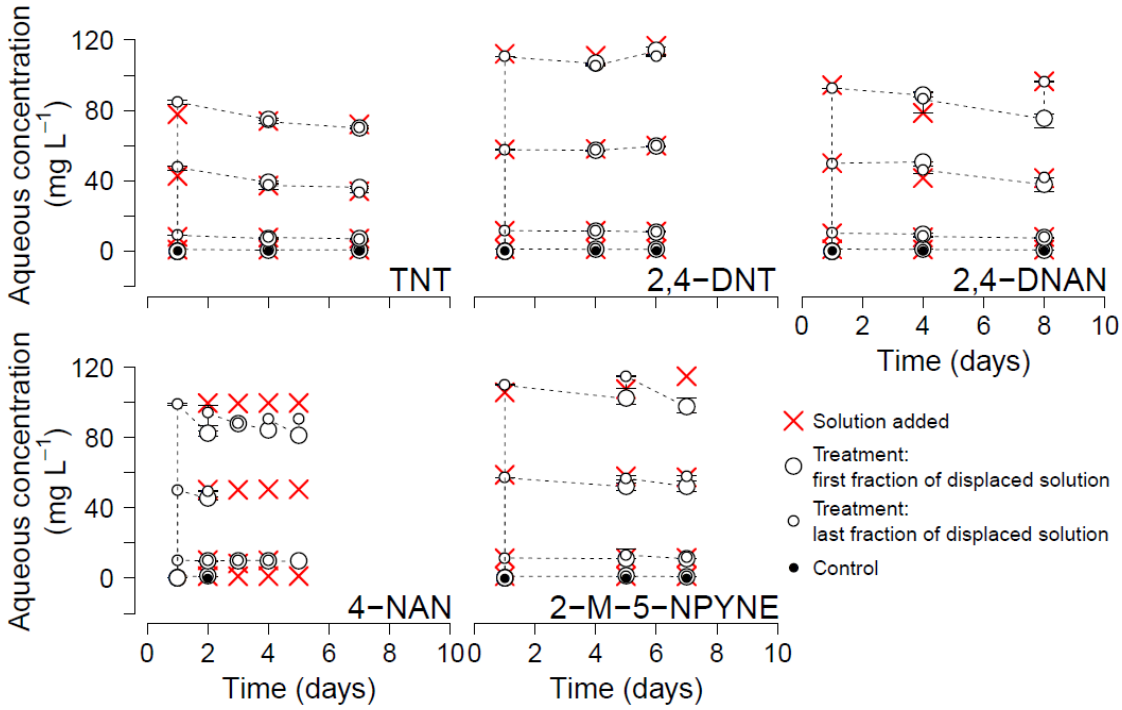

Figure A-2 Exposure concentrations over time for MCs and MLCs in toxicity screening with barley at five concentrations of solution added (nominal: Control, 1, 10, 50, and 100 mg L^{-1}). Legend: Solution added is the solution sampled just before being loaded into plant pots; Treatment are samples from displaced solutions of pots exposed to MCs or MLCs; first and last fraction of displaced solution refer to the first and last pore volume replenished daily; Control are samples from displaced solutions of untreated plant pots (not exposed to MCs or MLCs). Data presented as means and error bars represent the range.

Table A-3 Summary statistics for the fluctuation in measured exposure concentrations for MCs and MLCs during toxicity screening with barley [a].

Compound	NumDF[b]	DenDF[c]	F-value	p-value[d]
TNT	1.00E+00	1.41E+01	1.58E+00	2.29E-01
2,4-DNT	1.00E+00	2.54E+01	3.42E-02	8.55E-01
2,4-DNAN	1.00E+00	5.40E+01	1.04E+00	3.13E-01
4-NAN	1.00E+00	4.70E+01	1.55E-02	9.01E-01
2-M-5-NPYNE	1.00E+00	5.40E+01	2.24E-01	6.38E-01

[a] Time effect was analyzed for the four concentration of solutions added (nominal: 1, 10, 50, and 100 mg L^{-1}) altogether per MC or MLC. In cases of unbalanced ANOVA (e.g., missing data), a linear mixed-effect model analysis was conducted using Satterthwaite approximation for degrees of freedom to estimate p-values.
[b] Degrees of freedom numerator
[c] Degrees of freedom denominator
[d] A p-value ≤ 0.05 was accepted as significant

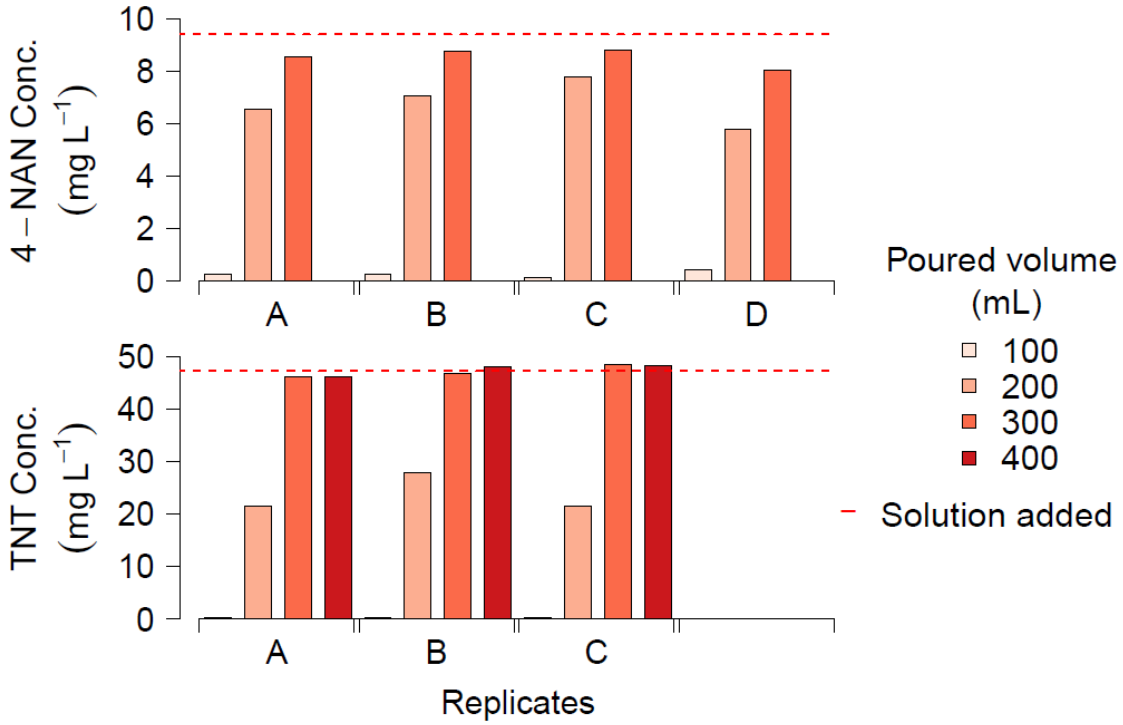

Figure A-3 Concentrations in displaced solutions collected at the end of each consecutive pore volume (pv, 100 mL per pv) on the first day of exposure to MCs and MLCs for selected chemicals during toxicity screening with barley. Solution added: Aqueous solution containing TNT or 4-NAN and being loaded to plant pots. Replicates: Plant pots subjected to the same solution added. Difference in TNT concentration between solution added and displaced solution collected from 4th pore volume were not statistically significant (p-value = 0.80).

A.3 Uptake Assays

Table A-4 Summary statistics for the fluctuation in measured exposure concentrations for MCs and MLCs during uptake assays with barley [a].

Compound	NumDF[b]	DenDF[c]	F-value	p-value[d]
TNT	1.00E+00	7.20E+01	1.82E+01	5.96E-05[e]
2,4-DNT	1.00E+00	6.59E+00	4.33E+00	7.86E-02
2,4-DNAN	1.00E+00	7.00E+01	2.78E+00	1.00E-01
4-NAN	1.00E+00	1.74E+01	3.80E-01	5.46E-01
2-M-5-NPYNE	1.00E+00	7.20E+01	2.22E-01	6.39E-01

[a] Time effect was analyzed for the four exposure times (1, 2, 3, and 4 weeks) altogether per MC or MLC. Unbalanced ANOVA (unequal number of observations over time due to destructive sampling across exposure weeks) was conducted through a linear mixed-effect model analysis using Satterthwaite approximation for degrees of freedom to estimate p-values
[b] Degrees of freedom numerator
[c] Degrees of freedom denominator
[d] A p-value ≤ 0.05 was accepted as significant
[e] Subsequent multiple comparisons test revealed a p-value = 0.90 for the difference between paired means of displaced solution collected on the 3rd and 4th weeks of exposure

Table A-5 Summary statistics for the significance of sorption of MCs and MLCs onto the solid growth medium (sand) during uptake assays with barley [a].

Compound	NumDF[b]	DenDF[c]	F-value	p-value[d]
TNT	1.00E+00	5.70E+01	1.71E-04	9.90E-01
2,4-DNT	1.00E+00	1.39E+01	1.73E+00	2.10E-01
2,4-DNAN	1.00E+00	5.50E+01	1.47E+00	2.30E-01
4-NAN	1.00E+00	3.70E+01	1.92E+00	1.74E-01
2-M-5-NPYNE	1.00E+00	8.05E+00	4.08E+00	7.78E-02

[a] Significance of sorption onto sand was analyzed comparing the concentrations of the solutions added and the displaced solutions sampled at the end of the daily replenishment from treated pots for the four exposure times (1, 2, 3, and 4 weeks) altogether per MC or MLC. Unbalanced ANOVA (unequal number of observations over time due to destructive sampling across exposure weeks) was conducted through a linear mixed-effect model analysis using Satterthwaite approximation for degrees of freedom to estimate p-values

[b] Degrees of freedom numerator

[c] Degrees of freedom denominator

[d] A p-value ≤ 0.05 was accepted as significant

Table A-6 Summary statistics for the significance of exposure time in the ratios of $\frac{C_{i_{Plant}}}{C_{i_{IW}}}$ for MCs and MLCs during uptake assays with barley [a].

Compound	Df	Sum Sq	Mean Sq	F-value	p-value[b]
TNT	3	1.83E-02	6.10E-03	2.19E+00	1.90E-01
2,4-DNT	3	3.72E-02	1.24E-02	2.32E+00	1.75E-01
2,4-DNAN	3	1.43E-01	4.76E-02	2.06E+00	2.07E-01
4-NAN	3	5.90E-01	1.97E-01	2.00E+01	7.17E-03[c]
2-M-5-NPYNE	3	3.32E-02	1.11E-02	6.49E-01	6.12E-01

[a] One-way ANOVA was used to assess the significance of exposure time on the ratio of concentration in the plant to concentration in the interstitial water, $\frac{C_{i_{Plant}}}{C_{i_{IW}}}$

[b] A p-value ≤ 0.05 was accepted as significant

[c] Subsequent multiple comparisons test revealed a p-value = 0.90 for the difference between paired means of $\frac{C_{i_{Plant}}}{C_{i_{IW}}}$ from the 3rd and 4th weeks of exposure

Table A-7 Ratios of $\frac{C_{i_{Plant}}}{C_{i_{IW}}}$ [b] for the compounds evaluated in uptake assays with barley.

Compound	Trial #	Exposure Time	Plant Mass	Concentration in Plant[c]	Concentration in Interstitial Water[d]	$\log\left(\frac{C_{i_{Plant}}}{C_{i_{IW}}}\right)$
		days	g_{dwt}[a]	mg kg_{dwt}^{-1}	mg L^{-1}	L kg_{dwt}^{-1}
TNT	1st	9	3.82E-01	4.36E+01	8.74E+00	6.97E-01
TNT	1st	9	4.07E-01	5.32E+01	9.37E+00	7.54E-01
TNT	1st	9	4.00E-01	4.41E+01	9.35E+00	6.73E-01
TNT	1st	16	5.68E-01	3.53E+01	7.15E+00	6.93E-01
TNT	1st	16	5.26E-01	2.72E+01	7.05E+00	5.86E-01
TNT	1st	16	5.63E-01	2.58E+01	7.11E+00	5.59E-01
TNT	1st	23	5.23E-01	2.56E+01	6.00E+00	6.30E-01
TNT	1st	23	4.79E-01	2.46E+01	5.84E+00	6.26E-01
TNT	1st	30	5.40E-01	3.16E+01	7.09E+00	6.49E-01
TNT	1st	30	4.41E-01	2.22E+01	6.00E+00	5.69E-01
2,4-DNT	1st	8	4.19E-01	5.83E+01	9.07E+00	8.08E-01
2,4-DNT	1st	8	6.28E-01	5.68E+01	9.09E+00	7.96E-01
2,4-DNT	1st	15	4.26E-01	6.65E+01	9.07E+00	8.65E-01

2,4-DNT	1st	15	4.96E-01	5.82E+01	8.98E+00	8.11E-01
2,4-DNT	1st	22	4.30E-01	5.09E+01	9.84E+00	7.14E-01
2,4-DNT	1st	22	4.36E-01	3.96E+01	9.82E+00	6.05E-01
2,4-DNT	1st	22	4.50E-01	5.98E+01	9.85E+00	7.83E-01
2,4-DNT	1st	29	3.76E-01	4.92E+01	9.44E+00	7.17E-01
2,4-DNT	1st	29	3.77E-01	3.79E+01	9.49E+00	6.01E-01
2,4-DNT	1st	29	3.19E-01	5.49E+01	9.39E+00	7.67E-01
2,4-DNAN	1st	22	3.85E-01	2.04E+02	7.56E+00	1.43E+00
2,4-DNAN	1st	22	3.62E-01	2.20E+02	7.71E+00	1.46E+00
2,4-DNAN	1st	29	3.92E-01	2.11E+02	7.98E+00	1.42E+00
2,4-DNAN	1st	29	5.25E-01	1.16E+02	8.10E+00	1.15E+00
2,4-DNAN	2nd	8	3.70E-01	7.49E+01	9.76E+00	8.85E-01
2,4-DNAN	2nd	8	3.44E-01	2.41E+02	1.24E+01	1.29E+00
2,4-DNAN	2nd	8	4.37E-01	7.13E+01	9.75E+00	8.64E-01
2,4-DNAN	2nd	15	3.78E-01	1.45E+02	1.01E+01	1.16E+00
2,4-DNAN	2nd	15	3.82E-01	1.76E+02	9.62E+00	1.26E+00
2,4-DNAN	2nd	15	5.23E-01	1.37E+02	9.64E+00	1.15E+00
2,4-DNAN	2nd	22	4.73E-01	1.17E+02	1.06E+01	1.04E+00
2,4-DNAN	2nd	22	4.87E-01	1.59E+02	1.09E+01	1.16E+00
2,4-DNAN	2nd	29	2.77E-01	2.37E+02	1.07E+01	1.35E+00
2,4-DNAN	2nd	29	4.28E-01	2.55E+02	1.05E+01	1.39E+00

4-NAN	1st	8	5.72E-01	1.03E+01	9.73E+00	2.51E-02
4-NAN	1st	8	4.72E-01	6.91E+00	9.84E+00	-1.53E-01
4-NAN	1st	15	4.27E-01	1.07E+01	9.66E+00	4.65E-02
4-NAN	1st	15	3.12E-01	7.28E+00	9.31E+00	-1.07E-01
4-NAN	1st	22	6.56E-01	2.39E+01	9.71E+00	3.91E-01
4-NAN	1st	22	5.85E-01	3.31E+01	9.84E+00	5.27E-01
4-NAN	1st	29	3.40E-01	3.01E+01	9.69E+00	4.93E-01
4-NAN	1st	29	2.73E-01	3.51E+01	9.62E+00	5.62E-01
4-NAN	2nd	22	7.22E-01	2.56E+01	7.28E+00	5.46E-01
4-NAN	2nd	22	7.05E-01	4.08E+01	6.99E+00	7.67E-01
4-NAN	2nd	29	7.50E-01	3.61E+01	7.48E+00	6.84E-01
4-NAN	2nd	29	7.94E-01	3.68E+01	7.54E+00	6.88E-01
4-NAN	3rd	22	5.79E-01	2.76E+01	7.23E+00	5.82E-01
4-NAN	3rd	22	5.83E-01	2.81E+01	7.27E+00	5.87E-01
4-NAN	3rd	29	4.64E-01	2.02E+01	7.31E+00	4.42E-01
4-NAN	3rd	29	5.27E-01	2.32E+01	7.25E+00	5.06E-01
4-NAN	3rd	29	6.04E-01	2.41E+01	7.26E+00	5.21E-01
4-NAN	4th	23	4.35E-01	2.05E+01	7.43E+00	4.41E-01
4-NAN	4th	23	3.87E-01	1.81E+01	7.50E+00	3.84E-01
4-NAN	4th	23	3.29E-01	2.50E+01	7.53E+00	5.22E-01
4-NAN	4th	30	4.00E-01	2.41E+01	7.62E+00	5.00E-01

4-NAN	4th	30	5.53E-01	1.50E+01	7.63E+00	2.92E-01
4-NAN	4th	30	5.85E-01	1.73E+01	7.65E+00	3.54E-01
2-M-5-NPYNE	1st	8	5.77E-01	4.30E+01	1.10E+01	5.94E-01
2-M-5-NPYNE	1st	8	4.53E-01	3.19E+01	1.09E+01	4.66E-01
2-M-5-NPYNE	1st	8	4.38E-01	3.26E+01	1.11E+01	4.66E-01
2-M-5-NPYNE	1st	15	5.35E-01	4.73E+01	9.68E+00	6.89E-01
2-M-5-NPYNE	1st	15	6.19E-01	2.40E+01	1.03E+01	3.67E-01
2-M-5-NPYNE	1st	15	7.02E-01	2.20E+01	9.84E+00	3.50E-01
2-M-5-NPYNE	1st	22	7.18E-01	2.80E+01	1.02E+01	4.39E-01
2-M-5-NPYNE	1st	22	7.67E-01	1.83E+01	1.02E+01	2.52E-01
2-M-5-NPYNE	1st	29	7.61E-01	2.79E+01	1.01E+01	4.40E-01
2-M-5-NPYNE	1st	29	6.35E-01	3.09E+01	1.02E+01	4.82E-01

[a] dwt: dry weight

[b] $C_{i_{Plant}}$: concentration of compound i in barley (mg kg_{dwt}^{-1}), $C_{i_{IW}}$: concentration of compound i in the interstitial water, which was measured in the displaced solution (mg L^{-1})

[c] Plant = shoots + roots

[d] Measured in the displaced solution

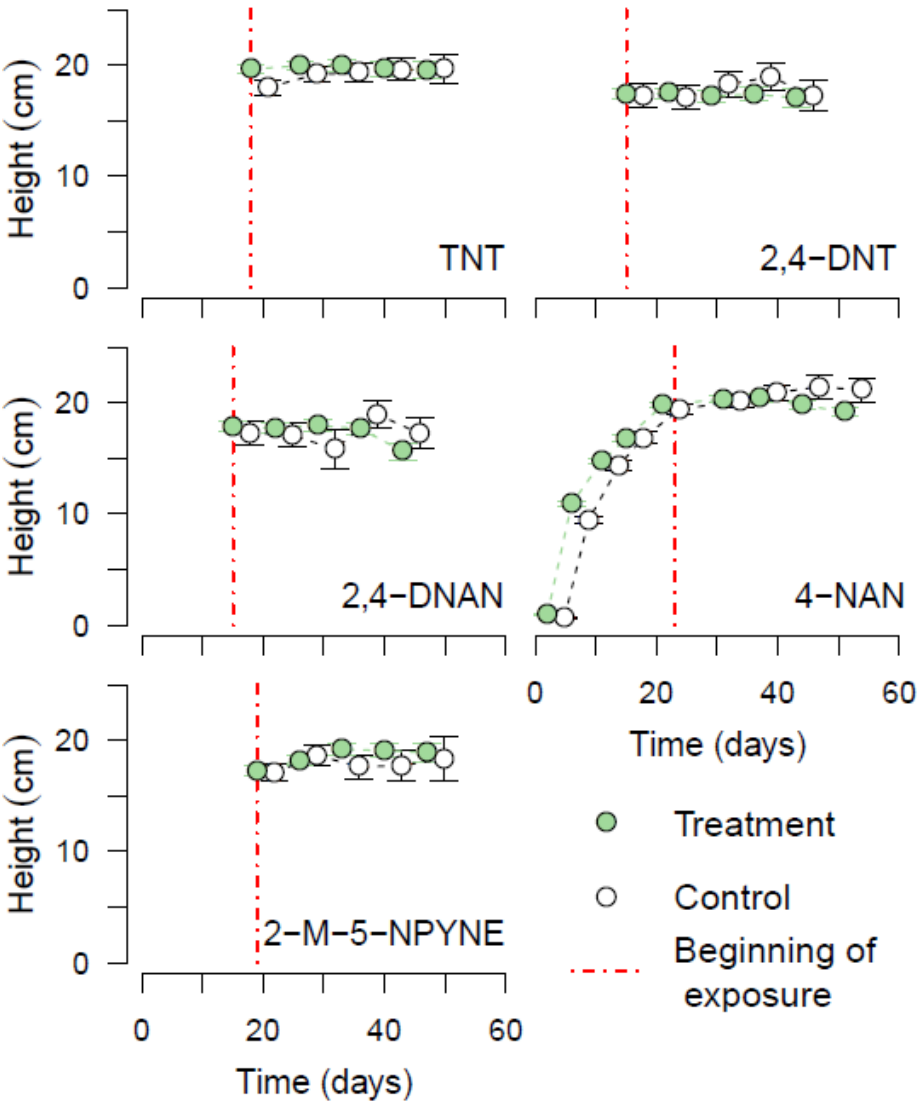

Figure A-4 Biomass profiles (shoot height) for barley exposed to individual MCs, or MLCs, during uptake assays. Legend: Treatment are plant pots exposed to MCs or MLCs at a nominal concentration of 10 mg L^{-1}; Control are untreated plant pots (not exposed to MCs or MLCs). Displaying 2nd trial for 2,4-DNAN and 1st trial for 4-NAN. Data presented as means ± standard error of the mean (SEM).

A.4 Plant-Water Partitioning vs. BCF

Table A-8 Plant-water partition coefficients (K_{PW}) for 4-NAN with barley and the summary statistics for the significance of contact time (kinetics) on log K_{PW} values [a].

Contact time	Replicate	log K_{PW}
h		L kg_{dwt}^{-1}
24	A	1.16E+00
24	B	1.13E+00
24	C	1.19E+00
48	A	1.07E+00
48	B	1.13E+00
48	C	1.19E+00
144	A	1.09E+00
144	B	1.12E+00
144	C	1.03E+00

Summary statistics

	Df	Sum Sq	Mean Sq	*F*	p-value[b]
Contact time	2	9.56E-03	4.78E-03	2.34E+00	1.77E-01
Residuals	6	1.23E-02	2.04E-03		

[a] One-way ANOVA was used to assess the significance of contact time on the 4-NAN log K_{PW} values

[b] A p-value ≤ 0.05 was accepted as significant

Table A-9 Summary statistics for the significance of the concentration of the initial solution added on log K_{PW} values [a].

Compound	t-test	Df	p-value[b]
2,5-DM-4-NANE	1.79E+00	2.68E+00	1.83E-01
2-M-5-NPYNE	-4.53E+00	1.16E+00	1.12E-01
2,4-DNAN	1.61E+00	9.79E+00	1.38E-01
4-NAN	1.86E+00	1.39E+00	2.56E-01
2,4-DNT	-2.26E+00	3.23E+00	1.02E-01
TNT	2.27E-01	4.59E+00	8.30E-01
RDX	2.09E+00	1.24E+00	2.44E-01

[a] Two-tailed t-tests assuming unequal variances were used to assess the significance of the concentration of the initial solution added on the log K_{PW} values
[b] A p-value ≤ 0.05 was accepted as significant

Table A-10 Plant-Water Partition Coefficients (K_{PW}) for the compounds evaluated.

Compound	Trial #	Nominal Concentration of Initial Solution Added[a]	Plant Mass	Concentration in Plant[c]	Concentration in Water Phase[c]	log K_{PW}[e]	Exposure[f]
		mg L^{-1}	g_{dwt}[b]	mg kg_{dwt}^{-1}	mg L^{-1}	L kg_{dwt}^{-1}	
2,5-DM-4-NANE	1st	10	4.31E-01	3.06E+01[d]	5.04E+00	7.83E-01	Low
2,5-DM-4-NANE	1st	10	5.17E-01	4.28E+01	3.87E+00	1.04E+00	Low
2,5-DM-4-NANE	1st	10	3.94E-01	3.71E+01	4.85E+00	8.84E-01	Low
2,5-DM-4-NANE	1st	100	4.34E-01	2.68E+02	4.17E+01	8.07E-01	High
2,5-DM-4-NANE	1st	100	4.38E-01	2.43E+02	4.31E+01	7.50E-01	High
2,5-DM-4-NANE	1st	100	4.18E-01	2.24E+02	4.45E+01	7.02E-01	High
HMX	1st	4	2.75E-01	1.32E+01	1.95E+00	8.32E-01	High
HMX	1st	4	2.23E-01	1.66E+01	2.03E+00	9.13E-01	High
HMX	1st	4	2.08E-01	1.39E+01	2.22E+00	7.97E-01	High
2-M-5-NPYNE	1st	16	6.67E-01	4.29E+01	6.41E+00	8.25E-01	Low
2-M-5-NPYNE	1st	16	6.68E-01	5.59E+01	6.96E+00	9.05E-01	Low
2-M-5-NPYNE	1st	160	2.18E-01	1.04E+03	9.95E+01	1.02E+00	High
2-M-5-NPYNE	1st	160	1.91E-01	1.09E+03	1.00E+02	1.04E+00	High

2,4-DNAN	1st	10	3.99E-01	6.32E+01	4.24E+00	1.17E+00	Low
2,4-DNAN	1st	10	4.23E-01	6.94E+01	3.73E+00	1.27E+00	Low
2,4-DNAN	1st	10	4.76E-01	6.88E+01	3.67E+00	1.27E+00	Low
2,4-DNAN	1st	10	4.79E-01	3.87E+01	4.63E+00	9.22E-01	Low
2,4-DNAN	1st	10	3.62E-01	6.33E+01	4.10E+00	1.19E+00	Low
2,4-DNAN	1st	10	3.10E-01	1.01E+02	3.84E+00	1.42E+00	Low
2,4-DNAN	2nd	10	3.59E-01	7.63E+01	4.76E+00	1.21E+00	Low
2,4-DNAN	2nd	10	3.37E-01	7.67E+01	4.99E+00	1.19E+00	Low
2,4-DNAN	3rd	10	4.25E-01	5.03E+01	4.10E+00	1.09E+00	Low
2,4-DNAN	3rd	10	4.19E-01	5.53E+01	3.95E+00	1.15E+00	Low
2,4-DNAN	3rd	100	3.71E-01	5.69E+02	4.26E+01	1.13E+00	High
2,4-DNAN	3rd	100	4.24E-01	5.29E+02	4.15E+01	1.11E+00	High
2,4-DNT	1st	6	4.60E-01	3.30E+01	2.37E+00	1.14E+00	Low
2,4-DNT	1st	6	5.39E-01	3.24E+01	2.03E+00	1.20E+00	Low
2,4-DNT	1st	60	4.22E-01	3.86E+02	2.00E+01	1.29E+00	High
2,4-DNT	1st	60	4.30E-01	3.97E+02	2.27E+01	1.24E+00	High
2,4-DNT	2nd	60	1.40E+00	2.04E+02	1.30E+01	1.20E+00	High
2,4-DNT	2nd	60	3.40E-01	5.32E+02	2.37E+01	1.35E+00	High
4-NAN	1st	10	3.79E-01	7.83E+01	4.25E+00	1.27E+00	Low
4-NAN	1st	10	2.73E-01	6.66E+01	4.41E+00	1.18E+00	Low
4-NAN	1st	10	4.31E-01	7.67E+01	2.37E+00	1.51E+00	Low

4-NAN	1st	10	3.85E-01	7.06E+01	3.79E+00	1.27E+00	Low
4-NAN	1st	10	3.58E-01	8.28E+01	3.99E+00	1.32E+00	Low
4-NAN	1st	10	2.54E-01	8.87E+01	3.91E+00	1.36E+00	Low
4-NAN	2nd	10	3.75E-01	7.06E+01	4.35E+00	1.21E+00	Low
4-NAN	2nd	10	3.10E-01	7.18E+01	4.98E+00	1.16E+00	Low
4-NAN	2nd	10	3.65E-01	7.05E+01	4.33E+00	1.21E+00	Low
4-NAN	1st	100	5.24E-01	5.75E+02	5.50E+01	1.02E+00	High
4-NAN	1st	100	2.83E-01	8.07E+02	5.19E+01	1.19E+00	High
TNT	1st	10	3.16E-01	5.34E+01	2.97E+00	1.25E+00	Low
TNT	1st	10	4.19E-01	4.66E+01	2.44E+00	1.28E+00	Low
TNT	2nd	10	3.63E-01	5.18E+01	2.86E+00	1.26E+00	Low
TNT	2nd	10	2.37E-01	7.33E+01	2.94E+00	1.40E+00	Low
TNT	2nd	10	2.41E-01	7.98E+01	3.14E+00	1.40E+00	Low
TNT	2nd	100	2.41E-01	7.32E+02	3.65E+01	1.30E+00	High
TNT	2nd	100	1.96E-01	9.09E+02	4.31E+01	1.32E+00	High
RDX	2nd	4	2.11E-01	5.14E+01[d]	1.02E+00	1.70E+00	Low
RDX	2nd	4	2.16E-01	5.22E+01	9.79E-01	1.73E+00	Low
RDX	2nd	4	2.93E-01	3.59E+01	1.07E+00	1.52E+00	Low
RDX	1st	40	2.85E-01	3.59E+02	1.36E+01	1.42E+00	High
RDX	1st	40	3.04E-01	2.03E+02	1.86E+01	1.04E+00	High

[a] Difference with respect to measured concentration was never > 20%
[b] dwt: dry weight
[c] Measured at the end of the 24 h equilibration period
[d] Due to failure to completely avoid overlap of 2,5-DM-4-NANE and RDX peaks with background signals in plant extracts samples, all concentrations in plant tissues at the end of the 24 h equilibration period were calculated by mass balance for 2,5-DM-4-NANE and RDX
[e] Ratio of concentration in plant to concentration in water phase, both measured at the end of the 24 h equilibration period
[f] Calculated as the ratio of the nominal concentration of initial solution added to the aqueous solubility. Ratios ranged from 0.01 to 0.09 and 0.06 to 0.87 for the low and high exposures, respectively.

Table A-11 Time course data obtained from Sunahara [20] and Dodard et al. [30], and estimated degradation rates for MCs [a].

Compound	Total time[b]	Time[c]	$C_{i_{Plant}}(t)$[a]		Fitted Parameters		Median K_{PW}	Median BCF
			Observed	Predicted	$C_{i_{Plant}}(0)$ (SEM)[a]	$k_{degradation}$ (SEM)[a]		
	days	days	mg kg_{dwt}^{-1}		mg kg_{dwt}^{-1}	d^{-1}	L kg_{dwt}^{-1}	L kg_{dwt}^{-1}
2,4-DNAN	0	0	5.25E+01[d]	5.25E+01	5.25E+01	6.63E-02	1.51E+01	2.33E+01
	19	19	1.49E+01	1.49E+01				
2,4-DNT	21	0	3.20E+00[e]	3.13E+00	3.13E+00 (3.34E-01)	8.32E-02 (2.16E-02)	1.67E+01	5.19E+00
	28	7	1.50E+00	1.75E+00				
	35	14	1.20E+00	9.77E-01				
TNT	14	0	2.04E+01[e]	2.03E+01	2.03E+01 (9.91E-01)	1.89E-01 (2.35E-02)	2.00E+01	4.25E+00
	21	7	5.00E+00	5.42E+00				
	28	14	1.70E+00	1.44E+00				
	35	21	1.70E+00	3.85E-01				

[a] An exponential decay model was fitted to the concentration in the plant ($C_{i_{Plant}}(t)$) time course data to obtain the maximum concentration in the plant ($C_{i_{Plant}}(0)$) and degradation rate ($k_{\text{degradation}}$): $C_{i_{Plant}}(t) = C_{i_{Plant}}(0)\, e^{(-k_{degradation}t)}$. SEM: Standard error of the mean

[b] Time starting from beginning of exposure

[c] Time starting from when maximum concentration in the plant was observed

[d] Assumed to be equal to the sum of the parent compound and transformation product at 19 days in absence of an initial value; data measured in the shoots from a soil exposure at 4.7 mg kg_{dwt}^{-1}

[e] All the time course data for 2,4-DNT and TNT were measurements in the roots from soil exposures at 10 and 100 mg kg_{dwt}^{-1}, respectively

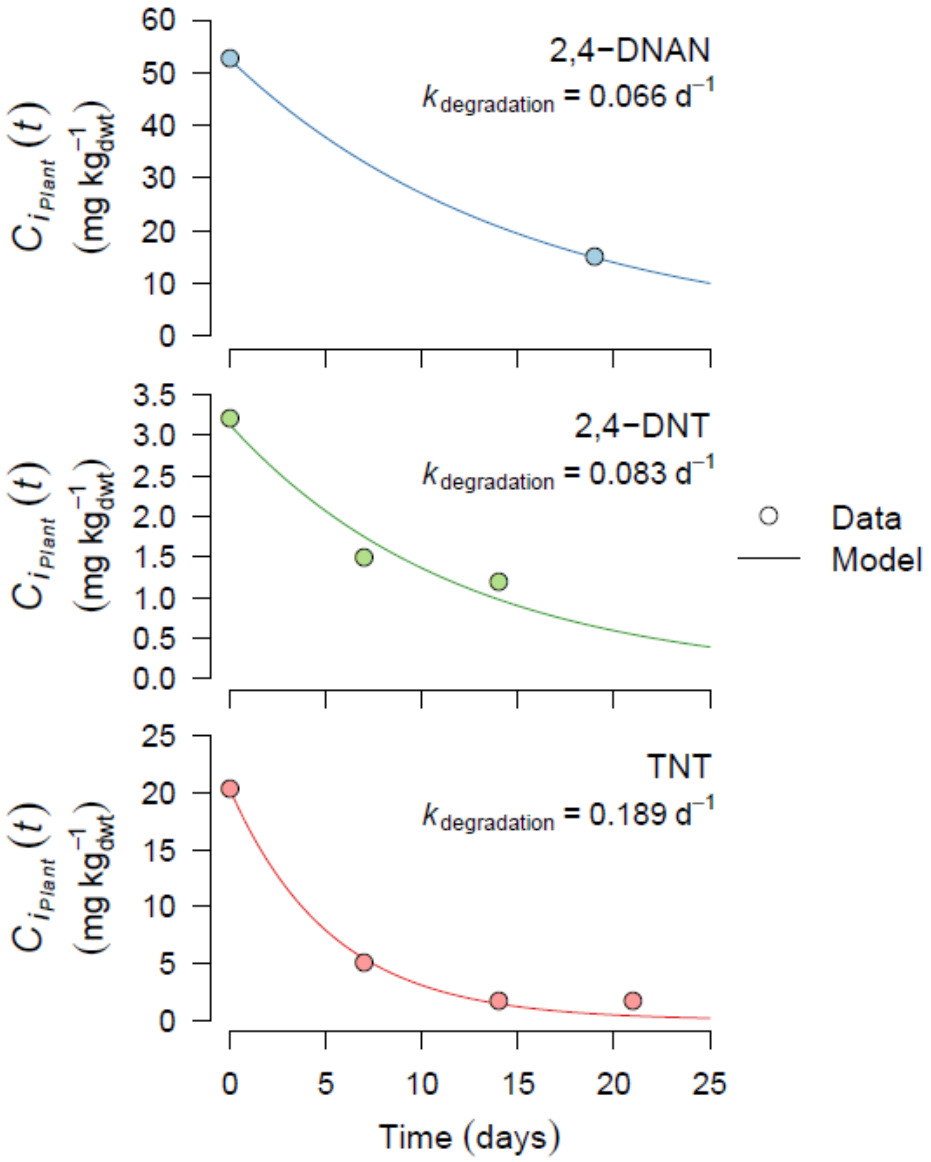

Figure A-5 Concentration in the plant ($C_{i_{Plant}}(t)$) over time and estimated degradation rates ($k_{degradation}$) for MCs. An exponential decay model fitted to time course data obtained from Sunahara [20] and Dodard et al. [30] (Table A-11 in Appendix A)

Appendix B

MODEL PARAMETERS AND DATA FOR pp–LFERs PREDICTION OF MUNITIONS COMPOUNDS BIOCONCENTRATION IN PLANTS

References cited in this appendix are listed in the "REFERENCES" section of Chapter 3.

B.1 Munitions Compounds (MCs) and Munitions-Like Compounds (MLCs)

Table B-1 Selected characteristics and physicochemical properties of the MCs and MLCs.

Class	Compound[a]	CAS #	Molecular Weight	Structure	Aqueous Solubility[b] mg L^{-1}	log K_{OW}[b]
MCs: Nitroaromatics	TNT	118-96-7	227.13	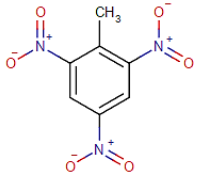	115	1.60
	2,4-DNT	121-14-2	182.14	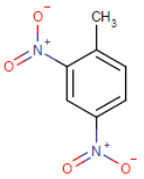	200	1.98

	2,4-DNAN	119-27-7	198.14	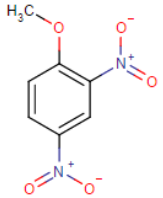	155	1.58[c]
MCs: Nitramines	RDX	121-82-4	222.12	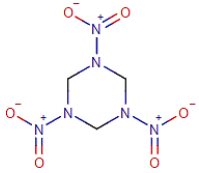	60	0.87
	HMX	2691-41-0	296.16	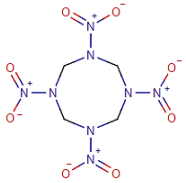	5	0.16
MLCs	4-NAN	100-17-4	153.14	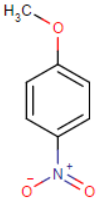	590	2.03
	2-M-5-NPYNE	5446-92-4	154.13	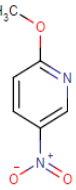	1406[d]	1.55

2,5-DM-4-NANE	6313-37-7	198.18	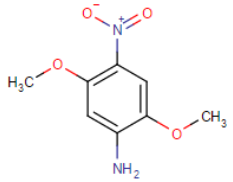	1801[d]	1.63[d]

[a] Chemicals: 2,4,6-trinitrotoluene (TNT); 2,4-dinitrotoluene (2,4-DNT); 2,4-dinitroanisole (2,4-DNAN); hexahydro-1,3,5-trinitro-1,3,5-triazine (RDX); octahydro-1,3,5,7-tetranitro-1,3,5,7-tetrazocine (HMX); 4-nitroanisole (4-NAN); 2-methoxy-5-nitropyridine (2-M-5-NPYNE); 2,5-dimethoxy-4-nitroaniline (2,5-DM-4-NANE)

[b] Experimental data from EPI Suite database [55]

[c] Experimental value from Hawari et al. [56]

[d] Estimate from EPI Suite [55] in absence of an experimental value

B.2 Polyparameter Linear Free Energy Relationship (pp–LFER) Models

Table B-2 Plant cuticle-water partition coefficients (K_{Cut}) data.

Compound[a]	CAS #	Obs. log K_{OW}[b]	Plant Species[e]	Plant common name[f]	Plant tissue[g]	Obs. log K_{Cut}[h]	Source[i]
methanol	67-56-1	-0.77	*L. esculentum*	Tomato frt.	MX	-1.09	[9]
acetonitrile	75-05-8	-0.34	*L. esculentum*	Tomato frt.	MX	-0.27	[9]
ethanol	64-17-5	-0.31	*L. esculentum*	Tomato frt.	MX	-0.86	[9]
1,4-dioxane	123-91-1	-0.27	*L. esculentum*	Tomato frt.	MX	-0.56	[9]
propanone	67-64-1	-0.24	*L. esculentum*	Tomato frt.	MX	-0.39	[9]
propan-2-ol	67-63-0	0.05	*L. esculentum*	Tomato frt.	MX	-0.60	[9]
HMX	2691-41-0	0.16	*H. vulgare*	Barley	Whole	1.580	This work
propan-1-ol	71-23-8	0.25	*L. esculentum*	Tomato frt.	MX	-0.30	[9]
acrylonitrile	107-13-1	0.25	*L. esculentum*	Tomato frt.	MX	0.02	[9]
butanone	78-93-3	0.29	*L. esculentum*	Tomato frt.	MX	-0.16	[9]
2-methylpropan-2-ol	75-65-0	0.35	*L. esculentum*	Tomato frt.	MX	-0.37	[9]
1-C-2,3-E	106-89-8	0.45	*L. esculentum*	Tomato frt.	MX	0.49	[9]
tetrahydrofuran	109-99-9	0.46	*L. esculentum*	Tomato frt.	MX	0.12	[9]
butan-2-ol	78-92-2	0.61	*L. esculentum*	Tomato frt.	MX	-0.09	[9]

pyridine	110-86-1	0.65	*L. esculentum*	Tomato frt.	MX	0.39	[9]
ethyl acetate	141-78-6	0.73	*L. esculentum*	Tomato frt.	MX	0.37	[9]
2-methylpropan-1-ol	78-83-1	0.76	*L. esculentum*	Tomato frt.	MX	0.11	[9]
cyclohexanone	108-94-1	0.81	*L. esculentum*	Tomato frt.	MX	0.32	[9]
1-nitropropane	108-03-2	0.87	*L. esculentum*	Tomato frt.	MX	0.95	[9]
RDX	121-82-4	0.87	*H. vulgare*	Barley	Whole	1.964	This work
RDX	121-82-4	0.87	*H. vulgare*	Barley	Whole	2.384	This work
butan-1-ol	71-36-3	0.88	*L. esculentum*	Tomato frt.	MX	0.24	[9]
2-methylbutan-2-ol	75-85-4	0.89	*L. esculentum*	Tomato frt.	MX	0.11	[9]
pentan-2-ol	6032-29-7	1.19	*L. esculentum*	Tomato frt.	MX	0.46	[9]
propyl acetate	109-60-4	1.24	*L. esculentum*	Tomato frt.	MX	0.80	[9]
dichloromethane	75-09-2	1.25	*L. esculentum*	Tomato frt.	MX	1.42	[9]
4-MP-2	108-10-1	1.31	*L. esculentum*	Tomato frt.	MX	0.80	[9]
phenol	108-95-2	1.46	*L. esculentum*	Tomato frt.	MX	1.64	[57]
phenol	108-95-2	1.46	*F. elastica*	Rubber plant lf.	MX	1.69	[57]
phenol	108-95-2	1.46	*C. annuum*	Green pepper frt.	MX	1.67	[57]
phenol	108-95-2	1.46	*C. annuum*	Pepper frt.	MX	2.334	[58]
1,2-dichloroethane	107-06-2	1.48	*L. esculentum*	Tomato frt.	MX	1.46	[9]
pentan-1-ol	71-41-0	1.51	*L. esculentum*	Tomato frt.	MX	0.76	[9]
2-M-5-NPYNE	5446-92-4	1.55	*H. vulgare*	Barley	Whole	1.598	This work
2-M-5-NPYNE	5446-92-4	1.55	*H. vulgare*	Barley	Whole	1.761	This work

2,4-DNAN	119-27-7	1.58[d]	*H. vulgare*	Barley	Whole	1.921	This work
2,4-DNAN	119-27-7	1.58	*H. vulgare*	Barley	Whole	1.849	This work
TNT	118-96-7	1.60	*H. vulgare*	Barley	Whole	2.052	This work
TNT	118-96-7	1.60	*H. vulgare*	Barley	Whole	2.046	This work
2,5-DM-4-NANE	6313-37-7	1.63[c]	*H. vulgare*	Barley	Whole	1.637	This work
2,5-DM-4-NANE	6313-37-7	1.63	*H. vulgare*	Barley	Whole	1.487	This work
metribuzin	21087-64-9	1.70	*P. laurocerasus*	Cherry laurel lf.	CM	1.484	[59]
3-methylpentan-3-ol	77-74-7	1.71[c]	*L. esculentum*	Tomato frt.	MX	0.61	[9]
hexan-2-ol	626-93-7	1.76	*L. esculentum*	Tomato frt.	MX	1.01	[9]
butyl acetate	123-86-4	1.78	*L. esculentum*	Tomato frt.	MX	1.34	[9]
2-nitrophenol	88-75-5	1.79	*L. esculentum*	Tomato frt.	MX	1.99	[57]
2-nitrophenol	88-75-5	1.79	*F. elastica*	Rubber plant lf.	MX	1.99	[57]
2-nitrophenol	88-75-5	1.79	*C. annuum*	Green pepper frt.	MX	2.04	[57]
benzoic acid	65-85-0	1.87	*C. annuum*	Green pepper frt.	MX	1.58	[57]
benzoic acid	65-85-0	1.87	*P. laurocerasus*	Rubber plant lf.	CM	1.679	[59]
benzoic acid	65-85-0	1.87	*G. biloba*	Ginkgo lf.	CM	1.724	[59]
benzoic acid	65-85-0	1.87	*J. regia*	Eng. walnut lf.	CM	1.719	[59]
4-nitrophenol	100-02-7	1.91	*L. esculentum*	Tomato frt.	MX	1.91	[57]
4-nitrophenol	100-02-7	1.91	*C. aurantium*	Bitter orange lf.	MX	1.76	[57]
4-nitrophenol	100-02-7	1.91	*F. elastica*	Rubber plant lf.	MX	1.89	[57]
4-nitrophenol	100-02-7	1.91	*C. annuum*	Green pepper frt.	MX	2.03	[57]

4-nitrophenol	100-02-7	1.91	*P. laurocerasus*	Cherry laurel lf.	CM	1.773	[59]
3-chloroprop-1-ene	107-05-1	1.93[c]	*L. esculentum*	Tomato frt.	MX	1.66	[9]
1,2-dibromoethane	106-93-4	1.96	*L. esculentum*	Tomato frt.	MX	1.75	[9]
trichloromethane	67-66-3	1.97	*L. esculentum*	Tomato frt.	MX	1.84	[9]
1,2-dichloropropane	78-87-5	1.98	*L. esculentum*	Tomato frt.	MX	1.96	[9]
2,4-DNT	121-14-2	1.98	*H. vulgare*	Barley	Whole	1.906	This work
2,4-DNT	121-14-2	1.98	*H. vulgare*	Barley	Whole	2.003	This work
hexan-1-ol	111-27-3	2.03	*L. esculentum*	Tomato frt.	MX	1.29	[9]
4-NAN	100-17-4	2.03	*H. vulgare*	Barley	Whole	1.839[i]	This work
4-NAN	100-17-4	2.03	*H. vulgare*	Barley	Whole	2.009	This work
trichloronitromethane	76-06-2	2.09	*L. esculentum*	Tomato frt.	MX	2.13	[9]
1,1-dichloroethene	75-35-4	2.13	*L. esculentum*	Tomato frt.	MX	2.04	[9]
benzene	71-43-2	2.13	*L. esculentum*	Tomato frt.	MX	2.00	[9]
benzene	71-43-2	2.13	*L. multiflorum*	Annual rye	Whole	2.097[h]	[29]
1-NAA	86-87-3	2.24	*L. esculentum*	Tomato frt.	MX	2.31	[57]
1-NAA	86-87-3	2.24	*C. aurantium*	Bitter orange lf.	MX	2.25	[57]
1-NAA	86-87-3	2.24	*C. annuum*	Green pepper frt.	MX	2.43	[57]
salicylic acid	69-72-7	2.26	*P. laurocerasus*	Cherry laurel lf.	CM	2.087	[59]
salicylic acid	69-72-7	2.26	*G. biloba*	Ginkgo lf.	CM	2.028	[59]
salicylic acid	69-72-7	2.26	*J. regia*	Eng. walnut lf.	CM	1.981	[59]
2-M-1,3-D	78-79-5	2.42	*L. esculentum*	Tomato frt.	MX	2.09	[9]

trichloroethene	79-01-6	2.42	*L. esculentum*	Tomato frt.	MX	2.56	[9]
1,1,1-trichloroethane	71-55-6	2.49	*L. esculentum*	Tomato frt.	MX	2.44	[9]
atrazine	1912-24-9	2.61	*L. esculentum*	Tomato frt.	MX	2.13	[57]
atrazine	1912-24-9	2.61	*C. aurantium*	Bitter orange lf.	MX	2.17	[57]
atrazine	1912-24-9	2.61	*F. elastica*	Rubber plant lf.	MX	2.15	[57]
atrazine	1912-24-9	2.61	*C. annuum*	Green pepper frt.	MX	2.20	[57]
atrazine	1912-24-9	2.61	*P. laurocerasus*	Cherry laurel lf.	CM	1.899	[59]
toluene	108-88-3	2.73	*L. esculentum*	Tomato frt.	MX	2.50	[9]
2,4-D	94-75-7	2.81	*L. esculentum*	Tomato frt.	MX	2.79	[57]
2,4-D	94-75-7	2.81	*C. aurantium*	Bitter orange lf.	MX	3.20	[57]
2,4-D	94-75-7	2.81	*F. elastica*	Rubber plant lf.	MX	3.20	[57]
2,4-D	94-75-7	2.81	*C. annuum*	Green pepper frt.	MX	3.26	[57]
2,4-D	94-75-7	2.81	*P. laurocerasus*	Cherry laurel lf.	CM	2.628	[59]
2,4-D	94-75-7	2.81	*G. biloba*	Ginkgo lf.	CM	2.630	[59]
2,4-D	94-75-7	2.81	*J. regia*	Eng. walnut lf.	CM	2.624	[59]
tetrachloromethane	56-23-5	2.83	*L. esculentum*	Tomato frt.	MX	2.49	[9]
chlorobenzene	108-90-7	2.84	*L. esculentum*	Tomato frt.	MX	2.70	[9]
1-naphthalenol	90-15-3	2.85	*S. lycopersicum*	Tomato frt.	MX	2.906	[60]
1-naphthalenol	90-15-3	2.85	*M. domestica*	Apple frt.	MX	3.038	[60]
1-naphthalenol	90-15-3	2.85	*C. annuum*	Pepper frt.	MX	2.931	[60]
1-naphthalenol	90-15-3	2.85	*C. annuum*	Pepper frt.	MX	3.009	[58]

triadimenol	55219-65-3	2.90	*L. esculentum*	Tomato frt.	CM	3.37	[57]
triadimenol	55219-65-3	2.90	*C. aurantium*	Bitter orange lf.	CM	3.37	[57]
triadimenol	55219-65-3	2.90	*F. elastica*	Rubber plant lf.	CM	3.26	[57]
triadimenol	55219-65-3	2.90	*C. annuum*	Green pepper frt.	CM	3.37	[57]
styrene	100-42-5	2.95	*L. esculentum*	Tomato frt.	MX	2.83	[9]
o-xylene	95-47-6	3.12	*L. esculentum*	Tomato frt.	MX	2.90	[9]
ethylbenzene	100-41-4	3.15	*L. esculentum*	Tomato frt.	MX	2.82	[9]
naphthalene	91-20-3	3.30	*S. lycopersicum*	Tomato frt.	MX	3.382[f,g]	[60]
naphthalene	91-20-3	3.30	*M. domestica*	Apple frt.	MX	3.418	[60]
naphthalene	91-20-3	3.30	*C. annuum*	Pepper frt.	MX	3.373	[60]
naphthalene	91-20-3	3.30	*C. annuum*	Pepper frt.	MX	3.386[g]	[58]
2,4,5-T	93-76-5	3.31	*L. esculentum*	Tomato frt.	MX	3.24	[57]
2,4,5-T	93-76-5	3.31	*C. aurantium*	Bitter orange lf.	MX	3.20	[57]
2,4,5-T	93-76-5	3.31	*F. elastica*	Rubber plant lf.	MX	3.20	[57]
2,4,5-T	93-76-5	3.31	*C. annuum*	Green pepper frt.	MX	3.26	[57]
tetrachloroethene	127-18-4	3.40	*L. esculentum*	Tomato frt.	MX	3.05	[9]
1,2-dichlorobenzene	95-50-1	3.43	*L. multiflorum*	Annual rye	Whole	3.158	[29]
1,2-dichlorobenzene	95-50-1	3.43	*L. arundinaceium*	Tall fescue	Whole	3.161	[29]
1,2-dichlorobenzene	95-50-1	3.43	*F. rubra*	Red fescue	Whole	3.155	[29]
1,2-dichlorobenzene	95-50-1	3.43	*S. oleracea*	Spinach	Whole	3.063	[29]
cyclohexane	110-82-7	3.44	*L. esculentum*	Tomato frt.	MX	3.13	[9]

bitertanol	55179-31-2	4.16	*L. esculentum*	Tomato frt.	CM	3.91	[57]
bitertanol	55179-31-2	4.16	*C. aurantium*	Bitter orange lf.	CM	3.77	[57]
bitertanol	55179-31-2	4.16	*F. elastica*	Rubber plant lf.	CM	3.95	[57]
bitertanol	55179-31-2	4.16	*C. annuum*	Green pepper frt.	CM	3.85	[57]
phenanthrene	85-01-8	4.46	*S. lycopersicum*	Tomato frt.	MX	4.739[g]	[61]
phenanthrene	85-01-8	4.46	*M. domestica*	Apple frt.	MX	4.756	[61]
phenanthrene	85-01-8	4.46	*S. tuberosum*	Potato tuber	MX	4.295	[61]
phenanthrene	85-01-8	4.46	*V. heyneana*	Grape frt.	MX	4.587	[61]
phenanthrene	85-01-8	4.46	*C. annuum*	Pepper frt.	MX	4.859	[58]
phenanthrene	85-01-8	4.46	*L. multiflorum*	Annual rye	Whole	4.408	[29]
limonene	138-86-3	4.57	*L. esculentum*	Tomato frt.	MX	4.09	[9]
heptane	142-82-5	4.66	*L. esculentum*	Tomato frt.	MX	4.47	[9]
pentachlorophenol	87-86-5	5.12	*L. esculentum*	Tomato frt.	MX	4.70	[57]
pentachlorophenol	87-86-5	5.12	*C. aurantium*	Bitter orange lf.	MX	4.46	[57]
pentachlorophenol	87-86-5	5.12	*F. elastica*	Rubber plant lf.	MX	4.60	[57]
pentachlorophenol	87-86-5	5.12	*C. annuum*	Green pepper frt.	MX	4.72	[57]
hexachlorobenzene	118-74-1	5.73	*L. esculentum*	Tomato frt.	MX	5.85	[57]
hexachlorobenzene	118-74-1	5.73	*C. aurantium*	Bitter orange lf.	MX	5.79	[57]
hexachlorobenzene	118-74-1	5.73	*F. elastica*	Rubber plant lf.	MX	6.01	[57]
hexachlorobenzene	118-74-1	5.73	*C. annuum*	Green pepper frt.	MX	5.82	[57]
perylene	198-55-0	6.25	*L. esculentum*	Tomato frt.	MX	6.49	[57]

perylene	198-55-0	6.25	*C. aurantium*	Bitter orange lf.	MX	6.59	[57]
perylene	198-55-0	6.25	*F. elastica*	Rubber plant lf.	MX	6.58	[57]
perylene	198-55-0	6.25	*C. annuum*	Green pepper frt.	MX	6.58	[57]

[a] 1-C-2,3-E: 1-chloro-2,3-epoxypropane; 4-methylpentan-2-one: 4-MP-2; 1-NAA: 1-naphthaleneacetic acid; 2-M-1,3-D: 2-methylbuta-1,3-diene; 2,4-D: 2,4-dichlorophenoxyacetic acid; 2,4,5-T: 2,4,5-trichlorophenoxyacetic acid; all other abbreviations explained in Table B-1 in Appendix B

[b] Experimental data from EPI Suite database [55]

[c] Estimate from EPI Suite [55] in absence of an experimental value

[d] Experimental value from Hawari et al. [56]

[e] As reported in the references. *L. esculentum*: *Lycopersicum esculentum* Mill; *F. elastica*: *Ficus elastica* Roxb. var. decora; *C. annuum*: *Capiscum annuum* L.; *C. aurantium*: *Citrus aurantium* L.; *P. laurocerasus*: *Prunus laurocerasus* L.; *G. biloba*: *Ginkgo biloba* L.; *J. regia*: *Juglans regia* L.; *S. lycopersicum*: *Solanum lycopersicum*; *M. domestica*: *Malus domestica*; *S. tuberosum*: *Solanum tuberosum*; *V. heyneana*: *Vitis heyneana* Roem. et Schult; *L. multiflorum*: *Lolium multiflorum* Lam.; *L. arundinaceium*: *Lolium arundinaceium*; *F. rubra*: *Festuca rubra* L.; *S. oleracea*: *Spinacia oleracea*; *H. vulgare*: *Hordeum vulgare* L.

[f] frt.: fruit; lf.: leaf; Eng.: English

[g] MX: cuticle matrix (the dewaxed CM); CM: cuticular membrane; Whole: plant material including shoots and roots

[h] Observed log plant cuticle-water partition coefficient (L_{water} $kg_{cuticle}^{-1}$). Number of decimal figures correspond to those reported in the source for the log value

[i] Chen et al. [60] report nonlinear behavior for some of the isotherms, only those partition coefficients obtained with linear isotherms were taken ($Ce/Cs = 0.005$; where Ce is the equilibrium concentration and Cs is the aqueous solubility). Data from Chen et al. [60], Chen et al. [58], and Li and Chen [61] are for the cuticular fraction referred as number 2 in the sources. Only data for shoots were taken from Barbour et al. [29]. Data from "This work" were used as the average among each low and high treatments (Table A-10 in Appendix A)

Table B-3 Plant cuticle membrane–water partition coefficients (K_{CM}) and plant cuticle matrix–water partition coefficients (K_{MX}) for undissociated organic compounds from Sabljic et al. [57] and the summary statistics for the significance of the cuticular component on the plant cuticle–water partition coefficient (K_{Cut}).

Compound	CAS #	log $K_{CM\ or\ MX}$[a]					
		C. aurantium		*F. elastica*		*C. annuum*	
		CM	MX	CM	MX	CM	MX
phenol	108-95-2	NA	NA	1.51	1.69	1.59	1.67
2-nitrophenol	88-75-5	NA	NA	1.84	1.99	1.92	2.04
4-nitrophenol	100-02-7	1.79	1.76	1.80	1.89	1.97	2.03
atrazine	1912-24-9	2.15	2.17	2.16	2.15	2.19	2.20
pentachlorophenol	87-86-5	4.42	4.46	4.55	4.60	4.66	4.72
hexachlorobenzene	118-74-1	5.70	5.79	5.74	6.01	5.80	5.82
perylene	198-55-0	6.45	6.59	6.20	6.58	6.55	6.58

Summary statistics[b]

	Df	t stat	p-value[c]
Cuticle component	36	-0.143	0.887

[a] $L_{water}\ kg_{cuticle}^{-1}$. Species abbreviations defined in Table B-2 in Appendix B
[b] t-test: Two-Sample Assuming Unequal Variances
[c] A p-value ≤ 0.05 was accepted as significant

Table B-4 Absolv estimated Abraham Parameters (Absolv–AP) and K_{Cut} predicted using polyparameter linear free energy relationships (pp–LFERs) with Absolv–AP.

Compound[a]	Obs. log K_{Cut}[b]	E	S	A	B	V	Pred. log K_{Cut}[c]	
							Platts and Abraham[d]	This work[e]
methanol	-1.09	0.210	0.442	0.313	0.303	0.308	-0.669	0.194
acetonitrile	-0.27	0.189	0.722	0.001	0.202	0.404	0.150	0.685
ethanol	-0.86	0.208	0.446	0.313	0.306	0.449	-0.133	0.425
1,4-dioxane	-0.56	0.293	0.578	0.000	0.437	0.681	0.392	0.809
propanone	-0.39	0.217	0.670	0.000	0.337	0.547	0.195	0.692
propan-2-ol	-0.60	0.216	0.435	0.313	0.337	0.590	0.300	0.613
HMX	1.580	1.769	3.132	0.000	2.841	1.660	-5.804	-0.426
propan-1-ol	-0.30	0.206	0.451	0.313	0.309	0.590	0.403	0.657
acrylonitrile	0.02	0.311	0.784	0.000	0.256	0.502	0.360	0.893
butanone	-0.16	0.215	0.674	0.000	0.340	0.688	0.731	0.923
2-methylpropan-2-ol	-0.37	0.189	0.388	0.313	0.347	0.731	0.814	0.798
1-C-2,3-E	0.49	0.386	0.546	0.001	0.249	0.604	0.930	1.161
tetrahydrofuran	0.12	0.253	0.424	0.000	0.225	0.622	1.070	1.075
butan-2-ol	-0.09	0.214	0.439	0.313	0.340	0.731	0.836	0.844
pyridine	0.39	0.600	0.822	0.000	0.399	0.675	0.607	1.252
ethyl acetate	0.37	0.067	0.578	0.000	0.364	0.747	0.815	0.795

2-methylpropan-1-ol	0.11	0.214	0.439	0.313	0.340	0.731	0.836	0.844
cyclohexanone	0.32	0.423	0.770	0.000	0.322	0.861	1.565	1.506
1-nitropropane	0.95	0.225	0.716	0.001	0.248	0.706	1.166	1.150
RDX	1.964	1.382	2.412	0.000	2.131	1.245	-4.451	-0.215
RDX	2.384	1.382	2.412	0.000	2.131	1.245	-4.451	-0.215
butan-1-ol	0.24	0.204	0.455	0.313	0.312	0.731	0.938	0.888
2-methylbutan-2-ol	0.11	0.187	0.393	0.313	0.350	0.872	1.349	1.030
pentan-2-ol	0.46	0.212	0.444	0.313	0.343	0.872	1.372	1.076
propyl acetate	0.80	0.065	0.582	0.000	0.367	0.888	1.350	1.026
dichloromethane	1.42	0.216	0.382	0.088	0.000	0.494	1.442	1.218
4-MP-2	0.80	0.221	0.667	0.000	0.374	0.970	1.700	1.342
phenol	1.64	0.784	0.903	0.499	0.389	0.775	0.861	1.439
phenol	1.69	0.784	0.903	0.499	0.389	0.775	0.861	1.439
phenol	1.67	0.784	0.903	0.499	0.389	0.775	0.861	1.439
phenol	2.334	0.784	0.903	0.499	0.389	0.775	0.861	1.439
1,2-dichloroethane	1.46	0.376	0.479	0.001	0.102	0.635	1.675	1.490
pentan-1-ol	0.76	0.202	0.459	0.313	0.315	0.872	1.474	1.120
2-M-5-NPYNE	1.598	0.933	1.489	0.000	0.709	1.049	0.722	1.698
2-M-5-NPYNE	1.761	0.933	1.489	0.000	0.709	1.049	0.722	1.698
2,4-DNAN	1.921	1.159	1.929	0.000	0.522	1.264	2.281	2.723
2,4-DNAN	1.849	1.159	1.929	0.000	0.522	1.264	2.281	2.723

TNT	2.052	1.389	2.345	0.000	0.407	1.380	3.170	3.441
TNT	2.046	1.389	2.345	0.000	0.407	1.380	3.170	3.441
2,5-DM-4-NANE	1.637	1.268	1.814	0.297	0.849	1.390	1.395	2.280
2,5-DM-4-NANE	1.487	1.268	1.814	0.297	0.849	1.390	1.395	2.280
metribuzin	1.484	1.463	1.210	0.211	1.528	1.620	-0.078	1.573
3-methylpentan-3-ol	0.61	0.185	0.397	0.313	0.353	1.013	1.885	1.261
hexan-2-ol	1.01	0.210	0.448	0.313	0.346	1.013	1.908	1.307
butyl acetate	1.34	0.063	0.587	0.000	0.370	1.028	1.882	1.256
2-nitrophenol	1.99	0.955	1.237	0.112	0.353	0.949	1.849	2.200
2-nitrophenol	1.99	0.955	1.237	0.112	0.353	0.949	1.849	2.200
2-nitrophenol	2.04	0.955	1.237	0.112	0.353	0.949	1.849	2.200
benzoic acid	1.58	0.749	1.075	0.572	0.443	0.932	1.122	1.530
benzoic acid	1.679	0.749	1.075	0.572	0.443	0.932	1.122	1.530
benzoic acid	1.724	0.749	1.075	0.572	0.443	0.932	1.122	1.530
benzoic acid	1.719	0.749	1.075	0.572	0.443	0.932	1.122	1.530
4-nitrophenol	1.91	1.054	1.473	0.670	0.486	0.949	0.983	1.811
4-nitrophenol	1.76	1.054	1.473	0.670	0.486	0.949	0.983	1.811
4-nitrophenol	1.89	1.054	1.473	0.670	0.486	0.949	0.983	1.811
4-nitrophenol	2.03	1.054	1.473	0.670	0.486	0.949	0.983	1.811
4-nitrophenol	1.773	1.054	1.473	0.670	0.486	0.949	0.983	1.811
3-chloroprop-1-ene	1.66	0.250	0.377	0.001	0.083	0.611	1.626	1.332

1,2-dibromoethane	1.75	0.742	0.643	0.001	0.102	0.740	2.235	2.114
trichloromethane	1.84	0.335	0.484	0.117	0.005	0.617	1.916	1.551
1,2-dichloropropane	1.96	0.384	0.468	0.001	0.132	0.776	2.112	1.680
2,4-DNT	1.906	1.120	1.775	0.000	0.310	1.206	2.963	2.992
2,4-DNT	2.003	1.120	1.775	0.000	0.310	1.206	2.963	2.992
hexan-1-ol	1.29	0.201	0.464	0.313	0.318	1.013	2.010	1.352
4-NAN	1.839	0.890	1.359	0.000	0.425	1.090	2.073	2.275
4-NAN	2.009	0.890	1.359	0.000	0.425	1.090	2.073	2.275
trichloronitromethane	2.13	0.482	0.871	0.000	0.176	0.791	1.883	1.752
1,1-dichloroethene	2.04	0.352	0.458	0.000	0.096	0.592	1.526	1.400
benzene	2.00	0.556	0.692	0.000	0.115	0.716	1.958	1.827
benzene	2.097	0.556	0.692	0.000	0.115	0.716	1.958	1.827
1-NAA	2.31	1.466	1.403	0.572	0.505	1.442	3.156	3.148
1-NAA	2.25	1.466	1.403	0.572	0.505	1.442	3.156	3.148
1-NAA	2.43	1.466	1.403	0.572	0.505	1.442	3.156	3.148
salicylic acid	2.087	0.910	1.101	0.704	0.396	0.990	1.565	1.859
salicylic acid	2.028	0.910	1.101	0.704	0.396	0.990	1.565	1.859
salicylic acid	1.981	0.910	1.101	0.704	0.396	0.990	1.565	1.859
2-M-1,3-D	2.09	0.228	0.245	0.000	0.157	0.727	1.818	1.351
trichloroethene	2.56	0.505	0.642	0.000	0.108	0.715	1.973	1.776
1,1,1-trichloroethane	2.44	0.308	0.438	0.000	0.015	0.758	2.488	1.789

atrazine	2.13	1.258	1.241	0.363	0.886	1.620	2.340	2.533
atrazine	2.17	1.258	1.241	0.363	0.886	1.620	2.340	2.533
atrazine	2.15	1.258	1.241	0.363	0.886	1.620	2.340	2.533
atrazine	2.20	1.258	1.241	0.363	0.886	1.620	2.340	2.533
atrazine	1.899	1.258	1.241	0.363	0.886	1.620	2.340	2.533
toluene	2.50	0.581	0.634	0.000	0.116	0.857	2.543	2.093
2,4-D	2.79	1.045	1.414	0.572	0.577	1.376	2.347	2.388
2,4-D	3.20	1.045	1.414	0.572	0.577	1.376	2.347	2.388
2,4-D	3.20	1.045	1.414	0.572	0.577	1.376	2.347	2.388
2,4-D	3.26	1.045	1.414	0.572	0.577	1.376	2.347	2.388
2,4-D	2.628	1.045	1.414	0.572	0.577	1.376	2.347	2.388
2,4-D	2.630	1.045	1.414	0.572	0.577	1.376	2.347	2.388
2,4-D	2.624	1.045	1.414	0.572	0.577	1.376	2.347	2.388
tetrachloromethane	2.49	0.420	0.551	0.000	0.000	0.739	2.496	1.926
chlorobenzene	2.70	0.704	0.772	0.000	0.112	0.839	2.506	2.223
1-naphthalenol	2.906	1.502	1.227	0.499	0.447	1.144	2.360	2.826
1-naphthalenol	3.038	1.502	1.227	0.499	0.447	1.144	2.360	2.826
1-naphthalenol	2.931	1.502	1.227	0.499	0.447	1.144	2.360	2.826
1-naphthalenol	3.009	1.502	1.227	0.499	0.447	1.144	2.360	2.826
triadimenol	3.37	1.786	1.911	0.228	1.240	2.188	3.216	3.517
triadimenol	3.37	1.786	1.911	0.228	1.240	2.188	3.216	3.517

triadimenol	3.26	1.786	1.911	0.228	1.240	2.188	3.216	3.517
triadimenol	3.37	1.786	1.911	0.228	1.240	2.188	3.216	3.517
styrene	2.83	0.703	0.696	0.000	0.170	0.955	2.752	2.301
o-xylene	2.90	0.605	0.577	0.000	0.117	0.998	3.128	2.357
ethylbenzene	2.82	0.579	0.639	0.000	0.119	0.998	3.079	2.324
naphthalene	3.382	1.275	1.016	0.000	0.173	1.085	3.457	3.215
naphthalene	3.418	1.275	1.016	0.000	0.173	1.085	3.457	3.215
naphthalene	3.373	1.275	1.016	0.000	0.173	1.085	3.457	3.215
naphthalene	3.386	1.275	1.016	0.000	0.173	1.085	3.457	3.215
2,4,5-T	3.24	1.155	1.514	0.572	0.498	1.499	3.176	2.890
2,4,5-T	3.20	1.155	1.514	0.572	0.498	1.499	3.176	2.890
2,4,5-T	3.20	1.155	1.514	0.572	0.498	1.499	3.176	2.890
2,4,5-T	3.26	1.155	1.514	0.572	0.498	1.499	3.176	2.890
tetrachloroethene	3.05	0.605	0.727	0.000	0.123	0.837	2.413	2.077
1,2-dichlorobenzene	3.158	0.831	0.854	0.000	0.099	0.961	3.078	2.612
1,2-dichlorobenzene	3.161	0.831	0.854	0.000	0.099	0.961	3.078	2.612
1,2-dichlorobenzene	3.155	0.831	0.854	0.000	0.099	0.961	3.078	2.612
1,2-dichlorobenzene	3.063	0.831	0.854	0.000	0.099	0.961	3.078	2.612
cyclohexane	3.13	0.210	0.278	0.000	0.019	0.845	2.820	1.806
bitertanol	3.91	2.464	2.270	0.228	1.349	2.674	4.925	4.955
bitertanol	3.77	2.464	2.270	0.228	1.349	2.674	4.925	4.955

bitertanol	3.95	2.464	2.270	0.228	1.349	2.674	4.925	4.955
bitertanol	3.85	2.464	2.270	0.228	1.349	2.674	4.925	4.955
phenanthrene	4.739	1.993	1.340	0.000	0.232	1.454	4.951	4.599
phenanthrene	4.756	1.993	1.340	0.000	0.232	1.454	4.951	4.599
phenanthrene	4.295	1.993	1.340	0.000	0.232	1.454	4.951	4.599
phenanthrene	4.587	1.993	1.340	0.000	0.232	1.454	4.951	4.599
phenanthrene	4.859	1.993	1.340	0.000	0.232	1.454	4.951	4.599
phenanthrene	4.408	1.993	1.340	0.000	0.232	1.454	4.951	4.599
limonene	4.09	0.450	0.322	0.000	0.205	1.323	4.051	2.539
heptane	4.47	-0.003	0.196	0.000	0.045	1.095	3.597	1.920
pentachlorophenol	4.70	1.270	1.129	0.704	0.000	1.387	4.938	3.751
pentachlorophenol	4.46	1.270	1.129	0.704	0.000	1.387	4.938	3.751
pentachlorophenol	4.60	1.270	1.129	0.704	0.000	1.387	4.938	3.751
pentachlorophenol	4.72	1.270	1.129	0.704	0.000	1.387	4.938	3.751
hexachlorobenzene	5.85	1.330	1.232	0.000	0.000	1.451	5.539	4.254
hexachlorobenzene	5.79	1.330	1.232	0.000	0.000	1.451	5.539	4.254
hexachlorobenzene	6.01	1.330	1.232	0.000	0.000	1.451	5.539	4.254
hexachlorobenzene	5.82	1.330	1.232	0.000	0.000	1.451	5.539	4.254
perylene	6.49	3.318	1.841	0.000	0.310	1.954	7.169	6.903
perylene	6.59	3.318	1.841	0.000	0.310	1.954	7.169	6.903
perylene	6.58	3.318	1.841	0.000	0.310	1.954	7.169	6.903

perylene	6.58	3.318	1.841	0.000	0.310	1.954	7.169	6.903

[a] 1-C-2,3-E: 1-chloro-2,3-epoxypropane; 4-methylpentan-2-one: 4-MP-2; 1-NAA: 1-naphthaleneacetic acid; 2-M-1,3-D: 2-methylbuta-1,3-diene; 2,4-D: 2,4-dichlorophenoxyacetic acid; 2,4,5-T: 2,4,5-trichlorophenoxyacetic acid
[b] Observed log plant cuticle-water partition coefficient (L $kg_{cuticle}^{-1}$); data sources in Table B-2 in Appendix B
[c] pp–LFER–predicted log plant cuticle-water partition coefficient (L $kg_{cuticle}^{-1}$)
[d] Reported by Platts and Abraham [9], pp–LFER shown in Eq. (3-2)
[e] Obtained in this work with a multiple linear regression analysis fitting the general Abraham polyparameter model (Eq. (3-1)) to the data compiled in Table B-2 in Appendix B; resulting pp–LFER shown in Table B-7 in Appendix B

Table B-5 Absolv–AP and S, A, and B Experimentally derived Abraham Parameters (Exp–AP) for 4-NAN, RDX, HMX, and TNT and K_{Cut} predicted using pp–LFERs with Absolv–AP and Exp–AP.

Compound[a]	Obs. log K_{Cut}[b]	E	S	A	B	V	Pred. log K_{Cut}[c]	
							Platts and Abraham[d]	This work[e]
methanol	-1.09	0.210	0.442	0.313	0.303	0.308	-0.668	-0.443
acetonitrile	-0.27	0.189	0.722	0.001	0.202	0.404	0.152	0.218
ethanol	-0.86	0.208	0.446	0.313	0.306	0.449	-0.133	-0.013
1,4-dioxane	-0.56	0.293	0.578	0.000	0.437	0.681	0.392	0.212
propanone	-0.39	0.217	0.670	0.000	0.337	0.547	0.196	0.143
propan-2-ol	-0.60	0.216	0.435	0.313	0.337	0.590	0.302	0.313
HMX	1.580	1.769	2.774	0.684	1.136	1.660	0.980	1.708
propan-1-ol	-0.30	0.206	0.451	0.313	0.309	0.590	0.403	0.418
acrylonitrile	0.02	0.311	0.784	0.000	0.256	0.502	0.361	0.398
butanone	-0.16	0.215	0.674	0.000	0.340	0.688	0.731	0.573
2-methylpropan-2-ol	-0.37	0.189	0.388	0.313	0.347	0.731	0.816	0.697
1-C-2,3-E	0.49	0.386	0.546	0.001	0.249	0.604	0.931	0.793
tetrahydrofuran	0.12	0.253	0.424	0.000	0.225	0.622	1.071	0.848
butan-2-ol	-0.09	0.214	0.439	0.313	0.340	0.731	0.837	0.744
pyridine	0.39	0.600	0.822	0.000	0.399	0.675	0.606	0.574
ethyl acetate	0.37	0.067	0.578	0.000	0.364	0.747	0.817	0.554

2-methylpropan-1-ol	0.11	0.214	0.439	0.313	0.340	0.731	0.837	0.744
cyclohexanone	0.32	0.423	0.770	0.000	0.322	0.861	1.563	1.341
1-nitropropane	0.95	0.225	0.716	0.001	0.248	0.706	1.167	1.009
RDX	1.964	1.382	2.249	0.491	0.637	1.245	1.487	2.088
RDX	2.384	1.382	2.249	0.491	0.637	1.245	1.487	2.088
butan-1-ol	0.24	0.204	0.455	0.313	0.312	0.731	0.938	0.848
2-methylbutan-2-ol	0.11	0.187	0.393	0.313	0.350	0.872	1.351	1.127
pentan-2-ol	0.46	0.212	0.444	0.313	0.343	0.872	1.373	1.174
propyl acetate	0.80	0.065	0.582	0.000	0.367	0.888	1.352	0.985
dichloromethane	1.42	0.216	0.382	0.088	0.000	0.494	1.442	1.333
4-MP-2	0.80	0.221	0.667	0.000	0.374	0.970	1.702	1.330
phenol	1.64	0.784	0.903	0.499	0.389	0.775	0.862	1.134
phenol	1.69	0.784	0.903	0.499	0.389	0.775	0.862	1.134
phenol	1.67	0.784	0.903	0.499	0.389	0.775	0.862	1.134
phenol	2.334	0.784	0.903	0.499	0.389	0.775	0.862	1.134
1,2-dichloroethane	1.46	0.376	0.479	0.001	0.102	0.635	1.677	1.475
pentan-1-ol	0.76	0.202	0.459	0.313	0.315	0.872	1.473	1.279
2-M-5-NPYNE	1.598	0.933	1.489	0.000	0.709	1.049	0.721	0.765
2-M-5-NPYNE	1.761	0.933	1.489	0.000	0.709	1.049	0.721	0.765
2,4-DNAN	1.921	1.159	1.929	0.000	0.522	1.264	2.280	2.372
2,4-DNAN	1.849	1.159	1.929	0.000	0.522	1.264	2.280	2.372

TNT	2.052	1.389	1.809	0.012	0.683	1.380	2.255	2.252
TNT	2.046	1.389	1.809	0.012	0.683	1.380	2.255	2.252
2,5-DM-4-NANE	1.637	1.268	1.814	0.297	0.849	1.390	1.394	1.567
2,5-DM-4-NANE	1.487	1.268	1.814	0.297	0.849	1.390	1.394	1.567
metribuzin	1.484	1.463	1.210	0.211	1.528	1.620	-0.076	-0.332
3-methylpentan-3-ol	0.61	0.185	0.397	0.313	0.353	1.013	1.886	1.558
hexan-2-ol	1.01	0.210	0.448	0.313	0.346	1.013	1.908	1.605
butyl acetate	1.34	0.063	0.587	0.000	0.370	1.028	1.883	1.412
2-nitrophenol	1.99	0.955	1.237	0.112	0.353	0.949	1.848	1.906
2-nitrophenol	1.99	0.955	1.237	0.112	0.353	0.949	1.848	1.906
2-nitrophenol	2.04	0.955	1.237	0.112	0.353	0.949	1.848	1.906
benzoic acid	1.58	0.749	1.075	0.572	0.443	0.932	1.122	1.399
benzoic acid	1.679	0.749	1.075	0.572	0.443	0.932	1.122	1.399
benzoic acid	1.724	0.749	1.075	0.572	0.443	0.932	1.122	1.399
benzoic acid	1.719	0.749	1.075	0.572	0.443	0.932	1.122	1.399
4-nitrophenol	1.91	1.054	1.473	0.670	0.486	0.949	0.983	1.528
4-nitrophenol	1.76	1.054	1.473	0.670	0.486	0.949	0.983	1.528
4-nitrophenol	1.89	1.054	1.473	0.670	0.486	0.949	0.983	1.528
4-nitrophenol	2.03	1.054	1.473	0.670	0.486	0.949	0.983	1.528
4-nitrophenol	1.773	1.054	1.473	0.670	0.486	0.949	0.983	1.528
3-chloroprop-1-ene	1.66	0.250	0.377	0.001	0.083	0.611	1.624	1.379

1,2-dibromoethane	1.75	0.742	0.643	0.001	0.102	0.740	2.235	2.071
trichloromethane	1.84	0.335	0.484	0.117	0.005	0.617	1.917	1.794
1,2-dichloropropane	1.96	0.384	0.468	0.001	0.132	0.776	2.111	1.801
2,4-DNT	1.906	1.120	1.775	0.000	0.310	1.206	2.964	3.011
2,4-DNT	2.003	1.120	1.775	0.000	0.310	1.206	2.964	3.011
hexan-1-ol	1.29	0.201	0.464	0.313	0.318	1.013	2.009	1.710
4-NAN	1.839	0.890	1.292	0.030	0.398	1.090	2.196	2.114
4-NAN	2.009	0.890	1.292	0.030	0.398	1.090	2.196	2.114
trichloronitromethane	2.13	0.482	0.871	0.000	0.176	0.791	1.883	1.755
1,1-dichloroethene	2.04	0.352	0.458	0.000	0.096	0.592	1.527	1.345
benzene	2.00	0.556	0.692	0.000	0.115	0.716	1.956	1.810
benzene	2.097	0.556	0.692	0.000	0.115	0.716	1.956	1.810
1-NAA	2.31	1.466	1.403	0.572	0.505	1.442	3.157	3.285
1-NAA	2.25	1.466	1.403	0.572	0.505	1.442	3.157	3.285
1-NAA	2.43	1.466	1.403	0.572	0.505	1.442	3.157	3.285
salicylic acid	2.087	0.910	1.101	0.704	0.396	0.990	1.565	1.911
salicylic acid	2.028	0.910	1.101	0.704	0.396	0.990	1.565	1.911
salicylic acid	1.981	0.910	1.101	0.704	0.396	0.990	1.565	1.911
2-M-1,3-D	2.09	0.228	0.245	0.000	0.157	0.727	1.818	1.428
trichloroethene	2.56	0.505	0.642	0.000	0.108	0.715	1.975	1.800
1,1,1-trichloroethane	2.44	0.308	0.438	0.000	0.015	0.758	2.489	2.161

atrazine	2.13	1.258	1.241	0.363	0.886	1.620	2.340	2.128
atrazine	2.17	1.258	1.241	0.363	0.886	1.620	2.340	2.128
atrazine	2.15	1.258	1.241	0.363	0.886	1.620	2.340	2.128
atrazine	2.20	1.258	1.241	0.363	0.886	1.620	2.340	2.128
atrazine	1.899	1.258	1.241	0.363	0.886	1.620	2.340	2.128
toluene	2.50	0.581	0.634	0.000	0.116	0.857	2.544	2.268
2,4-D	2.79	1.045	1.414	0.572	0.577	1.376	2.349	2.486
2,4-D	3.20	1.045	1.414	0.572	0.577	1.376	2.349	2.486
2,4-D	3.20	1.045	1.414	0.572	0.577	1.376	2.349	2.486
2,4-D	3.26	1.045	1.414	0.572	0.577	1.376	2.349	2.486
2,4-D	2.628	1.045	1.414	0.572	0.577	1.376	2.349	2.486
2,4-D	2.630	1.045	1.414	0.572	0.577	1.376	2.349	2.486
2,4-D	2.624	1.045	1.414	0.572	0.577	1.376	2.349	2.486
tetrachloromethane	2.49	0.420	0.551	0.000	0.000	0.739	2.496	2.245
chlorobenzene	2.70	0.704	0.772	0.000	0.112	0.839	2.505	2.319
1-naphthalenol	2.906	1.502	1.227	0.499	0.447	1.144	2.360	2.588
1-naphthalenol	3.038	1.502	1.227	0.499	0.447	1.144	2.360	2.588
1-naphthalenol	2.931	1.502	1.227	0.499	0.447	1.144	2.360	2.588
1-naphthalenol	3.009	1.502	1.227	0.499	0.447	1.144	2.360	2.588
triadimenol	3.37	1.786	1.911	0.228	1.240	2.188	3.218	2.875
triadimenol	3.37	1.786	1.911	0.228	1.240	2.188	3.218	2.875

triadimenol	3.26	1.786	1.911	0.228	1.240	2.188	3.218	2.875
triadimenol	3.37	1.786	1.911	0.228	1.240	2.188	3.218	2.875
styrene	2.83	0.703	0.696	0.000	0.170	0.955	2.753	2.449
o-xylene	2.90	0.605	0.577	0.000	0.117	0.998	3.130	2.725
ethylbenzene	2.82	0.579	0.639	0.000	0.119	0.998	3.079	2.699
naphthalene	3.382	1.275	1.016	0.000	0.173	1.085	3.455	3.265
naphthalene	3.418	1.275	1.016	0.000	0.173	1.085	3.455	3.265
naphthalene	3.373	1.275	1.016	0.000	0.173	1.085	3.455	3.265
naphthalene	3.386	1.275	1.016	0.000	0.173	1.085	3.455	3.265
2,4,5-T	3.24	1.155	1.514	0.572	0.498	1.499	3.178	3.274
2,4,5-T	3.20	1.155	1.514	0.572	0.498	1.499	3.178	3.274
2,4,5-T	3.20	1.155	1.514	0.572	0.498	1.499	3.178	3.274
2,4,5-T	3.26	1.155	1.514	0.572	0.498	1.499	3.178	3.274
tetrachloroethene	3.05	0.605	0.727	0.000	0.123	0.837	2.412	2.197
1,2-dichlorobenzene	3.158	0.831	0.854	0.000	0.099	0.961	3.076	2.849
1,2-dichlorobenzene	3.161	0.831	0.854	0.000	0.099	0.961	3.076	2.849
1,2-dichlorobenzene	3.155	0.831	0.854	0.000	0.099	0.961	3.076	2.849
1,2-dichlorobenzene	3.063	0.831	0.854	0.000	0.099	0.961	3.076	2.849
cyclohexane	3.13	0.210	0.278	0.000	0.019	0.845	2.821	2.344
bitertanol	3.91	2.464	2.270	0.228	1.349	2.674	4.924	4.462
bitertanol	3.77	2.464	2.270	0.228	1.349	2.674	4.924	4.462

bitertanol	3.95	2.464	2.270	0.228	1.349	2.674	4.924	4.462
bitertanol	3.85	2.464	2.270	0.228	1.349	2.674	4.924	4.462
phenanthrene	4.739	1.993	1.340	0.000	0.232	1.454	4.953	4.719
phenanthrene	4.756	1.993	1.340	0.000	0.232	1.454	4.953	4.719
phenanthrene	4.295	1.993	1.340	0.000	0.232	1.454	4.953	4.719
phenanthrene	4.587	1.993	1.340	0.000	0.232	1.454	4.953	4.719
phenanthrene	4.859	1.993	1.340	0.000	0.232	1.454	4.953	4.719
phenanthrene	4.408	1.993	1.340	0.000	0.232	1.454	4.953	4.719
limonene	4.09	0.450	0.322	0.000	0.205	1.323	4.052	3.274
heptane	4.47	-0.003	0.196	0.000	0.045	1.095	3.596	2.869
pentachlorophenol	4.70	1.270	1.129	0.704	0.000	1.387	4.938	5.013
pentachlorophenol	4.46	1.270	1.129	0.704	0.000	1.387	4.938	5.013
pentachlorophenol	4.60	1.270	1.129	0.704	0.000	1.387	4.938	5.013
pentachlorophenol	4.72	1.270	1.129	0.704	0.000	1.387	4.938	5.013
hexachlorobenzene	5.85	1.330	1.232	0.000	0.000	1.451	5.539	5.163
hexachlorobenzene	5.79	1.330	1.232	0.000	0.000	1.451	5.539	5.163
hexachlorobenzene	6.01	1.330	1.232	0.000	0.000	1.451	5.539	5.163
hexachlorobenzene	5.82	1.330	1.232	0.000	0.000	1.451	5.539	5.163
perylene	6.49	3.318	1.841	0.000	0.310	1.954	7.171	6.947
perylene	6.59	3.318	1.841	0.000	0.310	1.954	7.171	6.947
perylene	6.58	3.318	1.841	0.000	0.310	1.954	7.171	6.947

perylene	6.58	3.318	1.841	0.000	0.310	1.954	7.171	6.947

[a] 1-C-2,3-E: 1-chloro-2,3-epoxypropane; 4-methylpentan-2-one: 4-MP-2; 1-NAA: 1-naphthaleneacetic acid; 2-M-1,3-D: 2-methylbuta-1,3-diene; 2,4-D: 2,4-dichlorophenoxyacetic acid; 2,4,5-T: 2,4,5-trichlorophenoxyacetic acid
[b] Observed log plant cuticle-water partition coefficient (L $kg_{cuticle}^{-1}$); data sources in Table B-2 in Appendix B
[c] pp–LFER–predicted log plant cuticle-water partition coefficient (L $kg_{cuticle}^{-1}$)
[d] Reported by Platts and Abraham [9], pp–LFER shown in Eq. (3-2)
[e] Obtained in this work with a multiple linear regression analysis fitting the general Abraham polyparameter model (Eq. (3-1)) to the data compiled in Table B-2 in Appendix B; resulting pp–LFER shown in Table B-7 in Appendix B

Table B-6 Quantum Chemically estimated Abraham Parameters (QCAP) and K_{Cut} predicted using pp–LFERs with QCAP.

Compound[a]	Obs. log K_{Cut}[b]	E	S	A	B	V	Pred. log K_{Cut}[c]	
							Platts and Abraham[d]	This work[e]
methanol	-1.09	0.473	0.549	0.586	0.378	0.295	-1.053	-1.269
acetonitrile	-0.27	0.504	0.837	0.106	0.417	0.391	-0.694	-0.607
ethanol	-0.86	0.564	0.522	0.562	0.391	0.424	-0.524	-0.864
1,4-dioxane	-0.56	0.729	0.837	0.011	0.592	0.668	-0.146	-0.452
propanone	-0.39	0.630	0.712	0.046	0.485	0.515	-0.331	-0.576
propan-2-ol	-0.60	0.654	0.524	0.513	0.422	0.554	-0.066	-0.515
HMX	1.580	1.165	2.451	0.635	1.050	1.631	1.018	1.727
propan-1-ol	-0.30	0.643	0.538	0.528	0.406	0.556	-0.012	-0.421
acrylonitrile	0.02	0.701	0.783	0.114	0.332	0.488	0.169	0.221
butanone	-0.16	0.692	0.668	0.033	0.461	0.649	0.353	0.013
2-methylpropan-2-ol	-0.37	0.744	0.515	0.489	0.469	0.679	0.300	-0.294
1-C-2,3-E	0.49	0.710	0.893	0.095	0.329	0.640	0.745	0.882
tetrahydrofuran	0.12	0.747	0.477	0.013	0.361	0.605	0.712	0.263
butan-2-ol	-0.09	0.743	0.517	0.503	0.365	0.682	0.729	0.277
pyridine	0.39	1.055	0.753	0.091	0.430	0.642	0.604	0.356
ethyl acetate	0.37	0.667	0.735	0.033	0.464	0.716	0.560	0.281

2-methylpropan-1-ol	0.11	0.756	0.523	0.552	0.358	0.676	0.715	0.278
cyclohexanone	0.32	0.931	0.735	0.002	0.526	0.809	0.842	0.394
1-nitropropane	0.95	0.675	0.826	0.071	0.351	0.680	0.830	0.838
RDX	1.964	1.016	1.858	0.528	0.667	1.241	1.273	1.908
RDX	2.384	1.016	1.858	0.528	0.667	1.241	1.273	1.908
butan-1-ol	0.24	0.750	0.524	0.567	0.409	0.682	0.518	0.012
2-methylbutan-2-ol	0.11	0.819	0.493	0.474	0.434	0.804	0.993	0.351
pentan-2-ol	0.46	0.844	0.521	0.411	0.436	0.808	1.036	0.424
propyl acetate	0.80	0.772	0.728	0.031	0.460	0.844	1.143	0.787
dichloromethane	1.42	0.693	0.616	0.155	0.062	0.497	1.353	1.545
4-MP-2	0.80	0.896	0.650	0.042	0.463	0.898	1.442	0.932
phenol	1.64	1.192	0.952	0.821	0.190	0.735	1.579	1.828
phenol	1.69	1.192	0.952	0.821	0.190	0.735	1.579	1.828
phenol	1.67	1.192	0.952	0.821	0.190	0.735	1.579	1.828
phenol	2.334	1.192	0.952	0.821	0.190	0.735	1.579	1.828
1,2-dichloroethane	1.46	0.820	0.734	0.119	0.132	0.626	1.616	1.793
pentan-1-ol	0.76	0.841	0.536	0.566	0.398	0.814	1.128	0.580
2-M-5-NPYNE	1.598	1.428	1.257	0.105	0.591	1.019	1.425	1.401
2-M-5-NPYNE	1.761	1.428	1.257	0.105	0.591	1.019	1.425	1.401
2,4-DNAN	1.921	1.661	1.704	0.187	0.785	1.231	1.372	1.544
2,4-DNAN	1.849	1.661	1.704	0.187	0.785	1.231	1.372	1.544

TNT	2.052	1.656	1.886	0.302	0.752	1.344	1.812	2.220
TNT	2.046	1.656	1.886	0.302	0.752	1.344	1.812	2.220
2,5-DM-4-NANE	1.637	2.017	1.720	0.679	0.990	1.319	0.831	0.628
2,5-DM-4-NANE	1.487	2.017	1.720	0.679	0.990	1.319	0.831	0.628
metribuzin	1.484	2.091	1.439	0.751	0.870	1.516	2.216	1.700
3-methylpentan-3-ol	0.61	0.898	0.477	0.456	0.395	0.932	1.716	1.037
hexan-2-ol	1.01	0.956	0.534	0.496	0.373	0.937	1.816	1.229
butyl acetate	1.34	0.850	0.703	0.033	0.437	0.973	1.797	1.369
2-nitrophenol	1.99	1.415	1.061	0.179	0.407	0.904	1.765	1.777
2-nitrophenol	1.99	1.415	1.061	0.179	0.407	0.904	1.765	1.777
2-nitrophenol	2.04	1.415	1.061	0.179	0.407	0.904	1.765	1.777
benzoic acid	1.58	1.300	1.042	0.830	0.312	0.887	1.699	1.818
benzoic acid	1.679	1.300	1.042	0.830	0.312	0.887	1.699	1.818
benzoic acid	1.724	1.300	1.042	0.830	0.312	0.887	1.699	1.818
benzoic acid	1.719	1.300	1.042	0.830	0.312	0.887	1.699	1.818
4-nitrophenol	1.91	1.371	1.323	1.081	0.413	0.920	1.210	1.530
4-nitrophenol	1.76	1.371	1.323	1.081	0.413	0.920	1.210	1.530
4-nitrophenol	1.89	1.371	1.323	1.081	0.413	0.920	1.210	1.530
4-nitrophenol	2.03	1.371	1.323	1.081	0.413	0.920	1.210	1.530
4-nitrophenol	1.773	1.371	1.323	1.081	0.413	0.920	1.210	1.530
3-chloroprop-1-ene	1.66	0.801	0.597	0.089	0.126	0.589	1.556	1.580

1,2-dibromoethane	1.75	1.126	0.833	0.120	0.154	0.705	1.975	2.166
trichloromethane	1.84	0.810	0.521	0.172	0.005	0.629	2.203	2.267
1,2-dichloropropane	1.96	0.887	0.810	0.112	0.212	0.751	1.789	1.894
2,4-DNT	1.906	1.580	1.449	0.134	0.625	1.163	1.845	1.940
2,4-DNT	2.003	1.580	1.449	0.134	0.625	1.163	1.845	1.940
hexan-1-ol	1.29	0.948	0.560	0.535	0.418	0.942	1.616	1.000
4-NAN	1.839	1.426	1.187	0.101	0.552	1.059	1.771	1.689
4-NAN	2.009	1.426	1.187	0.101	0.552	1.059	1.771	1.689
trichloronitromethane	2.13	0.824	0.446	0.110	0.083	0.819	2.697	2.473
1,1-dichloroethene	2.04	0.847	0.380	0.096	-0.005	0.590	2.210	2.113
benzene	2.00	1.173	0.598	0.059	0.102	0.674	2.223	2.179
benzene	2.097	1.173	0.598	0.059	0.102	0.674	2.223	2.179
1-NAA	2.31	2.264	1.464	0.891	0.464	1.345	3.233	3.336
1-NAA	2.25	2.264	1.464	0.891	0.464	1.345	3.233	3.336
1-NAA	2.43	2.264	1.464	0.891	0.464	1.345	3.233	3.336
salicylic acid	2.087	1.390	1.061	0.974	0.294	0.933	1.921	2.048
salicylic acid	2.028	1.390	1.061	0.974	0.294	0.933	1.921	2.048
salicylic acid	1.981	1.390	1.061	0.974	0.294	0.933	1.921	2.048
2-M-1,3-D	2.09	1.114	0.473	0.062	0.105	0.678	2.242	2.035
trichloroethene	2.56	1.015	0.447	0.108	-0.014	0.713	2.794	2.715
1,1,1-trichloroethane	2.44	0.920	0.469	0.095	0.071	0.754	2.547	2.382

atrazine	2.13	2.098	1.218	0.536	0.606	1.531	3.561	3.108
atrazine	2.17	2.098	1.218	0.536	0.606	1.531	3.561	3.108
atrazine	2.15	2.098	1.218	0.536	0.606	1.531	3.561	3.108
atrazine	2.20	2.098	1.218	0.536	0.606	1.531	3.561	3.108
atrazine	1.899	2.098	1.218	0.536	0.606	1.531	3.561	3.108
toluene	2.50	1.315	0.606	0.056	0.121	0.802	2.729	2.588
2,4-D	2.79	1.722	1.438	1.062	0.531	1.347	2.567	2.635
2,4-D	3.20	1.722	1.438	1.062	0.531	1.347	2.567	2.635
2,4-D	3.20	1.722	1.438	1.062	0.531	1.347	2.567	2.635
2,4-D	3.26	1.722	1.438	1.062	0.531	1.347	2.567	2.635
2,4-D	2.628	1.722	1.438	1.062	0.531	1.347	2.567	2.635
2,4-D	2.630	1.722	1.438	1.062	0.531	1.347	2.567	2.635
2,4-D	2.624	1.722	1.438	1.062	0.531	1.347	2.567	2.635
tetrachloromethane	2.49	0.926	0.298	0.067	-0.016	0.759	3.011	2.734
chlorobenzene	2.70	1.340	0.677	0.090	0.097	0.804	2.803	2.783
1-naphthalenol	2.906	2.066	1.131	0.863	0.243	1.081	3.140	3.249
1-naphthalenol	3.038	2.066	1.131	0.863	0.243	1.081	3.140	3.249
1-naphthalenol	2.931	2.066	1.131	0.863	0.243	1.081	3.140	3.249
1-naphthalenol	3.009	2.066	1.131	0.863	0.243	1.081	3.140	3.249
triadimenol	3.37	2.342	1.837	0.391	1.121	2.066	3.506	2.913
triadimenol	3.37	2.342	1.837	0.391	1.121	2.066	3.506	2.913

triadimenol	3.26	2.342	1.837	0.391	1.121	2.066	3.506	2.913
triadimenol	3.37	2.342	1.837	0.391	1.121	2.066	3.506	2.913
styrene	2.83	1.672	0.815	0.082	0.171	0.891	2.985	2.952
o-xylene	2.90	1.444	0.638	0.053	0.151	0.925	3.152	2.938
ethylbenzene	2.82	1.428	0.614	0.054	0.132	0.928	3.241	3.022
naphthalene	3.382	2.055	0.936	0.077	0.202	1.018	3.535	3.499
naphthalene	3.418	2.055	0.936	0.077	0.202	1.018	3.535	3.499
naphthalene	3.373	2.055	0.936	0.077	0.202	1.018	3.535	3.499
naphthalene	3.386	2.055	0.936	0.077	0.202	1.018	3.535	3.499
2,4,5-T	3.24	1.931	1.458	1.087	0.528	1.472	3.171	3.178
2,4,5-T	3.20	1.931	1.458	1.087	0.528	1.472	3.171	3.178
2,4,5-T	3.20	1.931	1.458	1.087	0.528	1.472	3.171	3.178
2,4,5-T	3.26	1.931	1.458	1.087	0.528	1.472	3.171	3.178
tetrachloroethene	3.05	1.175	0.375	0.051	-0.018	0.836	3.445	3.196
1,2-dichlorobenzene	3.158	1.507	0.708	0.098	0.098	0.927	3.362	3.299
1,2-dichlorobenzene	3.161	1.507	0.708	0.098	0.098	0.927	3.362	3.299
1,2-dichlorobenzene	3.155	1.507	0.708	0.098	0.098	0.927	3.362	3.299
1,2-dichlorobenzene	3.063	1.507	0.708	0.098	0.098	0.927	3.362	3.299
cyclohexane	3.13	0.979	0.149	0.038	-0.039	0.784	3.311	2.847
bitertanol	3.91	3.568	2.283	0.370	1.311	2.498	4.973	4.312
bitertanol	3.77	3.568	2.283	0.370	1.311	2.498	4.973	4.312

bitertanol	3.95	3.568	2.283	0.370	1.311	2.498	4.973	4.312
bitertanol	3.85	3.568	2.283	0.370	1.311	2.498	4.973	4.312
phenanthrene	4.739	3.016	1.258	0.111	0.321	1.357	4.795	4.708
phenanthrene	4.756	3.016	1.258	0.111	0.321	1.357	4.795	4.708
phenanthrene	4.295	3.016	1.258	0.111	0.321	1.357	4.795	4.708
phenanthrene	4.587	3.016	1.258	0.111	0.321	1.357	4.795	4.708
phenanthrene	4.859	3.016	1.258	0.111	0.321	1.357	4.795	4.708
phenanthrene	4.408	3.016	1.258	0.111	0.321	1.357	4.795	4.708
limonene	4.09	1.567	0.600	0.038	0.192	1.214	4.210	3.744
heptane	4.47	1.105	0.122	0.055	-0.049	1.000	4.274	3.672
pentachlorophenol	4.70	2.141	0.896	1.067	0.175	1.354	4.524	4.273
pentachlorophenol	4.46	2.141	0.896	1.067	0.175	1.354	4.524	4.273
pentachlorophenol	4.60	2.141	0.896	1.067	0.175	1.354	4.524	4.273
pentachlorophenol	4.72	2.141	0.896	1.067	0.175	1.354	4.524	4.273
hexachlorobenzene	5.85	2.337	0.714	0.053	0.171	1.409	5.462	4.954
hexachlorobenzene	5.79	2.337	0.714	0.053	0.171	1.409	5.462	4.954
hexachlorobenzene	6.01	2.337	0.714	0.053	0.171	1.409	5.462	4.954
hexachlorobenzene	5.82	2.337	0.714	0.053	0.171	1.409	5.462	4.954
perylene	6.49	4.757	1.708	0.152	0.520	1.814	6.597	6.330
perylene	6.59	4.757	1.708	0.152	0.520	1.814	6.597	6.330
perylene	6.58	4.757	1.708	0.152	0.520	1.814	6.597	6.330

perylene	6.58	4.757	1.708	0.152	0.520	1.814	6.597	6.330

[a] 1-C-2,3-E: 1-chloro-2,3-epoxypropane; 4-methylpentan-2-one: 4-MP-2; 1-NAA: 1-naphthaleneacetic acid; 2-M-1,3-D: 2-methylbuta-1,3-diene; 2,4-D: 2,4-dichlorophenoxyacetic acid; 2,4,5-T: 2,4,5-trichlorophenoxyacetic acid

[b] Observed log plant cuticle-water partition coefficient (L $kg_{cuticle}^{-1}$); data sources in Table B-2 in Appendix B

[c] pp–LFER–predicted log plant cuticle-water partition coefficient (L $kg_{cuticle}^{-1}$)

[d] Reported by Platts and Abraham [9], pp–LFER shown in Eq. (3-2)

[e] Obtained in this work with a multiple linear regression analysis fitting the general Abraham polyparameter model (Eq. (3-1)) to the data compiled in Table B-2 in Appendix B; resulting pp–LFER shown in Table B-7 in Appendix B

Table B-7 Results of the K_{Cut} pp–LFER multiple linear regression analyses fitting the general Abraham polyparameter model (Eq. (3-1)) to K_{Cut} data using three different sources of solute descriptors[a].

Source of solute descriptors	Plant cuticle phase descriptors		Standard error	t value	p-value
Absolv–AP	c	0.144	0.222	0.648	5.18E-01
	e	1.200	0.224	5.363	3.39E-07
	s	0.039	0.265	0.148	8.83E-01
	a	-0.453	0.270	-1.681	9.50E-02
	b	-1.984	0.248	-8.013	4.36E-13
	v	1.700	0.295	5.766	5.15E-08
	77 compounds; N = 143; RMSE = 0.786; $R^2_{Adj.}$ = 0.747; SE = 0.803; F = 85.03				
Absolv–AP and Exp–AP	c	-0.403	0.159	-2.527	1.26E-02
	e	0.717	0.162	4.432	1.90E-05
	s	0.033	0.187	0.179	8.58E-01
	a	0.139	0.196	0.711	4.78E-01
	b	-4.027	0.238	-16.943	< 2E-16
	v	3.151	0.233	13.520	< 2E-16
	77 compounds; N = 143; RMSE = 0.542; $R^2_{Adj.}$ = 0.880; SE = 0.554; F = 208.9				
QCAP	c	-0.617	0.101	-6.120	9.25E-09

e	0.417	0.088	4.754	4.98E-06
s	0.919	0.168	5.488	1.90E-07
a	-0.546	0.102	-5.357	3.48E-07
b	-5.449	0.259	-21.016	< 2E-16
v	3.479	0.208	16.709	< 2E-16
77 compounds; N = 143; RMSE = 0.395; $R^2_{Adj.}$ = 0.936; SE = 0.403; F = 418.7				

[a] K_{Cut} dataset described in Table B-2 in Appendix B. N = number of data points used to estimate the regression equation coefficients, RMSE = root mean square error of prediction, $R^2_{Adj.}$= adjusted coefficient of determination, SE = regression residual standard error, and F = Fischer's F statistic

Table B-8 Quantum Chemically estimated Experimental Abraham Parameters (QCEAP) [39] for the estimation of log K_{OC} for MCs and MLCs[a].

Compound[b]	E	S	A	B	V
4-NAN	0.819	1.205	0.013	0.543	1.107
2,4-DNAN	1.156	1.769	0.050	0.744	1.280
2,5-DM-4-NANE	1.517	1.886	0.385	1.062	1.400
2-M-5-NPYNE	0.872	1.284	0.016	0.580	1.066
RDX	0.705	1.760	0.270	0.635	1.245
HMX	0.881	2.383	0.315	1.020	1.643
TNT	1.184	1.921	0.115	0.683	1.381
2,4-DNT	1.009	1.487	0.023	0.584	1.209

[a] The solute descriptors used to apply the K_{OC} pp–LFER by Kipka and Di Toro [41] were obtained with the regression equations for the QCEAP reported in Liang [39]. QCEAP are recommended over QCAP for existing pp–LFERs that were built using solute descriptors either derived from calibration to experimental measurements or estimated with functional group fragments contributions (e.g., Absolv–AP) [39]

[b] Abbreviations explained in Table B-1 in Appendix B

B.3 Prediction of Concentrations in Plants from Independent Uptake Assays

Table B-9 Data from published uptake assays with plants exposed to MCs, or MLCs, in the growth medium.

Compound	Plant[a]	Species[b]	Plant family	Plant part[c]	Exposure Medium	Exposure time	Concentration in plant	Concentration in exposure medium[d]	f_{oc}	Source[e]
						days	mg kg_{dwt}^{-1}	mg kg_{dwt}^{-1} or mg L^{-1}		
TNT	YN	*C. esculentus*	Cyperaceae	Shoots	Soil	45	27.799	11.269	0.024	[62]
TNT	YN	*C. esculentus*	Cyperaceae	Shoots	Soil	45	93.438	16.704	0.006	[62]
TNT	Barley	*H. vulgare*	Poaceae	Whole	Sand	30	26.014	6.230	NA	TW
2,4-DNT	PR	*L. perenne*	Poaceae	Shoots	Soil	14	2.800	1.000	0.013	[63]
2,4-DNT	PR	*L. perenne*	Poaceae	Shoots	Soil	14	2.800	5.000	0.013	[63]
2,4-DNT	Barley	*H. vulgare*	Poaceae	Whole	Sand	29	48.712	9.639	NA	TW
RDX	PR	*L. perenne*	Poaceae	Shoots	Soil	42	119.000	11.100	0.007	[64]
RDX	PR	*L. perenne*	Poaceae	Shoots	Soil	42	804.000	104.000	0.007	[64]
RDX	PR	*L. perenne*	Poaceae	Shoots	Soil	42	764.000	1014.000	0.007	[64]
RDX	PR	*L. perenne*	Poaceae	Shoots	Soil	42	1690.000	8867.000	0.007	[64]
RDX	PR	*L. perenne*	Poaceae	Shoots	Soil	55	1083.000	10.000	0.029	[65]
RDX	PR	*L. perenne*	Poaceae	Shoots	Soil	55	5217.000	59.200	0.026	[65]

RDX	PR	*L. perenne*	Poaceae	Shoots	Soil	55	2948.000	153.900	0.022	[65]
RDX	PR	*L. perenne*	Poaceae	PT	Soil	55	806.000	13.800	0.037	[66]
RDX	PR	*L. perenne*	Poaceae	PT	Soil	55	2055.000	645.000	0.073	[66]
RDX	PR	*L. perenne*	Poaceae	PT	Soil	55	3886.000	855.500	0.100	[66]
RDX	PR	*L. perenne*	Poaceae	PT	Soil	55	3068.000	1540.500	0.164	[66]
RDX	PR	*L. perenne*	Poaceae	Shoots	Soil	34	387.567	10.000	0.013	[63]
RDX	PR	*L. perenne*	Poaceae	Shoots	Soil	34	1965.800	30.000	0.013	[63]
RDX	PR	*L. perenne*	Poaceae	Shoots	Soil	34	2221.400	100.000	0.013	[63]
RDX	Alfalfa	*M. sativa*	Fabaceae	PT	Soil	55	187.000	13.800	0.037	[66]
RDX	Alfalfa	*M. sativa*	Fabaceae	PT	Soil	55	3997.000	645.000	0.073	[66]
RDX	Alfalfa	*M. sativa*	Fabaceae	PT	Soil	55	4355.000	855.500	0.100	[66]
RDX	Alfalfa	*M. sativa*	Fabaceae	PT	Soil	55	4155.000	1540.500	0.164	[66]
RDX	Corn	*Z. mays*	Poaceae	APT	Soil	34	120.000	12.500	0.036	[67]
RDX	Corn	*Z. mays*	Poaceae	APT	Soil	34	300.000	25.000	0.036	[67]
RDX	Corn	*Z. mays*	Poaceae	APT	Soil	34	802.000	50.000	0.036	[67]
RDX	Corn	*Z. mays*	Poaceae	APT	Soil	34	1210.000	100.000	0.036	[67]
RDX	Corn	*Z. mays*	Poaceae	APT	Soil	28	695.000	220.000	0.036	[67]
RDX	Corn	*Z. mays*	Poaceae	APT	Soil	28	602.000	494.000	0.036	[67]
RDX	Corn	*Z. mays*	Poaceae	APT	Soil	28	649.000	903.000	0.036	[67]
RDX	Corn	*Z. mays*	Poaceae	APT	Water	28	95.000	6.000	NA	[67]
RDX	Corn	*Z. mays*	Poaceae	APT	Water	28	171.000	13.000	NA	[67]

RDX	Corn	*Z. mays*	Poaceae	APT	Water	28	300.000	21.000	NA	[67]
RDX	Soybean	*G. max*	Fabaceae	APT	Soil	34	104.000	12.500	0.036	[67]
RDX	Soybean	*G. max*	Fabaceae	APT	Soil	34	181.000	25.000	0.036	[67]
RDX	Soybean	*G. max*	Fabaceae	APT	Soil	34	314.000	50.000	0.036	[67]
RDX	Soybean	*G. max*	Fabaceae	APT	Soil	34	492.000	100.000	0.036	[67]
RDX	Soybean	*G. max*	Fabaceae	APT	Soil	28	322.000	220.000	0.036	[67]
RDX	Soybean	*G. max*	Fabaceae	APT	Soil	28	358.000	494.000	0.036	[67]
RDX	Soybean	*G. max*	Fabaceae	APT	Soil	28	274.000	903.000	0.036	[67]
RDX	Soybean	*G. max*	Fabaceae	APT	Soil	28	76.000	6.000	NA	[67]
RDX	Soybean	*G. max*	Fabaceae	APT	Soil	28	138.000	13.000	NA	[67]
RDX	Soybean	*G. max*	Fabaceae	APT	Soil	28	168.000	21.000	NA	[67]
RDX	Sorghum	*S. Sudanese*	Poaceae	APT	Soil	34	94.000	12.500	0.036	[67]
RDX	Sorghum	*S. Sudanese*	Poaceae	APT	Soil	34	314.000	25.000	0.036	[67]
RDX	Sorghum	*S. Sudanese*	Poaceae	APT	Soil	34	1052.000	50.000	0.036	[67]
RDX	Sorghum	*S. Sudanese*	Poaceae	APT	Soil	34	1414.000	100.000	0.036	[67]
RDX	Sorghum	*S. Sudanese*	Poaceae	APT	Soil	28	1133.000	220.000	0.036	[67]
RDX	Sorghum	*S. Sudanese*	Poaceae	APT	Soil	28	975.000	494.000	0.036	[67]
RDX	Sorghum	*S. Sudanese*	Poaceae	APT	Soil	28	1218.000	903.000	0.036	[67]
RDX	Sorghum	*S. Sudanese*	Poaceae	APT	Water	28	72.000	6.000	NA	[67]
RDX	Sorghum	*S. Sudanese*	Poaceae	APT	Water	28	196.000	13.000	NA	[67]
RDX	Sorghum	*S. Sudanese*	Poaceae	APT	Water	28	436.000	21.000	NA	[67]

RDX	Wheat	*T. aestivum*	Poaceae	APT	Soil	34	290.000	12.500	0.036	[67]
RDX	Wheat	*T. aestivum*	Poaceae	APT	Soil	34	888.000	25.000	0.036	[67]
RDX	Wheat	*T. aestivum*	Poaceae	APT	Soil	34	1723.000	50.000	0.036	[67]
RDX	Wheat	*T. aestivum*	Poaceae	APT	Soil	34	2828.000	100.000	0.036	[67]
RDX	Wheat	*T. aestivum*	Poaceae	APT	Soil	28	1597.000	220.000	0.036	[67]
RDX	Wheat	*T. aestivum*	Poaceae	APT	Soil	28	1680.000	494.000	0.036	[67]
RDX	Wheat	*T. aestivum*	Poaceae	APT	Soil	28	1915.000	903.000	0.036	[67]
RDX	Wheat	*T. aestivum*	Poaceae	APT	Water	28	65.000	6.000	NA	[67]
RDX	Wheat	*T. aestivum*	Poaceae	APT	Water	28	239.000	13.000	NA	[67]
RDX	Wheat	*T. aestivum*	Poaceae	APT	Water	28	408.000	21.000	NA	[67]
HMX	PR	*L. perenne*	Poaceae	Shoots	Soil	42	39.000	3.900	0.007	[64]
HMX	PR	*L. perenne*	Poaceae	Shoots	Soil	42	201.000	107.000	0.007	[64]
HMX	PR	*L. perenne*	Poaceae	Shoots	Soil	42	206.000	1099.000	0.007	[64]
HMX	PR	*L. perenne*	Poaceae	Shoots	Soil	42	325.000	9282.000	0.007	[64]
HMX	PR	*L. perenne*	Poaceae	Shoots	Soil	55	29.800	1.600	0.029	[65]
HMX	PR	*L. perenne*	Poaceae	Shoots	Soil	55	101.700	7.000	0.026	[65]
HMX	PR	*L. perenne*	Poaceae	Shoots	Soil	55	62.300	17.200	0.022	[65]
HMX	PR	*L. perenne*	Poaceae	PT	Soil	55	26.000	8.600	0.073	[66]
HMX	PR	*L. perenne*	Poaceae	PT	Soil	55	50.000	16.900	0.100	[66]
HMX	PR	*L. perenne*	Poaceae	PT	Soil	55	43.000	41.000	0.164	[66]
HMX	Alfalfa	*M. sativa*	Fabaceae	PT	Soil	55	65.000	8.600	0.073	[66]

HMX	Alfalfa	*M. sativa*	Fabaceae	PT	Soil	55	84.000	16.900	0.100	[66]
HMX	Alfalfa	*M. sativa*	Fabaceae	PT	Soil	55	66.000	41.000	0.164	[66]
HMX	Alfalfa	*M. sativa*	Fabaceae	Whole	Soil	77	289.300	32.300	0.020	[68]
HMX	BB	*P. vulgaris*	Fabaceae	Whole	Soil	77	123.300	32.300	0.020	[68]
HMX	Canola	*B. rapa*	Brassicaceae	Whole	Soil	77	223.500	32.300	0.020	[68]
HMX	PR	*L. perenne*	Poaceae	Whole	Soil	77	459.700	32.300	0.020	[68]
HMX	Wheat	*T. aestivum*	Poaceae	Whole	Soil	77	295.100	32.300	0.020	[68]
2,4-DNAN	PR	*L. perenne*	Poaceae	Shoots	Soil	19	1.059	0.474	0.012	[69]
2,4-DNAN	PR	*L. perenne*	Poaceae	Shoots	Soil	19	2.085	0.796	0.012	[69]
2,4-DNAN	PR	*L. perenne*	Poaceae	Shoots	Soil	19	2.893	1.808	0.012	[69]
2,4-DNAN	PR	*L. perenne*	Poaceae	Shoots	Soil	19	4.723	2.977	0.012	[69]
2,4-DNAN	PR	*L. perenne*	Poaceae	Shoots	Soil	19	14.908	4.699	0.012	[69]
2,4-DNAN	Barley	*H. vulgare*	Poaceae	Whole	Sand	29	192.209	10.681	NA	TW
4-NAN	Barley	*H. vulgare*	Poaceae	Whole	Sand	30	26.573	7.886	NA	TW
2-M-5-NPYNE	Barley	*H. vulgare*	Poaceae	Whole	Sand	29	26.268	10.180	NA	TW

[a] Plant common name; YN: Yellow Nutsedge; PR: Perennial ryegrass; BB: Bush bean

[b] *C. esculentus: Cyperus esculentus*; *H. vulgare*: *Hordeum vulgare*; *L. perenne: Lolium perenne*; *M. sativa: Medicago sativa*; *Z. mays: Zea mays*; *G. max: Glycine max*; *S. Sudanese: Sorghum sudanese*; *T. aestivum: Triticum aestivum*; *P. vulgaris: Phaseolus vulgaris*; *B. rapa: Brassica rapa*

[c] PT: Plant tissue; APT: Aerial plant tissue

[d] Concentration in the exposure medium (e.g., soil, sand, water). Exposure concentrations in sand are reported in this work (Table A-7 in Appendix A) as the concertation in the interstitial water (mg L^{-1})

[e] TW: This work (Table A-7 in Appendix A)

Table B-10 Predicted values for soil organic carbon–water partition coefficient (K_{OC}), concentration in interstitial water, and concentration in plant for MCs and MLCs in published uptake assays[a].

Compound	Obs. concentration in plant	Pred. log K_{OC}[b]	Pred. concentration in interstitial water[c]	Pred. concentration in interstitial water_corrected[d]	Pred. concentration in plant	Residuals[e]
	mg kg_{dwt}^{-1}	L kg^{-1}	mg L^{-1}	mg L^{-1}	mg kg_{dwt}^{-1}	
TNT	27.799	2.236	2.724	2.724	83.462	0.477
TNT	93.438	2.236	17.004	17.004	520.921	0.746
TNT	26.014	NA	NA	NA	190.872	0.866
2,4-DNT	2.800	2.118	0.662	0.662	10.670	0.581
2,4-DNT	2.800	2.118	3.312	3.312	53.349	1.280
2,4-DNT	48.712	NA	NA	NA	155.276	0.503
RDX	119.000	1.592	47.355	47.355	708.773	0.775
RDX	804.000	1.592	443.686	59.700	893.544	0.046
RDX	764.000	1.592	4325.938	59.700	893.544	0.068
RDX	1690.000	1.592	37828.493	59.700	893.544	-0.277
RDX	1083.000	1.592	10.218	10.218	152.942	-0.850
RDX	5217.000	1.592	67.200	59.700	893.544	-0.766
RDX	2948.000	1.592	209.544	59.700	893.544	-0.518
RDX	806.000	1.592	11.143	11.143	166.784	-0.684

RDX	2055.000	1.592	263.953	59.700	893.544	-0.362
RDX	3886.000	1.592	253.454	59.700	893.544	-0.638
RDX	3068.000	1.592	280.360	59.700	893.544	-0.536
RDX	387.567	1.592	22.258	22.258	333.148	-0.066
RDX	1965.800	1.592	66.775	59.700	893.544	-0.342
RDX	2221.400	1.592	222.585	59.700	893.544	-0.396
RDX	187.000	1.592	11.143	11.143	166.784	-0.050
RDX	3997.000	1.592	263.953	59.700	893.544	-0.651
RDX	4355.000	1.592	253.454	59.700	893.544	-0.688
RDX	4155.000	1.592	280.360	59.700	893.544	-0.667
RDX	120.000	1.592	8.888	8.888	133.028	0.045
RDX	300.000	1.592	17.776	17.776	266.056	-0.052
RDX	802.000	1.592	35.552	35.552	532.112	-0.178
RDX	1210.000	1.592	71.104	59.700	893.544	-0.132
RDX	695.000	1.592	156.428	59.700	893.544	0.109
RDX	602.000	1.592	351.251	59.700	893.544	0.172
RDX	649.000	1.592	642.065	59.700	893.544	0.139
RDX	95.000	NA	NA	NA	89.803	-0.024
RDX	171.000	NA	NA	NA	194.574	0.056
RDX	300.000	NA	NA	NA	314.312	0.020
RDX	104.000	1.592	8.888	8.888	133.028	0.107

RDX	181.000	1.592	17.776	17.776	266.056	0.167
RDX	314.000	1.592	35.552	35.552	532.112	0.229
RDX	492.000	1.592	71.104	59.700	893.544	0.259
RDX	322.000	1.592	156.428	59.700	893.544	0.443
RDX	358.000	1.592	351.251	59.700	893.544	0.397
RDX	274.000	1.592	642.065	59.700	893.544	0.513
RDX	76.000	NA	NA	NA	89.803	0.072
RDX	138.000	NA	NA	NA	194.574	0.149
RDX	168.000	NA	NA	NA	314.312	0.272
RDX	94.000	1.592	8.888	8.888	133.028	0.151
RDX	314.000	1.592	17.776	17.776	266.056	-0.072
RDX	1052.000	1.592	35.552	35.552	532.112	-0.296
RDX	1414.000	1.592	71.104	59.700	893.544	-0.199
RDX	1133.000	1.592	156.428	59.700	893.544	-0.103
RDX	975.000	1.592	351.251	59.700	893.544	-0.038
RDX	1218.000	1.592	642.065	59.700	893.544	-0.135
RDX	72.000	NA	NA	NA	89.803	0.096
RDX	196.000	NA	NA	NA	194.574	-0.003
RDX	436.000	NA	NA	NA	314.312	-0.142
RDX	290.000	1.592	8.888	8.888	133.028	-0.338
RDX	888.000	1.592	17.776	17.776	266.056	-0.523

RDX	1723.000	1.592	35.552	35.552	532.112	-0.510
RDX	2828.000	1.592	71.104	59.700	893.544	-0.500
RDX	1597.000	1.592	156.428	59.700	893.544	-0.252
RDX	1680.000	1.592	351.251	59.700	893.544	-0.274
RDX	1915.000	1.592	642.065	59.700	893.544	-0.331
RDX	65.000	NA	NA	NA	89.803	0.140
RDX	239.000	NA	NA	NA	194.574	-0.089
RDX	408.000	NA	NA	NA	314.312	-0.113
HMX	39.000	1.524	19.470	5.000	49.244	0.101
HMX	201.000	1.524	534.172	5.000	49.244	-0.611
HMX	206.000	1.524	5486.496	5.000	49.244	-0.622
HMX	325.000	1.524	46338.172	5.000	49.244	-0.820
HMX	29.800	1.524	1.913	1.913	18.843	-0.199
HMX	101.700	1.524	9.298	5.000	49.244	-0.315
HMX	62.300	1.524	27.404	5.000	49.244	-0.102
HMX	26.000	1.524	4.118	4.118	40.560	0.193
HMX	50.000	1.524	5.859	5.000	49.244	-0.007
HMX	43.000	1.524	8.732	5.000	49.244	0.059
HMX	65.000	1.524	4.118	4.118	40.560	-0.205
HMX	84.000	1.524	5.859	5.000	49.244	-0.232
HMX	66.000	1.524	8.732	5.000	49.244	-0.127

HMX	289.300	1.524	48.375	5.000	49.244	-0.769
HMX	123.300	1.524	48.375	5.000	49.244	-0.399
HMX	223.500	1.524	48.375	5.000	49.244	-0.657
HMX	459.700	1.524	48.375	5.000	49.244	-0.970
HMX	295.100	1.524	48.375	5.000	49.244	-0.778
2,4-DNAN	1.059	2.021	0.452	0.452	2.928	0.441
2,4-DNAN	2.085	2.021	0.759	0.759	4.911	0.372
2,4-DNAN	2.893	2.021	1.724	1.724	11.157	0.586
2,4-DNAN	4.723	2.021	2.839	2.839	18.372	0.590
2,4-DNAN	14.908	2.021	4.481	4.481	28.997	0.289
2,4-DNAN	192.209	NA	NA	NA	69.109	-0.444
4-NAN	26.573	NA	NA	NA	71.281	0.429
2-M-5-NPYNE	26.268	NA	NA	NA	47.338	0.256

[a] Dataset described in Table B-2 in Appendix B

[b] Prediction made using K_{OC} pp–LFER model developed by Kipka and Di Toro [41] Eq. (3-3). Not applicable (NA) for experiments performed using sand or water as the growth medium

[c] NA for experiments performed using sand or water as the growth medium given that the concentrations in the interstitial water or bulk water are measured and directly reported in the data sources

[d] Predicted concentrations in interstitial water that exceeded solubility limits were corrected to be at the solubility of the compound, listed in Table B-1 in Appendix B

[e] Calculated as: (Pred. log concentration in plant) - (Obs. log concentration in plant)

Appendix C

MODEL PARAMETERS AND DATA FOR PARTION–BASED PREDICTION OF MUNITIONS COMPOUNDS BIOCONCENTRATION IN WORMS

References cited in this appendix are listed in the "REFERENCES" section of Chapter 4.

C.1 Munitions Compounds (MCs) and Munitions-Like Compounds (MLCs)

Table C-1 Selected characteristics and physicochemical properties of the MCs and MLCs included in the worm lipid–water pp–LFER and the model validation.

Class	Compound[a]	CAS #	Molecular Weight	Structure	Aqueous Solubility[b] mg L^{-1}	log K_{OW}[b]
MCs: Nitroaromatics	2,4-DNAN	119-27-7	198.14	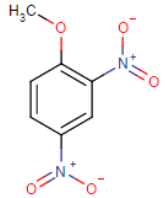	155	1.58[c]

MCs: Nitramines	RDX	121-82-4	222.12	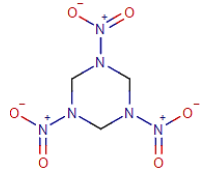	60	0.87
	HMX	2691-41-0	296.16	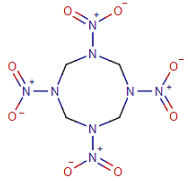	5	0.16
	NQ	556-88-7	104.07	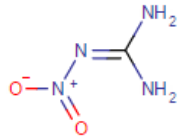	4400	-0.89
MLCs	2-A-4-NAN	99-59-2	168.15	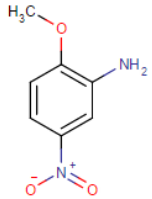	115	1.47
	2-M-5-NPYNE	5446-92-4	154.13	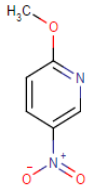	1406[d]	1.55

	3,5-DN-o-TAME	148-01-6	225.16	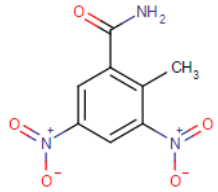	1000	0.19[d]
	4-NAN	100-17-4	153.14	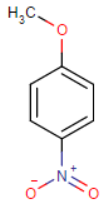	590	2.03

[a] 2,4-DNAN: 2,4-dinitroanisole; RDX: hexahydro-1,3,5-trinitro-1,3,5-triazine; HMX: octahydro-1,3,5,7-tetranitro-1,3,5,7-tetrazocine; NQ: nitroguanidine; 2-A-4-NAN: 2-amino-4-nitroanisole; 2-M-5-NPYNE: 2-methoxy-5-nitropyridine; 3,5-DN-o-TAME: 3,5-dinitro-o-toluamide; 4-NAN: 4-nitroanisole.
[b] Experimental data from EPI Suite database [35]
[c] Experimental value from Hawari et al. [40]
[d] Estimate from EPI Suite [35] in absence of an experimental value

Table C-2 Worm bioconcentration factors (BCFs) dataset.

Compound[a]	CAS #	Chemical class[b]	log K_{OW}[c]	Exposure medium	Worm species[f]	Aquatic or terrestrial	Obs. log BCF[h]	Source
NQ	556-88-7	MC	-0.89	Soil	*E. andrei*	terra	-0.211	0
3,5-DN-o-TAME	148-01-6	MLC	0.19[d]	Sand	*E. andrei*	terra	0.778	41
RDX	121-82-4	MC	0.87	Soil	*E. andrei*	terra	0.740	29
RDX	121-82-4	MC	0.87	Soil	*E. andrei*	terra	0.602	29
RDX	121-82-4	MC	0.87	Soil	*E. andrei*	terra	0.663	29
RDX	121-82-4	MC	0.87	Soil	*E. andrei*	terra	0.699	29
RDX	121-82-4	MC	0.87	Soil	*E. andrei*	terra	0.633	29
RDX	121-82-4	MC	0.87	Soil	*E. andrei*	terra	0.748	29
RDX	121-82-4	MC	0.87	Soil	*E. andrei*	terra	0.740	29
RDX	121-82-4	MC	0.87	Water	*E. andrei*	terra	1.114	29
RDX	121-82-4	MC	0.87	Water	*L. variegatus*	aqua	0.380	28
2-A-4-NAN	99-59-2	MLC	1.47	Soil	*E. andrei*	terra	-0.087	0
2-M-5-NPYNE	5446-92-4	MLC	1.55	Sand	*E. andrei*	terra	1.041	41
2,4-DNAN	119-27-7	MC	1.58[e]	Soil	*E. andrei*	terra	1.185	0
4-NAN	100-17-4	MLC	2.03	Sand	*E. andrei*	terra	1.672	41
simazine	122-34-9	pesticide	2.18	Water	*L. terrestris*	terra	2.161	15
3-chlorophenol	108-43-0	cL-phenol	2.5	Water	*E. fetida*	terra	0.845	16

3-chlorophenol	108-43-0	cL-phenol	2.5	Water	*E. fetida*	terra	1.230	[16]
3-chlorophenol	108-43-0	cL-phenol	2.5	Water	*L. rubellus*	terra	2.009	[16]
3-chlorophenol	108-43-0	cL-phenol	2.5	Water	*L. rubellus*	terra	2.090	[16]
3,4-dichlorophenol	95-77-2	cL-phenol	3.33	Water	*E. fetida*	terra	1.431	[16]
3,4-dichlorophenol	95-77-2	cL-phenol	3.33	Water	*E. fetida*	terra	1.380	[16]
3,4-dichlorophenol	95-77-2	cL-phenol	3.33	Water	*L. rubellus*	terra	1.301	[16]
3,4-dichlorophenol	95-77-2	cL-phenol	3.33	Water	*L. rubellus*	terra	1.613	[16]
1,2,3-TCB	87-61-6	org-chlorine	4.05	Water	*E. andrei*	terra	3.103	[18]
γ-HCH	58-89-9	pesticide	4.14	Sediment	*T. tubifex*	aqua	3.279	[27]
γ-HCH	58-89-9	pesticide	4.14	Water	*L. terrestris*	terra	3.380	[42]
α-HCH	319-84-6	pesticide	4.14	Sediment	*T. tubifex*	aqua	2.674	[27]
fluorene	86-73-7	PAH	4.18	Water	*L. variegatus*	aqua	2.519	[43]
fluorene	86-73-7	PAH	4.18	Water	*L. variegatus*	aqua	2.580	[43]
fluorene	86-73-7	PAH	4.18	Water	*L. variegatus*	aqua	2.690	[43]
1,3,5-TCB	108-70-3	org-chlorine	4.19	Water	*E. andrei*	terra	2.824	[18]
anthracene	120-12-7	PAH	4.45	Water	*L. variegatus*	aqua	3.134	[43]
anthracene	120-12-7	PAH	4.45	Water	*L. variegatus*	aqua	3.107	[43]
anthracene	120-12-7	PAH	4.45	Water	*L. variegatus*	aqua	3.146	[43]
anthracene	120-12-7	PAH	4.45	Water	*L. variegatus*	aqua	3.143	[43]
anthracene	120-12-7	PAH	4.45	Water	*L. variegatus*	aqua	3.152	[43]
phenanthrene	85-01-8	PAH	4.46	Sediment	*T. tubifex*[g]	aqua	4.263	[44,45]

1,2,3,4-TCB	634-66-2	org-chlorine	4.6	Water	*E. andrei*	terra	3.748	[18]
1,2,3,4-TCB	634-66-2	org-chlorine	4.6	Sediment	*T. tubifex*	aqua	5.797	[44,45]
HCBT	87-68-3	vinyl halide	4.78	Sediment	*T. tubifex*	aqua	4.462	[27]
pyrene	129-00-0	PAH	4.88	Water	*L. variegatus*	aqua	3.299	[43]
pyrene	129-00-0	PAH	4.88	Water	*L. variegatus*	aqua	3.303	[43]
pyrene	129-00-0	PAH	4.88	Water	*L. variegatus*	aqua	3.279	[43]
pyrene	129-00-0	PAH	4.88	Water	*L. variegatus*	aqua	3.176	[43]
pyrene	129-00-0	PAH	4.88	Water	*L. variegatus*	aqua	3.079	[43]
fluoranthene	206-44-0	PAH	5.16	Water	*M. rubroniveus*	aqua	4.037	[43]
fluoranthene	206-44-0	PAH	5.16	Sediment	*T. tubifex*	aqua	4.953	[44,45]
PChB	608-93-5	org-chlorine	5.17	Sediment	*T. tubifex*	aqua	4.279	[27]
PChB	608-93-5	org-chlorine	5.17	Water	*E. andrei*	terra	4.096	[18]
PChB	608-93-5	org-chlorine	5.17	Sediment	*T. tubifex*	aqua	5.972	[44,45]
2,3,4,5,6-PCT	877-11-2	org-chlorine	5.62	Sediment	*T. tubifex*	aqua	4.447	[27]
HCB	118-74-1	org-chlorine	5.73	Sediment	*T. tubifex*	aqua	4.380	[27]
HCB	118-74-1	org-chlorine	5.73	Water	*E. andrei*	terra	4.506	[18]
HCB	118-74-1	org-chlorine	5.73	Water	*E. andrei*	terra	4.614	[18]
HCB	118-74-1	org-chlorine	5.73	Water	*L. terrestris*	terra	4.290	[15]
HCB	118-74-1	org-chlorine	5.73	Sediment	*T. tubifex*	aqua	6.408	[44,45]
1,2,3,4-TCN	20020-02-4	cL-PAH	5.75	Sediment	*T. tubifex*	aqua	4.322	[27]
B[a]A	56-55-3	PAH	5.76	Sediment	*T. tubifex*	aqua	5.828	[44,45]

chrysene	218-01-9	PAH	5.81	Sediment	*T. tubifex*	aqua	5.658	[44,45]

[a] 1,2,3-TCB: 1,2,3-trichlorobenzene; γ-HCH: γ-hexachlorocyclohexane; α-HCH: α-hexachlorocyclohexane; 1,3,5-TCB: 1,3,5-trichlorobenzene; 1,2,3,4-TCB: 1,2,3,4-tetrachlorobenzene; HCBT: hexachlorobutadiene; PChB: pentachlorobenzene; 2,3,4,5,6-PCT: 2,3,4,5,6-pentachlorotoluene; HCB: hexachlorobenzene; 1,2,3,4-TCN: 1,2,3,4-tetrachloronaphthalene; B[a]A: benzo[a]anthracene. For all other abbreviations see Table C-1 in Appendix C

[b] cL-phenol: chlorinated phenol; org-chlorine: organochlorine; PAH: polycyclic aromatic hydrocarbon; cL-PAH: chlorinated PAH

[c] Experimental data from EPI Suite database [35]

[d] Estimate from EPI Suite [35] in absence of an experimental value

[e] Experimental value from Hawari et al. [40]

[f] *E. andrei*: *Eisenia andrei*; *L. variegatus*: *Lumbriculus variegatus*; *L. terrestris*: *Lumbricus terrestris*; *E. fetida*: *Eisenia fetida*; *L. rubellus*: *Lumbricus rubellus*; *T. tubifex*: *Tubifex tubifex*; *M. rubroniveus*: *Monopylephorus rubroniveus*

[g] More than 90% of the culture used in the studies reported in Kraaij et al. [44] and Kraaij et al. [45] consisted of the species *Limnodrilus hoffmeisteri* and *Tubifex tubifex* (both family Tubificidae)

[h] Observed log BCF (L kg_{dwt}^{-1}). Values from Lord et al. [15] are K_{Lipid}, and were transformed using the corresponding mass fraction of lipid from Table C-4 in Appendix C. Values from Kraaij et al. [44] and Kraaij et al. [45] were calculated using the concentration in the worm lipid in Kraaij et al. [44] and the concentration in the pore water (untreated sediment) reported in Kraaij et al. [45]; biota-to-sediment accumulation factor (BSAF) and the concentration in the sediment for the 2 days aging time ("contact time" in source) treatment reported in Kraaij et al. [44] were used to obtain the concentration in the worm lipid

Table C-3 Worm mass fraction of dry weight (f_{dwt}), fraction of lipid (f_{Lipid}), and fraction of protein ($f_{Protein}$) obtained from the literature.

Species[a]	Aquatic or terrestrial	f_{dwt}[b] kg kg_{wwt}^{-1}	Qlty.[d]	f_{Lipid} kg kg_{wwt}^{-1}	Qlty.	f_{Lipid} kg kg_{dwt}^{-1}	Qlty.	$f_{Protein}$ kg kg_{wwt}^{-1}	Qlty.	$f_{Protein}$ kg kg_{dwt}^{-1}	Qlty.	Source
E. andrei	terra	NA[c]	NA	0.010	Msrd.	0.067	Calc.					[18]
E. andrei	terra	0.15	Calc.	NA	NA	NA	NA					[29]
E. andrei	terra	NA	NA	0.023	Msrd.	0.153	Calc.					[46]
E. andrei	terra	NA	NA	NA	NA	0.142	Msrd.					[41]
E. andrei	terra	NA	NA	NA	NA	0.105	Msrd.					[41]
E. andrei	terra	NA	NA	NA	NA	0.121	Msrd.					[41]
E. fetida	terra	0.157	Msrd.	0.019	Msrd.	0.120	Msrd.	0.110	Msrd.	0.702	Msrd.	[47]
L.terrestris	terra	NA	NA	0.012	Msrd.	0.075	Calc.					[48]
L.terrestris	terra	0.164	Msrd.	0.016	Msrd.	0.098	Msrd.	0.105	Msrd.	0.640	Msrd.	[49]
L. variegatus	aqua	0.19	Msrd.	0.015	Calc.	0.080	Msrd.					[50]
L. variegatus	aqua	NA	NA	0.010	Msrd.	0.053	Calc.					[51]
L. variegatus	aqua	NA	NA	0.011	Msrd.	0.055	Calc.					[52]
T. tubifex	aqua	0.14	Msrd.	0.027	Msrd.	0.197	Msrd.					[53]
T. tubifex	aqua	0.13	Msrd.	0.010	Msrd.	0.080	Msrd.					[27]
T. tubifex	aqua	NA	NA	0.030	Msrd.	0.219	Calc.					[44]

[a] Abbreviations defined in Table C-1 in Appendix C.
[b] dwt: dry weight; wwt: wet or fresh weight
[c] Not available
[d] Quality of the values in the column immediately to the left. Calc.: values calculated with information either provided in the source (e.g., ratio of BCF to BCF_{Lipid} for f_{Lipid}) or listed in this table. When f_{dwt} was unavailable from the source, calc. f_{Lipid} dwt values were obtained with the average f_{dwt} values listed in this table for the corresponding species. Msrd.: values measured and reported explicitly in the source or elsewhere referred to by the source

Table C-4 Worm mass fractions of lipid (f_{Lipid}), protein ($f_{Protein}$), dry weight (f_{dwt}), and water (f_{Water}) used for the prediction of worms BCFs[a].

Compound[b]	Obs. log BCF[b]	Worm species[b]	f_{Lipid} (kg kg_{wwt}^{-1})	$f_{Protein}$ (kg kg_{wwt}^{-1})	f_{dwt} (kg kg_{wwt}^{-1})	f_{Water} (kg kg_{wwt}^{-1})[c]
NQ	-0.211	*E. andrei*	0.017	0.108	0.150	0.850
3,5-DN-o-TAME	0.778	*E. andrei*	0.016	0.108	0.150	0.850
RDX	0.740	*E. andrei*	0.017	0.108	0.150	0.850
RDX	0.602	*E. andrei*	0.017	0.108	0.150	0.850
RDX	0.663	*E. andrei*	0.017	0.108	0.150	0.850
RDX	0.699	*E. andrei*	0.017	0.108	0.150	0.850
RDX	0.633	*E. andrei*	0.017	0.108	0.150	0.850
RDX	0.748	*E. andrei*	0.017	0.108	0.150	0.850
RDX	0.740	*E. andrei*	0.017	0.108	0.150	0.850
RDX	1.114	*E. andrei*	0.017	0.108	0.150	0.850
RDX	0.380	*L. variegatus*	0.012	0.108	0.190	0.810
2-A-4-NAN	-0.087	*E. andrei*	0.017	0.108	0.150	0.850
2-M-5-NPYNE	1.041	*E. andrei*	0.018	0.108	0.150	0.850
2,4-DNAN	1.185	*E. andrei*	0.017	0.108	0.150	0.850
4-NAN	1.672	*E. andrei*	0.021	0.108	0.150	0.850
simazine	2.161	*L. terrestris*	0.014	0.105	0.164	0.836

3-chlorophenol	0.845	*E. fetida*	0.019	0.110	0.157	0.843
3-chlorophenol	1.230	*E. fetida*	0.019	0.110	0.157	0.843
3-chlorophenol	2.009	*L. rubellus*	0.018	0.108	0.157	0.843
3-chlorophenol	2.090	*L. rubellus*	0.018	0.108	0.157	0.843
3,4-dichlorophenol	1.431	*E. fetida*	0.019	0.110	0.157	0.843
3,4-dichlorophenol	1.380	*E. fetida*	0.019	0.110	0.157	0.843
3,4-dichlorophenol	1.301	*L. rubellus*	0.018	0.108	0.157	0.843
3,4-dichlorophenol	1.613	*L. rubellus*	0.018	0.108	0.157	0.843
1,2,3-TCB	3.103	*E. andrei*	0.010	0.108	0.150	0.850
γ-HCH	3.279	*T. tubifex*	0.010	0.108	0.130	0.870
γ-HCH	3.380	*L. terrestris*	0.010	0.108	0.130	0.870
α-HCH	2.674	*T. tubifex*	0.014	0.105	0.164	0.836
fluorene	2.519	*L. variegatus*	0.011	0.108	0.190	0.810
fluorene	2.580	*L. variegatus*	0.011	0.108	0.190	0.810
fluorene	2.690	*L. variegatus*	0.011	0.108	0.190	0.810
1,3,5-TCB	2.824	*E. andrei*	0.010	0.108	0.150	0.850
anthracene	3.134	*L. variegatus*	0.011	0.108	0.190	0.810
anthracene	3.107	*L. variegatus*	0.011	0.108	0.190	0.810
anthracene	3.146	*L. variegatus*	0.011	0.108	0.190	0.810
anthracene	3.143	*L. variegatus*	0.011	0.108	0.190	0.810
anthracene	3.152	*L. variegatus*	0.011	0.108	0.190	0.810

phenanthrene	4.263	*T. tubifex*[g]	0.030	0.108	0.135	0.865
1,2,3,4-TCB	3.748	*E. andrei*	0.010	0.108	0.150	0.850
1,2,3,4-TCB	5.797	*T. tubifex*	0.030	0.108	0.135	0.865
HCBT	4.462	*T. tubifex*	0.010	0.108	0.130	0.870
pyrene	3.299	*L. variegatus*	0.011	0.108	0.190	0.810
pyrene	3.303	*L. variegatus*	0.011	0.108	0.190	0.810
pyrene	3.279	*L. variegatus*	0.011	0.108	0.190	0.810
pyrene	3.176	*L. variegatus*	0.011	0.108	0.190	0.810
pyrene	3.079	*L. variegatus*	0.011	0.108	0.190	0.810
fluoranthene	4.037	*M. rubroniveus*	0.017	0.108	0.153	0.847
fluoranthene	4.953	*T. tubifex*	0.030	0.108	0.135	0.865
PChB	4.279	*T. tubifex*	0.010	0.108	0.130	0.870
PChB	4.096	*E. andrei*	0.010	0.108	0.150	0.850
PChB	5.972	*T. tubifex*	0.030	0.108	0.135	0.865
2,3,4,5,6-PCT	4.447	*T. tubifex*	0.010	0.108	0.130	0.870
HCB	4.380	*T. tubifex*	0.010	0.108	0.130	0.870
HCB	4.506	*E. andrei*	0.010	0.108	0.150	0.850
HCB	4.614	*E. andrei*	0.010	0.108	0.150	0.850
HCB	4.290	*L. terrestris*	0.014	0.105	0.164	0.836
HCB	6.408	*T. tubifex*	0.030	0.108	0.135	0.865
1,2,3,4-TCN	4.322	*T. tubifex*	0.010	0.108	0.130	0.870

B[a]A	5.828	*T. tubifex*	0.030	0.108	0.135	0.865
chrysene	5.658	*T. tubifex*	0.030	0.108	0.135	0.865

[a] Values obtained from the literature, sources in Table C-2 in Appendix C. Average of values for the corresponding species were taken when not available in or elsewhere referred to by the source of the worm BCF (Table C-3 in Appendix C). If the species was not listed in Table C-3 in Appendix C, the average among the values for the corresponding worm type (i.e., terrestrial or aquatic) was taken

[b] Values and abbreviations described in Table C-2 in Appendix C

[c] Calculated as: 1-f_{dwt}

Table C-5 Quantum Chemically estimated Abraham Parameters (QCAP) and Quantum Chemically estimated Experimental Abraham Parameters (QCEAP) [a] from Liang [31] used for the prediction of the worms BCFs dataset[b].

Compound[c]	Chemical class[c]	QCAP					QCEAP				
		E	*S*	*A*	*B*	*V*	*E*	*S*	*A*	*B*	*V*
NQ	MC	0.840	1.025	1.310	0.558	0.652	0.679	1.001	0.851	0.777	0.683
3,5-DN-o-TAME	MLC	1.560	2.629	0.487	0.855	1.462	1.314	2.590	0.227	0.704	1.448
RDX	MC	1.020	1.859	0.528	0.667	1.241	0.668	1.746	0.285	0.638	1.236
RDX	MC	1.020	1.859	0.528	0.667	1.241	0.668	1.746	0.285	0.638	1.236
RDX	MC	1.020	1.859	0.528	0.667	1.241	0.668	1.746	0.285	0.638	1.236
RDX	MC	1.020	1.859	0.528	0.667	1.241	0.668	1.746	0.285	0.638	1.236
RDX	MC	1.020	1.859	0.528	0.667	1.241	0.668	1.746	0.285	0.638	1.236
RDX	MC	1.020	1.859	0.528	0.667	1.241	0.668	1.746	0.285	0.638	1.236
RDX	MC	1.020	1.859	0.528	0.667	1.241	0.668	1.746	0.285	0.638	1.236
RDX	MC	1.020	1.859	0.528	0.667	1.241	0.668	1.746	0.285	0.638	1.236
RDX	MC	1.020	1.859	0.528	0.667	1.241	0.668	1.746	0.285	0.638	1.236
2-A-4-NAN	MLC	1.730	1.430	0.548	0.666	1.133	1.223	1.514	0.306	0.694	1.187
2-M-5-NPYNE	MLC	1.430	1.258	0.105	0.591	1.019	0.870	1.278	0.018	0.579	1.065
2,4-DNAN	MC	1.660	1.704	0.187	0.785	1.231	1.144	1.757	0.056	0.745	1.276
4-NAN	MLC	1.430	1.188	0.101	0.552	1.059	0.819	1.200	0.016	0.543	1.105

simazine	pesticide	1.990	1.199	0.541	0.635	1.402	1.213	1.313	0.297	0.689	1.481
3-chlorophenol	cL-phenol	1.370	0.972	0.937	0.139	0.866	0.923	0.945	0.581	0.177	0.885
3-chlorophenol	cL-phenol	1.370	0.972	0.937	0.139	0.866	0.923	0.945	0.581	0.177	0.885
3-chlorophenol	cL-phenol	1.370	0.972	0.937	0.139	0.866	0.923	0.945	0.581	0.177	0.885
3-chlorophenol	cL-phenol	1.370	0.972	0.937	0.139	0.866	0.923	0.945	0.581	0.177	0.885
3,4-dichlorophenol	cL-phenol	1.530	0.945	1.041	0.138	0.992	1.003	0.941	0.647	0.190	1.020
3,4-dichlorophenol	cL-phenol	1.530	0.945	1.041	0.138	0.992	1.003	0.941	0.647	0.190	1.020
3,4-dichlorophenol	cL-phenol	1.530	0.945	1.041	0.138	0.992	1.003	0.941	0.647	0.190	1.020
3,4-dichlorophenol	cL-phenol	1.530	0.945	1.041	0.138	0.992	1.003	0.941	0.647	0.190	1.020
1,2,3-TCB	org-chlorine	1.690	0.718	0.101	0.108	1.051	0.861	0.729	0.017	0.055	1.098
γ-HCH	pesticide	1.700	1.347	0.341	0.438	1.545	0.873	1.325	0.153	0.392	1.583
γ-HCH	pesticide	1.700	1.370	0.361	0.434	1.543	0.886	1.347	0.166	0.385	1.579
α-HCH	pesticide	1.700	1.347	0.341	0.438	1.545	0.873	1.325	0.153	0.392	1.583
fluorene	PAH	2.590	1.164	0.082	0.311	1.279	1.715	1.350	-0.020	0.191	1.357
fluorene	PAH	2.590	1.164	0.082	0.311	1.279	1.715	1.350	-0.020	0.191	1.357
fluorene	PAH	2.590	1.164	0.082	0.311	1.279	1.715	1.350	-0.020	0.191	1.357
1,3,5-TCB	org-chlorine	1.750	0.731	0.133	0.075	1.063	0.916	0.746	0.036	0.012	1.110
anthracene	PAH	1.993	1.340	0.000	0.232	1.454	1.116	1.345	-0.081	0.068	1.487
anthracene	PAH	1.993	1.340	0.000	0.232	1.454	1.116	1.345	-0.081	0.068	1.487
anthracene	PAH	1.993	1.340	0.000	0.232	1.454	1.116	1.345	-0.081	0.068	1.487
anthracene	PAH	1.993	1.340	0.000	0.232	1.454	1.116	1.345	-0.081	0.068	1.487

anthracene	PAH	1.993	1.340	0.000	0.232	1.454	1.116	1.345	-0.081	0.068	1.487
phenanthrene	PAH	3.020	1.258	0.111	0.321	1.357	2.100	1.524	-0.009	0.174	1.449
1,2,3,4-TCB	org-chlorine	1.900	0.689	0.110	0.133	1.173	0.973	0.737	0.019	0.086	1.234
1,2,3,4-TCB	org-chlorine	1.90	0.69	0.11	0.13	1.17	0.973	0.737	0.019	0.086	1.234
HCBT	vinyl halide	1.770	0.517	0.072	0.087	1.320	0.696	0.519	-0.005	0.061	1.383
pyrene	PAH	2.600	1.517	0.000	0.251	1.585	1.656	1.628	-0.095	0.036	1.635
pyrene	PAH	2.600	1.517	0.000	0.251	1.585	1.656	1.628	-0.095	0.036	1.635
pyrene	PAH	2.600	1.517	0.000	0.251	1.585	1.656	1.628	-0.095	0.036	1.635
pyrene	PAH	2.600	1.517	0.000	0.251	1.585	1.656	1.628	-0.095	0.036	1.635
pyrene	PAH	2.600	1.517	0.000	0.251	1.585	1.656	1.628	-0.095	0.036	1.635
fluoranthene	PAH	3.530	1.390	0.112	0.370	1.495	2.532	1.748	-0.020	0.191	1.607
fluoranthene	PAH	3.530	1.390	0.112	0.370	1.495	2.532	1.748	-0.020	0.191	1.607
PChB	org-chlorine	2.130	0.725	0.088	0.136	1.294	1.120	0.805	-0.003	0.071	1.364
PChB	org-chlorine	2.130	0.725	0.088	0.136	1.294	1.120	0.805	-0.003	0.071	1.364
PChB	org-chlorine	2.130	0.725	0.088	0.136	1.294	1.120	0.805	-0.003	0.071	1.364
2,3,4,5,6-PCT	org-chlorine	1.223	1.069	0.000	0.000	1.469	0.296	0.877	-0.071	-0.146	1.463
HCB	org-chlorine	2.340	0.715	0.053	0.171	1.409	1.235	0.832	-0.030	0.106	1.492
HCB	org-chlorine	2.340	0.715	0.053	0.171	1.409	1.235	0.832	-0.030	0.106	1.492
HCB	org-chlorine	2.340	0.715	0.053	0.171	1.409	1.235	0.832	-0.030	0.106	1.492
HCB	org-chlorine	2.340	0.715	0.053	0.171	1.409	1.235	0.832	-0.030	0.106	1.492
HCB	org-chlorine	2.340	0.715	0.053	0.171	1.409	1.235	0.832	-0.030	0.106	1.492

1,2,3,4-TCN	cL-PAH	2.920	0.915	0.092	0.240	1.501	1.791	1.146	-0.017	0.138	1.604
B[a]A	PAH	2.712	1.664	0.000	0.290	1.823	1.673	1.766	-0.107	0.053	1.873
chrysene	PAH	2.712	1.664	0.000	0.290	1.823	1.673	1.766	-0.107	0.053	1.873

[a] The solute descriptors used to apply the K_{Lipid} and $K_{Protein}$ pp–LFERs by Kuo and Di Toro [30,33] were obtained with the regression equations for the QCEAP provided in Liang [31]. QCEAP are recommended over QCAP to apply existing pp–LFERs that were built using solute descriptors either derived from calibration to experimental measurements or estimated with functional group fragments contributions [31].
[b] Dataset described in Table C-2 in Appendix C.
[c] Values and abbreviations described in Table C-2 in Appendix C

Table C-6 Predicted worm BCFs using the partition–based model (Eq. (4-3)) with K_{Lipid} pp–LFER either from Kuo and Di Toro [30,33] (Eq. (4-5)) or from this work (Eq. (4-11)), and $K_{Protein}$ pp–LFER from Kuo and Di Toro [30,33] (Eq. (4-6))[a].

Compound[b]	Obs. log BCF[b]	K_{Lipid} pp–LFER from Kuo and Di Toro [30,33]			K_{Lipid} pp–LFER from this work		
		Pred. log BCF[c]	Square error[d]	Residuals[e]	Pred. log BCF[c]	Square error[d]	Residuals[e]
NQ	-0.211	0.759	9.41E-01	0.970	0.759	9.41E-01	0.970
3,5-DN-o-TAME	0.778	0.909	1.70E-02	0.130	0.781	1.06E-05	0.003
RDX	0.740	0.884	2.05E-02	0.143	0.794	2.84E-03	0.053
RDX	0.602	0.884	7.92E-02	0.281	0.794	3.67E-02	0.192
RDX	0.663	0.884	4.87E-02	0.221	0.794	1.71E-02	0.131
RDX	0.699	0.884	3.41E-02	0.185	0.794	8.97E-03	0.095
RDX	0.633	0.884	6.25E-02	0.250	0.794	2.57E-02	0.160
RDX	0.748	0.884	1.83E-02	0.135	0.794	2.07E-03	0.045
RDX	0.740	0.884	2.05E-02	0.143	0.794	2.84E-03	0.053
RDX	1.114	0.884	5.31E-02	-0.230	0.794	1.03E-01	-0.320
RDX	0.380	0.735	1.26E-01	0.354	0.664	8.06E-02	0.284
2-A-4-NAN	-0.087	0.991	1.16E+00	1.078	0.938	1.05E+00	1.025
2-M-5-NPYNE	1.041	1.054	1.58E-04	0.013	1.057	2.33E-04	0.015
2,4-DNAN	1.185	0.954	5.30E-02	-0.230	0.881	9.23E-02	-0.304

4-NAN	1.672	1.277	1.56E-01	-0.395	1.366	9.35E-02	-0.306
simazine	2.161	1.741	1.76E-01	-0.420	2.293	1.74E-02	0.132
3-chlorophenol	0.845	1.731	7.84E-01	0.886	1.206	1.30E-01	0.361
3-chlorophenol	1.230	1.731	2.50E-01	0.500	1.206	5.83E-04	-0.024
3-chlorophenol	2.009	1.703	9.32E-02	-0.305	1.187	6.75E-01	-0.822
3-chlorophenol	2.090	1.703	1.49E-01	-0.387	1.187	8.15E-01	-0.903
3,4-dichlorophenol	1.431	2.141	5.04E-01	0.710	1.683	6.34E-02	0.252
3,4-dichlorophenol	1.380	2.141	5.79E-01	0.761	1.683	9.18E-02	0.303
3,4-dichlorophenol	1.301	2.112	6.58E-01	0.811	1.656	1.26E-01	0.355
3,4-dichlorophenol	1.613	2.112	2.49E-01	0.499	1.656	1.90E-03	0.044
1,2,3-TCB	3.103	3.030	5.34E-03	-0.073	3.055	2.32E-03	-0.048
γ-HCH	3.279	2.829	2.02E-01	-0.449	2.975	9.20E-02	-0.303
γ-HCH	3.380	2.820	3.14E-01	-0.561	2.903	2.28E-01	-0.478
α-HCH	2.674	2.877	4.14E-02	0.204	3.024	1.23E-01	0.350
fluorene	2.519	3.332	6.61E-01	0.813	2.916	1.58E-01	0.398
fluorene	2.580	3.332	5.65E-01	0.752	2.916	1.13E-01	0.336
fluorene	2.690	3.332	4.12E-01	0.642	2.916	5.10E-02	0.226
1,3,5-TCB	2.824	3.233	1.68E-01	0.410	3.152	1.08E-01	0.328
anthracene	3.134	3.772	4.08E-01	0.639	3.262	1.65E-02	0.128
anthracene	3.107	3.772	4.43E-01	0.665	3.262	2.39E-02	0.155
anthracene	3.146	3.772	3.92E-01	0.626	3.262	1.34E-02	0.116

anthracene	3.143	3.772	3.96E-01	0.629	3.262	1.41E-02	0.119
anthracene	3.152	3.772	3.85E-01	0.620	3.262	1.20E-02	0.110
phenanthrene	4.263	4.398	1.83E-02	0.135	3.776	2.37E-01	-0.487
1,2,3,4-TCB	3.748	3.453	8.69E-02	-0.295	3.709	1.57E-03	-0.040
1,2,3,4-TCB	5.797	3.968	3.35E+00	-1.829	4.224	2.48E+00	-1.574
HCBT	4.462	4.139	1.05E-01	-0.324	4.925	2.14E-01	0.462
pyrene	3.299	4.495	1.43E+00	1.197	3.647	1.21E-01	0.349
pyrene	3.303	4.495	1.42E+00	1.192	3.647	1.18E-01	0.344
pyrene	3.279	4.495	1.48E+00	1.217	3.647	1.36E-01	0.369
pyrene	3.176	4.495	1.74E+00	1.319	3.647	2.22E-01	0.471
pyrene	3.079	4.495	2.01E+00	1.416	3.647	3.23E-01	0.568
fluoranthene	4.037	4.664	3.93E-01	0.627	3.914	1.52E-02	-0.123
fluoranthene	4.953	4.958	2.73E-05	0.005	4.207	5.56E-01	-0.746
PChB	4.279	4.049	5.30E-02	-0.230	4.342	4.05E-03	0.064
PChB	4.096	3.986	1.19E-02	-0.109	4.280	3.41E-02	0.185
PChB	5.972	4.502	2.16E+00	-1.470	4.796	1.38E+00	-1.176
2,3,4,5,6-PCT	4.447	4.466	3.40E-04	0.018	4.280	2.80E-02	-0.167
HCB	4.380	4.434	2.87E-03	0.054	4.936	3.09E-01	0.556
HCB	4.506	4.372	1.81E-02	-0.134	4.874	1.35E-01	0.368
HCB	4.614	4.372	5.88E-02	-0.243	4.874	6.73E-02	0.259
HCB	4.290	4.484	3.74E-02	0.193	4.986	4.84E-01	0.696

HCB	6.408	4.887	2.31E+00	-1.521	5.389	1.04E+00	-1.019
1,2,3,4-TCN	4.322	4.771	2.02E-01	0.449	4.949	3.93E-01	0.627
B[a]A	5.828	5.699	1.66E-02	-0.129	4.944	7.81E-01	-0.884
chrysene	5.658	5.699	1.71E-03	0.041	4.944	5.09E-01	-0.714

[a] Solute descriptors used for the K_{Lipid} pp–LFER obtained in this work (Eq. (4-11)) were QCAP, while those used for the K_{Lipid} and $K_{Protein}$ pp–LFERs by Kuo and Di Toro [30,33], (Eq. (4-5)) and (Eq. (4-6)), respectively, were QCEAP. Both QCAP and QCEAP were obtained from Liang [31] and are listed in Table C-5 in Appendix C. Mass fractions used for each worm component are listed in Table C-4 in Appendix C

[b] Values and abbreviations described in Table C-2 in Appendix C

[c] Predicted log BCF (L kg_{dwt}^{-1})

[d] Calculated as: [(Pred. log BCF) - (Obs. log BCF)]^2

[e] Calculated as: (Pred. log BCF) - (Obs. log BCF)

Table C-7 Statistics for the comparison of the lipid phase descriptors between the K_{Lipid} pp–LFERs from Kuo and Di Toro [30,33] (Eq. (4-5)) and the K_{Lipid} pp–LFERs from this work (Eq. (4-11))[a].

Lipid phase descriptor	This work	Standard error[b]	Kuo and Di Toro [30,33]	Standard error[b]	z-score	p–value[c]
c	0.751	0.780	0.84	0.14	-0.113	0.912
e	0.431	0.189	0.77	0.10	-1.581	0.114
s	-2.409	0.387	-1.1	0.19	-3.038	0.003
a	-0.787	0.393	-0.47	0.22	-0.703	0.484
b	-2.106	0.793	-3.52	0.20	1.730	0.084
v	4.553	0.673	3.37	0.13	1.726	0.084

[a] Results from a z–test with inhomogeneity of the error variances between the groups
[b] For the column to the left
[c] A p-value ≤ 0.05 was accepted as significant

Table C-8 Data from independent uptake assays with worms exposed to MCs in soil.

Compound[a]	Worm species[a]	Soil	Exposure time	Concentration in worm[d]	Concentration in soil	f_{oc}[e]	Source
			days	mg kg_{dwt}^{-1}	mg kg_{dwt}^{-1}	kg OC $kg_{dwt\ soil}^{-1}$	
RDX	*E. andrei*	soil SSL[c]	7	17.341	0.660	0.012	38
RDX	*E. andrei*	soil SSL	7	63.584	10.600	0.012	38
RDX	*E. andrei*	soil SSL	7	287.090	102.000	0.012	38
RDX	*E. andrei*	soil SSL	7	426.590	967.000	0.012	38
RDX	*E. andrei*	soil SSL	7	579.961	2850.000	0.012	38
RDX	*E. andrei*	soil SSL	7	920.520	9427.000	0.012	38
RDX	*E. fetida*	aged soil	28	41.000	645.000	0.063	37
RDX	*E. fetida*	aged soil	28	1698.000	855.500	0.086	37
RDX	*E. fetida*	sandy loam	14	61.173	8.000	0.012	54
RDX	*E. fetida*	sandy loam	14	102.213	16.000	0.012	54
RDX	*E. fetida*	sandy loam	14	186.615	32.000	0.012	54
RDX	*E. fetida*	sandy loam	14	284.956	64.000	0.012	54
RDX	*E. fetida*	sandy loam	14	306.637	128.000	0.012	54
2,4-DNAN	*E. andrei*	spiked soil	14	57.143	8.909	0.010	55
2,4-DNAN	*E. andrei*	spiked soil	14	100.840	19.822	0.010	55

2,4-DNAN	*E. andrei*	spiked soil	14	152.941	27.840	0.010	[55]
HMX	*E. andrei*	ammended soil	28	11.046	100.000	0.012	[39]
HMX	*E. andrei*	ammended soil	28	48.818	1000.000	0.012	[39]
HMX	*E. andrei*	ammended soil	28	501.106	10000.000	0.012	[39]
TNT[b]	*E. fetida*	sandy loam	14	5.190	6.000	0.012	[54]
TNT	*E. fetida*	sandy loam	14	12.111	12.000	0.012	[54]
TNT	*E. fetida*	sandy loam	14	31.575	24.000	0.012	[54]
TNT	*E. fetida*	sandy loam	14	98.616	48.000	0.012	[54]

[a] Abbreviations in Tables C-1 and C-8 in Appendix C
[b] [U-^{14}C]-TNT
[c] Sassafras sandy loam
[d] Values from Sarrazin et al. [38] taken as the average value per treatment. Values from Gong et al. [54] taken as the average of day 4 ("repeat") and day 14. Values from Sunahara [39] taken as the average of concentrations measured after day 5
[e] Mass fraction of organic carbon in the soil. If only mass fraction of organic matter (f_{OM}) in the soil was reported, a factor of 0.50 was used to convert f_{OM} to f_{OC} [36]

Table C-9 Values for f_{Lipid}, $f_{Protein}$, f_{dwt}, and f_{Water}, QCAP, and QCEAP [31] used for the prediction of the concentrations in worms from the independent uptake assays dataset[a].

Compound	Species	f_{Lipid}	$f_{Protein}$	f_{dwt}	f_{Water}	QCAP					QCEAP				
						E	S	A	B	V	E	S	A	B	V
RDX	*E. andrei*	0.017	0.108	0.150	0.850	1.020	1.859	0.528	0.668	1.241	0.668	1.747	0.285	0.639	1.236
RDX	*E. andrei*	0.017	0.108	0.150	0.850	1.020	1.859	0.528	0.668	1.241	0.668	1.747	0.285	0.639	1.236
RDX	*E. andrei*	0.017	0.108	0.150	0.850	1.020	1.859	0.528	0.668	1.241	0.668	1.747	0.285	0.639	1.236
RDX	*E. andrei*	0.017	0.108	0.150	0.850	1.020	1.859	0.528	0.668	1.241	0.668	1.747	0.285	0.639	1.236
RDX	*E. andrei*	0.017	0.108	0.150	0.850	1.020	1.859	0.528	0.668	1.241	0.668	1.747	0.285	0.639	1.236
RDX	*E. andrei*	0.017	0.108	0.150	0.850	1.020	1.859	0.528	0.668	1.241	0.668	1.747	0.285	0.639	1.236
RDX	*E. fetida*	0.019	0.110	0.157	0.843	1.020	1.859	0.528	0.668	1.241	0.668	1.747	0.285	0.639	1.236
RDX	*E. fetida*	0.019	0.110	0.157	0.843	1.020	1.859	0.528	0.668	1.241	0.668	1.747	0.285	0.639	1.236
RDX	*E. fetida*	0.019	0.110	0.157	0.843	1.020	1.859	0.528	0.668	1.241	0.668	1.747	0.285	0.639	1.236
RDX	*E. fetida*	0.019	0.110	0.157	0.843	1.020	1.859	0.528	0.668	1.241	0.668	1.747	0.285	0.639	1.236
RDX	*E. fetida*	0.019	0.110	0.157	0.843	1.020	1.859	0.528	0.668	1.241	0.668	1.747	0.285	0.639	1.236
RDX	*E. fetida*	0.019	0.110	0.157	0.843	1.020	1.859	0.528	0.668	1.241	0.668	1.747	0.285	0.639	1.236
RDX	*E. fetida*	0.019	0.110	0.157	0.843	1.020	1.859	0.528	0.668	1.241	0.668	1.747	0.285	0.639	1.236
2,4-DNAN	*E. andrei*	0.017	0.108	0.150	0.850	1.660	1.704	0.187	0.785	1.231	1.144	1.757	0.056	0.745	1.276
2,4-DNAN	*E. andrei*	0.017	0.108	0.150	0.850	1.660	1.704	0.187	0.785	1.231	1.144	1.757	0.056	0.745	1.276
2,4-DNAN	*E. andrei*	0.017	0.108	0.150	0.850	1.660	1.704	0.187	0.785	1.231	1.144	1.757	0.056	0.745	1.276

HMX	*E. andrei*	0.017	0.108	0.150	0.850	1.160	2.450	0.635	1.050	1.631	0.825	2.357	0.335	1.026	1.629
HMX	*E. andrei*	0.017	0.108	0.150	0.850	1.160	2.450	0.635	1.050	1.631	0.825	2.357	0.335	1.026	1.629
HMX	*E. andrei*	0.017	0.108	0.150	0.850	1.160	2.450	0.635	1.050	1.631	0.825	2.357	0.335	1.026	1.629
TNT	*E. fetida*	0.019	0.110	0.157	0.843	1.660	1.887	0.302	0.752	1.344	1.164	1.910	0.124	0.684	1.373
TNT	*E. fetida*	0.019	0.110	0.157	0.843	1.660	1.887	0.302	0.752	1.344	1.164	1.910	0.124	0.684	1.373
TNT	*E. fetida*	0.019	0.110	0.157	0.843	1.660	1.887	0.302	0.752	1.344	1.164	1.910	0.124	0.684	1.373
TNT	*E. fetida*	0.019	0.110	0.157	0.843	1.660	1.887	0.302	0.752	1.344	1.164	1.910	0.124	0.684	1.373

[a] Data presented in Table C-8 in Appendix C, including abbreviations. Values for f_{Lipid}, $f_{Protein}$, f_{Water}, and f_{dwt} are expressed as kg kg_{wwt}^{-1} and their sources are in Table C-3 in Appendix C; average of values for the corresponding species were taken when not available in or elsewhere referred to by the source of the worm concentration. The solute descriptors used to apply the K_{Lipid} and K_{Protein} pp–LFERs by Kuo and Di Toro [30,33] were obtained with the regression equations for the QCEAP provided in Liang [31]. QCEAP are recommended over QCAP to apply existing pp–LFERs that were built using solute descriptors either derived from calibration to experimental measurements or estimated with functional group fragments contributions [31].

Table C-10 Predicted values for soil organic carbon-water partition coefficient (K_{OC}), concentration in interstitial water, and concentration in worm for MCs data from independent uptake studies using the partition–based model (Eq. (4-12)) with K_{Lipid} pp–LFER from this work (Eq. (4-11)).

Compound[a]	Obs. concentration in worm[a]	Pred. log K_{OC}[b]	Pred. concentration in interstitial water	Pred. concentration in interstitial water_corrected[c]	Pred. concentration in worm[d]
	mg kg_{dwt}^{-1}	L kg^{-1}	mg L^{-1}	mg L^{-1}	mg kg_{dwt}^{-1}
RDX	17.341	1.532	1.617	1.617	10.055
RDX	63.584	1.532	25.976	25.976	161.493
RDX	287.090	1.532	249.962	59.700	371.149
RDX	426.590	1.532	2369.739	59.700	371.149
RDX	579.961	1.532	6984.237	59.700	371.149
RDX	920.520	1.532	23101.897	59.700	371.149
RDX	41.000	1.532	303.241	59.700	355.351
RDX	1698.000	1.532	291.180	59.700	355.351
RDX	61.173	1.532	20.457	20.457	121.767
RDX	102.213	1.532	40.915	40.915	243.535
RDX	186.615	1.532	81.829	59.700	355.351
RDX	284.956	1.532	163.658	59.700	355.351
RDX	306.637	1.532	327.316	59.700	355.351
2,4-DNAN	57.143	2.002	8.864	8.864	67.390

2,4-DNAN	100.840	2.002	19.722	19.722	149.942
2,4-DNAN	152.941	2.002	27.699	27.699	210.593
HMX	11.046	1.433	320.874	5.000	29.466
HMX	48.818	1.433	3208.740	5.000	29.466
HMX	501.106	1.433	32087.399	5.000	29.466
TNT	5.190	2.203	3.272	3.272	25.457
TNT	12.111	2.203	6.544	6.544	50.913
TNT	31.575	2.203	13.089	13.089	101.826
TNT	98.616	2.203	26.178	26.178	203.652

[a] Dataset described in Table C-8 in Appendix C

[b] Prediction made using K_{OC} pp–LFER model developed by Kipka and Di Toro [34] Eq. (4-7) and QCEAP described in Table C-9 in Appendix C

[c] Predicted concentrations in interstitial water that exceeded solubility limits were corrected to be at the solubility of the compound listed in Table C-1 in Appendix C

[d] The K_{Lipid} pp–LFER from this work (Eq. (4-11)) was used with the QCAP from Liang [31] in Table C-9 in Appendix C

Table C-11 Predicted values for soil organic carbon-water partition coefficient (K_{OC}), concentration in interstitial water, and concentration in worm for MCs data from independent uptake studies using the partition–based model (Eq. (4-9)) with K_{Lipid} pp–LFER obtained by Kuo and Di Toro [30,33] (Eq. (4-5)).

Compound[a]	Obs. concentration in worm[a]	Pred. log K_{OC}[b]	Pred. concentration in interstitial water	Pred. concentration in interstitial water_corrected[c]	Pred. concentration in worm
	mg kg_{dwt}^{-1}	L kg^{-1}	mg L^{-1}	mg L^{-1}	mg kg_{dwt}^{-1}
RDX	17.341	1.532	1.617	1.617	12.041
RDX	63.584	1.532	25.976	25.976	193.393
RDX	287.090	1.532	249.962	59.700	444.463
RDX	426.590	1.532	2369.739	59.700	444.463
RDX	579.961	1.532	6984.237	59.700	444.463
RDX	920.520	1.532	23101.897	59.700	444.463
RDX	41.000	1.532	303.241	59.700	435.585
RDX	1698.000	1.532	291.180	59.700	435.585
RDX	61.173	1.532	20.457	20.457	149.261
RDX	102.213	1.532	40.915	40.915	298.522
RDX	186.615	1.532	81.829	59.700	435.585
RDX	284.956	1.532	163.658	59.700	435.585
RDX	306.637	1.532	327.316	59.700	435.585
2,4-DNAN	57.143	2.002	8.864	8.864	76.970

2,4-DNAN	100.840	2.002	19.722	19.722	171.258
2,4-DNAN	152.941	2.002	27.699	27.699	240.531
HMX	11.046	1.433	320.874	5.000	30.796
HMX	48.818	1.433	3208.740	5.000	30.796
HMX	501.106	1.433	32087.399	5.000	30.796
TNT	5.190	2.203	3.272	3.272	41.012
TNT	12.111	2.203	6.544	6.544	82.024
TNT	31.575	2.203	13.089	13.089	164.048
TNT	98.616	2.203	26.178	26.178	328.096

[a] Dataset described in Table C-8 in Appendix C

[b] Prediction made using K_{OC} pp–LFER model developed by Kipka and Di Toro [34] Eq. (4-7) and QCEAP described in Table C-9 in Appendix C

[c] Predicted concentrations in interstitial water that exceeded solubility limits were corrected to be at the solubility of the compound, listed in Table C-1 in Appendix C

[d] The K_{Lipid} pp–LFER by Kuo and Di Toro [30,33] (Eq. (4-5)) was used with the QCEAP from Liang [31] in Table C-9 in Appendix C